UC Santa Barbara

UC Santa Barbara Electronic Theses and Dissertations

Title

Co-Optimization of Communication, Motion and Sensing in Mobile Robotic Operations

Permalink

https://escholarship.org/uc/item/5t05b568

Author

Yan, Yuan

Publication Date

2016

Peer reviewed|Thesis/dissertation

eScholarship.org Powered by the California Digital Library
University of California

University of California
Santa Barbara

Co-Optimization of Communication, Motion and Sensing in Mobile Robotic Operations

A dissertation submitted in partial satisfaction
of the requirements for the degree

Doctor of Philosophy
in
Electrical and Computer Engineering

by

Yuan Yan

Committee in charge:

Professor Yasamin Mostofi (Advisor), Chair
Professor Francesco Bullo (Committee Member)
Professor Joao Hespanha (Committee Member)
Professor Upamanyu Madhow (Committee Member)

March 2016

The Dissertation of Yuan Yan is approved.

Professor Francesco Bullo (Committee Member)

Professor Joao Hespanha (Committee Member)

Professor Upamanyu Madhow (Committee Member)

Professor Yasamin Mostofi (Advisor), Committee Chair

March 2016

Co-Optimization of Communication, Motion and Sensing in Mobile Robotic Operations

Copyright © 2016

by

Yuan Yan

I dedicate this dissertation to my wife, Meiyi Chen, for her endless love and support.

Acknowledgements

First, I would like to express my deepest gratitude to my advisor, Prof. Yasamin Mostofi, for her great guidance, patience, support and caring over the years. She is knowledgeable and hardworking, who not only inspired me with great research ideas but also patiently corrected my writings. I would never have finished my dissertation without her help.

I would like to thank my committee members, Prof. Francesco Bullo, Prof. Joao Hespanha and Prof. Upamanyu Madhow, not only for their precious time, but also for their valuable suggestions and comments to improve my dissertation. I would like to thank Prof. Rafael Fierro for his help for my research when I was a PhD student at University of New Mexico.

I would like to extend my gratitude to all the members in Prof. Yasamin Mostofi's research group, especially Alireza Ghaffarkhah, Alejandro Gonzalez-Ruiz and Mehrzad Malmirchegini, for their valuable opinions as excellent researchers, as well as kind help as good friends.

Finally, I would like to thank my family for their love and support. I would like to thank my wife, Meiyi Chen, for putting tremendous effort on our long-distance relationship for the last nine years. I would like to thank my mother, Hong Zhou, and my father, Songgen Yan, for providing me the best atmosphere they could for my education since I was a child.

Curriculum Vitæ

Yuan Yan

Education

2016	Ph.D. in Electrical and Computer Engineering (Expected), University of California, Santa Barbara.
2008	M.S. in Control Science and Engineering, Huazhong University of Science and Technology.
2006	B.S. in Control Science and Engineering, Huazhong University of Science and Technology.

Publications

- *Journal Publications*

  1. Y. Yan and Y. Mostofi, "Efficient Clustering and Path Planning Strategies for Robotic Data Collection," *IEEE Transactions on Control of Network Systems*, 2016, conditionally accepted.
  2. Y. Yan and Y. Mostofi, "To Go or Not to Go: On Energy-Aware and Communication-Aware Robotic Operation", *IEEE Transactions on Control of Network Systems*, 1(3): 218-231, September 2014.
  3. Y. Yan and Y. Mostofi, "Co-Optimization of Communication and Motion Planning of a Robotic Operation under Resource Constraints and in Fading Environments," *IEEE Transactions on Wireless Communications*, 12(4): 1562-572, April 2013.
  4. Y. Yan and Y. Mostofi, "Robotic Router Formation in Realistic Communication Environments – A Bit Error Rate Approach," *IEEE Transactions on Robotics*, 28(4): 810-827, August 2012.

- *Conference Publications*

  1. U. Ali, Y. Yan, Y. Mostofi and Y. Wardi, "An Optimal Control Approach for Communication and Motion Co-Optimization in Realistic Fading Environments," *IEEE American Control Conference*, June 2015.
  2. Y. Yan and Y. Mostofi, "An Efficient Clustering and Path Planning Strategy in Sensor Networks for Data Collection Based on Space-Filling Curves," *IEEE Conference on Decision and Control*, December 2014.
  3. Y. Yan and Y. Mostofi, "Efficient Communication-Aware Dynamic Coverage Using Space-Filling Curves," *IEEE American Control Conference*, June 2014.
  4. Y. Yan and Y. Mostofi, "Impact of Localization Errors on Wireless Channel Prediction in Mobile Robotic Networks," *IEEE Globecom Workshop on WiUAV*, December 2013.

5. Y. Yan, A. Ghaffarkhah and Y. Mostofi, "Communication and Path Planning Strategies of a Robotic Coverage Operation," *IEEE American Control Conference*, June 2013.
6. Y. Yan and Y. Mostofi, "Utilizing Mobility to Minimize the Total Communication and Motion Energy Consumption of a Robotic Operation," *IFAC Workshop on Distributed Estimation and Control in Networked Systems*, September 2012.
7. A. Ghaffarkhah, Y. Yan and Y. Mostofi, "Dynamic Coverage of Time-Varying Environments Using a Mobile Robot – A Communication-Aware Perspective," *IEEE Globecom Workshop on WiUAV*, December 2011.
8. Y. Yan and Y. Mostofi, "Co-Optimization of Communication and Motion Planning of a Robotic Operation in Fading Environments," *Asilomar Conference on Signals, Systems and Computers*, November 2011.
9. N. Bezzo, Y. Yan, R. Fierro and Y. Mostofi, "A Decentralized Connectivity Strategy for Mobile Router Swarms," *World Congress of the International Federation of Automatic Control*, August 2011.
10. Y. Yan and Y. Mostofi, "Robotic Router Formation – A Bit Error Rate Approach," *IEEE Military Communications Conference*, October 2010.

Awards

2014 University of California, Santa Barbara, Deans Fellowship

Abstract

Co-Optimization of Communication, Motion and Sensing in Mobile Robotic Operations

by

Yuan Yan

In recent years, there has been considerable interest in wireless sensor networks and networked robotic systems. In order to achieve the full potential of such systems, integrative approaches that design the communication, navigation and sensing aspects of the systems simultaneously are needed. However, most of the existing work in the control and robotic communities uses over-simplified disk models or path-loss-only models to characterize the communication in the network, while most of the work in networking and communication communities does not fully explore the benefits of motion.

This dissertation thus focuses on co-optimizing these three aspects simultaneously in realistic communication environments that experience path loss, shadowing and multi-path fading. We show how to integrate the probabilistic channel prediction framework, which allows the robots to predict the channel quality at unvisited locations, into the co-optimization design. In particular, we consider four different scenarios: 1) robotic router formation, 2) communication and motion energy co-optimization along a pre-defined trajectory, 3) communication and motion energy co-optimization with trajectory planning, and 4) clustering and path planning strategies for robotic data collection. Our theoretical, simulation and experimental results show that the proposed framework considerably outperforms the cases where the communication, motion and sensing aspects of the system are optimized separately, indicating the necessity of co-optimization. They further show the significant benefits of using realistic channel models, as compared to the case of using over-simplified disk models.

Contents

Chapter 1

Introduction

In recent years, considerable progress has been made in the area of mobile sensor networks and networked robotic systems. Such systems have broad applications in real world, including but not limited to coverage control [1–4], rendezvous [5, 6], target tracking [7–10], surveillance and security [11–13], flocking [14–16], formulation control [17–21], dynamic vehicle routing [22–24] and environmental monitoring [25, 26]. In such systems, the robots/sensors need to communicate with each other in order to work collaboratively and achieve given common goals. In many applications, the robots/sensors may further need to communicate with a remote station (control center) to report their tasks or seek help from human operators [27]. As a result, the robots need to maintain a level of connectivity in order to achieve their tasks. In this dissertation, we aim to bring a foundational understanding to the impact of realistic communication links on the robotic system design, and show how to systematically co-optimize navigation, communication and sensing in realistic fading environments.

In this chapter, we first present motivating applications to show the importance of proper communication in the networked robotic systems. Then, we summarize the considered scenarios, review the related work in the literature and state the main contributions

of this thesis. Finally, we briefly summarize the organization of this dissertation.

1.1 Motivating Applications

In this part, we present a few applications of robotic systems where reliable communication is critical.

Robots for Surveillance, Security and Safety

Unmanned vehicles are envisioned to help with emergency response, search and rescue, and surveillance operations in near future. In such cases, each individual node has limited sensing and perception capabilities and the team has to perform the task cooperatively. Proper connectivity maintenance is thus considerably important in such scenarios and should be taken into account when path planning.

Mobile Relays for Connectivity Maintenance

In robotic router applications, unmanned vehicles are tasked with providing connectivity between two nodes that are otherwise disconnected due to possibly a large distance or fading. The mobile relays need to intelligently configure themselves into a reliable mesh network in order to build a temporary communication infrastructure. Such relay networks can have applications in many different areas from field robotics to smart homes where small robotic relays move to provide connectivity for users/computers that are in otherwise poorly-connected areas. As can be seen, the key in such application is to properly use motion capabilities to provide reliable communication services.

Unmanned Vehicles As Part of Our Everyday Life

It is envisioned that unmanned vehicles will soon be part of our everyday life. For instance, Amazon is developing a delivery system by using Unmanned Aerial Vehicles (UAV), which is known as Amazon Prime Air [28]. It is envisioned to allow the costumers to receive their packages in 30 minutes or less. During its operation, Prime Air may need to connect to a remote operator or other UAVs. It can then use its motion to move to better spots for connectivity.

Within a decade, self-driving cars can be part of our everyday life. Another popular application of robots is to provide tele-presence for medical care. In general, realizing such applications requires proper connectivity maintenance, path planning, and sensing.

1.2 Motivations and Contributions

In this dissertation, we focus on the co-optimization of the communication, motion and sensing strategies of mobile robots. The co-optimization is considerably important as the communication, motion and sensing decisions are highly coupled. For example, consider the case where a mobile robot needs to send some information bits to a remote station. Given a limited amount of energy, should the robot just send the information bits directly, or should it move to find a place that is good for communication and then send the bits? Clearly, the optimal decision of the robot depends on the current channel quality of the robot, the cost to move and the amount of information bits that needs to be sent. As another example, consider the case where a mobile robot needs to send a live streaming video of a target to a remote station. Should the robot move closer to the target for a better sensing quality, or should it move closer to the remote station for a better communication quality? On one hand, if the communication quality is poor, the remote station cannot receive a smooth streaming video. On the other hand, if the

sensing quality is poor, the remote station cannot get quality data. Clearly, the optimal decision, in terms of how much to move, depends on the sensing capability of the robot, the channel quality in the environment, and other system constraints. Therefore, the goal of this dissertation is to have an understanding of the co-optimization strategies in different scenarios and see the underlying tradeoffs in terms of communication, motion and sensing.

Traditionally, most of the work in robotics and control communities does not take communication issues into account when designing such systems. Instead, only the sensing and navigation aspects of the systems are investigated and over-simplified link models are assumed. Furthermore, the fact that each robot can now utilize mobility for better connectivity is not exploited. On the other hand, most of the work in the communication and networking communities are not concerned with path planning. In order to truly realize the full potentials of these systems, however, integrative approaches that properly optimize the communication, sensing and navigation issues are needed. Recently, such communication-aware navigation and/or sensing strategies have started to attract considerable attention [8, 9, 11, 22, 29–67].

This is the main motivation for the work in this thesis, i.e. to bring a foundational understanding to the rich space at the intersection of communication, motion and sensing in robotic networks. In order to co-optimize these aspects jointly, each robot needs to have a prediction of the channel quality at unvisited locations in the workspace. Most of the existing work uses disk models to model a wireless channel, i.e. it is assumed that two robots can communicate with each other if and only if the distance between them is smaller than some threshold. However, such over-simplified models do not suffice to model realistic fading channels. Fig. 1.1 shows a real indoor channel measurement (blue solid line) [68]. As can be seen, neither disk models nor path-loss-only models can capture the channel behaviors in practice. As a result, using such models may cause significant

performance degradation. See [9] for an example where using such models can cause instability in control over a wireless link. Hence, more sophisticated channel models are needed to design the networked robotic systems. In this dissertation, we use the probabilistic channel prediction framework that was proposed in [69–71] to predict the channel quality at unvisited locations. We briefly summarize this approach in Section 2.1. This thesis then shows how navigation, communication, and sensing can be co-optimized in realistic communication environments.

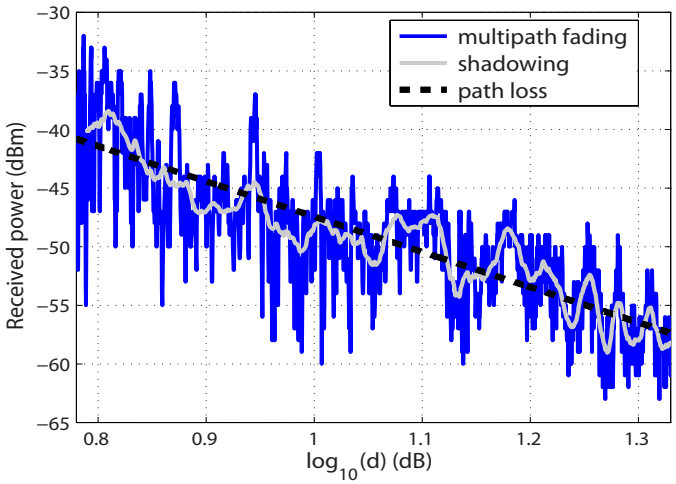

Figure 1.1: The figure shows an indoor channel measurement with three different channel dynamics marked [68].

In this dissertation, we consider four important aspects of robotic communication, motion and sensing co-optimization (each treated in a chapter). In the rest of this section, we review the related work in the literature, discuss our motivations, and summarize our contributions, for each chapter.

1.2.1 Robotic Router Formation

In Chapter 3, we mainly focus on understanding the fundamentals of co-optimizing motion and communication of a robotic network, without considering sensing issues. We then show how motion can be systematically optimized to ensure acceptable communication quality in realistic communication environments. More specifically, we consider a robotic router problem. In such problems, a transmitting node needs to maintain its connectivity to a receiving node over a large distance. Since the receiving node may need to get far due to possible exploratory missions, direct transmission may not be possible. Therefore, a number of robotic routers can be used to ensure robust communication between the two nodes. The routers will reconfigure themselves constantly in order to optimize the flow of information. A fundamental question is then as follows: Given specific transmitter/receiver locations and environmental/communication constraints, what is the optimum configuration of the routers and how can it be reached? Note that this scenario is directly related to the second application mentioned in Section 1.1, and the findings can also be used in robotic router applications for smart homes as well.

In the robotics and control community, algebraic-graph approaches attracted considerable attention for solving this problem. In [43], authors take Fiedler eigenvalue as a metric for the connectivity of a state-dependent graph, and use semidefinite programming to maximize it, subject to minimum distance constraints. In [44], a decentralized algorithm based on super-gradient and decentralized computation of Fiedler eigenvector is proposed. Similarly, a potential function is defined in [30], using spectral properties of the Laplacian matrix, in order to optimize connectivity while k-connectivity constraints are imposed in [45]. In [46], the ideas from [43, 44] and [45] are integrated to design a centralized control law for robotic routers. While the Fiedler eigenvalue is one measure of graph connectivity, it is rather a high-level measure, i.e. it does not measure the

communication reception quality. In [38], a spring-damper model is adopted to enforce the connectivity of a robotic operation, in an outdoor environment. A spring-damper model, on the other hand, still requires designing a function that translates the link quality to proper forces. In [47], two robotic router algorithms, namely known user trajectory algorithm and adversarial user trajectory algorithm, are proposed. More relevant communication-oriented metrics have also been utilized. Authors in [49] solve the mobility control problem by minimizing the communication energy cost, while in [50], the mobility control problem is investigated with the goal of maximizing the lifetime of the network. The aforementioned work, however, assumes an a priori-known disk or path-loss-only model for communication.

In the wireless sensor network community, optimal positioning of wireless sensors (or relays) has been studied [72, 73]. Similarly, in the communication literature, there has recently been a considerable interest in cooperative communication typically with the assumption of one relay node [74–78]. While communication-related metrics are used in these problems, most of the work from the communication or networking community has not been concerned with the control of motion, i.e. it is not on how a number of routers can plan their motions to optimally position themselves. For instance, the issue of online channel prediction does not even come up.

This motivates us to investigate the robotic router problem in realistic fading environments by jointly optimizing communication and motion.

Contributions

We start by using the Bit Error Rate (BER) of the end receiver as our performance metric. Then, the optimum configuration of the nodes is the one that results in the smallest possible BER at the receiving node. We show how this metric results in a different robotic configuration as compared to other approaches such as maximizing Fiedler eigen-

value of a graph. Moreover, we are interested in the robust operation of a robotic router network in a realistic communication environment which naturally experiences different forms of fading. We show how the probabilistic channel prediction framework of Section 2.1 can be properly integrated with the robotic router optimization and mathematically characterize properties of the optimal solution. This allows each robot to constantly make a distributed decision on where to move such that the whole network converges to the configuration that minimizes the end-to-end BER.

Furthermore, we characterize the robotic router formulation problem from the angle of power minimization. We show how robotic routers should position themselves and adjust their transmit power such that the total power consumption is minimized while the required link quality is satisfied. We further extend this analysis to the case where both communication and motion costs are taken into consideration, and show the underlying tradeoffs.

Finally, our proposed framework is verified with real channel data by both simulation and experimental results. In particular, our results show considerably performance improvement (an order of magnitude) over the state-of-the-art. We also show how localization errors will affect the performance of our framework illustrating interesting interplay between fading and localization errors.

1.2.2 Co-Optimization Along a Fixed Trajectory

As is established, energy resource of a mobile robot is typically very limited. Thus, a robot needs to efficiently plan the usage of its limited energy for its motion, communication, sensing and computation during the operation. Among these, it is reported that motion and communication are two major consumers [34]. While individual optimization of communication and motion energy consumption has been heavily but separately

explored in the communications/networking [79–83] and robotics literature [84–93], co-optimization of communication and motion energy consumption has received little attention so far. In [34], the authors proposed an efficient algorithm to find the path that minimizes the motion and communication energy costs. In [52], the authors proposed algorithms to optimize the relay configuration in a data-intensive wireless sensor network, in order to minimize the total communication and motion energy costs of the sensors. In [53], the authors designed an algorithm to maximize the lifetime of the wireless sensor network, while considering both the communication and motion costs of the sensors. In [54], the authors proposed an optimal control approach to minimize the communication and motion energy costs in a one-dimensional robotic router network.

However, simplified path-loss-only models are utilized to model the communication channels in the aforementioned papers. This motivates us to investigate how realistic communication channels will affect the communication and motion design of the robotic systems, when minimizing the total energy cost, *including both the communication and motion energy costs*. Hence, in our second scenario, we consider the case where a mobile robot is tasked with sending a fixed number of given bits of information to a remote station in a limited operation time, as it travels along a pre-defined trajectory. We aim to design both the motion and communication strategies of the robot in a realistic fading environment that experiences channel fading. We are interested in mathematically understanding when/to what extend it is beneficial for the robot to spend its energy on motion and when/to what extend it is more beneficial to spend its energy on communication (or when to do both). Note that this scenario is related to the first and third applications mentioned in Section 1.1.

Contributions

We propose a motion and communication co-optimization framework that allows the robot to schedule its motion speed, transmission rate and stop time along the pre-defined trajectory, while minimizing its overall energy consumption and satisfying a target BER. Such a planning approach, in realistic fading environments, requires a prediction of the link quality at places over the pre-defined trajectory that have not yet been visited by the robot. We show how the probabilistic channel prediction framework allows the robot to predict the shadowing and path loss components of the channel over the trajectory and plan its motion and communication strategies accordingly. In particular, we prove that in order to save energy, the robot should move faster (slower) and send fewer (more) bits at the locations that have worse (better) predicted channel quality. We furthermore prove that if the robot must stop, it should then stop only once and at the location with the best predicted channel quality. We also mathematically characterize two special scenarios, namely the heavy-task load and the light-task load cases, in order to have a better understanding of the optimum strategy.

The aforementioned optimization framework is a one-time planning at the beginning of the operation. As the robot moves along the trajectory, it can measure the true value of the channel and fine tune its strategy accordingly. Along this line, we also propose an additional stop-time online adaptation strategy to further optimize the stop location as the robot moves along its trajectory and measures the true value of the channel. For this case, we show that the problem can be posed as a nested form of multi-stage stochastic program, whose global optimum solution we mathematically characterize.

Finally, we show how to extend our results to the case of online data gathering, where the robot needs to collect information from a number of Points of Interest (POIs) along its trajectory and transmit them to the remote station. Our simulation results show that

our proposed framework results in a considerable performance improvement.

1.2.3 Co-Optimization With Trajectory Planning

Mobile robots can navigate the workspace to actively look for places that are good for communication and/or sensing. Hence, in our third scenario, we extend the previous case and integrate the trajectory design into the whole optimization framework. More specifically, we consider the problem where a mobile robot needs to visit a number of POIs in a workspace, gather their generated bits of information (time-invariant quantities), and transmit the collected bits to a remote station. Similar to the previous case, the robot has to operate in a realistic communication environment. It further needs to minimize the total energy consumption, *including both motion and communication energy costs*, and finish the gathering/transmission task successfully in a given limited time, and under a reception quality constraint. We are then interested in the co-optimization of the communication and motion strategies of the robot such that it finds the optimal trajectory and optimally plans its communication and motion strategies, which include motion speed, stop times, communication transmission rate and power.

This considered scenario is related to data muling and vehicle routing literature [22, 39–41]. In such problems, a number of robots are utilized to visit a number of POIs and collect their information. The main problem is then how to plan the paths of the robots or coordinate their sensing. Proper connectivity maintenance based on realistic link metrics as well as co-optimization of energy resources, however, have not been considered in this context. In [35, 55], the authors developed a communication-aware dynamic coverage framework that deploys a group of mobile agents to periodically cover a number of time-varying POIs. However, the emphasis was on persistent information collection, as opposed to deviating from the main trajectory for better connectivity. Furthermore,

no theories were developed for the case where there could be transmissions along the whole trajectory. Another class of related problems is utilizing mobile sinks/relays to prolong the lifetime of a sensor network [42, 56–60]. In such problems, the main focus is typically on designing new algorithms to jointly optimize the mobility of the sinks/relays and the routing protocols of the networks. However, most of the work uses simplified path-loss-only models for communication.

Contributions

It is a common assumption that motion costs more than communication and therefore it is always better to increase the transmit power of a robot instead of moving to a spot that is better for communication. In this scenario, we first develop a framework that mathematically characterizes if and under what condition (as a function of communication and motion parameters) this assumption is correct by co-optimizing the usage of both communication and motion energy costs. We refer to this as the "To Go or Not To Go" problem and characterize key properties of it as part of our whole setup.

Based on these findings, we then solve the overall problem of finding the optimal trajectory that covers all the POIs and adapting the corresponding optimal communication and motion strategies (transmission rate/power, motion speed and stop times) along the whole trajectory for successful task accomplishment under resource constraints. Since the overall problem becomes considerably challenging, we assume that the route between each two POIs is pre-defined. Then, we show how this problem can be posed as a Mixed Integer Linear Program (MILP) and characterize several key properties of the co-optimized communication and motion solution. For instance, among other properties, we derive conditions under which the optimal trajectory (i.e. the optimal order to visit all the POIs) becomes the minimum-length one as well as conditions under which the trajectory can deviate considerably from the minimum-length one to end at the location with

the highest channel quality in the workspace. We also show that, between each two POIs, the robot should send faster at the regions where the predicted channel quality is higher. Moreover, should the robot stop, it should only stop at the points where the predicted channel quality is better than the remaining part of the optimal trajectory. Overall, our derived mathematical conditions are functions of both the motion and communication parameters, including motion power cost, predicted channel quality, the number of bits that needs to be sent and the given time budget, and clearly show the interplay between communication and motion.

Similar to the previous scenario, we mainly focus on the initial planning of the robot. However, the same framework can be applied for online adaptation as the robot better learns its environment during the operation. More specifically, the robot can re-solve our proposed optimization framework, with updated model parameters, after visiting each POI. The computational complexity of a continuous optimal online adaptation, however, could be considerable. Thus, we also propose a simpler sub-optimal online strategy to adapt to the initial uncertainty of channel learning.

Finally, our simulation results with real channel and motion parameters confirm the analysis and show considerable energy saving.

1.2.4 Clustering and Path Planning Strategies for Robotic Data Collection

In the wireless sensor network literature, one application of mobile robots is to harvest data from a wireless sensor network [60, 94–97]. In such a scenario, the sensors can be scheduled to transmit information bits to a mobile robot when it gets closer to them, resulting in a smaller communication cost. Along this line, various approaches have been proposed for addressing different issues such as path planning and speed control of the

mobile robots [94, 95, 97]. Visiting each individual sensor, however, can result in long latencies and high motion energy consumption.

Clustering is another popular approach for energy saving [98,99]. In such a framework, the sensors are grouped into a number of clusters with an elected cluster head to manage the data collection in its corresponding cluster. However, each cluster head may need to incur high energy to process and forward the gathered information bits to a remote station.

Naturally, the ideas of clustering and using mobile robots for data collection can be integrated to overcome their individual shortcomings. More specifically, mobile robots can considerably reduce the communication burden of the sensors in each cluster by moving close to the corresponding cluster to collect the data. At the same time, clustering can reduce the motion burden of the robot as it only needs to collect data from one point in the cluster, rather than visiting each sensor individually. Along this line, a number of heuristic approaches have been proposed [100–103]. These approaches, however, do not consider realistic fading communication channels. Furthermore, [100–102] do not consider motion cost of the robot. [103], on the other hand, considers the motion cost but does not consider trajectory design, assuming fixed trajectories.

In Chapter 6, we consider a scenario where a mobile robot is tasked with periodically collecting up-to-date data from a wireless sensor network. Our goal is to minimize the total energy cost of the system, including the motion cost of the robot and the communication cost of the sensors to the robot in realistic fading environments. We propose an efficient strategy that jointly optimizes the clustering and path planning of the robot by using space-filling curves. More specifically, the robot first groups the sensors into a number of clusters. A stop position is then chosen in each cluster for the robot to collect the data from the sensors in the corresponding cluster. The robot then periodically visits all the stop positions and gathers the data from the network. As before, we consider

communication over realistic fading links and utilize the probabilistic channel assessment framework.

Contributions

The main challenge of the considered problem is that we need to jointly optimize the number of clusters, the clustering strategy, the stop positions, and the path and motion strategy of the robot. As we shall see, this becomes a mixed integer nonlinear program which is difficult to solve. We then propose a computationally-efficient approach to solve this problem by using space-filling curves [104]. More specifically, by utilizing space-filling curves and their locality property, we show how the coupled clustering, stop position selection, path planning and motion strategy design problems can be solved sub-optimally but very efficiently as a series of convex optimization problems. Using space-filling curves not only results in an efficient systematic design but also allows us to derive an upper bound on the total energy consumption of the operation, relating it to key motion, communication, and system parameters. For instance, the bound shows how the resulting number of clusters is related to the communication and motion parameters of the network. We start our analysis by considering the case where the sensors are uniformly distributed in the workspace and then extend it to the case of non-uniformly-distributed sensors. Finally, our simulation results, with real channel and motion parameters, confirm that considerable energy saving can be achieved as compared to the case of no clustering.

1.3 Organization

The rest of the dissertation is organized as follows. In Chapter 2, we review the channel prediction framework that allows the robot to predict the channel quality at

unvisited locations based on a small number of a priori-collected channel samples in the same environment [69, 70]. We then discuss the communication and motion models that will be used in this dissertation. Chapter 3 solves the robotic router formation problem in realistic communication environments. In Chapter 4, we propose how to co-optimize communication and motion strategies along a fixed trajectory. Chapter 5 then extends this scenario and integrates the trajectory design into the co-optimization framework. In Chapter 6, we focus on joint clustering and path planning for robotic data collection in realistic communication environments, where we propose computationally-efficient strategies based on using space-filling curves. Finally, we conclude in Chapter 7.

Chapter 2

Backgrounds

As discussed in Chapter 1, over-simplified channel models do not suffice to model realistic wireless channels in multi-robotic systems. Hence, in this chapter, we first summarize the work of [69, 70] which proposes the probabilistic channel prediction framework that allows the robot to predict the channel quality at unvisited locations based on a small number of a priori-collected channel samples in the same environment. We shall see that the commonly used disk model is a special case of the general probabilistic channel prediction framework, and that assuming disk models can result in a considerable performance degradation in realistic scenarios. We then discuss two communication metrics, namely Bit Error Rate (BER) and communication power/energy, that will be used in this dissertation. Finally, we present the motion energy models. We start from the most complete model which includes the impact of both acceleration and velocity of the robot. We then show two simplified motion models that only take the velocity into account.

2.1 Probabilistic Channel Prediction Framework

As shown in the communication literature [105], the received Channel to Noise Ratio (CNR) can be modeled as a multi-scale random process with three components: path loss, shadow fading (shadowing) and multipath fading. The slowest dynamic, path loss, is associated with the signal attenuation due to the distance-dependent power falloff. Shadowing is a faster variation because of the blocking objects between the transmitter and receiver. Finally, multipath fading is an even faster variation caused by the multiple replicas of the transmitted signal arrive at the receiver due to the reflections and scatterings from the surrounding objects. Fig. 1.1 shows a set of real channel data with three different channel dynamics marked [68].

Let $\gamma(q, q_b)$ denote the received CNR in the transmission from the robot at position q to the remote station at position q_b. By using a 2D non-stationary random field model, we have the following characterization for $\gamma(q, q_b)$ (in dB):

$$\gamma_{\mathrm{dB}}(q, q_b) = \alpha_{\mathrm{PL,dB}} - 10\, n_{\mathrm{PL}} \log_{10}\left(\|q - q_b\|\right) + \gamma_{\mathrm{SH}}(q, q_b) + \gamma_{\mathrm{MP}}(q, q_b), \tag{2.1}$$

where $\gamma_{\mathrm{dB}}(q, q_b) = 10 \log_{10}\left(\gamma(q, q_b)\right)$, $\alpha_{\mathrm{PL,dB}}$ and n_{PL} are the path loss parameters, and $\gamma_{\mathrm{SH}}(q, q_b)$ and $\gamma_{\mathrm{MP}}(q, q_b)$ are independent random variables representing the effects of shadowing and multipath fading in dB, respectively [105]. In this part, we briefly summarize how the robot can probabilistically assess the spatial variations of the instantaneous received CNR, using a small number of a priori CNR measurements in the same environment.[1]

Let $\mathcal{Q} = \left\{q_1, \cdots, q_{m_\mathcal{Q}}\right\}$ denote the set of the positions corresponding to the small

[1]Note that the a priori CNR measurements can be collected in the environment before the operation by using a mobile robot (or a robotic team). With the prevalence of smartphones, it is also possible to get the data from the history of the locations of the smartphone users and their corresponding received signal quality.

number of the a priori CNR measurements available to the robot, where $m_{\mathcal{Q}}$ represents the total number of a priori samples. The stacked vector of the received CNR measurements (in dB) can then be expressed by $Y_{\mathcal{Q}} = H_{\mathcal{Q}}\theta_{\rm PL} + \omega_{\rm SH,\mathcal{Q}} + \omega_{\rm MP,\mathcal{Q}}$, where $H_{\mathcal{Q}} = [\mathbf{1}_{m_{\mathcal{Q}}} \ -D_{\mathcal{Q}}]$, $\mathbf{1}_{m_{\mathcal{Q}}}$ denotes the $m_{\mathcal{Q}}$-dimensional vector of all ones, $D_{\mathcal{Q}} = \big[10\log_{10}(\|q_1 - q_b\|)\cdots 10\log_{10}(\|q_{m_{\mathcal{Q}}} - q_b\|)\big]^{\rm T}$, $\theta_{\rm PL} = [\alpha_{\rm PL,dB} \ \ n_{\rm PL}]^{\rm T}$, $\omega_{\rm SH,\mathcal{Q}} = \big[\gamma_{\rm SH}(q_1,q_b)\cdots\gamma_{\rm SH}(q_{m_{\mathcal{Q}}},q_b)\big]^{\rm T}$ and $\omega_{\rm MP,\mathcal{Q}} = \big[\gamma_{\rm MP}(q_1,q_b) \ \cdots \ \gamma_{\rm MP}(q_{m_{\mathcal{Q}}},q_b)\big]^{\rm T}$. Based on the commonly-used lognormal distribution for shadowing and its reported exponential spatial correlation [105], $\omega_{\rm SH,\mathcal{Q}}$ is a zero-mean Gaussian random vector with the covariance matrix $\Omega_{\mathcal{Q}} \in \mathbb{R}^{m_{\mathcal{Q}}\times m_{\mathcal{Q}}}$, where $\big[\Omega_{\mathcal{Q}}\big]_{i,j} = \xi^2_{\rm dB}\exp(-\|q_i - q_j\|/\beta)$ for $i,j \in \{1,\cdots,m_{\mathcal{Q}}\}$, with $\xi^2_{\rm dB}$ and β denoting the variance of the shadowing component in dB and its decorrelation distance, respectively. Let $\rho^2_{\rm dB}$ represent the power of multipath fading component (in dB) and $I_{m_{\mathcal{Q}}}$ be the $m_{\mathcal{Q}}$-dimensional identity matrix. We have the following lemma for estimating the underlying model parameters:

Lemma 1 ([69, 70]) *Define $\chi^2_{\rm dB} \triangleq \xi^2_{\rm dB} + \rho^2_{\rm dB}$. Then, the Least Square (LS) estimation of the channel parameters is given as follows:*

$$\begin{aligned}
\hat{\theta}_{\rm PL} &= (H_{\mathcal{Q}}^{\rm T}H_{\mathcal{Q}})^{-1}H_{\mathcal{Q}}^{\rm T}Y_{\mathcal{Q}},\\
\hat{\chi}^2_{\rm dB} &= \frac{1}{m_{\mathcal{Q}}}Y_{H_{\mathcal{Q}}}^{\rm T}Y_{H_{\mathcal{Q}}},\\
\hat{\theta}_{\rm SH} &= (J_{\mathcal{Q}}^{\rm T}W J_{\mathcal{Q}})^{-1}J_{\mathcal{Q}}^{\rm T}W\varsigma,\\
\hat{\rho}^2_{\rm dB} &= \hat{\chi}^2_{\rm dB} - \hat{\xi}^2_{\rm dB},
\end{aligned}$$

where $Y_{H_{\mathcal{Q}}} = \big(I_{m_{\mathcal{Q}}} - H_{\mathcal{Q}}(H_{\mathcal{Q}}^{\rm T}H_{\mathcal{Q}})^{-1}H_{\mathcal{Q}}^{\rm T}\big)Y_{\mathcal{Q}}$ and $\hat{\theta}_{\rm SH} = \big[\ln(\hat{\xi}^2_{\rm dB}) \ \ 1/\hat{\beta}\big]^{\rm T}$. Furthermore, $J_{\mathcal{Q}} = \big[\mathbf{1}_{|\mathcal{L}_{\mathcal{Q}}|} \ \ -G_{\mathcal{Q}}\big]$, $G_{\mathcal{Q}} = \big[l_1 \ \cdots \ l_{|\mathcal{L}_{\mathcal{Q}}|}\big]^{\rm T}$ and $\varsigma = \big[\ln(\hat{r}(l_1)) \ \cdots \ \ln(\hat{r}(l_{|\mathcal{L}_{\mathcal{Q}}|}))\big]^{\rm T}$, where $\hat{r}(l) = \big(\sum_{(i,j)\in\mathcal{A}(l)}\big[Y_{H_{\mathcal{Q}}}\big]_i\big[Y_{H_{\mathcal{Q}}}\big]_j\big)/|\mathcal{A}(l)|$ is the numerical estimation of the spatial correlation at distance l, with $\mathcal{A}(l) = \big\{(i,j) \ \big| \ q_i, q_j \in \mathcal{Q}, \big\|q_i - q_j\big\| = l\big\}$, and

$\mathcal{L}_{\mathcal{Q}} = \{l \mid 0 < \hat{r}(l) < \hat{\chi}^2_{\mathrm{dB}}\} = \{l_1, \cdots, l_{|\mathcal{L}_{\mathcal{Q}}|}\}$ *is the ordered set of acceptable possible distances among the samples. Finally,* W *is a constant weight matrix that can be chosen based on the assessment of the accuracy of the estimation of* $\hat{r}(l)$*.*

Then, based on the measurements available to the robot and conditioned on the channel parameters, the assessment of the received CNR at an unvisited position q is given by the following lemma:

Lemma 2 ([69, 70]) *A Gaussian random variable,* $\Upsilon_{\mathrm{dB}}(q, q_b)$*, with mean*

$$\begin{aligned}\overline{\Upsilon}_{\mathrm{dB}}(q, q_b) &= \mathbb{E}\big\{\gamma_{\mathrm{dB}}(q, q_b) \,\big|\, Y_{\mathcal{Q}}, \theta_{\mathrm{PL}}, \beta, \xi_{\mathrm{dB}}, \rho_{\mathrm{dB}}\big\} \\ &= \underbrace{H_q\, \theta_{\mathrm{PL}}}_{\textit{predicted path loss}} + \underbrace{\Psi^{\mathrm{T}}_{\mathcal{Q}}(q)\Phi^{-1}_{\mathcal{Q}}\big(Y_{\mathcal{Q}} - H_{\mathcal{Q}}\theta_{\mathrm{PL}}\big)}_{\textit{predicted shadowing}}, \end{aligned} \tag{2.2}$$

and variance

$$\begin{aligned}\sigma^2_{\mathrm{dB}}(q, q_b) &= \mathbb{E}\Big\{\big(\gamma_{\mathrm{dB}}(q, q_b) - \overline{\Upsilon}_{\mathrm{dB}}(q, q_b)\big)^2 \,\Big|\, Y_{\mathcal{Q}}, \theta_{\mathrm{PL}}, \beta, \xi_{\mathrm{dB}}, \rho_{\mathrm{dB}}\Big\} \\ &= \xi^2_{\mathrm{dB}} + \rho^2_{\mathrm{dB}} - \Psi^{\mathrm{T}}_{\mathcal{Q}}(q)\Phi^{-1}_{\mathcal{Q}}\Psi_{\mathcal{Q}}(q), \end{aligned} \tag{2.3}$$

can best characterize the path loss and shadowing components of CNR at q*, where* $H_q = \big[1 \;\; -10\log_{10}(\|q - q_b\|)\big]$*,* $\Phi_{\mathcal{Q}} = \Omega_{\mathcal{Q}} + \rho^2_{\mathrm{dB}} I_{m_{\mathcal{Q}}}$ *and* $\Psi_{\mathcal{Q}}(q) = \xi^2_{\mathrm{dB}}\big[\exp(-\|q - q_1\|/\beta) \cdots \exp(-\|q - q_{m_{\mathcal{Q}}}\|/\beta)\big]^{\mathrm{T}}$*.*

Then, the robot substitutes the estimated parameters of the channel (acquired from Lemma 1) in $\overline{\Upsilon}_{\mathrm{dB}}(q, q_b)$ and $\sigma^2_{\mathrm{dB}}(q, q_b)$ of Lemma 2 to assess the variations of the CNR in the workspace. We refer to $\overline{\Upsilon}_{\mathrm{dB}}(q, q_b)$ and $\sigma^2_{\mathrm{dB}}(q, q_b)$ as the predicted mean value and the prediction error variance, respectively. Essentially, this channel prediction framework models the wireless channel as a non-stationary Gaussian random process. Then, the CNR at an unvisited location can be predicted by conditioning on the available a priori

measurements in the same environment. It should be noted that this framework does not attempt to predict the multipath fading component of the channel since it typically decorrelates very fast. It rather assumes an uncorrelated Gaussian $\omega_{\mathrm{MP},\mathcal{Q}}$. The readers are referred to [69, 70] for more details on the performance of this framework with real data and in different environments.

When the predicted shadowing component of the channel is uncorrelated, i.e. $\beta \to 0$, it is easy to see that (2.2) and (2.3) can be simplified as follows:

$$\overline{\Upsilon}_{\mathrm{dB}}(q, q_b) = H_q\, \theta_{\mathrm{PL}}, \tag{2.4}$$

$$\sigma^2_{\mathrm{dB}}(q, q_b) = \xi^2_{\mathrm{dB}} + \rho^2_{\mathrm{dB}} = \chi^2_{\mathrm{dB}}. \tag{2.5}$$

In this case, the predicted mean value $\overline{\Upsilon}_{\mathrm{dB}}(q, q_b)$ only contains the path loss component, while the prediction error variance, $\sigma^2_{\mathrm{dB}}(q, q_b)$, contains the total channel variance, including both shadowing and multipath fading components. In practice, this could happen when the shadowing component of the channel is negligible as compared to the multipath fading component.

From (2.4) and (2.5), we can also see that the commonly used path-loss-only model in the literature is a special case when $\sigma^2_{\mathrm{dB}}(q, q_b) = 0$. Clearly, path-loss-only models completely ignore the impact of channel fading and, as a result, may cause significant performance degradation. In Chapter 3, we shall compare the performance of other more sophisticated channel prediction models to the path-loss-only one in the context of robotic router formation, in order to see the benefit of this probabilistic channel prediction framework.

2.2 Communication Models

Bit Error Rate (BER) characterizes the probability that a bit arrives in error (flipped) at the receiver and has been used extensively to characterize communication performance in the communication literature [105]. Another fundamental parameter that characterizes the performance of a communication channel is the received Signal to Noise Ratio (SNR). Received Signal to Noise Ratio is defined as the ratio of the received signal power divided by the receiver thermal noise power. The instantaneous received SNR directly impacts the BER and as a result the reception quality. Received SNR is proportional to CNR: received SNR equals to CNR times the transmit power.

BER shows how the received SNR, modulation, channel coding and other transmission parameters affect the performance [105]. As a result, a general expression for BER does not exist. Consider communication between a transmitter and receiver. Let b and $\hat{b}$ represent a transmitted bit (as part of a transmitted packet) and its reception (after passing through a decision device) respectively. Then, BER is defined as $p_b = \text{Prob}\{\hat{b} \neq b\}$. For an Additive White Gaussian Noise (AWGN) channel, BER can be represented or finely approximated by a Q function or an exponential function. In [105], a general approximation (an upper bound) for the BER of an M-ary Quadrature Amplitude Modulation (M-QAM) transmission is derived as follows:[2]

$$p_b \approx 0.2 \exp\left(-\frac{1.5}{M-1}\gamma_{\text{SNR}}(q,q_b)\right) = 0.2 \exp\left(-\frac{1.5}{M-1}\widetilde{P}_{\text{C}}\gamma(q,q_b)\right), \qquad (2.6)$$

where M is the modulation constellation size, $\widetilde{P}_{\text{C}}$ is the transmit power and $\gamma_{\text{SNR}}(q,q_b)$ denotes the received SNR. This approximation is tight (within 1 dB) for $M \geq 4$ and $0\,\text{dB} < \gamma_{\text{dB,SNR}}(q,q_b) < 30\,\text{dB}$. In this dissertation, we use this approximation to characterize BER of each reception.

[2]M-QAM is a common class of modulation in the communication literature.

Given a target BER, $p_{b,\text{th}}$, we can also find the minimum required transmit power based on (2.6) as follows:

$$\widetilde{P}_{\text{C}}(q, q_b) = \frac{M-1}{K\gamma(q, q_b)} = \frac{2^R - 1}{K\gamma(q, q_b)}, \tag{2.7}$$

where $K = -1.5/\ln(5p_{b,\text{th}})$, and $R = \log_2(M)$ denotes the spectral efficiency (transmission rate divided by bandwidth). As a result, the communication energy cost is given by:

$$\widetilde{E}_{\text{C}}(q, q_b) = \widetilde{P}_{\text{C}}(q, q_b)t_{\text{tr}} = \frac{M-1}{K\gamma(q, q_b)}t_{\text{tr}} = \frac{2^R - 1}{K\gamma(q, q_b)}t_{\text{tr}}, \tag{2.8}$$

where t_{tr} denotes the transmission time.

As shown in the previous section, since we are predicting the channel quality probabilistically, the anticipated communication energy cost $\widetilde{E}_{\text{C}}(q, q_b)$ becomes a random variable as well. We then take the average of $\widetilde{E}_{\text{C}}(q, q_b)$ (over the predicted channel) as our communication cost. Hence, we have

$$\begin{aligned} E_{\text{C}}(q, q_b) &= \mathbb{E}\left\{\widetilde{E}_{\text{C}}(q, q_b)\right\} = \mathbb{E}\left\{\widetilde{P}_{\text{C}}(q, q_b)\right\} t_{\text{tr}} \\ &= P_{\text{C}}(q, q_b)t_{\text{tr}} = \frac{2^R - 1}{K}\mathbb{E}\left\{\frac{1}{\Upsilon(q, q_b)}\right\} t_{\text{tr}}, \end{aligned} \tag{2.9}$$

where $P_{\text{C}}(q, q_b) = \big((2^R - 1)/K\big)\mathbb{E}\{1/\Upsilon(q, q_b)\}$ and $E_{\text{C}}(q, q_b)$ are the average communication power and average communication energy respectively, and $\Upsilon(q, q_b) = 10^{\Upsilon_{\text{dB}}(q,q_b)/10}$ denotes the predicted channel quality in the non-dB domain.

In addition to moving to a better place for connectivity, the robot can also optimize its average communication cost based on the predicted channel quality if it is allowed to adapt its spectral efficiency and transmission time. We next discuss a general adaptive rate extension for (2.9). Assume that R can be chosen from a set of integers $\mathcal{R} = \{R^0, R^1, \cdots, R^{n_r}\}$, where $0 = R^0 < R^1 < \cdots < R^{n_r}$ and n_r is the number of possible

non-zero spectral efficiencies for transmission. Then, given the target BER, the minimum required communication power for transmission with a spectral efficiency R^ℓ, for $\ell \in \{0, \cdots, n_r\}$, can be characterized as

$$\widetilde{P}_{\mathrm{C},\ell}(q, q_b) = \frac{2^{R^\ell} - 1}{K\gamma(q, q_b)}, \tag{2.10}$$

Note that the transmitter does not send any bits when $R = R^0$. As a result, we have $\widetilde{P}_{\mathrm{C},0}(q, q_b) = 0$. Then, the total communication energy cost of (2.8) can be generalized as:

$$\widetilde{E}_{\mathrm{C}}(q, q_b) = \sum_{\ell=1}^{n_r} \widetilde{P}_{\mathrm{C},\ell}(q, q_b) t_{\mathrm{tr},\ell}, \tag{2.11}$$

where $t_{\mathrm{tr},\ell}$ represents the communication time of using spectral efficiency R^ℓ. Similar to (2.9), we have

$$\begin{aligned} E_{\mathrm{C}}(q, q_b) &= \mathbb{E}\left\{\widetilde{E}_{\mathrm{C}}(q, q_b)\right\} = \sum_{\ell=1}^{n_r} \mathbb{E}\left\{\widetilde{P}_{\mathrm{C},\ell}(q, q_b)\right\} t_{\mathrm{tr},\ell} \\ &= \sum_{\ell=1}^{n_r} P_{\mathrm{C},\ell}(q, q_b) t_{\mathrm{tr},\ell} = \sum_{\ell=1}^{n_r} \frac{2^{R^\ell} - 1}{K} \mathbb{E}\left\{\frac{1}{\Upsilon(q, q_b)}\right\} t_{\mathrm{tr},\ell}, \end{aligned} \tag{2.12}$$

when R is subject to an integer constraint and $P_{\mathrm{C},\ell}(q, q_b) = \big((2^{R^\ell} - 1)/K\big)\mathbb{E}\{1/\Upsilon(q, q_b)\}$. In this case, the robot can adapt its spectral efficiency by choosing $t_{\mathrm{tr},\ell}$s.

Remark 1 *In this dissertation, we say the predicted channel quality is good (or bad) if* $\mathbb{E}\{1/\Upsilon(q, q_b)\}$ *is small (or large). From Section 2.1,* $\Upsilon(q, q_b)$ *is a lognormal random variable. Then, it is straightforward to show that*

$$\mathbb{E}\left\{\frac{1}{\Upsilon(q, q_b)}\right\} = \exp\left(\left(\frac{\ln 10}{10}\right)^2 \frac{\sigma^2_{\mathrm{dB}}(q, q_b)}{2}\right) \frac{1}{\overline{\Upsilon}(q, q_b)}, \tag{2.13}$$

where $\overline{\Upsilon}(q, q_b) = 10^{\overline{\Upsilon}_{\mathrm{dB}}(q, q_b)/10}$. *Therefore, the robot has a better predicted channel quality*

if the corresponding predicted mean value ($\overline{\Upsilon}(q, q_b)$) is relatively large and/or the prediction error variance ($\sigma^2_{\mathrm{dB}}(q, q_b)$) is relatively small. This is, in particular, a good measure of assessing the link quality. It not only takes into account the predicted mean value but also considers how much the robot trusts its prediction.

2.3 Motion Models

In this dissertation, we assume that the robot uses a DC motor for its motion. Then, the general motion power cost of the robot can be characterized as follows [87]:

$$P_{\mathrm{M}} = \begin{cases} \kappa_1 v^2 + \kappa_2 v + \kappa_3 u^2 + \kappa_4 + \kappa_5 u + \kappa_6 uv, & \text{if } v \neq 0 \text{ or } u \neq 0, \\ 0, & \text{if } v = 0 \text{ and } u = 0, \end{cases} \tag{2.14}$$

where P_{M} is the motion power cost, v and u denote the velocity and acceleration of the robot, respectively, and κ_i, for $i \in \{1, \cdots, 6\}$, are positive constants depending on the parameters of the motor, external load and the mechanical transmission system of the robot.

If the initial and final velocities of the robot are both zero when traveling from one position to another, we can neglect the last two terms in P_{M} when calculating the motion energy cost of the robot [87]. Then, the motion energy cost for traveling along a trajectory with length d, given a motion time t_{mo}, can be found by solving the following optimal

control problem:

$$\text{minimize} \quad \int_0^{t_{\text{mo}}} (\kappa_1 v^2 + \kappa_2 v + \kappa_3 u^2 + \kappa_4) d\tau = \int_0^{t_{\text{mo}}} (\kappa_1 v^2 + \kappa_3 u^2) d\tau + \kappa_2 d + \kappa_4 t_{\text{mo}} \tag{2.15}$$

$$\begin{aligned} \text{subject to} \quad & \dot{q} = v, \quad q(0) = 0, \quad q(t_{\text{mo}}) = d, \\ & \dot{v} = u, \quad v(0) = 0, \quad v(t_{\text{mo}}) = 0, \end{aligned}$$

where q denotes the position of the robot, $q(0) = 0$ and $q(t_{\text{mo}}) = d$ denote the initial and terminal positions of the robot, respectively, and $v(0) = 0$ and $v(t_{\text{mo}}) = 0$ are the initial and terminal velocities of the robot, respectively. Here, the control input we need to optimize is u. Note that for a fixed t_{mo}, equation (2.15) can be solved analytically by using the standard optimal control theory [106]. After several steps of calculations, we then have the following optimal control law:

$$u^\star(\tau) = \theta_1 \exp\left(\sqrt{\frac{\kappa_1}{\kappa_3}}\tau\right) + \theta_2 \exp\left(-\sqrt{\frac{\kappa_1}{\kappa_3}}\tau\right), \tag{2.16}$$

where

$$\begin{aligned} \theta_1 &= \frac{\sqrt{\frac{\kappa_1}{\kappa_3}} d}{\left(2\sqrt{\frac{\kappa_3}{\kappa_1}} - t_{\text{mo}}\right) \exp\left(\sqrt{\frac{\kappa_1}{\kappa_3}} t_{\text{mo}}\right) - 2\sqrt{\frac{\kappa_3}{\kappa_1}} - t_{\text{mo}}}, \\ \theta_2 &= -\theta_1 \exp\left(\frac{\kappa_1}{\kappa_3} t_{\text{mo}}\right). \end{aligned}$$

It can be shown that the optimal motion cost is then as follows:

$$E_{\mathrm{M}}(d, t_{\mathrm{mo}}) = \frac{\kappa_1 d^2}{t_{\mathrm{mo}} - 2\sqrt{\frac{\kappa_3}{\kappa_1}} \frac{\exp\left(\sqrt{\kappa_1/\kappa_3} t_{\mathrm{mo}}\right) - 1}{\exp\left(\sqrt{\kappa_1/\kappa_3} t_{\mathrm{mo}}\right) + 1}} + \kappa_2 d + \kappa_4 t_{\mathrm{mo}}. \tag{2.17}$$

We skip the details of the calculations for brevity. Note that $\lim_{t_{\mathrm{mo}} \to 0} E_{\mathrm{M}}(d, t_{\mathrm{mo}}) = \infty$ if $d > 0$. For convenience, we then define $E_{\mathrm{M}}(d, t_{\mathrm{mo}}) = \infty$ for the case where $t_{\mathrm{mo}} = 0$ and $d > 0$.

The following lemma shows the convexity of $E_{\mathrm{M}}(d, t_{\mathrm{mo}})$ with respect to t_{mo}.

Lemma 3 *$E_{\mathrm{M}}(d, t_{\mathrm{mo}})$ is a convex function of t_{mo} for $t_{\mathrm{mo}} \in (0, \infty)$.*

Proof: We show the convexity of (2.17) by characterizing its second-order derivative. For convenience, define the denominator of the first term of $E_{\mathrm{M}}(d, t_{\mathrm{mo}})$ as g_1. Then, we have $E_{\mathrm{M}}(d, t_{\mathrm{mo}}) = \kappa_1 d^2 / g_1 + \kappa_2 d + \kappa_4 t_{\mathrm{mo}}$. The second-order derivative of $E_{\mathrm{M}}(d, t_{\mathrm{mo}})$ with respect to t_{mo} can be found as follows:

$$\frac{\partial^2 E_{\mathrm{M}}(d, t_{\mathrm{mo}})}{\partial t_{\mathrm{mo}}^2} = \frac{\kappa_1 d^2 (2 g_1'^2 - g_1'' g_1)}{g_1^3}, \tag{2.18}$$

where $2g_1'^2 - g_1'' g_1 = 2g_2(\exp(\sqrt{\kappa_1/\kappa_3} t_{\mathrm{mo}}) - 1)/(\exp(\sqrt{\kappa_1/\kappa_3} t_{\mathrm{mo}}) + 1)^3$ with g_2 defined as $g_2 = \exp(2\sqrt{\kappa_1/\kappa_3} t_{\mathrm{mo}}) - 2\sqrt{\kappa_1/\kappa_3} t_{\mathrm{mo}} \exp(\sqrt{\kappa_1/\kappa_3} t_{\mathrm{mo}}) - 1$. Since

$$g_2' = 2\sqrt{\frac{\kappa_1}{\kappa_3}} \exp\left(\sqrt{\frac{\kappa_1}{\kappa_3}} t_{\mathrm{mo}}\right) \left(\exp\left(\sqrt{\frac{\kappa_1}{\kappa_3}} t_{\mathrm{mo}}\right) - 1 - \sqrt{\frac{\kappa_1}{\kappa_3}} t_{\mathrm{mo}} \right) > 0, \tag{2.19}$$

and $\lim_{t_{\mathrm{mo}} \to 0} g_2 = 0$, we have $g_2 > 0$, for $t_{\mathrm{mo}} \in (0, \infty)$. As a result, we have

$$\frac{\partial^2 E_{\mathrm{M}}(d, t_{\mathrm{mo}})}{\partial t_{\mathrm{mo}}^2} > 0. \tag{2.20}$$

Hence, $E_{\mathrm{M}}(d, t_{\mathrm{mo}})$ is a convex function of t_{mo}, for $t_{\mathrm{mo}} \in (0, \infty)$. ■

While (2.14) is the most general motion model, it is usually complicated to analyze. A simplified motion model is to neglect the impact of acceleration. The motion power can then be characterized as follows [85]:

$$P_{\mathrm{M}} = \kappa_1 v^2 + \kappa_2 v + \kappa_4, \quad \text{for } v \leq v_{\max}, \tag{2.21}$$

where P_{M} is the motion power, v and $v_{\max}$ denote the velocity of the robot and its upper bound respectively. This motion power model does not consider the impact of acceleration since it is negligible for many DC motors [85]. Consider the case where it takes t_{mo} seconds for the robot to travel a fixed length d at a constant velocity of v. Then, we have the following total energy consumption:

$$E_{\mathrm{M}}(d, t_{\mathrm{mo}}) = \underbrace{\frac{\kappa_1 d^2}{t_{\mathrm{mo}}} + \kappa_4 t_{\mathrm{mo}}}_{\widetilde{E}_{\mathrm{M}}(d, t_{\mathrm{mo}})} + \kappa_2 d, \quad \text{for } t_{\mathrm{mo}} \geq d/v_{\max}. \tag{2.22}$$

Note that the velocity only affects $\widetilde{E}_{\mathrm{M}}(d, t_{\mathrm{mo}})$. Also, the first term of $E_{\mathrm{M}}(d, t_{\mathrm{mo}})$ is inversely proportional to t_{mo} while the second term is linear in t_{mo}. Hence, the motion energy cost becomes large if the robot moves too fast or too slow, with the minimum achieved at

$$t_{\mathrm{mo}} = \begin{cases} \sqrt{\kappa_1/\kappa_4}\, d & \text{if } v_{\max} > \sqrt{\kappa_4/\kappa_1}, \\ d/v_{\max} & \text{if } v_{\max} \leq \sqrt{\kappa_4/\kappa_1}, \end{cases} \tag{2.23}$$

or equivalently at

$$v = \begin{cases} \sqrt{\kappa_4/\kappa_1} & \text{if } v_{\max} > \sqrt{\kappa_4/\kappa_1}, \\ v_{\max} & \text{if } v_{\max} \leq \sqrt{\kappa_4/\kappa_1}. \end{cases} \tag{2.24}$$

An simpler motion model is the linear motion model:

$$P_{\mathrm{M}} = \kappa_2 v + \kappa_4, \quad \text{for } v \leq v_{\max}. \tag{2.25}$$

This model is a very good fit to the Pioneer 3DX robot, when the velocity is smaller than 0.9 m/s [86]. Then, the motion energy cost for traveling along a trajectory with length d can be found as follows: $E_{\mathrm{M}}(d, t_{\mathrm{mo}}) = \kappa_2 d + \kappa_4 t_{\mathrm{mo}}$, where $t_{\mathrm{mo}} \geq d/v_{\max}$. Note that $E_{\mathrm{M}}(d, t_{\mathrm{mo}})$ is minimized when $t_{\mathrm{mo}} = d/v_{\max}$, i.e. when the robot travels with its maximum speed. In this case, the motion energy cost becomes

$$E_{\mathrm{M}}(d) = \kappa_{\mathrm{M}} d, \tag{2.26}$$

where $\kappa_{\mathrm{M}} = \kappa_2 + \kappa_4/v_{\max}$.

Chapter 3

Robotic Router Formation

In this chapter, we show how motion can be optimized to improve the communication quality in robotic systems. In particular, we consider a robotic router problem where a group of robotic routers needs to establish a reliable communication link from a transmitter to a receiver that are otherwise too far from each other. More specifically, there is a team of m robots spatially distributed in a given environment. Let node 1 indicate a transmitting node (TX) that needs to send information to node m, the receiving node (RX), which can be considerably far from node 1. The rest of the nodes will act as robotic routers by relaying the information, i.e. they spatially position themselves such that the flow of information is maximized from the transmitting node to the receiving one. Our goal is to find the optimum configuration in realistic communication environments and control the motion of the routers such that they converge to it (given stationary TX/RX). In this chapter, we use the terms 'robot' and 'node' interchangeably to represent all the agents, including the transmitter, the receiver and any router. We use the term 'router' to specifically indicate a robotic router. Furthermore, we consider stationary TX and RX nodes, in order to focus on the optimum configuration and motion planning of the routers

This chapter is an amended version of [107].

with realistic wireless channels and metrics. We, however, note that our framework can be extended to accommodate mobile TX and/or RX.

In this chapter, we use the end-to-end BER of the robotic route network, i.e. the BER at the receiving end node, as the performance metric. Therefore, we are interested in motion planning and optimization of router configuration, as well as characterizing the implication of BER for motion planning and control in realistic communication environments. Moreover, we assume a multihop topology for the robotic router network, i.e. each node relays the information received from its previous node, to the next one, until it reaches the RX node. This topology can be built by using a route discovery scheme from the ad-hoc routing literature, such as Dynamic Source Routing (DSR) [108] or Ad-hoc On-Demand Distance Vector Routing (AODV) [109]. Once a valid route is found, the transmitter will receive a packet containing a summary of the sequence of loop-free hops to the receiver, which can be used to deliver messages. See [108, 109] for more details. Each robot then broadcasts the received message once it receives it from its previous node. This process continues until the message reaches the final destination (receiving node). Our framework then focuses on co-optimizing the motion planning and communication performance metrics of this route. In other words, similar to other work on robotic router motion planning, we do not focus on the layer that corresponds to routing and topology discovery as there is a rich body of work on it in the ad-hoc routing literature. Instead, we focus on the integration of communication issues (physical layer) with motion planning (application layer). While we assume a multihop route in this chapter, our framework can also be extended to other topologies. For instance, in [110], we considered a diversity-based topology in which a node receives multiple copies of the transmitted information from different routers. The framework of this chapter can be extended to such topologies as well. It should be noted that we are not assuming a highly-dense network (such as swarms). Thus, we are not concerned with multiple access issues (such

as interference among the nodes) that can arise when the number of nodes, sharing the given resources, e.g. bandwidth, is considerably large. Then, BER is primarily affected by signal attenuation and fading rather than congestion and interference.

The rest of this chapter is organized as follows. In Section 3.1, we review different channel predictors that will be used based on the channel prediction framework introduced in Section 2.1. In Sections 3.2 and 3.3, we propose and extensively analyze our robotic router optimization framework. We further show the performance of the proposed framework and compare with the state-of-the-art. In Section 3.4, we look at the the robotic router optimization problem from the angle of power optimization and characterize the corresponding properties. Finally, in Section 3.5, we show real experimental results to further verify the effectiveness of our framework.

3.1 Overview of Different Channel Predictors

In this chapter, we shall characterize the properties of different channel predictors and compare their performance. We start from the case where we only predict the path loss component of the channel without considering the impact of channel fading (known as path-loss-only model in the literature). From the discussions in Section 2.1, we then have

$$\overline{\Upsilon}_{\mathrm{dB}}(q, q_b) = \overline{\Upsilon}_{\mathrm{dB,Det,PL}}(q, q_b) = \alpha_{\mathrm{PL,dB}} - 10\, n_{\mathrm{PL}} \log_{10}\left(\|q - q_b\|\right), \tag{3.1}$$

$$\sigma^2_{\mathrm{dB}}(q, q_b) = \sigma^2_{\mathrm{dB,Det,PL}}(q, q_b) = 0, \tag{3.2}$$

where $\overline{\Upsilon}_{\mathrm{dB,Det,PL}}(q, q_b)$ and $\sigma^2_{\mathrm{dB,Det,PL}}(q, q_b)$ denote the predicted path loss component of the channel and its prediction error variance respectively. We refer to this predictor as the *Deterministic Path Loss Predictor* which will serve as a benchmark for performance

comparisons.

Next, we consider the case of uncorrelated shadowing. We have

$$\overline{\Upsilon}_{\mathrm{dB}}(q, q_b) = \overline{\Upsilon}_{\mathrm{dB,Prob,PL}}(q, q_b) = \alpha_{\mathrm{PL,dB}} - 10\, n_{\mathrm{PL}} \log_{10}\big(\|q - q_b\|\big), \tag{3.3}$$

$$\sigma^2_{\mathrm{dB}}(q, q_b) = \sigma^2_{\mathrm{dB,Prob,PL}}(q, q_b) = \chi^2_{\mathrm{dB}}. \tag{3.4}$$

We refer to this predictor as the *Probabilistic Path Loss Predictor*. As compared to the *Deterministic Path Loss Predictor*, it also takes shadowing and multipath fading into account but assumes uncorrelated shadowing. Next, we consider the *Deterministic Path Loss/Shadowing Predictor*:

$$\begin{aligned}\overline{\Upsilon}_{\mathrm{dB}}(q, q_b) &= \overline{\Upsilon}_{\mathrm{dB,Det,PL/SH}}(q, q_b) \\ &= \alpha_{\mathrm{PL,dB}} - 10\, n_{\mathrm{PL}} \log_{10}\big(\|q - q_b\|\big) + \Psi^{\mathrm{T}}_{\mathcal{Q}}(q)\Phi^{-1}_{\mathcal{Q}}\big(Y_{\mathcal{Q}} - H_{\mathcal{Q}}\theta_{\mathrm{PL}}\big),\end{aligned} \tag{3.5}$$

$$\sigma^2_{\mathrm{dB}}(q, q_b) = \sigma^2_{\mathrm{dB,Det,PL/SH}}(q, q_b) = 0, \tag{3.6}$$

and the *Probabilistic Path Loss/Shadowing Predictor*:

$$\begin{aligned}\overline{\Upsilon}_{\mathrm{dB}}(q, q_b) &= \overline{\Upsilon}_{\mathrm{dB,Prob,PL/SH}}(q, q_b) \\ &= \alpha_{\mathrm{PL,dB}} - 10\, n_{\mathrm{PL}} \log_{10}\big(\|q - q_b\|\big) + \Psi^{\mathrm{T}}_{\mathcal{Q}}(q)\Phi^{-1}_{\mathcal{Q}}\big(Y_{\mathcal{Q}} - H_{\mathcal{Q}}\theta_{\mathrm{PL}}\big),\end{aligned} \tag{3.7}$$

$$\sigma^2_{\mathrm{dB}}(q, q_b) = \sigma^2_{\mathrm{dB,Prob,PL/SH}}(q, q_b) = \xi^2_{\mathrm{dB}} + \rho^2_{\mathrm{dB}} - \Psi^{\mathrm{T}}_{\mathcal{Q}}(q)\Phi^{-1}_{\mathcal{Q}}\Psi_{\mathcal{Q}}(q), \tag{3.8}$$

where $\overline{\Upsilon}_{\mathrm{dB,Det,PL/SH}}(q, q_b)$ and $\overline{\Upsilon}_{\mathrm{dB,Prob,PL/SH}}(q, q_b)$ denote the predicted mean values, and $\sigma^2_{\mathrm{dB,Det,PL/SH}}(q, q_b)$ and $\sigma^2_{\mathrm{dB,Prob,PL/SH}}(q, q_b)$ represent the corresponding prediction error variances. Note that both predictors take the shadowing correlation into account. The difference is that the latter also takes the prediction error variance into account.

As mentioned in Section 2.1, the previous channel predictors cannot predict the mul-

tipath fading component. In order to take advantage of the rapid variations of multipath fading, after the routers converge to a configuration based on the planning using the previous *Probabilistic Path Loss/Shadowing Predictor*, it can jitter around a small local area, in order to gather additional measurements on multipath fading, and finds the optimum position based on the new samples. We refer to this approach as the *Probabilistic Path Loss/Shadowing Predictor with jitter*.

It is straightforward to see that the channel predictors above are ordered from the most simplified model to the most complete one. As such, we expect that the performance improves as the model becomes more complete, which will be verified by the results of the following sections. This comes at the cost of an increase in the computation. As the communication modeling gets more complete, it requires more information to build the corresponding correlation functions (not that much more though). Consequently, building the correlation functions increases the computation. For instance, if we only know the channel a priori at a couple of locations, then it may be harder to develop the *Probabilistic Path Loss/Shadowing Predictor* as compared to the *Probabilistic Path Loss Predictor*. The routers can also start with a more simplified approach and switch to a better one as they gather more channel samples. Fig. 3.1 compares the performance and computational complexity of different predictors.

3.2 Robotic Router Optimization Considering only Path Loss

In this section, we start by developing the foundation of robotic router optimization using BER as a metric by considering only the path loss component of the channel. This analysis will then serve as a benchmark for our derivations in the subsequent sections,

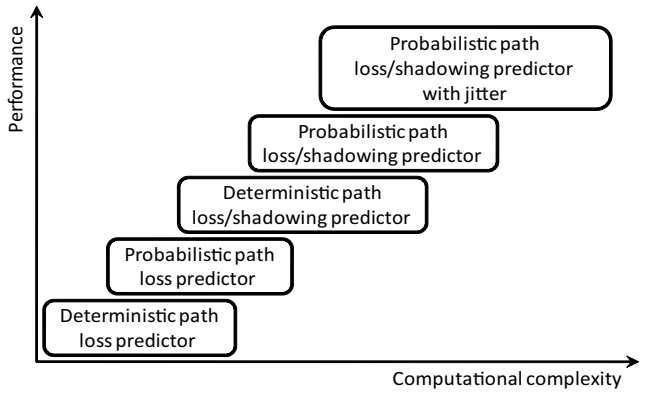

Figure 3.1: Summary of the performance and computational complexity of different predictors.

where we take fading into account.

3.2.1 Objective Function

Based on the *Deterministic Path Loss Predictor*, we have the following model for the received SNR in the transmission from the i^{th} robot to the j^{th} one:

$$\overline{\Upsilon}_{\text{SNR,Det,PL}}(q_i, q_j) = \overline{\Upsilon}_{\text{SNR,Det,PL},i,j} = \frac{\alpha_{\text{SNR,PL},i,j}}{\|q_i - q_j\|^{n_{\text{PL}}}} = \frac{\alpha_{\text{SNR,PL},i,j}}{d_{i,j}^{n_{\text{PL}}}}, \tag{3.9}$$

where q_i and q_j are the positions of robots i and j respectively, $d_{i,j} = \|q_i - q_j\|$ is the distance between robots i and j, $\alpha_{\text{SNR,PL},i,j}$ and n_{PL} are the path loss parameters, and $\overline{\Upsilon}_{\text{SNR,Det,PL}}(q_i, q_j)$ and $\overline{\Upsilon}_{\text{SNR,Det,PL},i,j}$ are the predicted SNR of the *Deterministic Path Loss Predictor*. Note that $\overline{\Upsilon}_{\text{SNR,Det,PL},i,j} = P_{\text{C},i}\overline{\Upsilon}_{\text{Det,PL},i,j}$ and $\alpha_{\text{SNR,PL},i,j} = P_{\text{C},i}\alpha_{\text{PL},i,j}$, where $P_{\text{C},i}$ is the transmit power of robot i, $\alpha_{\text{PL},i,j} = 10^{\alpha_{\text{PL,dB},i,j}/10}$, and $\alpha_{\text{PL,dB},i,j}$ is defined in (2.1). Also, note that the channel is considered deterministic in this case.

Without loss of generality, we label the robots as follows: node 1 represents the transmitter, node 2 represents the node that directly receives the information from the transmitter, and so on. Then, we have the following approximated expression, for the

probability of correct reception, at the receiving end node:

$$p_c(\text{RX}) \approx p_c(\{m\}|\{m-1\})p_c(\{m-1\}) \approx \prod_{i=2}^{m} p_c(\{i\}|\{i-1\}), \tag{3.10}$$

where $p_c(\{i\})$ represents the probability of correct reception of a bit at node i, and $P_c(\{i\}|\{i-1\})$ denotes the conditional probability of correct reception of a bit at the i^{th} node, given correct reception at node $i-1$. Assume that M-QAM modulation is used for communication between the robots. By combining (2.6) and (3.10), we have the following objective function to maximize:[1]

$$p_c(\text{RX}) = \prod_{i=2}^{m} \left(1 - 0.2 \, \exp\left(-c\overline{\Upsilon}_{\text{SNR,Det,PL},i-1,i}\right)\right), \tag{3.11}$$

where $c = 1.5/(M-1)$. Then the goal of the routers is to position themselves such that $p_c(\text{RX})$ is maximized.

Remark 2 *The approximation of (3.11) is based on only considering correct receptions, i.e. if a bit gets flipped a number of times but is correctly received at the end, we do not consider such a case as a correct reception. As a result, the approximation of (3.11) becomes a lower bound on* $p_c(\text{RX})$*. The approximation can also be justified by considering the fact that the probability of one bit flip is typically low (less than* 10^{-3}*). As a result, the probability of more than one flip is typically negligible, which also justifies the approximation of (3.11).*

Remark 3 *Note that as* $d_{i-1,i} \to 0$*,* $1 - 0.2 \exp(-c\overline{\Upsilon}_{\text{SNR,Det,PL},i-1,i}) \to 1$*, and*

$$\frac{\partial(1 - 0.2 \exp(-c\overline{\Upsilon}_{\text{SNR,Det,PL},i-1,i}))}{\partial d_{i-1,i}} \to 0. \tag{3.12}$$

[1]Note that $p_c(\text{RX}) = 1 - p_b(\text{RX})$, where $p_b(\text{RX})$ is the BER of the receiving node.

Hence, we define $1 - 0.2\ \exp(-c\overline{\Upsilon}_{\mathrm{SNR,Det,PL},i-1,i}) = 1$ *and*

$$\frac{\partial(1 - 0.2\ \exp(-c\overline{\Upsilon}_{\mathrm{SNR,Det,PL},i-1,i}))}{\partial d_{i-1,i}} = 0, \tag{3.13}$$

if $d_{i-1,i} = 0$. *Then,* $p_c(\mathrm{RX})$ *is continuously differentiable in its domain.*

3.2.2 Optimum Configuration of Robotic Routers

Define $q = [q_1^{\mathrm{T}}\ q_2^{\mathrm{T}}\ \cdots\ q_m^{\mathrm{T}}]^{\mathrm{T}}$ and $q_r = [q_2^{\mathrm{T}}\ q_3^{\mathrm{T}}\ \cdots\ q_{m-1}^{\mathrm{T}}]^{\mathrm{T}}$. Moreover, we assume that all the robotic routers are first-order systems: $\dot{q}_i = v_i$, for $i \in \{2, \cdots, m-1\}$. Let $\mathcal{W} \subset \mathbb{R}^2$ denote the valid workspace of the robots. Then, we have the following optimization problem (over q_r) by considering the objective function of (3.11):

$$\begin{aligned} &\text{maximize} \quad J(q_r) = \sum_{i=2}^{m} \ln\left(1 - 0.2\ \exp\left(-c\overline{\Upsilon}_{\mathrm{SNR,Det,PL},i-1,i}\right)\right) \\ &\text{subject to} \quad q_i \in \mathcal{W}, \quad \forall\ i \in \{2, \cdots, m-1\}, \end{aligned} \tag{3.14}$$

where $\overline{\Upsilon}_{\mathrm{SNR,Det,PL},i-1,i} = \alpha_{\mathrm{SNR,PL},i-1,i}/d_{i-1,i}^{n_{\mathrm{PL}}}$ and $d_{i-1,i} = \|q_{i-1} - q_i\|$, for $i \in \{2, \cdots, m\}$.

Lemma 4 *If*

$$n_{\mathrm{PL}} + 1 \leq \min_i \left\{ \frac{n_{\mathrm{PL}} c\overline{\Upsilon}_{\mathrm{SNR,Det,PL},i-1,i}}{1 - 0.2\ \exp(-c\overline{\Upsilon}_{\mathrm{SNR,Det,PL},i-1,i})} \right\} \tag{3.15}$$

all the time, then the optimization problem of (3.14) is concave for a convex $\mathcal{W}$.

Proof: Let $J_i(q_r) = \ln(1 - 0.2\ \exp(-c\overline{\Upsilon}_{\mathrm{SNR,Det,PL},i-1,i}))$ and

$$\eta_{i-1,i} = \frac{\partial \overline{\Upsilon}_{\mathrm{SNR,Det,PL},i-1,i}}{\partial d_{i-1,i}} \nabla_{q_i} d_{i-1,i}.$$

Then, for $\forall\ i \in \{2, \cdots, m-1\}$:

$$\begin{aligned}\nabla^2_{q_i} J_i = &\left(\frac{\partial^2 J_i}{\partial \overline{\Upsilon}^2_{\text{SNR,Det,PL},i-1,i}} + \frac{\partial J_i}{\partial \overline{\Upsilon}_{\text{SNR,Det,PL},i-1,i}} \frac{n_{\text{PL}}+1}{n_{\text{PL}}\,\overline{\Upsilon}_{\text{SNR,Det,PL},i-1,i}}\right)\eta_{i-1,i}\eta^{\text{T}}_{i-1,i} \\ &+ \frac{\partial J_i}{\partial \overline{\Upsilon}_{\text{SNR,Det,PL},i-1,i}} \frac{1}{n_{\text{PL}}\,\overline{\Upsilon}_{\text{SNR,Det,PL},i-1,i}}(\eta_{i-1,i}\eta^{\text{T}}_{i-1,i} - \|\eta_{i-1,i}\|^2 I_2) \\ \preceq &\left(\frac{\partial^2 J_i}{\partial \overline{\Upsilon}^2_{\text{SNR,Det,PL},i-1,i}} + \frac{\partial J_i}{\partial \overline{\Upsilon}_{\text{SNR,Det,PL},i-1,i}} \frac{n_{\text{PL}}+1}{n_{\text{PL}}\,\overline{\Upsilon}_{\text{SNR,Det,PL},i-1,i}}\right)\eta_{i-1,i}\eta^{\text{T}}_{i-1,i}.\end{aligned} \tag{3.16}$$

Furthermore, it can be shown that $\nabla^2_{q_{i-1}} J_i = \nabla^2_{q_i} J_i = -\nabla_{q_{i-1}} \nabla_{q_i} J_i$ for $\forall\ i \in \{3, \cdots, m-1\}$. Let $\psi_i = \nabla^2_{q_i} J_i$ and $\psi'_{m-1} = \nabla^2_{q_{m-1}} J_m$. We have, $\nabla^2_{q_i} J = \sum_{j=i}^{i+1} \psi_j$ if $i \in \{2, \cdots, m-2\}$, and $\nabla^2_{q_i} J = \psi_{m-1} + \psi'_{m-1}$ if $i = m-1$, which results in the following Hessian Matrix $H = \nabla^2_{q_r} J$:

$$H = \begin{bmatrix} \sum_{j=2}^{3} \psi_j & -\psi_3 & 0 & \cdots & 0 \\ -\psi_3 & \sum_{j=3}^{4} \psi_j & -\psi_4 & \cdots & 0 \\ \vdots & \vdots & \vdots & \ddots & \vdots \\ 0 & 0 & 0 & -\psi_{m-1} & \psi_{m-1} + \underbrace{\psi'_{m-1}}_{=\psi_m} \end{bmatrix}. \tag{3.17}$$

We can then write H as a sum of matrices H_i such that the nonzero blocks of each H_i are only related to ψ_i. It is then easy to show that a sufficient condition to make (3.17) negative semidefinite is to force all ψ_is to be negative semidefinite for $i \in \{2, \cdots, m\}$. From (3.16), this means that

$$\frac{\partial^2 J_i}{\partial \overline{\Upsilon}^2_{\text{SNR,Det,PL},i-1,i}} + \frac{\partial J_i}{\partial \overline{\Upsilon}_{\text{SNR,Det,PL},i-1,i}} \frac{n_{\text{PL}}+1}{n_{\text{PL}}\,\overline{\Upsilon}_{\text{SNR,Det,PL},i-1,i}} \leq 0, \tag{3.18}$$

for all i, or

$$n_{\mathrm{PL}} + 1 \leq \min_i \left\{ \frac{n_{\mathrm{PL}} c \overline{\Upsilon}_{\mathrm{SNR,Det,PL},i-1,i}}{1 - 0.2 \, \exp(-c \overline{\Upsilon}_{\mathrm{SNR,Det,PL},i-1,i})} \right\}. \tag{3.19}$$

■

Remark 4 *One way to ensure the condition of Lemma* 4 *is to enforce*

$$\min_i \left\{ \overline{\Upsilon}_{\mathrm{SNR,Det,PL},i-1,i} \right\} \geq \frac{n_{\mathrm{PL}} + 1}{n_{\mathrm{PL}} c} = \frac{(M-1)(n_{\mathrm{PL}} + 1)}{1.5 n_{\mathrm{PL}}}, \tag{3.20}$$

which is a stronger condition. This condition implies that all the robots need to maintain a minimum received SNR. This requirement increases as the modulation constellation size (M*) increases. However, since* M *is usually around* $4 \sim 8$*, it should be easy to satisfy this condition most of the time. For instance, for real channel measurements of Fig. 3.8, the estimated path loss exponent is* $\hat{n}_{\mathrm{PL}} = 2.32$*. Then, the sufficient condition of Lemma 4 is satisfied if* $\min_i \left\{ \overline{\Upsilon}_{\mathrm{SNR,Det,PL},i-1,i} \right\} \geq 4.57$ dB *for* $M = 4$*.*

We then propose the following control law:

$$v_i = \kappa \nabla_{q_i} J(q_r) = \kappa \left(\frac{\partial J_i(q_r)}{\partial d_{i-1,i}} \frac{q_i - q_{i-1}}{d_{i-1,i}} + \frac{\partial J_{i+1}(q_r)}{\partial d_{i,i+1}} \frac{q_i - q_{i+1}}{d_{i,i+1}} \right), \tag{3.21}$$

where κ is a positive constant and J_i is as defined in Lemma 4. Then the system will converge to the optimum configuration asymptotically under the condition of Lemma 4. Since the control input v_i only depends on the information of node i and the nodes in its vicinity, control of motion can be implemented in a decentralized way.

Next, we characterize some of the properties of the optimum solution for the optimization problem of (3.14).

Lemma 5 *In the absence of obstacles, the global optimum of (3.14) is achieved when all the routers stand on the line segment between* q_1 *and* q_m*.*

Proof: Assume that the robotic routers have reached the optimal configuration but they are not on the line between the transmitter and receiver. It can be easily seen that by projecting all the q_is to the line that passes through q_1 and q_m, the transmission distances will get smaller, resulting in a higher $p_c(\mathrm{RX})$. If any projection falls out of the line segment between q_1 and q_m, there is always a position on the line segment that results in a lower BER. Therefore, the global optimum can only be achieved when all the routers stand on the line segment between q_1 and q_m. ■

Remark 5 *Note that Lemma 5 holds for any objective function that is a decreasing function of $d_{i-1,i}$ for $i \in \{2, \cdots, m\}$.*

Based on Lemma 5, we have the following simplified optimization problem, in the absence of obstacles:

$$\begin{aligned} \text{maximize} \quad & J(d) = \sum_{i=2}^{m} \ln(1 - 0.2 \exp(-c\overline{\Upsilon}_{\mathrm{SNR,Det,PL},i-1,i})) \\ \text{subject to} \quad & d_{i-1,i} \geq 0, \ \forall\, i \in \{2, \cdots, m\}, \quad \mathbf{1}_{m-1}^{\mathrm{T}} d = D, \end{aligned} \tag{3.22}$$

where $d = [d_{1,2}\ d_{2,3}\ \cdots\ d_{m-1,m}]^{\mathrm{T}}$, $\mathbf{1}_{m-1}$ is the $(m-1)$-dimensional vector with all entries equal to 1, and $D = \|q_1 - q_m\|$.

Lemma 6 *Assume that the concavity condition of Lemma 4 holds. Then, the optimal solution of (3.22) satisfies the following properties:*

1. *if $\alpha_{\mathrm{SNR,PL},i-1,i} > \alpha_{\mathrm{SNR,PL},j-1,j}$, then $d^{\star}_{i-1,i} > d^{\star}_{j-1,j}$,*
2. *if $\alpha_{\mathrm{SNR,PL},i-1,i} = \alpha_{\mathrm{SNR,PL},j-1,j}$, then $d^{\star}_{i-1,i} = d^{\star}_{j-1,j}$,*

where $d^{\star}_{i-1,i}$ is the optimum distance between nodes $i-1$ and i.

Proof: Clearly, the optimization problem of (3.22) is concave if the condition in Lemma 4 holds. Consider the dual function of the primal problem of (3.22):

$$g_J(d,\lambda,\nu)=\sum_{i=2}^{m}J_i(d)-\sum_{i=2}^{m}\lambda_{i-1,i}d_{i-1,i}+\nu(\mathbf{1}_{m-1}^{\mathrm{T}}d-D), \tag{3.23}$$

where $\lambda_{i-1,i}$ and ν are Lagrange multipliers. For a concave optimization problem, the optimal primal and dual solutions satisfy the following Karush-Kuhn-Tucker (KKT) conditions [111]: $\partial J_i(d^\star)/\partial d^\star_{i-1,i}-\lambda^\star_{i-1,i}+\nu^\star=0$; $\lambda^\star_{i-1,i}d^\star_{i-1,i}=0$; $d^\star_{i-1,i}\geq 0$; $\lambda^\star_{i-1,i}\geq 0$; $\mathbf{1}_{m-1}^{\mathrm{T}}d^\star-D=0$, where $d^\star_{i-1,i}$, $\lambda^\star_{i-1,i}$ and $\nu^\star$ are the optimal points. This results in the following required condition:

$$\frac{\partial J_i(d^\star)}{\partial d^\star_{i-1,i}}=\frac{\partial J_j(d^\star)}{\partial d^\star_{j-1,j}}. \tag{3.24}$$

Due to the concavity of the objective function, $\partial J_i(d)/\partial d_{i-1,i}$ is strictly decreasing with respect to $d_{i-1,i}$. It is also straightforward to show that $\partial J_i(d)/\partial d_{i-1,i}$ is strictly increasing with respect to $\alpha_{\mathrm{SNR,PL},i-1,i}$. Therefore, the required condition of (3.24) can only be satisfied when $d^\star_{i-1,i}>d^\star_{j-1,j}$ if $\alpha_{\mathrm{SNR,PL},i-1,i}>\alpha_{\mathrm{SNR,PL},j-1,j}$. Similarly, if $\alpha_{\mathrm{SNR,PL},i-1,i}=\alpha_{\mathrm{SNR,PL},j-1,j}$, equation (3.24) holds if and only if $d^\star_{i-1,i}=d^\star_{j-1,j}$, which completes the proof. ■

Lemma 6 indicates that the routers should be equally spaced between the transmitter and receiver if the transceivers of all the robots are homogenous and all the links have the same underlying path loss parameters.[2] However, if a link experiences a lower $\alpha_{\mathrm{SNR,PL},i-1,i}$ (for instance due to a lower transmit power), then the corresponding nodes of that link should get closer to each other, in order to achieve a better overall performance.

[2]The second condition has to do with the size of the space of operation and its environmental features. For instance, if the operation is over a larger space, then the probability of having the same path loss parameters, over the whole space, is lower.

3.2.3 Motion Planning for the Optimization of Robotic Routers

In the previous section, we characterized the optimum configuration of the routers for different scenarios by mainly assuming a convex workspace (or no environmental constraints in some cases). In this part, we extend our analysis and consider motion planning to achieve the optimum configuration in the presence of obstacles. We extend the control law of (3.21), in order to include obstacle avoidance, using a similar approach in [46]. In this approach, the robotic routers are assumed to operate in a walled environment, which will allow us to add the obstacle avoidance as linear constraints. Let $N_\perp$ represent the outward normal vector of one side of a walled obstacle. Then, the i^{th} router will avoid colliding with that side of the obstacle, by enforcing the following:

$$\langle N_\perp, \dot{q}_i \rangle = \langle N_\perp, v_i \rangle \geq 0. \tag{3.25}$$

We will then have the following optimization problem, by considering the objective function of the previous section, obstacles, and control of motion:

$$\text{maximize} \quad \langle \nabla_{q_r} J, v \rangle \tag{3.26}$$

$$\text{subject to} \quad W_\perp v \geq 0, \tag{3.27}$$

where $W_\perp$ is the collection of all the constraints similar to (3.25) caused by all the obstacles. Hence, at q_r, the routers can first compute $\nabla_{q_r} J$ and $W_\perp$, then find v by solving (3.27). In case of a mobile transmitter or receiver, their dynamics can also be included. The optimization framework of (3.27) basically tries to guide the robots in the direction of the gradient as much as possible, given the constraints of the environment. It can also be implemented in a decentralized manner since each node only needs the information of the nodes in its vicinity. Note that any obstacle can be approximated by

a walled obstacle. However, the computational complexity can go up, depending on the shape of the original obstacle and the required approximation accuracy.

We next compare the performance of our proposed BER approach with that of graph-theoretic approaches, which are commonly used for robotic router optimization. In order to have a compatible setup, we need to translate our SNR model to a link weight between 0 and 1 (which is a common approach in graph-theoretic literature). Consider the following cutoff version of our SNR model:

$$\overline{\Upsilon}_{\mathrm{SNR,Det,PL},i,j}(d_{i,j}) = \begin{cases} \alpha_{\mathrm{SNR,PL},i,j}/\underline{r}^{n_{\mathrm{PL}}} & \text{if } d_{i,j} < \underline{r}, \\ 0 & \text{if } d_{i,j} > \overline{r}, \\ \alpha_{\mathrm{SNR,PL},i,j}/d_{i,j}^{n_{\mathrm{PL}}} & \text{otherwise,} \end{cases} \tag{3.28}$$

where $\underline{r}$ is the saturation distance, $\overline{r}$ is the cutoff distance, and n_{PL} is the path loss exponent. We can then translate this model to link weights as follows:

$$w_{i,j}(d_{i,j}) = \begin{cases} 1 & \text{if } d_{i,j} < \underline{r}, \\ 0 & \text{if } d_{i,j} > \overline{r}, \\ (\underline{r}/d_{i,j})^{n_{\mathrm{PL}}} & \text{otherwise.} \end{cases} \tag{3.29}$$

Consider the case where both the transmitting and receiving nodes are stationary. We next compare the performance of our proposed BER approach with the graph-theoretic approach of [46], in which the Fiedler eigenvalue is maximized (similar comparisons should hold with other eigenvalue-based approaches). The following parameters are used: $\underline{r} = 1$ meter, $\alpha_{\mathrm{SNR,PL},i,j} = 2500$, and $\overline{r} = 35.4$ meters.

Fig. 3.2 and 3.3 show the trajectories of four robots for the cases of minimizing the BER and maximizing the Fiedler eigenvalue respectively. It can be seen that the final robotic router configurations are not the same. To see the end-to-end performance, Fig.

3.4 shows the end-to-end BER of the two approaches. Multihop topology is implemented in both cases. It can be seen that our proposed approach performs considerably better (an order of magnitude) and results in a much smaller BER. The figure further confirms that only considering graph-theoretic metrics may not be suitable for the optimization of robotic routers and that communication-oriented metrics of the end-to-end performance, such as BER, should also be considered.

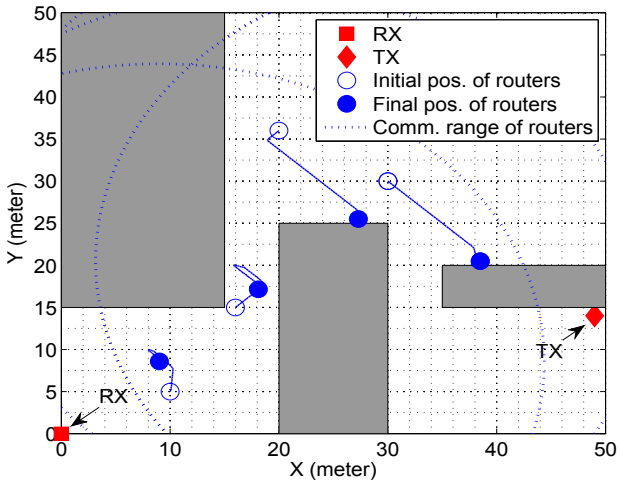

Figure 3.2: Robotic router optimization through minimizing the BER (our proposed approach) – gray areas show the obstacles.

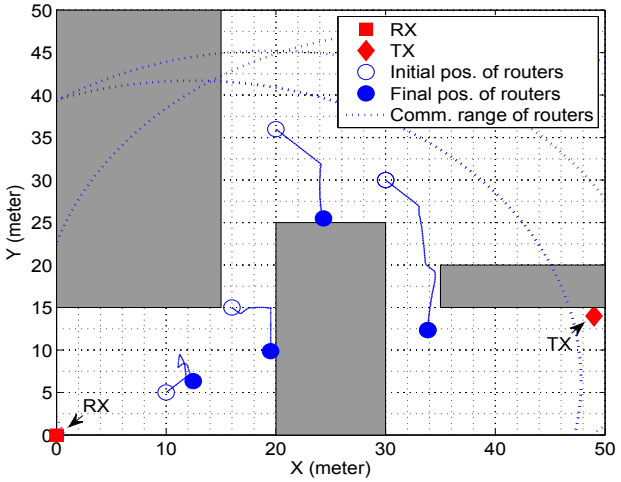

Figure 3.3: Robotic router optimization through maximizing the Fiedler eigenvalue [46] – gray areas show the obstacles.

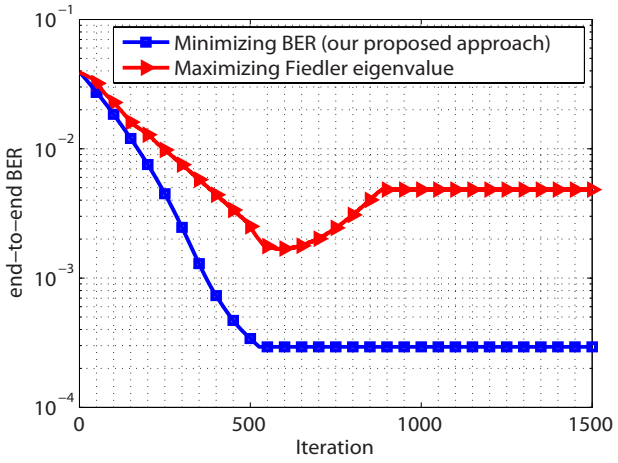

Figure 3.4: Comparison of our proposed approach with the case where Fiedler eigenvalue is maximized – It can be seen that our proposed approach performs considerably better.

3.3 Robotic Router Optimization in Fading Environments

In this part, we propose a framework for robotic router position optimization and motion planning in fading environments and discuss the underlying tradeoffs.

3.3.1 Objective Function

In this part, we derive the objective function when the predicted channel is random, i.e. when we use the *Probabilistic Path Loss/Shadowing Predictor* or the *Probabilistic Path Loss Predictor*. As shown in Section 3.2, our end-to-end performance metric is

$$p_c(\mathrm{RX}) = \prod_{i=2}^{m} \left(1 - 0.2 \exp\left(-c\, 10^{\frac{\Upsilon_{\mathrm{SNR,dB},i-1,i}}{10}}\right)\right), \tag{3.30}$$

where $\Upsilon_{\mathrm{SNR,dB},i-1,i}$ is the predicted SNR from robot $i-1$ to i in the dB domain. In this case, however, $\Upsilon_{\mathrm{SNR,dB},i-1,i}$ is a Gaussian random variable whose mean and variance can be estimated using either the *Probabilistic Path Loss/Shadowing Predictor* or the

Probabilistic Path Loss Predictor. This results in a stochastic $p_c(\text{RX})$. A proper approach common in such cases is to maximize the average of it over the predicted distribution of the channels. This results in the following:

$$\begin{aligned} &\text{maximize} \quad \mathbb{E}\left\{\prod_{i=2}^{m}\left(1-0.2\,\exp\left(-c10^{\frac{\Upsilon_{\text{SNR,dB},i-1,i}}{10}}\right)\right)\right\} \\ &\text{subject to} \quad q_i \in \mathcal{W}, \quad \forall\, i \in \{2,\cdots,m-1\}. \end{aligned} \tag{3.31}$$

While this optimization problem can be solved numerically, we next show how further simplification is also possible. Based on the aforementioned lognormal distribution for fading, the received SNR from the i^{th} node to the j^{th} one is a random variable with the following distribution:

$$p_{\log}(\Upsilon_{\text{SNR},i,j}) = \frac{1}{\sqrt{2\pi}a\sigma_{\text{dB},i,j}\Upsilon_{\text{SNR},i,j}}\exp\left(-\frac{(\Upsilon_{\text{SNR,dB},i,j}-\overline{\Upsilon}_{\text{SNR,dB},i,j})^2}{2\sigma^2_{\text{dB},i,j}}\right), \tag{3.32}$$

where $a = \ln 10/10$, and $\overline{\Upsilon}_{\text{SNR,dB},i,j}$ and $\sigma_{\text{dB},i,j}$ are the mean and standard deviation of $\Upsilon_{\text{SNR,dB},i-1,i}$, respectively. The first and second moments of $\Upsilon_{\text{SNR},i,j}$ can then be found as

$$\mathbb{E}\{\Upsilon_{\text{SNR},i,j}\} = \overline{\Upsilon}_{\text{SNR},i,j}\exp\left(0.5(a\sigma_{\text{dB},i,j})^2\right), \tag{3.33}$$

$$\mathbb{E}\{\Upsilon^2_{\text{SNR},i,j}\} = \overline{\Upsilon}^2_{\text{SNR},i,j}\exp\left(2(a\sigma_{\text{dB},i,j})^2\right), \tag{3.34}$$

respectively. Following [112], we can approximate a lognormal distribution with a gamma distribution, with the same first and second moments:

$$p_{\text{gam}}(\Upsilon_{\text{SNR},i,j}) = \frac{\Upsilon^{\varphi_{i,j}-1}_{\text{SNR},i,j}}{(\vartheta_{i,j}\overline{\Upsilon}_{\text{SNR},i,j})^{\varphi_{i,j}}\Gamma(\varphi_{i,j})}\exp\left(-\frac{\Upsilon_{\text{SNR},i,j}}{\vartheta_{i,j}\overline{\Upsilon}_{\text{SNR},i,j}}\right), \tag{3.35}$$

where $\varphi_{i,j} = (\exp((a\sigma_{\mathrm{dB},i,j})^2) - 1)^{-1}$, $\vartheta_{i,j} = \exp(1.5(a\sigma_{\mathrm{dB},i,j})^2) - \exp(0.5(a\sigma_{\mathrm{dB},i,j})^2)$, and $\Gamma(\cdot)$ represents the gamma function. As $\sigma_{\mathrm{dB},i,j}$ decreases, this approximation becomes better [112]. We then have the following:

$$\begin{aligned}\mathbb{E}\{p_c(\mathrm{RX})\} &= \prod_{i=2}^{m}\left(1 - 0.2\mathbb{E}\left\{\exp\left(-c\,10^{\frac{\Upsilon_{\mathrm{SNR,dB},i-1,i}}{10}}\right)\right\}\right) \\ &= \prod_{i=2}^{m}\left(1 - 0.2\left(1 + c\vartheta_{i-1,i}10^{\frac{\overline{\Upsilon}_{\mathrm{SNR,dB},i-1,i}}{10}}\right)^{-\varphi_{i-1,i}}\right), \end{aligned} \tag{3.36}$$

where the second line can be confirmed using the distribution of (3.35) and after a few lines of derivations. Note that in writing (3.36), we assumed that all the channels are statistically independent, which is an appropriate assumption for several wireless scenarios. We then have the following optimization problem:

$$\begin{aligned}&\text{maximize} \quad \sum_{i=2}^{m}\ln\left(1 - 0.2\left(1 + c\vartheta_{i-1,i}10^{\frac{\overline{\Upsilon}_{\mathrm{SNR,dB},i-1,i}}{10}}\right)^{-\varphi_{i-1,i}}\right) \\ &\text{subject to} \quad q_i \in \mathcal{W}, \quad \forall\, i \in \{2,\cdots,m-1\}.\end{aligned} \tag{3.37}$$

Then, we can use either $\overline{\Upsilon}_{\mathrm{SNR,dB,Prob,PL/SH},i-1,i}$ of (3.7) and $\sigma_{\mathrm{dB,Prob,PL/SH},i-1,i}$ of (3.8) for $\overline{\Upsilon}_{\mathrm{SNR,dB},i-1,i}$ and $\sigma_{\mathrm{dB},i-1,i}$ respectively, or $\overline{\Upsilon}_{\mathrm{SNR,dB,Prob,PL},i-1,i}$ of (3.3) and $\sigma_{\mathrm{dB,Prob,PL},i-1,i}$ of (3.4) for $\overline{\Upsilon}_{\mathrm{SNR,dB},i-1,i}$ and $\sigma_{\mathrm{dB},i-1,i}$ respectively, depending on our channel prediction strategy. Note that we have $\overline{\Upsilon}_{\mathrm{SNR,dB,Prob,PL},i-1,i} = P_{\mathrm{C},i-1}\overline{\Upsilon}_{\mathrm{dB,Prob,PL},i-1,i}$ and $\overline{\Upsilon}_{\mathrm{SNR,dB,Prob,PL/SH},i-1,i} = P_{\mathrm{C},i-1}\overline{\Upsilon}_{\mathrm{dB,Prob,PL/SH},i-1,i}$.

3.3.2 Optimum Configuration of Robotic Routers

In Lemmas 4 and 6, we derived conditions for guaranteeing the optimality of our robotic router optimization framework for the *Deterministic Path Loss Predictor* and showed the properties of the optimum solution. In this section, we first extend Lem-

mas 4 and 6 to fading environments. Specifically, we characterize the properties of the optimization problem of (3.37) for the case of the *Probabilistic Path Loss predictor*, i.e. $\overline{\Upsilon}_{\mathrm{SNR,dB},i-1,i} = \overline{\Upsilon}_{\mathrm{SNR,dB,Prob,PL},i-1,i}$ and $\sigma_{\mathrm{dB},i-1,i} = \sigma_{\mathrm{dB,Prob,PL},i-1,i}$. We then have the following optimization problem:

$$\begin{aligned} &\text{maximize} \quad \overline{J}(q_r) = \sum_{i=2}^{m} \ln(1 - 0.2(1 + c\vartheta_{\mathrm{PL},i-1,i}\overline{\Upsilon}_{\mathrm{SNR,Prob,PL},i-1,i})^{-\varphi_{\mathrm{PL},i-1,i}}) \\ &\text{subject to} \quad q_i \in \mathcal{W}, \quad \forall\, i \in \{2, \cdots, m-1\}, \end{aligned} \tag{3.38}$$

where $\vartheta_{\mathrm{PL},i-1,i} = \exp(1.5(a\sigma_{\mathrm{dB,Prob,PL},i-1,i})^2) - \exp(0.5(a\sigma_{\mathrm{dB,Prob,PL},i-1,i})^2)$ and $\varphi_{\mathrm{PL},i-1,i} = (\exp((a\sigma_{\mathrm{dB,Prob,PL},i-1,i})^2) - 1)^{-1}$.

Lemma 7 *If* $\sigma_{\mathrm{dB,Prob,PL},i-1,i} < \sqrt{\ln(n_{\mathrm{PL}}+1)}/a$ *and*

$$\overline{\Upsilon}_{\mathrm{SNR,Prob,PL},i-1,i} \geq \frac{n_{\mathrm{PL}}+1}{n_{\mathrm{PL}}c}\left(\varphi_{\mathrm{PL},i-1,i}\vartheta_{\mathrm{PL},i-1,i} - \frac{\vartheta_{\mathrm{PL},i-1,i}}{n_{\mathrm{PL}}}\right)^{-1} \tag{3.39}$$

all the time, then the optimization problem of (3.38) is concave for a convex $\mathcal{W}$.

Proof: Let $\overline{J}_i(q_r) = \ln(1 - 0.2(1 + c\vartheta_{\mathrm{PL},i-1,i}\overline{\Upsilon}_{\mathrm{SNR,Prob,PL},i-1,i})^{-\varphi_{\mathrm{PL},i-1,i}})$. Similar to Lemma 4, it is sufficient to force

$$\frac{\partial^2 \overline{J}_i}{\partial \overline{\Upsilon}^2_{\mathrm{SNR,Prob,PL},i-1,i}} + \frac{\partial \overline{J}_i}{\partial \overline{\Upsilon}_{\mathrm{SNR,Prob,PL},i-1,i}} \frac{n_{\mathrm{PL}}+1}{n_{\mathrm{PL}}\overline{\Upsilon}_{\mathrm{SNR,Prob,PL},i-1,i}} \leq 0, \tag{3.40}$$

for all i, to guarantee the concavity, which results in the following sufficient condition:

$$\overline{\Upsilon}_{\mathrm{SNR,Prob,PL},i-1,i} \geq \frac{n_{\mathrm{PL}}+1}{n_{\mathrm{PL}}c}\left(\varphi_{\mathrm{PL},i-1,i}\vartheta_{\mathrm{PL},i-1,i} - \frac{\vartheta_{\mathrm{PL},i-1,i}}{n_{\mathrm{PL}}}\right)^{-1}, \tag{3.41}$$

if $\sigma_{\mathrm{dB,Prob,PL},i-1,i} < \sqrt{\ln(n_{\mathrm{PL}}+1)}/a$. ■

If there is no obstacle on the line segment between the transmitter and receiver, Lemma 5 clearly holds, resulting in the following simplified optimization problem, on the

line segment between the transmitter and receiver:

$$\begin{aligned} &\text{maximize} \quad \overline{J}(d) = \sum_{i=2}^{m} \ln(1 - 0.2(1 + c\vartheta_{\mathrm{PL},i-1,i}\overline{\Upsilon}_{\mathrm{SNR,Prob,PL},i-1,i})^{-\varphi_{\mathrm{PL},i-1,i}}) \\ &\text{subject to} \quad d_{i-1,i} \geq 0, \forall\ i \in \{2, \cdots, m\}, \quad \mathbf{1}_{m-1}^{T} d = D. \end{aligned} \tag{3.42}$$

Lemma 8 *Assume that the concavity condition in Lemma 7 holds. Then, the optimal solution of (3.42) satisfies the following properties:*

1. *if* $\alpha_{\mathrm{SNR,PL},i-1,i} > \alpha_{\mathrm{SNR,PL},j-1,j}$ *and* $\sigma_{\mathrm{dB,Prob,PL},i-1,i} = \sigma_{\mathrm{dB,Prob,PL},j-1,j}$, *then* $d^{\star}_{i-1,i} > d^{\star}_{j-1,j}$,

2. *if* $\alpha_{\mathrm{SNR,PL},i-1,i} = \alpha_{\mathrm{SNR,PL},j-1,j}$,

$$\overline{\Upsilon}_{\mathrm{SNR,Prob,PL},i-1,i} \geq \frac{\exp\left(1.5\exp((a\sigma_{\mathrm{dB,Prob,PL},i-1,i})^2) - 0.5\right) - 1}{c\vartheta_{\mathrm{PL},i-1,i}}, \tag{3.43}$$

$$\overline{\Upsilon}_{\mathrm{SNR,Prob,PL},j-1,j} \geq \frac{\exp\left(1.5\exp((a\sigma_{\mathrm{dB,Prob,PL},j-1,j})^2) - 0.5\right) - 1}{c\vartheta_{\mathrm{PL},j-1,j}} \tag{3.44}$$

   and $\sigma_{\mathrm{dB,Prob,PL},i-1,i} > \sigma_{\mathrm{dB,Prob,PL},j-1,j}$, *then* $d^{\star}_{i-1,i} < d^{\star}_{j-1,j}$,

3. *if* $\alpha_{\mathrm{SNR,PL},i-1,i} = \alpha_{\mathrm{SNR,PL},j-1,j}$ *and* $\sigma_{\mathrm{dB,Prob,PL},i-1,i} = \sigma_{\mathrm{dB,Prob,PL},j-1,j}$, *then* $d^{\star}_{i-1,i} = d^{\star}_{j-1,j}$,

where $d^{\star}_{i-1,i}$ *is the optimum distance between nodes* $i-1$ *and* i.

Proof: Similar to Lemma 6, the optimal solution of (3.42) satisfies the KKT conditions, which results in the following:

$$\frac{\partial \overline{J}_i(d^{\star})}{\partial d^{\star}_{i-1,i}} = \frac{\partial \overline{J}_j(d^{\star})}{\partial d^{\star}_{j-1,j}}. \tag{3.45}$$

Parts 1 and 3 can then be proved similar to Lemma 6. For the proof of Part 2, let $\partial\overline{J}_i/\partial\overline{\Upsilon}_{\mathrm{SNR,Prob,PL},i-1,i} = 0.2c/f_{i-1,i}$, where

$$f_{i-1,i} = \exp\left(-0.5(a\sigma_{\mathrm{dB,Prob,PL},i-1,i})^2\right) \times \left((1+c\vartheta_{\mathrm{PL},i-1,i}\overline{\Upsilon}_{\mathrm{SNR,Prob,PL},i-1,i})^{\varphi_{\mathrm{PL},i-1,i}+1} - 0.2(1+c\vartheta_{\mathrm{PL},i-1,i}\overline{\Upsilon}_{\mathrm{SNR,Prob,PL},i-1,i})\right). \tag{3.46}$$

Then,

$$\frac{\partial f_{i-1,i}}{\partial\sigma_{\mathrm{dB,Prob,PL},i-1,i}} < a^2(1+c\vartheta_{\mathrm{PL},i-1,i}\overline{\Upsilon}_{\mathrm{SNR,Prob,PL},i-1,i})^{\varphi_{\mathrm{PL},i-1,i}+1}\varphi^2_{\mathrm{PL},i-1,i} \times \exp\left(0.5(a\sigma_{\mathrm{dB,Prob,PL},i-1,i})^2\right)\sigma_{\mathrm{dB,Prob,PL},i-1,i} \times \left(3\exp((a\sigma_{\mathrm{dB,Prob,PL},i-1,i})^2) - 1 - 2\ln(1+c\vartheta_{\mathrm{PL},i-1,i}\overline{\Upsilon}_{\mathrm{SNR,Prob,PL},i-1,i})\right). \tag{3.47}$$

Therefore, $\partial f_{i-1,i}/\partial\sigma_{\mathrm{dB,Prob,PL},i-1,i}$ is negative if:

$$\overline{\Upsilon}_{\mathrm{SNR,Prob,PL},i-1,i} \geq \frac{\exp\left(1.5\exp((a\sigma_{\mathrm{dB,Prob,PL},i-1,i})^2) - 0.5\right) - 1}{c\vartheta_{\mathrm{PL},i-1,i}}. \tag{3.48}$$

If (3.48) is satisfied for i and j, then $\partial\overline{J}_i/\partial\overline{\Upsilon}_{\mathrm{SNR,Prob,PL},i-1,i}$ and $\partial\overline{J}_j/\partial\overline{\Upsilon}_{\mathrm{SNR,Prob,PL},j-1,j}$ are monotonically increasing, with respect to $\sigma_{\mathrm{dB,Prob,PL},i-1,i}$ and $\sigma_{\mathrm{dB,Prob,PL},j-1,j}$ respectively. Assume that the optimal solution of (3.42) is $d^\star_{i-1,i} = d^\star_{j-1,j}$ if $\alpha_{\mathrm{SNR,PL},i-1,i} = \alpha_{\mathrm{SNR,PL},j-1,j}$ and $\sigma_{\mathrm{dB,Prob,PL},i-1,i} > \sigma_{\mathrm{dB,Prob,PL},j-1,j}$. Then, $\partial\overline{J}_i(d^\star)/\partial d^\star_{i-1,i} < \partial\overline{J}_j(d^\star)/\partial d^\star_{j-1,j}$. Therefore, equation (3.45) can only be achieved by increasing $\partial\overline{J}_i(d^\star)/\partial d^\star_{i-1,i}$ or equivalently decreasing $\partial\overline{J}_j(d^\star)/\partial d^\star_{j-1,j}$. By the concavity condition, we know that $\partial\overline{J}_i(d)/\partial d_{i-1,i}$ is decreasing with respect to $d_{i-1,i}$. Hence, the optimal configuration is achieved iff $d^\star_{i-1,i} < d^\star_{j-1,j}$. ■

Remark 6 *As compared to the conditions of* $\overline{\Upsilon}_{\mathrm{SNR,Det,PL},i-1,i}$ *in Lemmas* 4 *and 6, the*

sufficient conditions of Lemmas 7 and 8, not only require that the average SNR (distance-dependent path loss) is above a minimum level but also need the variations of fading around this average to be small. As an example, consider the real channel measurements of Fig. 3.8, where the estimated path loss exponent is $\hat{n}_{\mathrm{PL}} = 2.32$*, and standard deviation of fading is* $\sigma_{\mathrm{dB,Prob,PL},i-1,i} = 4.66$*. The first condition of Lemma 7 is then satisfied since* $\sigma_{\mathrm{dB,Prob,PL},i-1,i} < \sqrt{\ln(2.32+1)}/a$*. The second condition of Lemma 7, as well as the second condition of Part 2 of Lemma 8, can further be satisfied if* $\overline{\Upsilon}_{\mathrm{SNR,dB,Prob,PL},i-1,i} \geq$ 13.58 dB*, which, for instance, happens in a continuous area around the transmitter that mounts to 44.6% of the whole basement. Thus, with the proper use of a couple of routers, the required conditions can be satisfied, depending on the initial positions of the routers.*

The first and third parts of Lemma 8 show similar properties to Lemma 6. In fading environments, average BER is also monotonically increasing with $\sigma_{\mathrm{dB,Prob,PL},i-1,i}$, i.e. the fading level of the channel. The second part of Lemma 8 then shows that, in order to compensate for the performance degradation in the links with larger $\sigma_{\mathrm{dB,Prob,PL},i-1,i}$s, the routers should form a configuration in which the distances of those links are smaller.

3.3.3 Performance of the Proposed Robotic Router Optimization Framework

In this part, we show the performance of our proposed 5 strategies of Section 3.1 in fading environments. For all the approaches, the performance measure is the average end-to-end BER. In general, a realistic channel and the resulting optimization problem may have many local maxima (see Fig. 1.1 for example). Hence, there is no general control law to drive the routers to the global optimum even with perfect channel knowledge. Therefore, in our framework, each router uses a localized window search approach to solve the optimization problem iteratively, starting from its initial position. More specifically,

the router uses the proposed channel prediction strategies, in order to calculate the BER and the overall objective function in a local window around its current position, finds the motion direction that maximizes the objective function by searching the local window, and moves one step in that direction. The performance of this approach depends on the window size and channel prediction quality. If the window size is large enough and the prediction quality is good, then the router is more likely to find the global optimum.

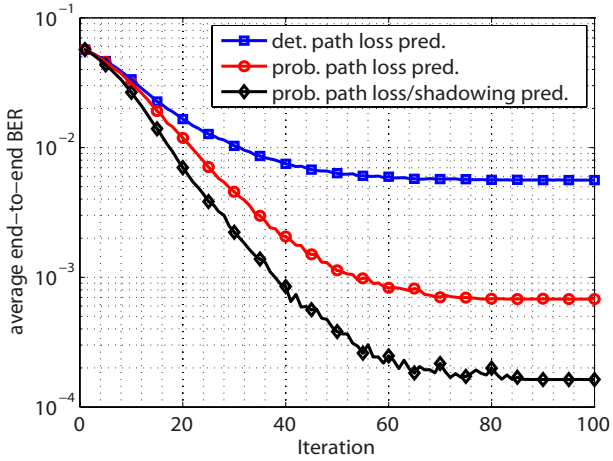

Figure 3.5: Performance of the proposed approaches in optimizing a robotic router network in a fading environment – comparison of the *Deterministic Path Loss Predictor*, *Probabilistic Path Loss predictor* and *Probabilistic Path Loss/Shadowing Predictor*. The channels are generated by the probabilistic channel simulator [68] with $n_{\mathrm{PL}} = 2$, $\xi_{\mathrm{dB}} = 10$ and $\beta = 10$ meters. The multipath fading is generated as uncorrelated Rician fading with parameter $K_{\mathrm{ric}} = 5$. As can be seen, the proposed *Probabilistic Path Loss predictor* and *Probabilistic Path Loss/Shadowing Predictor* perform considerably better.

First, consider the case of one router with no obstacles in the environment and the channel that is generated using the probabilistic channel simulator [68]. Since the performance depends on the initial position of the router and the specific generated channel, we average the performance of each case over several runs of different channel samples (but with the same underlying parameters) as well as random initial router position. Fig. 3.5, 3.6 and 3.7 show the performance of these approaches. In all the cases, the router uses only 5% a priori random channel measurements in the environment, in order to estimate

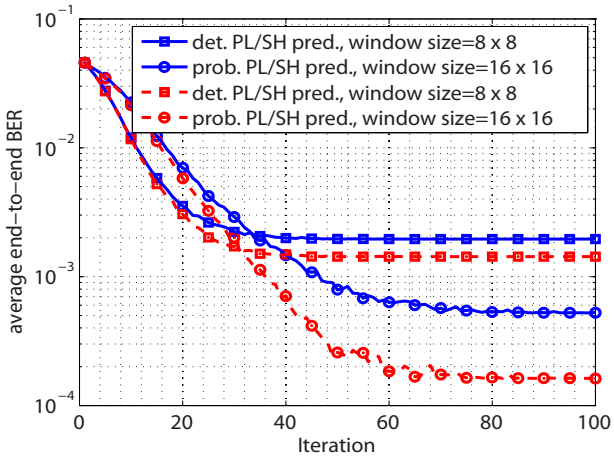

Figure 3.6: Performance of the proposed approaches in optimizing a robotic router network in a fading environment – comparison of the *Deterministic Path Loss Predictor* and *Probabilistic Path Loss/Shadowing Predictor*. The channels are generated by the probabilistic channel simulator [68] with $n_{\mathrm{PL}} = 2$, $\xi_{\mathrm{dB}} = 8$ and $\beta = 10$ meters. The multipath fading is generated as uncorrelated Rician fading with parameter $K_{\mathrm{ric}} = 5$.

the underlying channel parameters.

Fig. 3.5 compares the performance of the *Deterministic Path Loss Predictor*, *Probabilistic Path Loss predictor* and *Probabilistic Path Loss/Shadowing Predictor*, where a local window search size of 16 meters × 16 meters is utilized. The environment is taken to be a square of size 40 meters × 40 meters for all the three figures. As can be seen, the *Deterministic Path Loss Predictor* performs the worst, since it does not account for channel fading. By taking the variance caused by fading into account, the *Probabilistic Path Loss predictor* performs much better (around one order of magnitude). Finally, by considering the channel spatial correlation, the *Probabilistic Path Loss/Shadowing Predictor* performs the best.

Next, Fig. 3.6 compares the performance of the robotic router formation, for the *Deterministic Path Loss/Shadowing Predictor* and *Probabilistic Path Loss/Shadowing Predictor* and two different local window search sizes. As expected, the probabilistic case has a better performance and the improvement increases as the size of the search

window increases.

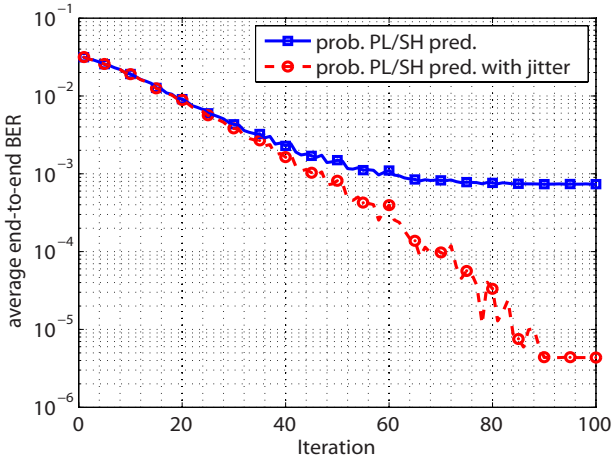

Figure 3.7: Impact of adding jitter to mitigate multipath fading. The channels are generated by the probabilistic channel simulator [68] with $n_{\mathrm{PL}} = 2$, $\xi_{\mathrm{dB}} = 4$ and $\beta = 10$ meters. The multipath fading is generated as uncorrelated Rician fading with parameter $K_{\mathrm{ric}} = 2$.

Finally, Fig. 3.7 shows the performance with the added jitter strategy. The local window search size is 16 meters $\times$ 16 meters, the environment size is 40 meters $\times$ 40 meters and the jitter area is 1.6 meters $\times$ 1.6 meters. Since multipath fading is unpredictable, it can severely degrade the prediction performance. Hence, the router can benefit considerably from the proposed jitter strategy as can be seen.

Next, we show the performance of the proposed framework in the presence of obstacles and by using the parameters of a real channel. We also compare the performance to the existing Fiedler eigenvalue approach. For comparison, we consider a cutoff version of our average SNR model similar to (3.28), which translates to link weights, as described for (3.29). We use the Pioneer robot of Fig. 3.8 (left) to make several measurements. Fig. 3.8 (right) shows a color map of the communication signal strength in the area of interest [68]. Using the proposed approach of Section 2.1, we extract the underlying parameters of the measured channel to be as follows: $\hat{\alpha}_{\mathrm{SNR,PL}} = 3320$, $\hat{n}_{\mathrm{PL}} = 2.32$, $\hat{\xi}^2_{\mathrm{dB}} = 11.68$, $\hat{\beta} = 1.20$ and $\hat{\rho}^2_{\mathrm{dB}} = 9.99$.

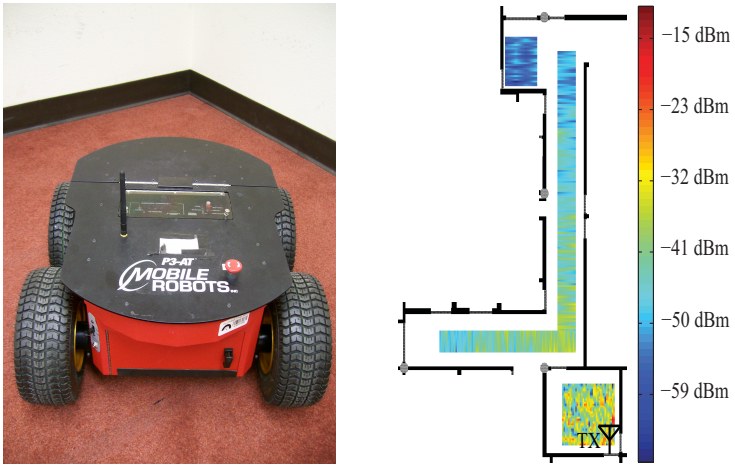

Figure 3.8: Experimental testbed and channel measurements. The left figure shows a Pioneer robot that gathered the measurements, and the right one shows the measured communication signal strength map to the TX marked on the figure.

Then, we simulate the performance of robotic router formation in an environment with the same underlying channel parameters. Fig. 3.9 shows the trajectories of four routers for the case of the *Probabilistic Path Loss predictor* (left) and maximizing the Fiedler eigenvalue (right) respectively. As can be seen, the optimum configurations of the two approaches are different, similar to Fig. 3.2 and 3.3. By maximizing the Fiedler eigenvalue, two nodes almost converge to the same position, which is a waste of the resources. Fig. 3.10 then compares the average BER of the two approaches. Similar to Section 3.2.3, our proposed approach performs considerably better.[3] In Section 3.5, we will further verify the effectiveness of our framework by running a preliminary experiment.

[3]In Fig. 3.9 (right), two routers almost converge to the same location for maximizing the Fiedler eigenvalue approach because of the environmental constraints. The routers will spread out for both cases, if we use 3 routers instead. In this case, the average end-to-end BER for maximizing Fiedler eigenvalue approach is 1.5×10^{-3}, while the average end-to-end BER by using our proposed *Probabilistic Path Loss predictor* approach, is 3.1×10^{-4}. It can be seen that our approach still outperforms considerably.

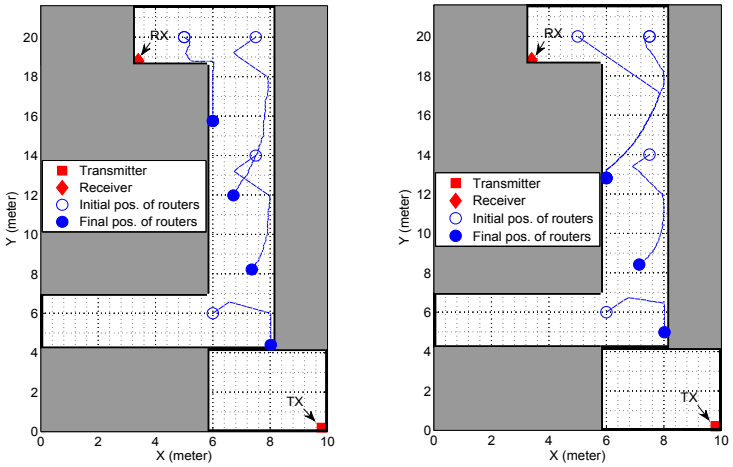

Figure 3.9: Robotic router optimization in a fading environment. The left figure shows the optimum configuration by using the *Probabilistic Path Loss predictor* (our proposed approach) while the right figure shows the optimum configuration by maximizing the Fiedler eigenvalue [46] – gray areas show the obstacles.

3.4 Communication and Motion Power Management in Robotic Routers

In several applications, robotic networks have to work under power constraints. Thus, in this section, we extend our framework and consider the optimization of robotic routers under power constraints. The limited power can be utilized for communication or motion, which results in interesting underlying tradeoffs. The motion and communication costs depend on the scenario. For instance, if the robot is in a bad location in terms of communication, then it may be more cost effective to move as compared to increasing the transmission power. If that is not the case, the motion can cost more. We will explore such tradeoffs in Section 3.4.3. But first we begin by understanding the impact of communication power limitations without considering motion costs in Sections 3.4.1 and 3.4.2. We then extend our analysis to explore the underlying tradeoffs between motion and communication.

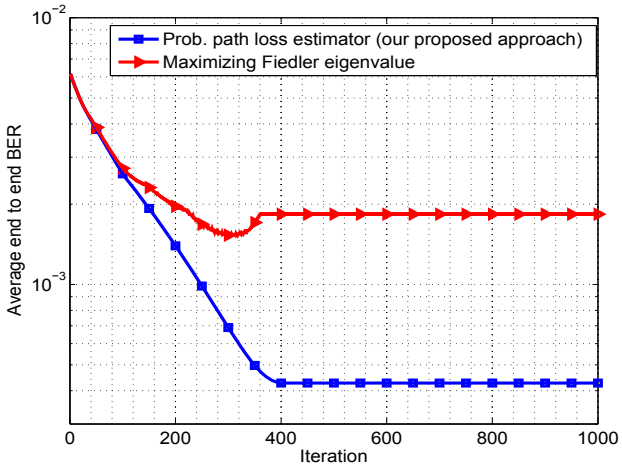

Figure 3.10: Comparison of our proposed approach with the case where Fiedler eigenvalue is maximized in a fading environment – It can be seen that our proposed approach performs considerably better.

3.4.1 Robotic Router Optimization under Transmit Power Constraints Considering Only Path Loss

In the previous sections, we considered the case where the transmit power of each robot was fixed. In this part, we consider the case where each robot can adapt its transmit power. The goal is then to minimize the overall power consumption of the network while maintaining a minimum required reception quality for all the links.

Consider the case where the *Deterministic Path Loss Predictor* is used for channel prediction. Let $p_{b,i-1,i,\text{th}}$ and $p_{b,i-1,i}$ represent the maximum tolerable BER and the true BER in the transmission from node $i-1$ to node i respectively.[4] We require that $p_{b,i-1,i} \leq p_{b,i-1,i,\text{th}}$, for all $i \in \{2, \cdots, m\}$, which results in $\overline{\Upsilon}_{\text{SNR,Det,PL},i-1,i} \geq \overline{\Upsilon}_{\text{SNR},i-1,i,\text{th}}$, where $\overline{\Upsilon}_{\text{SNR},i-1,i,\text{th}}$ is the corresponding SNR threshold using (2.6): $\overline{\Upsilon}_{\text{SNR},i-1,i,\text{th}} = -(M-1)\ln(5p_{b,i-1,i,\text{th}})/1.5$. In this part, we are interested in minimizing the overall transmission power while maintaining the minimum required link quality. For the case of no obstacles, it can be easily confirmed that the optimum solution of this problem also lies on the line

[4]Note that $p_{b,i-1,i,\text{th}}$ should be a function of the total number of nodes, as well as the end-to-end performance requirement, in order to properly utilize the routers.

segment between the transmitter and receiver. We then have the following optimization problem, considering communication power minimization:

$$\begin{aligned} \text{minimize} \quad & J_{\mathrm{RR}}(P_{\mathrm{C}}, d) = \mathbf{1}_{m-1}^{\mathrm{T}} P_{\mathrm{C}} \\ \text{subject to} \quad & \overline{\Upsilon}_{\mathrm{SNR},i-1,i,\mathrm{th}} d_{i-1,i}^{n_{\mathrm{PL}}} \leq \alpha_{\mathrm{PL},i-1,i} P_{\mathrm{C},i-1}, \;\; d_{i-1,i} \geq 0, \; \forall \; i \in \{2, \cdots, m\}, \\ & \mathbf{1}_{m-1}^{\mathrm{T}} d = D, \end{aligned} \tag{3.49}$$

where $P_{\mathrm{C}} = [P_{\mathrm{C},1} \; P_{\mathrm{C},2} \; \cdots \; P_{\mathrm{C},m-1}]^{\mathrm{T}}$, $d = [d_{1,2} \; d_{2,3} \; \cdots \; d_{m-1,m}]^{\mathrm{T}}$, $D = \|q_1 - q_m\|$ and $P_{\mathrm{C},i}$ is the transmit power of node i.

Lemma 9 *The solution to the optimization problem of (3.49) is*

$$d_{i-1,i}^{\star} = \frac{\left(\dfrac{\alpha_{\mathrm{PL},i-1,i}}{\overline{\Upsilon}_{\mathrm{SNR},i-1,i,\mathrm{th}}} \right)^{\frac{1}{n_{\mathrm{PL}}-1}}}{\displaystyle\sum_{j=2}^{m} \left(\dfrac{\alpha_{\mathrm{PL},j-1,j}}{\overline{\Upsilon}_{\mathrm{SNR},j-1,j,\mathrm{th}}} \right)^{\frac{1}{n_{\mathrm{PL}}-1}}} D \tag{3.50}$$

and $P_{\mathrm{C},i-1}^{\star} = \overline{\Upsilon}_{\mathrm{SNR},i-1,i,\mathrm{th}} d_{i-1,i}^{\star n_{\mathrm{PL}}} / \alpha_{\mathrm{PL},i-1,i}$*, for all* $i \in \{2, \cdots, m\}$.

Proof: It can be easily confirmed that the objective function and all the constraints of (3.49) are convex functions of variables d and P_{C}. Consider the dual function of the primal problem:

$$\begin{aligned} g_{J_{\mathrm{RR}}}(P_{\mathrm{C}}, d, \lambda, \mu, \nu) = & \sum_{i=2}^{m} \lambda_{i-1,i} (\overline{\Upsilon}_{\mathrm{SNR},i-1,i,\mathrm{th}} d_{i-1,i}^{n_{\mathrm{PL}}} - \alpha_{\mathrm{PL},i-1,i} P_{\mathrm{C},i-1}) + \mathbf{1}_{m-1}^{\mathrm{T}} P_{\mathrm{C}} \\ & - \sum_{i=2}^{m} \mu_{i-1,i} d_{i-1,i} + \nu (\mathbf{1}_{m-1}^{\mathrm{T}} d - D), \end{aligned} \tag{3.51}$$

where $\lambda_{i-1,i}$, $\mu_{i-1,i}$ and ν are Lagrange multipliers. Therefore, KKT conditions must be

satisfied:

$$\begin{aligned}
1-\lambda^{\star}_{i-1,i}\alpha_{\mathrm{PL},i-1,i}&=0,\\
n_{\mathrm{PL}}\lambda^{\star}_{i-1,i}{d^{\star}_{i-1,i}}^{n_{\mathrm{PL}}-1}\overline{\Upsilon}_{\mathrm{SNR},i-1,i,\mathrm{th}}+\nu^{\star}-\mu^{\star}_{i-1,i}&=0,\\
\lambda^{\star}_{i-1,i}(\overline{\Upsilon}_{\mathrm{SNR},i-1,i,\mathrm{th}}{d^{\star}_{i-1,i}}^{n_{\mathrm{PL}}}-\alpha_{\mathrm{PL},i-1,i}P^{\star}_{\mathrm{C},i-1})&=0,\\
\mu^{\star}_{i-1,i}d^{\star}_{i-1,i}=0,\quad \lambda^{\star}_{i-1,i}\geq 0,\quad \mu^{\star}_{i-1,i}&\geq 0,\\
d^{\star}_{i-1,i}\geq 0,\quad \alpha_{\mathrm{PL},i-1,i}P^{\star}_{\mathrm{C},i-1}-\overline{\Upsilon}_{\mathrm{SNR},i-1,i,\mathrm{th}}{d^{\star}_{i-1,i}}^{n_{\mathrm{PL}}}&\geq 0,\ \forall\ i,\\
\mathbf{1}^{\mathrm{T}}_{m-1}d^{\star}-D&=0,
\end{aligned}$$

where $P^{\star}_{\mathrm{C},i-1}$, $d^{\star}_{i-1,i}$, $\lambda^{\star}_{i-1,i}$, $\mu^{\star}_{i-1,i}$ and $\nu^{\star}$ are the optimal points. Then, we have

$$\left(\frac{\overline{\Upsilon}_{\mathrm{SNR},i-1,i,\mathrm{th}}}{\alpha_{\mathrm{PL},i-1,i}}\right)^{\frac{1}{n_{\mathrm{PL}}-1}} d^{\star}_{i-1,i}=\left(\frac{\overline{\Upsilon}_{\mathrm{SNR},j-1,j,\mathrm{th}}}{\alpha_{\mathrm{PL},j-1,j}}\right)^{\frac{1}{n_{\mathrm{PL}}-1}} d^{\star}_{j-1,j}, \tag{3.52}$$

which results in the optimum solution of Lemma 9. ■

If $\overline{\Upsilon}_{\mathrm{SNR},i-1,i,\mathrm{th}}/\alpha_{\mathrm{PL},i-1,i}=\overline{\Upsilon}_{\mathrm{SNR},j-1,j,\mathrm{th}}/\alpha_{\mathrm{PL},j-1,j}$, for $\forall\ i,j\in\{2,\cdots,m\}$, all the routers should be equally-spaced between the transmitter and receiver.

The analysis of this section then allows us to mathematically characterize the benefit we gain by using robotic routers, as compared to increasing the communication power of the transmitting node in order to have a direct transmission. We next formulate this. From the solution of Lemma 9, we know that the total power consumption, for the case of robotic router, is:

$$J^{\star}_{\mathrm{RR}}=\sum_{i=2}^{m}P^{\star}_{\mathrm{C},i-1}=\frac{D^{n_{\mathrm{PL}}}}{\left(\sum_{i=2}^{m}\left(\frac{\alpha_{\mathrm{PL},i-1,i}}{\overline{\Upsilon}_{\mathrm{SNR},i-1,i,\mathrm{th}}}\right)^{\frac{1}{n_{\mathrm{PL}}-1}}\right)^{n_{\mathrm{PL}}-1}}, \tag{3.53}$$

and the total power consumption for direct transmission, without using robotic routers,

is $P_{\mathrm{C,DT}} = \overline{\Upsilon}_{\mathrm{SNR},1,m,\mathrm{th}} D^{n_{\mathrm{PL}}}/\alpha_{\mathrm{PL},1,m}$, where $\overline{\Upsilon}_{\mathrm{SNR},1,m,\mathrm{th}}$ is the required SNR from the TX node to the RX. Without loss of generality, assume that $\alpha_{\mathrm{PL},1,m} = \alpha_{\mathrm{PL},i-1,i} = \alpha_{\mathrm{PL}}$ and $p_{b,i-1,i,\mathrm{th}} = p_{b,\mathrm{th}}$ for $\forall\ i \in \{2,3,\cdots,m\}$. Then, in order to have the same end-to-end performance ($p_{b,1,m,\mathrm{th}}$) for both cases, the following target bit error rate can be used for each link, for the case of using robotic routers: $p_{b,\mathrm{th}} = 1-(1-p_{b,1,m,\mathrm{th}})^{\frac{1}{m-1}}$, which results in $\overline{\Upsilon}_{\mathrm{SNR},1,m,\mathrm{th}} = -(M-1)\ln(5p_{b,1,m,\mathrm{th}})/1.5$ and $\overline{\Upsilon}_{\mathrm{SNR},i-1,i,\mathrm{th}} = -(M-1)\ln(5(1-(1-p_{b,1,m,\mathrm{th}})^{\frac{1}{m-1}}))/1.5$. Then, we have the following power ratio:

$$\frac{J^{\star}_{\mathrm{RR}}}{P_{\mathrm{C,DT}}} = \frac{\ln\left(5\left(1-(1-p_{b,1,m,\mathrm{th}})^{\frac{1}{m-1}}\right)\right)}{\ln(5p_{b,1,m,\mathrm{th}})(m-1)^{n_{\mathrm{PL}}-1}}. \tag{3.54}$$

From (3.54), it can be seen that the ratio decreases as n_{PL} (the exponent of distance-dependent path loss) increases. This is due to the fact that the signal strength drops faster as n_{PL} increases. Thus, the direct transmission case has to increase the transmit power considerably. Furthermore, if m (the total number of robots) increases, the ratio decreases, as expected. This result can also be interpreted as follows. If both systems are given equal communication power, the robotic router case will perform considerably better. Fig. 3.11 shows $J^{\star}_{\mathrm{RR}}/P_{\mathrm{C,DT}}$ of (3.54) with $p_{b,1,m,\mathrm{th}} = 10^{-3}$. As can be seen, the robotic router network can reduce communication power consumption considerably as n_{PL} or m increases.

We conclude this part by noting that the benefits of utilizing robotic routers is beyond just saving on the overall communication power. They also provide robustness through reconfigurability. For instance, if we have a mobile TX and RX nodes, depending on their positions, the direct link quality can degrade considerably. The router network can then reconfigure properly to ensure reliable flow of information.

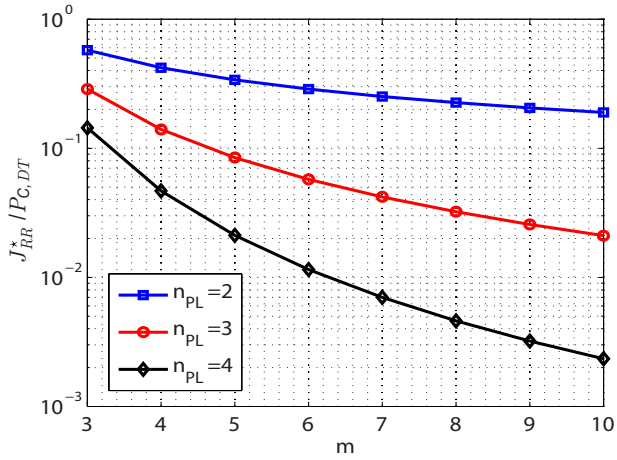

Figure 3.11: Comparing the performance of a robotic router network to that of a direct transmission, in terms of total power consumption. The y-axis shows the power ratio of (3.54).

3.4.2 Robotic Router Optimization under Transmit Power Constraints in Fading Environments

We next consider the impact of power constraints on robotic router optimization in fading environments. Similar to the previous section, we minimize the total power consumption while requiring each link to maintain a minimum acceptable performance. In this case, the performance is measured by the average BER, as discussed in Section 3.3. Let $\overline{p}_{b,i-1,i,\text{th}}$ denote the maximum acceptable average BER for the link between the $(i-1)^{\text{th}}$ and i^{th} node, i.e. we require that $\overline{p}_{b,i-1,i} \leq \overline{p}_{b,i-1,i,\text{th}}$ for all $i \in \{2, \cdots, m\}$. This requirement translates to the following SNR requirement, by using the moment generating function of a gamma distribution (see the derivations of (3.36)):

$$\overline{\Upsilon}_{\text{SNR},i-1,i} \geq \frac{\left(5\overline{p}_{b,i-1,i,\text{th}}\right)^{-\frac{1}{\varphi_{i-1,i}}} - 1}{c\vartheta_{i-1,i}} = \overline{\Upsilon}'_{\text{SNR},i-1,i,\text{th}}, \tag{3.55}$$

where $\varphi_{i-1,i}$, $\vartheta_{i-1,i}$ and c are as defined in the previous sections. Consider the case of the *Probabilistic Path Loss predictor* of Section 3.1, which predicts the path loss and fading

variance. Then, the optimization problem of (3.49) can be modified as follows:

$$\begin{aligned} \text{minimize} \quad & J_{\mathrm{RR,FD}}(P_{\mathrm{C}}, d) = \mathbf{1}_{m-1}^{\mathrm{T}} P_{\mathrm{C}} \\ \text{subject to} \quad & \overline{\Upsilon}'_{\mathrm{SNR},i-1,i,\mathrm{th}} d_{i-1,i}^{n_{\mathrm{PL}}} \leq \alpha_{\mathrm{PL},i-1,i} P_{\mathrm{C},i-1}, \;\; d_{i-1,i} \geq 0, \; \forall \; i \in \{2, \cdots, m\}, \\ & \mathbf{1}_{m-1}^{\mathrm{T}} d = D, \end{aligned} \tag{3.56}$$

where

$$\overline{\Upsilon}'_{\mathrm{SNR},i-1,i,\mathrm{th}} = \frac{(5\overline{p}_{b,i-1,i,\mathrm{th}})^{-\frac{1}{\varphi_{\mathrm{PL},i-1,i}}} - 1}{c\vartheta_{\mathrm{PL},i-1,i}}, \tag{3.57}$$

$$\varphi_{\mathrm{PL},i-1,i} = (\exp((a\sigma_{\mathrm{dB,Prob,PL},i-1,i})^2) - 1)^{-1}, \tag{3.58}$$

$$\vartheta_{\mathrm{PL},i-1,i} = \exp(1.5(a\sigma_{\mathrm{dB,Prob,PL},i-1,i})^2) - \exp(0.5(a\sigma_{\mathrm{dB,Prob,PL},i-1,i})^2), \tag{3.59}$$

and $a = \ln 10/10$. Then Lemma 9 can characterize the solution of (3.56) by replacing $\overline{\Upsilon}_{\mathrm{SNR},i-1,i,\mathrm{th}}$ with $\overline{\Upsilon}'_{\mathrm{SNR},i-1,i,\mathrm{th}}$. Because of fading, however, $\overline{\Upsilon}'_{\mathrm{SNR},i-1,i,\mathrm{th}}$ is higher than $\overline{\Upsilon}_{\mathrm{SNR},i-1,i,\mathrm{th}}$ if we take $\overline{p}_{b,i-1,i,\mathrm{th}} = p_{b,i-1,i,\mathrm{th}}$. It is also easy to confirm that the two solutions become the same if $\sigma_{\mathrm{dB,Prob,PL},i-1,i} \to 0$ for all i, i.e., fading goes to zero.

We can now mathematically characterize how much we benefit from properly accounting for fading, as opposed to using only a path loss model (case of the *Deterministic Path Loss Predictor* of Section 3.1), for robotic router optimization in fading environments. Let $J^{\star}_{\mathrm{RR,FD}}$ denote the total power consumption of the robotic routers as a result of the optimization of (3.56). To have a fair comparison, assume that the robotic router system that only considers path loss and does not account for fading is given the same total power. Then, the best performance of the path-loss-only case is achieved by solving the

following optimization problem:

$$\begin{aligned} &\text{maximize} \quad \overline{\Upsilon}_{\mathrm{SNR,th}} \\ &\text{subject to} \quad \overline{\Upsilon}_{\mathrm{SNR,th}} d_{i-1,i}^{n_{\mathrm{PL}}} \leq \alpha_{\mathrm{PL},i-1,i} P_{\mathrm{C},i-1}, \;\; d_{i-1,i} \geq 0, \; \forall \; i \in \{2, \cdots, m\}, \\ &\qquad\qquad \mathbf{1}_{m-1}^{\mathrm{T}} P_{\mathrm{C}} = J_{\mathrm{RR,FD}}^{\star}, \quad \mathbf{1}_{m-1}^{\mathrm{T}} d = D, \end{aligned} \tag{3.60}$$

where $\overline{\Upsilon}_{\mathrm{SNR,th}}$ denotes the minimum acceptable SNR, which is taken to be the same for all the links, to facilitate mathematical derivations. By applying KKT conditions, optimum $\overline{\Upsilon}_{\mathrm{SNR,th}}$ can then be found to be:

$$\overline{\Upsilon}_{\mathrm{SNR,th}}^{\star} = \frac{J_{\mathrm{RR,FD}}^{\star}}{D^{n_{\mathrm{PL}}}} \left(\sum_{i=2}^{m} \alpha_{\mathrm{PL},i-1,i}^{\frac{1}{n_{\mathrm{PL}}-1}} \right)^{n_{\mathrm{PL}}-1}. \tag{3.61}$$

Therefore, the actual performance of the *Deterministic Path Loss Predictor* will be as follows in a fading environment:

$$\overline{p}_{b,\mathrm{FD}}(\mathrm{RX}) = 1 - \prod_{i=2}^{m} (1 - 0.2(1 + c\vartheta_{\mathrm{PL},i-1,i} \overline{\Upsilon}_{\mathrm{SNR,th}}^{\star})^{-\varphi_{\mathrm{PL},i-1,i}}). \tag{3.62}$$

Fig. 3.12 shows how much we lose by considering only path loss in a fading environment, for the case of one router. For this simulation, $\overline{p}_{b,1,2,\mathrm{th}} = \overline{p}_{b,2,3,\mathrm{th}} = 10^{-3}$, $n_{\mathrm{PL}} = 2$ and $c = 0.5$. We have an end-to-end BER 2×10^{-3} for the design in which fading is taken into account. The figure then compares $\overline{p}_{b,\mathrm{FD}}(\mathrm{RX})$ with this benchmark. As can be seen, by only considering path loss, we can achieve the same performance only if $\sigma_{\mathrm{dB,Prob,PL},1,2} = \sigma_{\mathrm{dB,Prob,PL},2,3}$. In this case, the optimum configuration of both cases will be the same. However, as we depart from this equality and as fading variances increase, we can lose orders of magnitude by not taking fading into account.

It should also be noted that the gap between the two performances will further increase if the *Deterministic Path Loss/Shadowing Predictor* or *Probabilistic Path Loss/*

Shadowing Predictor of the previous section is utilized (in that case we will also see a gap for $\sigma_{\text{dB,Prob,PL,1,2}} = \sigma_{\text{dB,Prob,PL,2,3}}$).

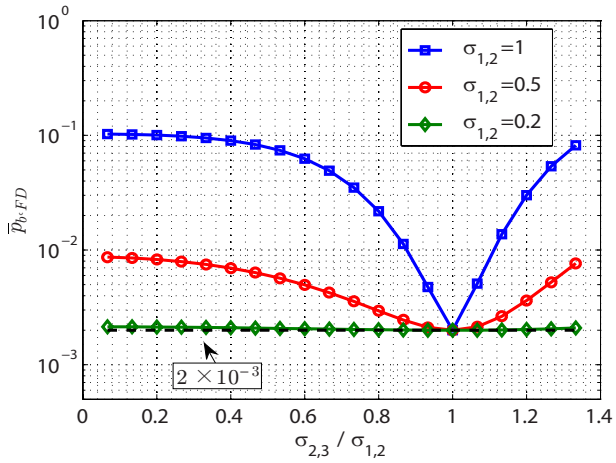

Figure 3.12: Impact of taking fading into account when designing robotic routers. The figure shows that we can experience a considerable performance loss if we only consider path loss (disk models) in fading environments.

3.4.3 Robotic Router Optimization Considering both Communication and Motion Costs

In the previous sections, we only considered the communication power consumption in the optimization of the routers. In this part, we extend our analysis and consider both communication and motion costs in order to understand the underlying tradeoffs. Consider the case where the TX needs to continuously send information to the RX, during time $[0, T]$. Robotic routers at positions q_is, where $i \in \{2, \cdots, m-1\}$, are cooperatively relaying the information using the multihop scheme. Our goal is to minimize the overall communication and motion costs of the entire network. First, consider only the path loss. Similar to Section 3.4.1, we assign each link a target performance requirement

($\overline{\Upsilon}_{\mathrm{SNR},i-1,i,\mathrm{th}}$). The required transmit power for each router is:

$$\begin{aligned} P_{\mathrm{C},i-1} &= \frac{\overline{\Upsilon}_{\mathrm{SNR},i-1,i,\mathrm{th}}}{\alpha_{\mathrm{PL},i-1,i}} d_{i-1,i}^{n_{\mathrm{PL}}} = -\frac{(M-1)\ln(5p_{b,i-1,i,\mathrm{th}})}{1.5\alpha_{\mathrm{PL},i-1,i}} d_{i-1,i}^{n_{\mathrm{PL}}} \\ &= C_{i-1,i}\|q_i - q_{i-1}\|^{n_{\mathrm{PL}}}. \end{aligned} \tag{3.63}$$

We then have the following optimization problem:

$$\begin{aligned} \text{minimize} \quad & \int_0^T \varpi \sum_{i=2}^{m-1} \|v_i\|^2 + \sum_{i=2}^{m} C_{i-1,i}\|q_i - q_{i-1}\|^{n_{\mathrm{PL}}} d\tau \\ \text{subject to} \quad & \dot{q}_i = v_i, \qquad \forall\ i \in \{2, \cdots, m-1\}, \end{aligned} \tag{3.64}$$

where ϖ is a positive constant (which allows the designer to properly weigh the two terms). Note that to facilitate analysis, in this section we model the motion cost as the square of the norm of the control input and only consider the case where $n_{\mathrm{PL}} = 2$. The Hamiltonian of (3.64) will then be

$$g = \varpi \sum_{i=2}^{m-1} \|v_i\|^2 + \sum_{i=2}^{m} C_{i-1,i}\|q_i - q_{i-1}\|^2 + \sum_{i=2}^{m-1} \lambda_i^{\mathrm{T}} v_i, \tag{3.65}$$

where λ_i is the Lagrange multiplier. By applying calculus of variations [106], we can find the necessary conditions for optimality as follows:

$$\begin{aligned} \frac{\partial g}{\partial v_i} &= 2\varpi v_i + \lambda_i = 0, \\ \frac{\partial g}{\partial q_i} &= 2C_{i-1,i}(q_i - q_{i-1}) + 2C_{i,i+1}(q_i - q_{i+1}), \\ \lambda_i(T) &= 0, \end{aligned} \tag{3.66}$$

for $\forall\ i \in \{2, \cdots, m-1\}$. Then, the optimal control law and trajectories of the routers can be found as follows for $t \in [0, T]$:

$$u^\star(t) = P\left(\text{diag}\left(\sqrt{\epsilon_i}\,\frac{\exp(\sqrt{\epsilon_i}t) - \exp(2\sqrt{\epsilon_i}T - \sqrt{\epsilon_i}t)}{1+\exp(2\sqrt{\epsilon_i}T)}\right)\otimes I_2\right)P^{-1}(q_r(0) - Z^{-1}V), \tag{3.67}$$

$$\begin{aligned} q_r^\star(t) = {} & P\left(\text{diag}\left(\frac{\exp(\sqrt{\epsilon_i}t) + \exp(2\sqrt{\epsilon_i}T - \sqrt{\epsilon_i}t)}{1+\exp(2\sqrt{\epsilon_i}T)}\right)\otimes I_2\right)P^{-1}q_r(0) \\ & - P\left(\text{diag}\left(\frac{\exp(\sqrt{\epsilon_i}t) + \exp(2\sqrt{\epsilon_i}T - \sqrt{\epsilon_i}t)}{1+\exp(2\sqrt{\epsilon_i}T)} - 1\right)\otimes I_2\right)P^{-1}Z^{-1}V, \end{aligned} \tag{3.68}$$

where

$$Z = \frac{1}{\varpi}\begin{bmatrix} \sum_{i=2}^{3} C_{i-1,i} & -C_{2,3} & \cdots & 0 \\ -C_{2,3} & \sum_{i=3}^{4} C_{i-1,i} & -C_{3,4} & \vdots \\ \vdots & \vdots & \ddots & \vdots \\ 0 & \cdots & -C_{m-2,m-1} & \sum_{i=m-1}^{m} C_{i-1,i} \end{bmatrix}\otimes I_2,$$

$q_r^{\mathrm{T}} = [q_2^{\mathrm{T}}\ \cdots\ q_{m-1}^{\mathrm{T}}]^{\mathrm{T}}$, $V = [C_{1,2}q_1^{\mathrm{T}}\ 0\ \cdots\ C_{m-1,m}q_m^{\mathrm{T}}]^{\mathrm{T}}/\varpi$, $P^{-1}ZP = \text{diag}(\epsilon_i)$, ϵ_i is the i^{th} eigenvalue of Z, $\otimes$ represents the Kronecker product, and $\text{diag}(\Delta_i)$ represents a diagonal matrix with Δ_is on its diagonals . Since $C_{i-1,i} > 0$ for $\forall\ i \in \{2, \cdots, m\}$, $Q \succ 0$.

For simplicity, consider the case where $C_{i-1,i} = C$ for all i. Then, C/ϖ denotes the ratio of communication to motion cost. As $C/\varpi \to 0$, $\epsilon_i \to 0$, for all i. Then, the second term on the right hand side of (3.68) goes to 0. Hence, $q_r^\star(t) \to q_r(0)$, which implies that the robotic routers are more likely to stay in their initial positions and simply increase their communication power. On the other hand, as $C/\varpi \to \infty$, $\epsilon_i \to \infty$, for all i, then the first term of (3.68) goes to zero, resulting in $q_r^\star(t) \to Z^{-1}V$ for $t \in (0, T]$. Next, we show that $Z^{-1}V$ is exactly the optimal solution of (3.49) for $n_{\text{PL}} = 2$, which implies that the robotic routers will move to the optimal communication configuration if the motion

cost is negligible.

Lemma 10 *The inverse of matrix Z has the following form:*

$$Z^{-1} = \varpi \begin{bmatrix} \dfrac{\displaystyle\sum_{i=3}^{m} \frac{1}{C_{i-1,i}}}{C_{1,2} \displaystyle\sum_{i=2}^{m} \frac{1}{C_{i-1,i}}} & \cdots & \dfrac{\dfrac{1}{C_{1,2}}}{C_{m-1,m} \displaystyle\sum_{i=2}^{m} \frac{1}{C_{i-1,i}}} \\ \dfrac{\displaystyle\sum_{i=4}^{m} \frac{1}{C_{i-1,i}}}{C_{1,2} \displaystyle\sum_{i=2}^{m} \frac{1}{C_{i-1,i}}} & \cdots & \dfrac{\displaystyle\sum_{i=2}^{3} \frac{1}{C_{i-1,i}}}{C_{m-1,m} \displaystyle\sum_{i=2}^{m} \frac{1}{C_{i-1,i}}} \\ \vdots & \cdots & \vdots \\ \dfrac{\dfrac{1}{C_{m-1,m}}}{C_{1,2} \displaystyle\sum_{i=2}^{m} \frac{1}{C_{i-1,i}}} & \cdots & \dfrac{\displaystyle\sum_{i=2}^{m-1} \frac{1}{C_{i-1,i}}}{C_{m-1,m} \displaystyle\sum_{i=2}^{m} \frac{1}{C_{i-1,i}}} \end{bmatrix} \otimes I_2.$$

Proof: It can be easily verified that $Z^{-1}Z = I_{2m-4}$. ■

By applying Lemma 10, we then have:

$$q_i^\star(t) \to \frac{\displaystyle\sum_{j=i+1}^{m} \frac{1}{C_{j-1,j}}}{\displaystyle\sum_{j=2}^{m} \frac{1}{C_{j-1,j}}} q_1 + \frac{\displaystyle\sum_{j=2}^{i} \frac{1}{C_{j-1,j}}}{\displaystyle\sum_{j=2}^{m} \frac{1}{C_{j-1,j}}} q_m, \tag{3.69}$$

if $C/\varpi \to \infty$, i.e., if the motion cost is negligible. This means that the routers should be on the line segment from the transmitter to the receiver, with the following optimum distances:

$$\|q_i - q_{i-1}\| = \frac{\dfrac{1}{C_{i-1,i}}}{\displaystyle\sum_{j=2}^{m} \frac{1}{C_{j-1,j}}} \|q_m - q_1\| = \frac{\dfrac{\alpha_{\mathrm{PL},i-1,i}}{\overline{\Upsilon}_{\mathrm{SNR},i-1,i,\mathrm{th}}}}{\displaystyle\sum_{j=2}^{m} \frac{\alpha_{\mathrm{PL},j-1,j}}{\overline{\Upsilon}_{\mathrm{SNR},j-1,j,\mathrm{th}}}} D.$$

As can be seen, this is exactly what we found in Lemma 9 for $n_{\mathrm{PL}} = 2$.

Fig. 3.13 shows the communication and motion tradeoffs for two cases. In the first

case, we have $M = 4$, $p_{b,i-1,i,\text{th}} = 10^{-3}$, $\alpha_{\text{PL},i-1,i} = 10^{-3}$ for all i, $T = 10$ and $\varpi = 5 \times 10^6$, resulting in $C/\varpi = 2.1 \times 10^{-3}$, which means that the communication cost is small, as compared to motion cost. In the second case, we have $M = 16$, $p_{b,i-1,i,\text{th}} = 10^{-6}$, $\alpha_{\text{PL},i-1,i} = 10^{-3}$ for all i, $T = 10$ and $\varpi = 10^3$, resulting in $C/\varpi = 122.1$, i.e. the communication cost is high as compared to the motion cost. As can be seen, when the communication cost is small, all the routers will stay close to the initial positions. On the hand, when the communication cost is high, all the routers will move to the solution of (3.49).

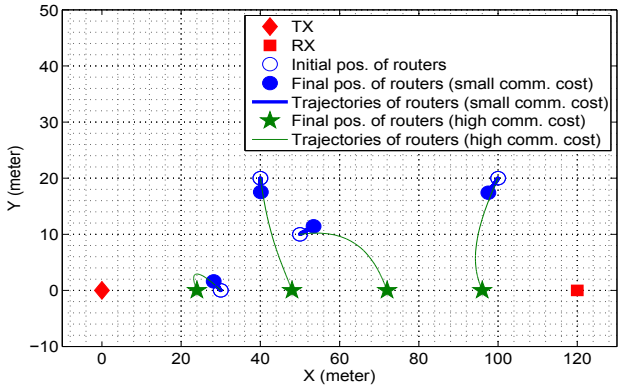

Figure 3.13: Communication and motion tradeoffs in robotic routers.

Extension to Fading Environments

We can readily extend the framework of (3.64) to fading environments, by considering the *Probabilistic Path Loss Predictor*. Similar to Section 3.4.2, we assign each link a minimum target average performance requirement ($\overline{\Upsilon}'_{\text{SNR},i-1,i,\text{th}}$). Then, the required transmit power for each router is:

$$P_{\text{C},i-1} = \frac{\overline{\Upsilon}'_{\text{SNR},i-1,i,\text{th}}}{\alpha_{\text{PL},i-1,i}} d_{i-1,i}^{n_{\text{PL}}} = C'_{i-1,i} d_{i-1,i}^{n_{\text{PL}}}. \tag{3.70}$$

We then have the following optimization framework:

$$\begin{aligned} \text{minimize} \quad & \int_0^T \varpi \sum_{i=2}^{m-1} \|v_i\|^2 + \sum_{i=2}^{m} C'_{i-1,i} \|q_{i-1} - q_i\|^{n_{\text{PL}}} d\tau \\ \text{subject to} \quad & \dot{q}_i = v_i, \qquad \forall\ i \in \{2, \cdots, m-1\}, \end{aligned} \tag{3.71}$$

As can be seen, all the analysis of this section holds for the case of $n_{\text{PL}} = 2$. Because of fading, however, $C'_{i-1,i}$ is larger than $C_{i-1,i}$ if we take $\overline{p}_{b,i-1,i,\text{th}} = p_{b,i-1,i,\text{th}}$. This implies that communication is more costly in fading environments, as expected. Also, as $\sigma_{\text{dB,PL},i-1,i} \to 0$, we have $C'_{i-1,i} \to C_{i-1,i}$, i.e. the solution of fading case converges to the path loss case if the variance of fading goes to 0. Note that only the *Probabilistic Path Loss predictor* approach is considered in (3.71). Hence, the performance can further be improved if the *Deterministic Path Loss/Shadowing Predictor* or *Probabilistic Path Loss/Shadowing Predictor* is utilized instead.

3.5 Preliminary Experimental Results

In Fig. 3.9 and 3.10, we simulated a robotic operation using the real channel data of Fig. 3.8. In this section, we show a preliminary robotic operation where a robot tries to maintain the connectivity of two stationary homogeneous routers in the basement of Department of Electrical and Computer Engineering at University of New Mexico. We emphasize that this is a preliminary test with the main goal of exploring the impact of localization errors. In particular, we discuss interesting interplays between the localization quality and channel correlation/learning quality. Fig. 3.14 shows the experimental setup where the positions of the TX and RX routers are marked. Fig. 3.8 (right) showed a color map of the received communication signal strength from the TX in this environment. We use the Pioneer robot of Fig. 3.8 (left) as a robotic router. The initial

position of the robot is marked with an empty circle in Fig. 3.14 (left). The robot uses a priori channel measurements that are collected in this environment, for motion planning, mounting to 1.04% to the TX and 1.24% to the RX. By using the probabilistic channel prediction framework of Section 2.1 (Lemmas 1 and 2), the robot then predicts the channel at unvisited locations.[5] It then finds its optimum position by solving the probabilistic optimization problem of (3.37) with the *Probabilistic Path Loss/Shadowing Predictor* through an exhaustive search.

The filled circle of Fig. 3.14 (left) shows the optimum position. As for motion planning, a simple strategy is used that finds a route that is parallel to the walls with minimum turns. Fig. 3.14 (left) shows the calculated route. The true route and final position, however, will be different, due to localization errors. The robot uses onboard gyroscope and wheel encoders for localization. Since this area of the basement is sloped, we also have a simple compensating function to control the direction. More sophisticated localization sensors/algorithms can also be used to improve the performance [113–115]. Fig. 3.14 (right) shows the probability density function of the distance of the true final position of the robot to the calculated optimum final position (filled circle of Fig. 3.14 (left)) after running the experiment for 10 times.

Fig. 3.15 (top) shows the signal strength from the TX and RX along the trajectory, while Fig. 3.15 (bottom) shows the simulated end-to-end BER based on the measurements of signal strength. The curves are averaged over 10 instants of running the experiment from the same initial position. As can be seen, the signal strength from the TX is low at the beginning, which results in a high BER. As the robot moves towards the final

[5]In general, localization errors can directly affect the channel assessment quality. Typically, however, channel assessment is mainly based on a very few measurements gathered at the beginning of the operation. Localization errors have not yet accumulated that much at the beginning of the operation, assuming the initial positions of the robots are known. Thus, its impact on channel learning may be negligible, as compared to the impact of channel parameter estimation errors or other channel learning uncertainties.

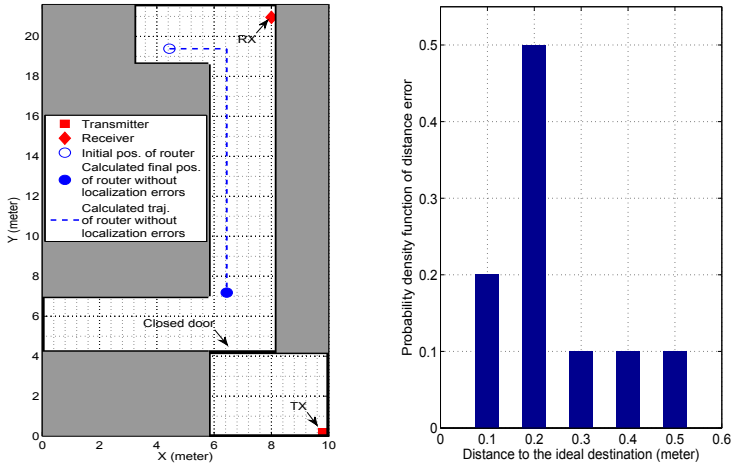

Figure 3.14: The left figure shows the initial position, calculated trajectory and calculated final position of the router, by using our proposed optimization framework and *Probabilistic Path Loss/Shadowing Predictor*. The right figure shows the pdf of the distance of the true final position of the robot to the calculated final position, after running the experiment 10 times, from the same initial position. The error is mainly due to localization errors.

position, the signal strength from the TX increases and the end-to-end BER decreases a few orders of magnitude. The fluctuations in the curves are caused by multipath fading. It is worth noting that the optimum position of the router based on the sparse samples of the channels is close to the TX. This makes sense as the closed door makes communication with the TX harder.

3.5.1 The Interplay Between Localization Quality and Channel Correlation/Learning Quality

Localization errors can impact the optimum positioning of the routers affecting the overall performance. However, the level of impact depends on the channel parameters. First, consider the case where the channel is dominated by multipath fading. Since the channel predictor (or any predictor for that matter) does not predict the multipath fading component, the final calculated optimum configuration does not experience the planned

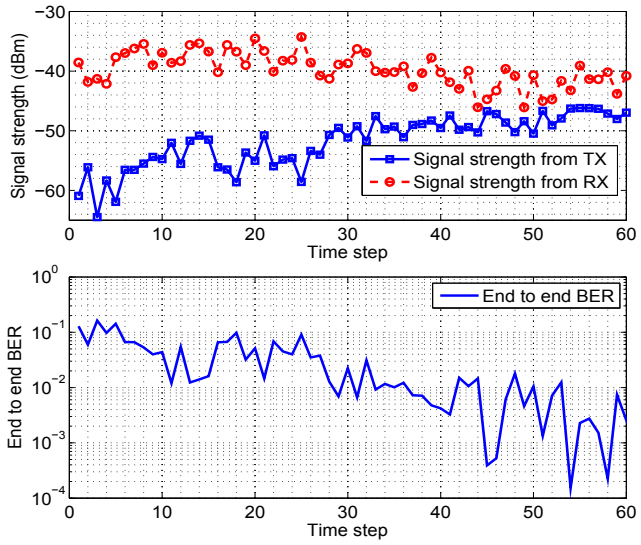

Figure 3.15: Signal strength from TX/RX along the trajectory (top) and the simulated end-to-end BER, based on the signal strength measurements (bottom).

channel qualities. The true performance at that configuration would be the same as any other configuration in its vicinity, due to multipath fading. Thus, the impact of multipath fading is similar to having localization errors in this case. In other words, localization errors do not impact the performance significantly. On the other hand, consider the case where multipath fading is negligible such that channel can be assessed almost perfectly. First, consider the case where shadowing decorrelation distance is large (channel stays correlated over a large distance). Then, small localization errors do not impact the performance that much since the true final position experiences highly-correlated channels with the calculated final position. However, if the decorrelation distance is small, localization errors can impact the performance. In summary, if the localization errors are small, with respect to the decorrelation distance, their impact on the performance of our proposed framework becomes negligible. Furthermore, as multipath fading increases, for any given localization quality and decorrelation distance, the impact of localization errors becomes smaller.

The simulation results of Fig. 3.16 verify our hypothesis, for the case where one

router tries to optimize the connectivity of two fixed nodes. In this simulation, the workspace is taken to be 40 meters $\times$ 40 meters, and the step size of the robot is 0.4 meter. The localization error is modeled as an additive zero mean Gaussian noise [115]. We assume that the robot has 5% a priori channel samples to predict the channel, using our *Probabilistic Path Loss/Shadowing Predictor*. The simulation is averaged over several runs of different channel samples (same underlying parameters) and start positions. The figure shows two curves. For the case of $\xi_{\text{dB}} = 8$ and $K_{\text{ric}} = 20$, multipath fading is negligible. The curve then shows that localization errors impact the performance more drastically as the localization error increases. For the case of $\xi_{\text{dB}} = 2$ and $K_{\text{ric}} = 0$, on the other hand, the channel is dominated by multipath fading. Then, the performance stays very similar to the case of no localization error, i.e. the performance is not as sensitive to localization errors.

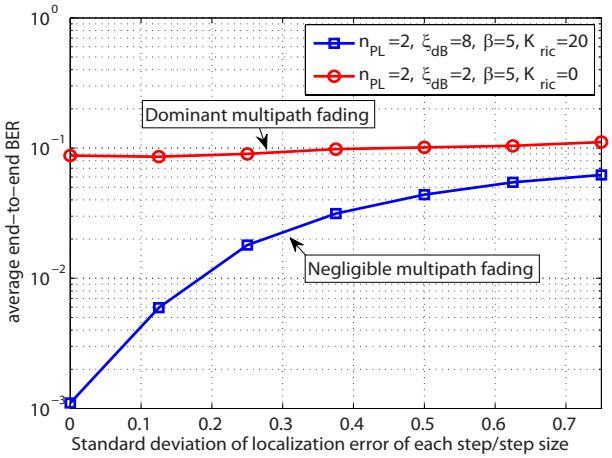

Figure 3.16: The interplay between localization quality and channel correlation/learning quality.

Chapter 4

Co-Optimization Along a Fixed Trajectory

Consider the scenario where a robot is tasked with sending a fixed number of a priori-given bits of information to a remote station in a limited operation time, and as it travels along a pre-defined trajectory $\mathcal{T}$ with length D. The pre-defined trajectory could be the only feasible path due to the environmental constraints such as obstacles. For instance, in a cluttered indoor office navigation problem, the only path from point A to point B may be across certain hallways. In Section 4.4 where we furthermore have online sensing, the pre-defined path could be the path dictated due to sensing constraints. In [39], the authors mention that in ocean sampling, the path is typically pre-defined. Furthermore, autonomous aircrafts may be restricted to fly along a particular trajectory to stay away from commercial air traffic or avoid detection by an adversary [39]. We assume that the robot operates in a realistic fading environment that naturally experiences path loss, shadowing and multipath fading. Moreover, we assume that the robot has some a priori collected channel samples in the same environment such that it can predict the channel

This chapter is an amended version of [116].

quality along the trajectory by utilizing the channel prediction framework introduced in Section 2.1. Then, the goal of the robot is to transmit the given information bits while minimizing the total energy consumption, which *includes both motion and communication energy costs*, and satisfying a target BER at the remote station.

Fig. 4.1 shows an example of the considered scenario. The robot starts from an initial position, follows the direction of $\mathcal{T}$, and transmits the needed information to the remote station before reaching its terminal position. In order to minimize the total energy cost, the robot needs to properly plan its motion speed/possible stop times, and schedule the transmission of the bits, based on the predicted channel quality along the trajectory. In this chapter, we solely focus on the communication and motion co-planning along a fixed trajectory, in order to have a good understanding on how the communication and motion affect each other when they are jointly optimized. However, co-planning the trajectory itself can also be integrated into the whole framework design and will be investigated in Chapter 5.

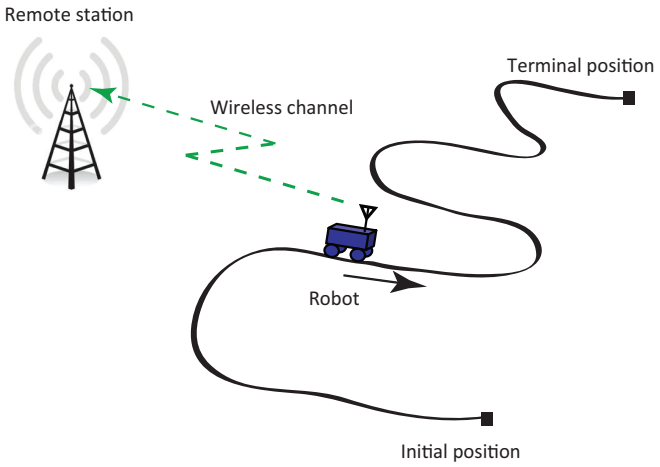

Figure 4.1: The robot needs to transmit a number of given bits to the remote station, under minimum energy cost (including both motion and communication energy consumption), while traveling along a pre-defined trajectory, and under a given time budget.

The rest of this chapter is organized as follows. In Section 4.1, we first propose a

co-optimization framework that allows the robot to plan its motion speed, transmission rate and stop time, based on its probabilistic prediction of the channel quality along the trajectory. Then, we characterize two special cases, namely the heavy-task load and light-task load cases, in order to have more intuitions on the co-optimization framework. Section 4.2 presents our additional stop-time online adaptation strategy to further fine tune the stop location as the robot moves along its trajectory and measures the true value of the channel. In Section 4.3, we verify the effectiveness of our proposed framework in a simulation environment. Finally, in Section 4.4, we extend our framework to the case where the robot needs to gather the information bits online along the pre-defined trajectory.

4.1 Problem Formulation

We divide the whole trajectory into N_{SH} sub-trajectories, $\mathcal{T}_i$s, for $i \in \{1, 2, \cdots, N_{\text{SH}}\}$, each with length d_i (see [70] for how to choose the length in practice). We assume small enough d_i such that the path loss and shadowing components of the channel can be assumed constant over each $\mathcal{T}_i$. The length d_i then depends on the length over which the channel can be considered stationary. To consider the most general case, we further allow d_is to be different from each other in order to account for the cases where the trajectory spans over a large area with changing environmental features (such as from indoor to outdoor), resulting in different stationary lengths in different parts of the trajectory. Note that the channel is still space-varying over each $\mathcal{T}_i$ due to multipath fading.

In this section, we show how the robot can co-plan its motion and communication, based on its prediction of the path loss and shadowing components of the channel over the sub-trajectories. Our one-time co-optimization happens at the beginning of the operation. In Section 4.2, we then show how the robot can furthermore fine tune its

strategy through online adaptation to the multipath component, as it moves along each sub-trajectory and measures the true value of the channel.

4.1.1 Co-Optimization of Communication and Motion

Assume that the robot uses the aforementioned probabilistic channel prediction framework of Section 2.1 to predict the received CNR over each sub-trajectory $\mathcal{T}_i$. Let $q_i \in \mathcal{T}_i$ represent a point along $\mathcal{T}_i$. Then, the CNR at $\mathcal{T}_i$ can be assessed as follows: $\Upsilon_{\rm dB}(q_i, q_b) \sim \mathcal{N}(\overline{\Upsilon}_{\rm dB}(q_i, q_b), \sigma^2_{\rm dB}(q_i, q_b))$, where q_b is the position of the remote station. In this chapter, we use communication energy model (2.9) and motion energy model (2.22). We then propose the following optimization framework to minimize the average total energy consumption (averaged over the distribution of the channel):

$$\begin{aligned}
\text{minimize} \quad & \widetilde{J}_{\rm SH} = \sum_{i=1}^{N_{\rm SH}} \underbrace{\frac{2^{\widetilde{R}_i}-1}{K}\mathbb{E}\left\{\frac{1}{\Upsilon_i}\right\}\widetilde{t}_{{\rm tr},i}}_{E_{{\rm C},i}\text{: ave. comm. energy cost along } \mathcal{T}_i} + \underbrace{\frac{\kappa_1 d_i^2}{\widetilde{t}_{{\rm mo},i}} + \kappa_4 \widetilde{t}_{{\rm mo},i}}_{E_{{\rm M},i}\text{: motion energy cost along } \mathcal{T}_i} \\
\text{subject to} \quad & \sum_{i=1}^{N_{\rm SH}} \widetilde{t}_{{\rm mo},i} + \widetilde{t}_{{\rm st},i} \le T_{\rm tot}, \quad \sum_{i=1}^{N_{\rm SH}} \widetilde{R}_i \widetilde{t}_{{\rm tr},i} = Q_{\rm tot}/B, \\
& \widetilde{R}_i \ge 0, \quad \widetilde{t}_{{\rm st},i} \ge 0, \quad \widetilde{t}_{{\rm tr},i} \ge 0, \quad \widetilde{t}_{{\rm mo},i} \ge d_i/v_{\max}, \\
& \widetilde{t}_{{\rm tr},i} \le \widetilde{t}_{{\rm mo},i} + \widetilde{t}_{{\rm st},i}, \ \forall\ i \in \{1, \cdots, N_{\rm SH}\},
\end{aligned} \tag{4.1}$$

where the unknown variables to solve for are $\widetilde{R}_i$, $\widetilde{t}_{{\rm tr},i}$, $\widetilde{t}_{{\rm mo},i}$ and $\widetilde{t}_{{\rm st},i}$, which denote the spectral efficiency, transmit time, motion time and stop time that are assigned to each $\mathcal{T}_i$ respectively.[1] Furthermore, Υ_i represents the non-dB version of $\Upsilon_{\rm dB}(q_i, q_b)$, i.e. $\Upsilon_i = \Upsilon(q_i, q_b) = 10^{\Upsilon_{\rm dB}(q_i,q_b)/10}$, $T_{\rm tot} \ge D/v_{\max}$ is the given operation time budget, $0 < Q_{\rm tot} < \infty$ is the total number of bits that needs to be sent, and B is the given fixed bandwidth.[2] As

[1] In practice, $\widetilde{R}_i$s should have certain integer constraints to ensure a proper modulation [105]. In this chapter, we do not consider such constraints for the sake of mathematical analysis.

[2] Note that (4.1) is infeasible if $T_{\rm tot} < D/v_{\max}$. Other feasibility issues can arise if maximum spectral efficiency and/or maximum transmit power are considered. While we do not consider these constraints

mentioned in Section 2.2, the required target BER is part of K: $K = -1.5/\ln(5p_{b,\text{th}})$. In the formulation of (4.1), we assume that the robot travels at a constant speed along each sub-trajectory. Moreover, since the robot moves along a fixed trajectory, the velocity of the robot only affects $\widetilde{E}_{\text{M}}$ in (2.22). Hence, the motion energy cost can be characterized by using $\widetilde{E}_{\text{M}}$.

Our optimization problem of (4.1) plans the motion speed/stop time of the robot (available time budget) and schedules the transmission of the given bits along each sub-trajectory, while minimizing the average total energy cost and satisfying the time budget and target BER. Note that motion energy can be minimized by using the velocity mentioned in Section 2.3. Thus, our co-optimization framework essentially plans the motion strategy, i.e. possibly costing more motion energy, to help save communication energy, resulting in an overall energy cost reduction. Since the robot can incur a large amount of motion energy if it moves too slowly, we introduced the stop time variables $\widetilde{t}_{\text{st},i}$s in (4.1), in order to allow the robot to stop during the operation if needed. Then, the total time that the robot can spend along $\mathcal{T}_i$ is $\widetilde{t}_{\text{mo},i} + \widetilde{t}_{\text{st},i}$, which includes both the motion and stop time durations. Hence, the transmit time $\widetilde{t}_{\text{tr},i}$ along $\mathcal{T}_i$ should always be smaller than or equal to $\widetilde{t}_{\text{mo},i} + \widetilde{t}_{\text{st},i}$: $\widetilde{t}_{\text{tr},i} \leq \widetilde{t}_{\text{mo},i} + \widetilde{t}_{\text{st},i}$. In Section 4.2, we will further show where the robot should stop along the sub-trajectory as it measures the real value of CNR.

There is no closed-form solution for (4.1). However, we can still characterize certain properties of the optimum solution, as we show next. In what follows, we use superscript $\star$ to represent the optimum solution (or value) of the corresponding optimization problem. First, we show that (4.1) can be simplified to another optimization problem with the same optimum value.

Lemma 11 *$f(t) = (2^{C/t} - 1)t$ is a non-increasing function of t for $t > 0$.*

here, we note that similar results can be derived.

Proof: The lemma can be easily confirmed by finding the first and second-order derivatives of $f(t)$. ■

Lemma 12 *The optimum solution of (4.1) is the same as the optimum solution of the following optimization problem:*

$$\begin{aligned} &\textit{minimize} \quad J_{\rm SH} = \sum_{i=1}^{N_{\rm SH}} \frac{2^{R_i}-1}{K} \mathbb{E}\left\{\frac{1}{\Upsilon_i}\right\}(t_{{\rm mo},i}+t_{{\rm st},i}) + \frac{\kappa_1 d_i^2}{t_{{\rm mo},i}} + \kappa_4 t_{{\rm mo},i} \\ &\textit{subject to} \quad \sum_{i=1}^{N_{\rm SH}} t_{{\rm mo},i}+t_{{\rm st},i} \le T_{\rm tot}, \quad \sum_{i=1}^{N_{\rm SH}} R_i(t_{{\rm mo},i}+t_{{\rm st},i}) = Q_{\rm tot}/B, \\ &\qquad R_i \ge 0, \quad t_{{\rm st},i} \ge 0, \quad t_{{\rm mo},i} \ge d_i/v_{\max}, \ \forall\ i \in \{1,\cdots,N_{\rm SH}\}. \end{aligned} \tag{4.2}$$

Proof: Note that (4.2) is a special case of (4.1) with $\widetilde{t}_{{\rm tr},i} = \widetilde{t}_{{\rm mo},i} + \widetilde{t}_{{\rm st},i}$ for all i, i.e. the communication transmission time is taken to be the same as the total time spent in each sub-trajectory. Let $\widetilde{R}_i^\star$, $\widetilde{t}_{{\rm tr},i}^\star$, $\widetilde{t}_{{\rm mo},i}^\star$ and $\widetilde{t}_{{\rm st},i}^\star$ represent the optimum solution of (4.1). From comparing the objective functions of (4.1) and (4.2), we can easily see that $\widetilde{J}_{\rm SH}^\star \le J_{\rm SH}^\star$. We then pick a feasible solution for (4.2) as follows: $t_{{\rm mo},i} = \widetilde{t}_{{\rm mo},i}^\star$, $t_{{\rm st},i} = \widetilde{t}_{{\rm st},i}^\star$, and $R_i = \begin{cases} \widetilde{R}_i^\star \widetilde{t}_{{\rm tr},i}^\star/(\widetilde{t}_{{\rm mo},i}^\star + \widetilde{t}_{{\rm st},i}^\star) & \text{if } \widetilde{R}_i^\star,\ \widetilde{t}_{{\rm tr},i}^\star > 0 \\ 0 & \text{otherwise} \end{cases}$. By using Lemma 11, we have $(2^{R_i}-1)(t_{{\rm mo},i}+t_{{\rm st},i}) \le (2^{\widetilde{R}_i^\star}-1)\widetilde{t}_{{\rm tr},i}^\star$, which results in $J_{\rm SH}^\star \le J_{\rm SH}(R_i, t_{{\rm mo},i}, t_{{\rm st},i}) \le \widetilde{J}_{\rm SH}^\star$. Thus, we must have $J_{\rm SH}^\star = \widetilde{J}_{\rm SH}^\star$. ■

Intuitively, it always costs less communication energy if the robot sends a fixed number of bits over a longer period of time, as it can then reduce the spectral efficiency (can send with a lower rate). This is what Lemma 12 indicates. It can be seen that the optimality of (4.1) can be achieved only if $\widetilde{t}_{{\rm tr},i} = \widetilde{t}_{{\rm mo},i} + \widetilde{t}_{{\rm st},i}$ for all i, i.e. the transmission time in each sub-trajectory is taken equal to the time spent in each sub-trajectory (the maximum possible). Note that (4.2) also reduces the dimension of the optimization problem. Based on Lemma 12, we can then characterize the properties of the optimum solution of (4.2)

instead of (4.1) in the rest of the chapter. Note that if $T_{\text{tot}} = D/v_{\max}$ in (4.2), then $t_{\text{mo},i} = d_i/v_{\max}$ and $t_{\text{st},i} = 0$ for all i, resulting in a simplified convex optimization problem which only has variable R_i. In this case, the robot does not have any freedom to plan its motion policy because of the limited time budget. The problem then becomes a spectral efficiency optimization problem, which can be characterized by using the approach in [79]. Hence, in the rest of the chapter, we focus on the case where $T_{\text{tot}} > D/v_{\max}$. Next, we present the following well-known theorem in optimization theory, which we use in our subsequent proofs.

Definition 1 (LICQ, [117]) *The Linear Independence Constraint Qualification (LICQ) holds if the gradients of the active constraints (those that reach equality) are linearly independent.*

Theorem 1 (First-Order Necessary Conditions, [117]) *Suppose that $p^\star$ is a local solution of a constrained optimization problem, that the objective function and the constraints are continuously differentiable, and that the LICQ holds at $p^\star$. Then there exists a Lagrange multiplier vector $\lambda^\star$, such that Karush-Kuhn-Tucker (KKT) conditions hold at $(p^\star, \lambda^\star)$.*

Then, we have the following regarding the optimum solution of (4.2).

Lemma 13 *The constraints of (4.2) satisfy the LICQ at the optimum point if $T_{\text{tot}} > D/v_{\max}$.*

Proof: The gradients of the active constraints with respect to the variable $\left[R_1 \cdots R_{N_{\text{SH}}} \,|\, t_{\text{mo},1} \cdots t_{\text{mo},N_{\text{SH}}} \,|\, t_{\text{st},1} \cdots t_{\text{st},N_{\text{SH}}}\right]^{\text{T}}$ are as follows: $\left[\mathbf{0}_{N_{\text{SH}}}^{\text{T}} \,|\, \mathbf{1}_{N_{\text{SH}}}^{\text{T}} \,|\, \mathbf{1}_{N_{\text{SH}}}^{\text{T}}\right]^{\text{T}}$ (if the first constraint is active), $\left[t_{\text{mo},1} + t_{\text{st},1} \cdots t_{\text{mo},N_{\text{SH}}} + t_{\text{st},N_{\text{SH}}} \,|\, R_1 \cdots R_{N_{\text{SH}}} \,|\, R_1 \cdots R_{N_{\text{SH}}}\right]^{\text{T}}$ (for the second constraint), $\left[\mathbf{e}_{N_{\text{SH}}}^{\text{T}}(i) \,|\, \mathbf{0}_{N_{\text{SH}}}^{\text{T}} \,|\, \mathbf{0}_{N_{\text{SH}}}^{\text{T}}\right]^{\text{T}}$ (if $R_i = 0$), $\left[\mathbf{0}_{N_{\text{SH}}}^{\text{T}} \,|\, \mathbf{e}_{N_{\text{SH}}}^{\text{T}}(i) \,|\, \mathbf{0}_{N_{\text{SH}}}^{\text{T}}\right]^{\text{T}}$ (if

$t_{\mathrm{mo},i} = d_i/v_{\max}$) and $\left[\mathbf{0}_{N_{\mathrm{SH}}}^{\mathrm{T}} \mid \mathbf{0}_{N_{\mathrm{SH}}}^{\mathrm{T}} \mid \mathbf{e}_{N_{\mathrm{SH}}}^{\mathrm{T}}(i)\right]^{\mathrm{T}}$ (if $t_{\mathrm{st},i} = 0$), where $\mathbf{e}_{N_{\mathrm{SH}}}(i)$ represents the N_{SH}-dimensional unit vector with the i^{th} entry equal to 1, and $\mathbf{0}_{N_{\mathrm{SH}}}$ and $\mathbf{1}_{N_{\mathrm{SH}}}$ denote N_{SH}-dimensional vectors of all 0 and 1 respectively. By assuming that $Q_{\mathrm{tot}} > 0$, we have $R_i^\star > 0$ for some $i \in \{1, \cdots, N_{\mathrm{SH}}\}$. Furthermore, if $T_{\mathrm{tot}} > D/v_{\max}$, then the first constraint and $t_{\mathrm{mo},i} \geq d_i/v_{\max}$, for all i, cannot be all active at the same time. Then, all the gradients of the active constraints cannot be linearly dependent at the optimum point in this case. Therefore, the constraints in (4.2) satisfy the LICQ at the optimum point. ■

Next, we show the properties of the optimum strategy based on Theorem 1 for the co-optimization of communication and motion.

Theorem 2 *The optimum motion speed ($v_i^\star$), transmission rate ($R_i^\star$) and stop time ($t_{\mathrm{st},i}^\star$) of (4.2) satisfy the following properties: if $\mathbb{E}\{1/\Upsilon_i\} < \mathbb{E}\{1/\Upsilon_j\}$, then $v_i^\star \leq v_j^\star$ and $R_i^\star \geq R_j^\star$ for $i, j \in \{1, \cdots, N_{\mathrm{SH}}\}$. Moreover, if $\mathbb{E}\{1/\Upsilon_i\}$ is above a certain threshold, then there is no transmission in the corresponding sub-trajectory ($R_i^\star = 0$). Finally, if $t_{\mathrm{st},i}^\star > 0$, then $\mathbb{E}\{1/\Upsilon_i\} = \min_{j\in\{1,\cdots,N_{\mathrm{SH}}\}}\{\mathbb{E}\{1/\Upsilon_j\}\}$, i.e. if the robot should stop, it stops at the sub-trajectory with the best predicted channel quality.*

Proof: We have the following dual function for the optimization problem of (4.2):

$$g_{J_{\mathrm{SH}}} = \sum_{i=1}^{N_{\mathrm{SH}}} \frac{2^{R_i}-1}{K}\mathbb{E}\left\{\frac{1}{\Upsilon_i}\right\}(t_{\mathrm{mo},i}+t_{\mathrm{st},i}) + \frac{\kappa_1 d_i^2}{t_{\mathrm{mo},i}} + \kappa_4 t_{\mathrm{mo},i} + \nu\left(\sum_{i=1}^{N_{\mathrm{SH}}} t_{\mathrm{mo},i} + t_{\mathrm{st},i} - T_{\mathrm{tot}}\right)$$
$$- \lambda\left(\sum_{i=1}^{N_{\mathrm{SH}}} R_i(t_{\mathrm{mo},i}+t_{\mathrm{st},i}) - Q_{\mathrm{tot}}/B\right) - \sum_{i=1}^{N_{\mathrm{SH}}}\pi_i R_i - \sum_{i=1}^{N_{\mathrm{SH}}}\epsilon_i t_{\mathrm{mo},i} - \sum_{i=1}^{N_{\mathrm{SH}}}\delta_i t_{\mathrm{st},i},$$

where π_i, ϵ_i, δ_i, ν and λ are Lagrange multipliers. From Lemma 13, the optimum solution

of (4.2) should satisfy the following KKT conditions:

$$\begin{aligned}
&\frac{\partial g_{J_{\mathrm{SH}}}}{\partial R_i} = \left(\frac{2^{R_i}\ln(2)}{K}\mathbb{E}\left\{\frac{1}{\Upsilon_i}\right\} - \lambda\right)(t_{\mathrm{mo},i} + t_{\mathrm{st},i}) - \pi_i = 0,\\
&\frac{\partial g_{J_{\mathrm{SH}}}}{\partial t_{\mathrm{mo},i}} = \frac{2^{R_i}-1}{K}\mathbb{E}\left\{\frac{1}{\Upsilon_i}\right\} - \lambda R_i - \frac{\kappa_1 d_i^2}{t_{\mathrm{mo},i}^2} + \kappa_4 + \nu - \epsilon_i = 0,\\
&\frac{\partial g_{J_{\mathrm{SH}}}}{\partial t_{\mathrm{st},i}} = \frac{2^{R_i}-1}{K}\mathbb{E}\left\{\frac{1}{\Upsilon_i}\right\} - \lambda R_i + \nu - \delta_i = 0,\\
&\nu\left(\sum_{i=1}^{N_{\mathrm{SH}}} t_{\mathrm{mo},i} + t_{\mathrm{st},i} - T_{\mathrm{tot}}\right) = 0,\\
&\lambda\left(\sum_{i=1}^{N_{\mathrm{SH}}} R_i(t_{\mathrm{mo},i} + t_{\mathrm{st},i}) - Q_{\mathrm{tot}}/B\right) = 0, \qquad \pi_i R_i = 0,\\
&\epsilon_i(t_{\mathrm{mo},i} - d_i/v_{\max}) = 0, \qquad \delta_i t_{\mathrm{st},i} = 0,\\
&R_i,\ t_{\mathrm{st},i},\ \delta_i,\ \epsilon_i,\ \lambda,\ \nu \geq 0, \qquad t_{\mathrm{mo},i} \geq d_i/v_{\max}.
\end{aligned}$$

Moreover, the first three KKT conditions can be further simplified as follows:

$$\begin{aligned}
&R_i^\star = \begin{cases} \log_2\left(\dfrac{\lambda^\star K}{\ln(2)}\Big/\mathbb{E}\left\{\dfrac{1}{\Upsilon_i}\right\}\right) & \text{if } i \in \mathcal{I},\\ 0 & \text{otherwise,}\end{cases}\\
&\frac{\kappa_1 d_i^2}{t_{\mathrm{mo},i}^{\star 2}} = \kappa_1 v_i^{\star 2} = \begin{cases} \lambda^\star\left(\dfrac{1}{\ln(2)} - R_i^\star\right) - \dfrac{1}{K}\mathbb{E}\left\{\dfrac{1}{\Upsilon_i}\right\} + \nu^\star + \kappa_4 - \epsilon_i^\star & \text{if } i \in \mathcal{I},\\ \nu^\star + \kappa_4 - \epsilon_i^\star & \text{otherwise,}\end{cases}\\
&\text{and } \ \delta_i^\star = \kappa_1 v_i^{\star 2} - \kappa_4 + \epsilon_i^\star,
\end{aligned} \tag{4.3}$$

where $\mathcal{I} = \{i \in \{1, \cdots, N_{\mathrm{SH}}\} \mid \mathbb{E}\{1/\Upsilon_i\} < \lambda^\star K/\ln(2)\}$.

From (4.3), it can be seen that $R_i^\star = 0$ if $\mathbb{E}\{1/\Upsilon_i\}$ is above the threshold $\lambda^\star K/\ln(2)$. This means that the robot does not transmit if the predicted channel quality is below a certain level. Furthermore, for $i, j \in \mathcal{I}$, we can see that $R_i^\star > R_j^\star$ if $\mathbb{E}\{1/\Upsilon_i\} < \mathbb{E}\{1/\Upsilon_j\}$. In summary, we have $R_i^\star \geq R_j^\star$ if $\mathbb{E}\{1/\Upsilon_i\} < \mathbb{E}\{1/\Upsilon_j\}$.

Next, consider $\kappa_1 v_i^{\star 2}$ in (4.3). It is straightforward to verify that $\kappa_1 v_i^{\star 2}+\epsilon_i^\star \leq \kappa_1 v_j^{\star 2}+\epsilon_j^\star$ if $\mathbb{E}\{1/\Upsilon_i\} < \mathbb{E}\{1/\Upsilon_j\}$. Note that the equality holds only if $i,j \in \{1,\cdots,N_{\rm SH}\}\backslash\mathcal{I}$. Suppose that $v_i^\star > v_j^\star$, then $0 \leq \epsilon_i^\star < \epsilon_j^\star$, resulting in $t_{{\rm mo},j}^\star = d_j/v_{\max}$, or equivalently $v_j^\star = v_{\max} \geq v_i^\star$. This contradicts the assumption that $v_i^\star > v_j^\star$. Hence, we have $v_i^\star \leq v_j^\star$ if $\mathbb{E}\{1/\Upsilon_i\} < \mathbb{E}\{1/\Upsilon_j\}$.

Finally, suppose that $t_{{\rm st},j}^\star > 0$ and $\mathbb{E}\{1/\Upsilon_j\} > \min_{k\in\{1,\cdots,N_{\rm SH}\}}\{\mathbb{E}\{1/\Upsilon_k\}\}$. Then there exists some $i \in \mathcal{I}$ such that $\mathbb{E}\{1/\Upsilon_i\} < \mathbb{E}\{1/\Upsilon_j\}$. This means that $\kappa_1 v_i^{\star 2}+\epsilon_i^\star < \kappa_1 v_j^{\star 2}+\epsilon_j^\star$, which results in $\delta_i^\star < \delta_j^\star$. Moreover, from the KKT conditions, we know that $\delta_j^\star = 0$ given $t_{{\rm st},j}^\star > 0$, which results in $\delta_i^\star < \delta_j^\star = 0$. This contradicts the constraint that $\delta_i \geq 0$. Hence, if $t_{{\rm st},i}^\star > 0$, then we must have $\mathbb{E}\{1/\Upsilon_i\} = \min_{j\in\{1,\cdots,N_{\rm SH}\}}\{\mathbb{E}\{1/\Upsilon_j\}\}$. ■

Theorem 2 shows that the robot should move slower at the locations that have higher predicted channel quality in order to send more bits. On the other hand, if the predicted channel quality is low, it should then speed up to escape from these regions quickly. Also, the robot should transmit faster (slower) at the locations that have higher (lower) predicted channel quality. If the predicted channel quality is too low, the robot should not transmit any information. As mentioned in Remark 1, we have $\mathbb{E}\{1/\Upsilon_i\} = \exp\big((\ln 10/10)^2\sigma_{{\rm dB},i}^2/2\big)/\overline{\Upsilon}_i$, which depends on the predicted mean value ($\overline{\Upsilon}_i$) and the prediction error variance ($\sigma_{{\rm dB},i}^2$). Hence, the robot moves slower and transmits faster at the locations that have larger predicted mean values and/or smaller prediction error variance. Finally, Theorem 2 says that if the robot must stop, it should then stop only once and at the location with the best predicted channel quality.

Corollary 1 *Let $k_{\rm best}$ denote the index where $\mathbb{E}\{1/\Upsilon_i\}$ has its minimum based on the predicted channel, i.e. $k_{\rm best} = \arg\min_{i\in\{1,\cdots,N_{\rm SH}\}}\{\mathbb{E}\{1/\Upsilon_i\}\}$. If $v_{\max} > \sqrt{\kappa_4/\kappa_1}$, we have $v_i^\star \geq \sqrt{\kappa_4/\kappa_1}$ for all i. Moreover, if $t_{{\rm st},k_{\rm best}}^\star > 0$, then $v_{k_{\rm best}}^\star = \sqrt{\kappa_4/\kappa_1}$. If $v_{\max} \leq \sqrt{\kappa_4/\kappa_1}$, we have $v_i^\star = v_{\max}$ for all i, and $t_{{\rm st},k_{\rm best}}^\star = T_{\rm tot} - D/v_{\max}$.*

Proof: From the proof of Theorem 2, we know that $\delta_i^\star = \kappa_1 v_i^{\star 2} - \kappa_4 + \epsilon_i^\star \geq 0$ for all i. Moreover, if $t^\star_{\mathrm{st},k_{\mathrm{best}}} > 0$, then we have $\delta^\star_{k_{\mathrm{best}}} = 0$. For the case of $v_{\max} > \sqrt{\kappa_4/\kappa_1}$, it is straightforward to verify that $\kappa_1 v_i^{\star 2} - \kappa_4 + \epsilon_i^\star \geq 0$ holds only if $v_i^\star \geq \sqrt{\kappa_4/\kappa_1}$. Furthermore, if $t^\star_{\mathrm{st},k_{\mathrm{best}}} > 0$, then $v^\star_{k_{\mathrm{best}}} = \sqrt{\kappa_4/\kappa_1}$. Similarly, for the case of $v_{\max} \leq \sqrt{\kappa_4/\kappa_1}$, the only possible solution is $v_i^\star = v_{\max}$ for all i, which also implies that $t^\star_{\mathrm{st},k_{\mathrm{best}}} = T_{\mathrm{tot}} - D/v_{\max}$. ■

Theorem 2 and Corollary 1 state that, in order to spend long enough time at the sub-trajectory where the predicted channel quality is the best, the robot stops at this location rather than reducing its speed below $\sqrt{\kappa_4/\kappa_1}$ if $v_{\max} > \sqrt{\kappa_4/\kappa_1}$ (or below $v_{\max}$ if $v_{\max} \leq \sqrt{\kappa_4/\kappa_1}$). As shown in Section 2.3, the aforementioned velocity minimizes the motion energy cost. Hence, the robot never reduces its speed below it in order to save the total energy.

Next, we consider the resulting optimum energy consumption of the robot. Consider the motion and communication energy costs ($E_{\mathrm{M},i}$ and $E_{\mathrm{C},i}$) as defined in (4.1). Define $E_{\mathrm{M,norm},i} \triangleq E_{\mathrm{M},i}/d_i = \kappa_1 d_i/t_{\mathrm{mo},i} + \kappa_4 t_{\mathrm{mo},i}/d_i$ and $E_{\mathrm{C,norm},i} \triangleq E_{\mathrm{C},i}/d_i = (2^{R_i} - 1)\mathbb{E}\{1/\Upsilon_i\}(t_{\mathrm{mo},i} + t_{\mathrm{st},i})/(d_i K)$ as the motion energy cost and the communication energy cost per unit length respectively. Then, based on the results of Theorem 2, we have the following corollary at the optimum solution, where $i, j \in \{1, \cdots, N_{\mathrm{SH}}\}$:

Corollary 2 *If* $\mathbb{E}\{1/\Upsilon_i\} < \mathbb{E}\{1/\Upsilon_j\}$*, then we have* $E^\star_{\mathrm{M,norm},i} \leq E^\star_{\mathrm{M,norm},j}$ *and* $E^\star_{\mathrm{C,norm},i} \geq E^\star_{\mathrm{C,norm},j}$.

Proof: From Theorem 2, we have $v_i^\star \leq v_j^\star$, $R_i^\star \geq R_j^\star$ and $t^\star_{\mathrm{st},i} \geq t^\star_{\mathrm{st},j}$ if $\mathbb{E}\{1/\Upsilon_i\} < \mathbb{E}\{1/\Upsilon_j\}$. Since $E_{\mathrm{C,norm},i}$ is monotonically increasing with respect to R_i and $t_{\mathrm{st},i}$, and is monotonically decreasing with respect to v_i, then $E^\star_{\mathrm{C,norm},i} \geq E^\star_{\mathrm{C,norm},j}$ if $\mathbb{E}\{1/\Upsilon_i\} < \mathbb{E}\{1/\Upsilon_j\}$. Moreover, from Corollary 1, we have $v_j^\star \geq v_i^\star \geq \sqrt{\kappa_4/\kappa_1}$ if $v_{\max} > \sqrt{\kappa_4/\kappa_1}$, and $v_j^\star = v_i^\star = v_{\max}$ if $v_{\max} \leq \sqrt{\kappa_4/\kappa_1}$. Since $E_{\mathrm{M,norm},i}$ is monotonically increasing

with respect to $v_i \geq \sqrt{\kappa_4/\kappa_1}$, then $E^{\star}_{\mathrm{M,norm},i} \leq E^{\star}_{\mathrm{M,norm},j}$ if $v_{\max} > \sqrt{\kappa_4/\kappa_1}$. Clearly, if $v_{\max} \leq \sqrt{\kappa_4/\kappa_1}$, then $E^{\star}_{\mathrm{M,norm},i} = E^{\star}_{\mathrm{M,norm},j}$. In summary, we have $E^{\star}_{\mathrm{M,norm},i} \leq E^{\star}_{\mathrm{M,norm},j}$ if $\mathbb{E}\{1/\Upsilon_i\} < \mathbb{E}\{1/\Upsilon_j\}$. ■

Corollary 2 shows that the robot should spend more motion energy per unit length to escape from the locations where the predicted channel quality is lower. Also, it should spend more communication energy per unit length to take advantage of the locations where the predicted channel quality is higher.

Remark 7 *So far, we assumed that κ_1, κ_2 and κ_4 are positive constants. Experimental results have shown that a linear model ($\kappa_1 = 0$) can also be used to approximate the motion energy cost for some types of robots, when the velocity is not very large [86], as discussed in Section 2.3. Furthermore, there could be cases where $\kappa_4 = 0$. Theorem 2 can be easily extended to address these special cases as we show in the next two lemmas.*

Lemma 14 *Consider the case where $\kappa_1 = 0$ and $\kappa_4 \neq 0$. The optimum motion speed ($v_i^{\star}$), transmission rate ($R_i^{\star}$) and stop time ($t^{\star}_{\mathrm{st},i}$) satisfy the following properties: $v_i^{\star} = v_{\max}$ for all i. If $\mathbb{E}\{1/\Upsilon_i\} < \mathbb{E}\{1/\Upsilon_j\}$, then $R_i^{\star} \geq R_j^{\star}$ for $i, j \in \{1, \cdots, N_{\mathrm{SH}}\}$. Moreover, if $\mathbb{E}\{1/\Upsilon_i\}$ is above a certain threshold, then there is no transmission in the corresponding sub-trajectory ($R_i^{\star} = 0$). Finally, $t^{\star}_{\mathrm{st},i} = T_{\mathrm{tot}} - D/v_{\max}$ if $\mathbb{E}\{1/\Upsilon_i\} = \min_{j\in\{1,\cdots,N_{\mathrm{SH}}\}}\{\mathbb{E}\{1/\Upsilon_j\}\}$.*

As compared to the results in Theorem 2, it can be seen that the robot always travels with its maximum velocity in this case since the distance to be travelled is given. Then the robot spends as much time as possible at the location that has the best predicted channel quality.[3]

[3]Note that if $\kappa_1 = \kappa_4 = 0$, Lemma 14 still holds except that the robot does not need to travel with its maximum speed along the sub-trajectory with the best predicted channel quality to achieve the optimality.

Lemma 15 *Consider the case where $\kappa_1 \neq 0$ and $\kappa_4 = 0$. The optimum motion speed ($v_i^\star$), transmission rate ($R_i^\star$) and stop time ($t_{\mathrm{st},i}^\star$) satisfy the following properties: if $\mathbb{E}\{1/\Upsilon_i\} < \mathbb{E}\{1/\Upsilon_j\}$, then $v_i^\star \leq v_j^\star$ and $R_i^\star \geq R_j^\star$ for $i, j \in \{1, \cdots, N_{\mathrm{SH}}\}$. Moreover, if $\mathbb{E}\{1/\Upsilon_i\}$ is above a certain threshold, then there is no transmission in the corresponding sub-trajectory ($R_i^\star = 0$). Finally, $t_{\mathrm{st},i}^\star = 0$ for all i.*

As compared to Theorem 2, the robot chooses to reduce its velocity rather than stopping, in order to save motion energy in this case.

Corollary 2 can similarly be generalized for the two cases discussed above. In the rest of the chapter, we assume that κ_1, κ_2 and κ_4 are positive constants.

4.1.2 Two Special Cases – Cases of Heavy-Task Load and Light-Task Load

In this section, we discuss two special cases of (4.2), namely the heavy-task load and the light-task load cases, in order to have a better understanding of the optimum design strategy.

Definition 2 *We say that the robot has a heavy-task load if $Q_{\mathrm{tot}}/T_{\mathrm{tot}}$ is considerably large, i.e. it needs to send a large number of bits in a relatively small given time budget. On the other hand, the robot has a light-task load if $Q_{\mathrm{tot}}/T_{\mathrm{tot}} \to 0$, i.e. it only needs to send a small number of bits under a relatively large time budget.*

Lemma 16 *Let k_{best} and k_{worst} denote the indices where $\mathbb{E}\{1/\Upsilon_i\}$ has its minimum and maximum based on the predicted channel respectively. If $v_{\max} > \sqrt{\kappa_4/\kappa_1}$ and $Q_{\mathrm{tot}}/T_{\mathrm{tot}} > \max\left\{B\big(\log_2\left(\mathbb{E}\left\{1/\Upsilon_{k_{\mathrm{worst}}}\right\}\right) - \log_2\left(\mathbb{E}\left\{1/\Upsilon_{k_{\mathrm{best}}}\right\}\right)\big), \eta\right\}$, where*

$$\eta = \max_{i\in\{1,\cdots,N_{\mathrm{SH}}\}} \left\{ B\log_2\left(\frac{K\kappa_1 v_{\max}^2 - \mathbb{E}\left\{1/\Upsilon_{k_{\mathrm{best}}}\right\} + \mathbb{E}\left\{1/\Upsilon_i\right\}}{\big(\log_2\left(\mathbb{E}\left\{1/\Upsilon_i\right\}\right) - \log_2\left(\mathbb{E}\left\{1/\Upsilon_{k_{\mathrm{best}}}\right\}\right)\big)\mathbb{E}\left\{1/\Upsilon_{k_{\mathrm{best}}}\right\}\ln(2)}\right)\right\}, \tag{4.4}$$

then we have: 1) $v_i^\star = v_{\max}$ *for all* $i \neq k_{\text{best}}$*, and* $v_{k_{\text{best}}}^\star = \max\left\{\sqrt{\kappa_4/\kappa_1}, d_{k_{\text{best}}}/(T_{\text{tot}} - \sum_{i\neq k_{\text{best}}} d_i/v_{\max})\right\}$*; and 2)* $t_{\text{st},k_{\text{best}}}^\star = \max\left\{T_{\text{tot}} - \sum_{i\neq k_{\text{best}}} d_i/v_{\max} - d_{k_{\text{best}}}\sqrt{\kappa_1/\kappa_4}, 0\right\}$*. Therefore, given an arbitrarily large* $v_{\max}$ *and an arbitrarily large* $Q_{\text{tot}}/T_{\text{tot}}$*, we have the following asymptotic behavior: 1)* $v_i^\star = v_{\max}$ *can become arbitrarily large for all* $i \neq k_{\text{best}}$*; 2)* $(t_{\text{mo},k_{\text{best}}}^\star + t_{\text{st},k_{\text{best}}}^\star)/T_{\text{tot}}$ *can become arbitrarily close to* 1*; and 3)* $R_{k_{\text{best}}}^\star(t_{\text{mo},k_{\text{best}}}^\star + t_{\text{st},k_{\text{best}}}^\star)/(Q_{\text{tot}}/B)$ *can become arbitrarily close to* 1*.*

Proof: From Theorem 2, it can be seen that

$$R_{k_{\text{best}}}^\star = \log_2\left(K\lambda^\star/\ln(2)\right) - \log_2\left(\mathbb{E}\left\{1/\Upsilon_{k_{\text{best}}}\right\}\right) \geq Q_{\text{tot}}/(BT_{\text{tot}}). \tag{4.5}$$

This is lower bounded by $Q_{\text{tot}}/(BT_{\text{tot}})$ since the robot has to send with at least as fast as the average rate ($Q_{\text{tot}}/(BT_{\text{tot}})$) at the place with the best predicted channel quality, in order to finish the task in the given time. Hence, if $Q_{\text{tot}}/T_{\text{tot}} > B\big(\log_2\left(\mathbb{E}\left\{1/\Upsilon_{k_{\text{worst}}}\right\}\right) - \log_2\left(\mathbb{E}\left\{1/\Upsilon_{k_{\text{best}}}\right\}\right)\big)$, we have $\mathbb{E}\left\{1/\Upsilon_i\right\} < K\lambda^\star/\ln(2)$ for all i. From (4.3), we then have the following for $i \neq k_{\text{best}}$:

$$\begin{aligned}
\kappa_1 v_i^{\star 2} - \kappa_1 v_{k_{\text{best}}}^{\star 2} &= \log_2\left(\mathbb{E}\left\{\frac{1}{\Upsilon_i}\right\}\Big/\mathbb{E}\left\{\frac{1}{\Upsilon_{k_{\text{best}}}}\right\}\right)\lambda^\star \\
&\quad + \frac{1}{K}\left(\mathbb{E}\left\{\frac{1}{\Upsilon_{k_{\text{best}}}}\right\} - \mathbb{E}\left\{\frac{1}{\Upsilon_i}\right\}\right) - \epsilon_i^\star + \epsilon_{k_{\text{best}}}^\star \\
&\geq \log_2\left(\mathbb{E}\left\{\frac{1}{\Upsilon_i}\right\}\Big/\mathbb{E}\left\{\frac{1}{\Upsilon_{k_{\text{best}}}}\right\}\right)\frac{\ln(2)}{K}2^{Q_{\text{tot}}/(BT_{\text{tot}})}\mathbb{E}\left\{\frac{1}{\Upsilon_{k_{\text{best}}}}\right\} \\
&\quad + \frac{1}{K}\left(\mathbb{E}\left\{\frac{1}{\Upsilon_{k_{\text{best}}}}\right\} - \mathbb{E}\left\{\frac{1}{\Upsilon_i}\right\}\right) - \epsilon_i^\star + \epsilon_{k_{\text{best}}}^\star \\
&> \kappa_1 v_{\max}^2 - \epsilon_i^\star + \epsilon_{k_{\text{best}}}^\star,
\end{aligned} \tag{4.6}$$

if $Q_{\text{tot}}/T_{\text{tot}} > \eta$. This equation implies that $\epsilon_i^\star > 0$ for all $i \neq k_{\text{best}}$. Hence, we have $v_i^\star = v_{\max}$ for all $i \neq k_{\text{best}}$, and $v_{k_{\text{best}}}^\star = \max\left\{\sqrt{\kappa_4/\kappa_1}, d_{k_{\text{best}}}/(T_{\text{tot}} - \sum_{i\neq k_{\text{best}}} d_i/v_{\max})\right\}$. Also, $t_{\text{st},k_{\text{best}}}^\star = \max\left\{T_{\text{tot}} - \sum_{i\neq k_{\text{best}}} d_i/v_{\max} - d_{k_{\text{best}}}\sqrt{\kappa_1/\kappa_4}, 0\right\}$. Therefore, given an

arbitrarily large $v_{\max}$, the asymptotic behavior can be easily verified. ■

Intuitively, if the task load is heavy, it is more important for the robot to minimize the communication energy cost. Lemma 16 says that, in this case, the robot will spend as long time as possible at the location that has the best predicted channel quality in order to save communication energy. To achieve this, the robot needs to travel with its maximum velocity to pass other places quickly.

Lemma 17 *Let k_{best} denote the index where $\mathbb{E}\{1/\Upsilon_i\}$ has its minimum based on the predicted channel. If $v_{\max} > \sqrt{\kappa_4/\kappa_1}$ and $Q_{\text{tot}}/T_{\text{tot}} \to 0$, then 1) $v_i^\star \to v_{k_{\text{best}}}^\star$ and $R_i^\star = 0$ for all $i \neq k_{\text{best}}$; 2) if $T_{\text{tot}} \geq \sqrt{\kappa_1/\kappa_4}D$, then $v_{k_{\text{best}}}^\star = \sqrt{\kappa_4/\kappa_1}$ and $t_{\text{st},k_{\text{best}}}^\star \to T_{\text{tot}} - \sqrt{\kappa_1/\kappa_4}D$; 3) if $T_{\text{tot}} < \sqrt{\kappa_1/\kappa_4}D$, then $v_{k_{\text{best}}}^\star \to D/T_{\text{tot}}$ and $t_{\text{st},k_{\text{best}}}^\star = 0$; and 4) $R_{k_{\text{best}}}^\star(t_{\text{mo},k_{\text{best}}}^\star + t_{\text{st},k_{\text{best}}}^\star)/(Q_{\text{tot}}/B) = 1$.*

Proof: From Theorem 2, we know that the robot moves slower or even stops along $\mathcal{T}_{k_{\text{best}}}$ (the sub-trajectory with the best predicted channel quality). Hence, the time budget allocated to $\mathcal{T}_{k_{\text{best}}}$ should be larger than or equal to $T_{\text{tot}}d_{k_{\text{best}}}/D$. Then, we have $R_{k_{\text{best}}}^\star = \log_2(K\lambda^\star/\ln(2)) - \log_2(\mathbb{E}\{1/\Upsilon_{k_{\text{best}}}\}) \leq Q_{\text{tot}}/(BT_{\text{tot}}d_{k_{\text{best}}}/D)$. Therefore, as $Q_{\text{tot}}/T_{\text{tot}} \to 0$, we have $\mathbb{E}\{1/\Upsilon_i\} > K\lambda^\star/\ln(2)$ for all $i \neq k_{\text{best}}$. This means that $R_i^\star = 0$ for all $i \neq k_{\text{best}}$, based on Theorem 2. Similar to the proof of Lemma 16, we then have

$$\begin{aligned}
0 \leq \kappa_1 v_i^{\star 2} - \kappa_1 v_{k_{\text{best}}}^{\star 2} &= \frac{1}{K}\mathbb{E}\left\{\frac{1}{\Upsilon_{k_{\text{best}}}}\right\} - \left(\frac{1}{\ln(2)} - R_{k_{\text{best}}}^\star\right)\lambda^\star - \epsilon_i^\star + \epsilon_{k_{\text{best}}}^\star \\
&\leq \frac{1}{K}\mathbb{E}\left\{\frac{1}{\Upsilon_{k_{\text{best}}}}\right\} - \left(\frac{1}{\ln(2)} - \frac{DQ_{\text{tot}}}{BT_{\text{tot}}d_{k_{\text{best}}}}\right)\frac{\ln(2)}{K}2^{Q_{\text{tot}}/(BT_{\text{tot}})}\mathbb{E}\left\{\frac{1}{\Upsilon_{k_{\text{best}}}}\right\} - \epsilon_i^\star + \epsilon_{k_{\text{best}}}^\star \\
&\leq \frac{1}{K}\mathbb{E}\left\{\frac{1}{\Upsilon_{k_{\text{best}}}}\right\} - \left(\frac{1}{\ln(2)} - \frac{DQ_{\text{tot}}}{BT_{\text{tot}}d_{k_{\text{best}}}}\right)\frac{\ln(2)}{K}2^{Q_{\text{tot}}/(BT_{\text{tot}})}\mathbb{E}\left\{\frac{1}{\Upsilon_{k_{\text{best}}}}\right\}, \qquad (4.7)
\end{aligned}$$

where the last inequality holds since $v_i^\star \geq v_{k_{\text{best}}}^\star$, resulting in $\epsilon_i^\star \geq \epsilon_{k_{\text{best}}}^\star$. As can be seen, as $Q_{\text{tot}}/T_{\text{tot}} \to 0$, the right hand side of (4.7) goes to 0. Thus, $v_i^\star \to v_{k_{\text{best}}}^\star$ for all $i \neq k_{\text{best}}$. Also, from Theorem 2, we have $t_{\text{st},i}^\star = 0$ for all $i \neq k_{\text{best}}$. Then, from Corollary

1, it is straightforward to show that $v^\star_{k_{\text{best}}} = \sqrt{\kappa_4/\kappa_1}$ and $t^\star_{\text{st},k_{\text{best}}} \to T_{\text{tot}} - \sqrt{\kappa_1/\kappa_4}D$ if $T_{\text{tot}} \geq \sqrt{\kappa_1/\kappa_4}D$, and $v^\star_{k_{\text{best}}} \to D/T_{\text{tot}}$ and $t^\star_{\text{st},k_{\text{best}}} = 0$ if $T_{\text{tot}} < \sqrt{\kappa_1/\kappa_4}D$. Finally, since $R^\star_i = 0$ for all $i \neq k_{\text{best}}$, we must have $R^\star_{k_{\text{best}}}(t^\star_{\text{mo},k} + t^\star_{\text{st},k_{\text{best}}})/(Q_{\text{tot}}/B) = 1$. ■

As compared to the heavy-task load case, it is more important to minimize the motion energy cost if the task load is light. Lemma 17 shows that in this case, the robot moves with an asymptotic constant speed of $\sqrt{\kappa_4/\kappa_1}$ along the whole trajectory in order to save motion energy. The constant speed is the speed that minimizes the motion energy if that speed can ensure achieving the task in the given time budget. If not, then the constant speed is D/T_{tot}. Finally, since there is only very limited number of bits to be sent, the robot only transmits at the location with the best predicted channel quality.

Remark 8 *Note that we only consider the case where $v_{\max} > \sqrt{\kappa_4/\kappa_1}$ in Lemmas 16 and 17. If $v_{\max} \leq \sqrt{\kappa_4/\kappa_1}$, then $v^\star_i = v_{\max}$ for all i, as we have shown in Corollary 1.*

4.2 Stop-Time Online Adaptation to Multipath Fading

As mentioned in Section 2.1, the channel along each $\mathcal{T}_i$ is still space-varying due to multipath fading, especially in rich scattering environments. Unlike path loss and shadowing, the multipath fading component of the channel is unpredictable. Hence, there is no efficient way of predicting its spatial variations ahead of time and planning accordingly. However, as the robot moves along each sub-trajectory, it can measure the true value of the channel and further fine tune its strategies, as we propose in this section. More specifically, we show how the robot can optimize its stop time location within a designated sub-trajectory, based on its online measurement of the channel and by using the computationally-efficient nested form of multi-stage stochastic programming [118].

From Corollary 1, we know that the total motion time of the whole operation is always less than or equal to $\sqrt{\kappa_1/\kappa_4}D$. Then, the robot will spend most of its time resource on the stop time, if the time budget is considerably larger than $\sqrt{\kappa_1/\kappa_4}D$. Therefore, carefully selecting the location of the stop time within the designated sub-trajectory (which is found in Section 4.1) can further reduce the energy consumption, as we show in this section.

Let $\mathcal{T}_i$ denote the sub-trajectory that was assigned a stop time based on (4.2). We divide $\mathcal{T}_i$ into $N_{\mathrm{MP},i}$ equal-length chunks, $\mathcal{T}_{i,j}$s, for $j \in \{1, \cdots, N_{\mathrm{MP},i}\}$, over which the channel is considered constant. Let $\gamma_{i,j}$ denote the CNR in $\mathcal{T}_{i,j}$. The process of online adaptation along $\mathcal{T}_i$ is summarized as follows. The robot obtains the optimum number of bits of information, and the motion and stop times that are assigned to $\mathcal{T}_i$ from (4.2). As the robot moves to $\mathcal{T}_{i,1}$, it measures $\gamma_{i,1}$. Then, it fine tunes its strategy based on the measurement of $\gamma_{i,1}$, and the estimation of $\gamma_{i,j}$ for $j \in \{2, \cdots, N_{\mathrm{MP},i}\}$. This process will go on until it reaches the end of $\mathcal{T}_i$. For those CNR values that the robot has not observed yet, it models them with the probabilistic channel prediction framework of Section 2.1, i.e. as lognormal random variables. More specifically, let $R_{i,j}$, $t_{\mathrm{mo},i,j}$ and $t_{\mathrm{st},i,j}$ be the spectral efficiency, motion time and stop time allocated to $\mathcal{T}_{i,j}$ respectively. Then, we have $R_{i,j} = R_i^\star$ and $t_{\mathrm{mo},i,j} = t_{\mathrm{mo},i}^\star/N_{\mathrm{MP},i}$ for all j, and we need to design a stop time strategy subject to $\sum_{j=1}^{N_{\mathrm{MP},i}} t_{\mathrm{st},i,j} = t_{\mathrm{st},i}^\star > 0$, where $R_i^\star$, $t_{\mathrm{mo},i}^\star$ and $t_{\mathrm{st},i}^\star$ are given by the solution of (4.2). Thus, the variables to solve for are $t_{\mathrm{st},i,j}$s.

In this section, we use multi-stage stochastic programming to design such a strategy [118]. In particular, we consider the nested form of the objective function, which allows us to solve the problem iteratively. Then, at step $\mathcal{T}_{i,j}$, for $j \in \{1, \cdots, N_{\mathrm{MP},i} - 1\}$, the

robot can solve the following optimization problem to decide how to use the stop time:

$$\begin{aligned} \text{minimize} \quad & J_{\mathrm{MP,st},i,j}(T_{\mathrm{st},i,j}) = \frac{2^{R_i^\star}-1}{K\gamma_{i,j}}\left(\sqrt{\frac{\kappa_1}{\kappa_4}}\frac{d_i}{N_{\mathrm{MP},i}} + t_{\mathrm{st},i,j}\right) + \frac{2\sqrt{\kappa_1\kappa_4}d_i}{N_{\mathrm{MP},i}} \\ & \qquad\qquad + \mathbb{E}\{J^\star_{\mathrm{MP,st},i,j+1}(T_{\mathrm{st},i,j+1})\} \\ \text{subject to} \quad & t_{\mathrm{st},i,j} + T_{\mathrm{st},i,j+1} = T_{\mathrm{st},i,j}, \quad t_{\mathrm{st},i,j},\, T_{\mathrm{st},i,j+1} \geq 0, \end{aligned}$$

where $T_{\mathrm{st},i,j+1} = t^\star_{\mathrm{st},i} - \sum_{\ell=1}^{j} t^\star_{\mathrm{st},i,\ell}$ denotes the remaining stop time available at step $\mathcal{T}_{i,j+1}$, and $J_{\mathrm{MP,st},i,j}$ is the average total energy cost from $\mathcal{T}_{i,j}$ to $\mathcal{T}_{i,N_{\mathrm{MP},i}}$. Note that $T_{\mathrm{st},i,1} = t^\star_{\mathrm{st},i}$, i.e. the remaining stop time at step $\mathcal{T}_{i,1}$ is equal to the stop time that is assigned to $\mathcal{T}_i$. Also, we use the fact that $t^\star_{\mathrm{mo},i} = \sqrt{\kappa_1/\kappa_4}d_i$ in (4.8).

The optimization problem of (4.8) minimizes the average total energy cost along the rest of $\mathcal{T}_i$, i.e. from $\mathcal{T}_{i,j}$ to $\mathcal{T}_{i,N_{\mathrm{MP},i}}$. Note that, at step $\mathcal{T}_{i,j}$, $\gamma_{i,j}$ is a constant since it has already been measured by the robot. Then the sum of the first and the second terms of the objective function in (4.8) represents the energy cost along $\mathcal{T}_{i,j}$. However, $J^\star_{\mathrm{MP,st},i,j+1}$, which is a function of $\gamma_{i,\ell}$, for $\ell \in \{j+1, \cdots, N_{\mathrm{MP},i}\}$, is still a random variable. Hence, we use the average of $J^\star_{\mathrm{MP,st},i,j+1}$ to represent the energy cost. The averaging is done over the distribution of the remaining unvisited channel samples in that sub-trajectory, which is characterized by using the probabilistic channel prediction framework.

Since solving the optimization problem at step $\mathcal{T}_{i,j}$ requires the average of the optimum value at step $\mathcal{T}_{i,j+1}$, i.e. $\mathbb{E}\{J^\star_{\mathrm{MP,st},i,j+1}(T_{\mathrm{st},i,j+1})\}$, equation (4.8) can be solved from the $(N_{\mathrm{MP},i}-1)^{\mathrm{th}}$ step, and then backtracked to the j^{th} step, which is similar to dynamic programming. Note that, at each step, equation (4.8) is a linear program, which can be solved uniquely. Then, we have the following optimum stop-time online adaptation strategy:

Lemma 18 *The optimum stop-time online adaptation strategy along $\mathcal{T}_{i,j}$, for $j \in \{1, \cdots,$*

$N_{\mathrm{MP},i}-1\}$, *is*

$$t^{\star}_{\mathrm{st},i,j}=\begin{cases} T_{\mathrm{st},i,j} & \text{if } \dfrac{1}{\gamma_{i,j}}\leq \underbrace{\mathbb{E}\left\{\min\left\{\dfrac{1}{\Upsilon_i},\cdots,\mathbb{E}\left\{\min\left\{\dfrac{1}{\Upsilon_i},\mathbb{E}\left\{\dfrac{1}{\Upsilon_i}\right\}\right\}\right\}\cdots\right\}\right\}}_{(N_{\mathrm{MP},i}-j)\text{ -step nested expectation}}. \\ 0 & \text{otherwise.}\end{cases} \tag{4.8}$$

Moreover, the average total energy cost along $\mathcal{T}_i$, after implementing (4.8), is[4]

$$\begin{aligned}\mathbb{E}\{J^{\star}_{\mathrm{MP,st},i,1}(t^{\star}_{\mathrm{st},i})\}=\frac{2^{R^{\star}_i}-1}{K}\Bigg(&\mathbb{E}\left\{\frac{1}{\Upsilon_i}\right\}\sqrt{\frac{\kappa_1}{\kappa_4}}d_i \\ &+\underbrace{\mathbb{E}\left\{\min\left\{\frac{1}{\Upsilon_i},\cdots,\mathbb{E}\left\{\min\left\{\frac{1}{\Upsilon_i},\mathbb{E}\left\{\frac{1}{\Upsilon_i}\right\}\right\}\right\}\cdots\right\}\right\}}_{N_{\mathrm{MP},i}\text{ -step nested expectation}}t^{\star}_{\mathrm{st},i}\Bigg)+2\sqrt{\kappa_1\kappa_4}d_i.\end{aligned} \tag{4.9}$$

Proof: Consider the $(N_{\mathrm{MP},i}-1)^{\mathrm{th}}$ step of the optimization problem of (4.8). It can be shown that $t^{\star}_{\mathrm{st},i,N_{\mathrm{MP},i}-1}=\begin{cases} T_{\mathrm{st},i,N_{\mathrm{MP},i}-1} & \text{if } 1/\gamma_{i,N_{\mathrm{MP},i}-1}\leq\mathbb{E}\{1/\Upsilon_i\} \\ 0 & \text{otherwise}\end{cases}$. Then, $J^{\star}_{\mathrm{MP,st},i,N_{\mathrm{MP},i}-1}(T_{\mathrm{st},i,N_{\mathrm{MP},i}-1})=((2^{R^{\star}_i}-1)/K)\big((\mathbb{E}\{1/\Upsilon_i\}+1/\gamma_{i,N_{\mathrm{MP},i}-1})\sqrt{\kappa_1/\kappa_4}d_i/N_{\mathrm{MP},i}+\min\{1/\gamma_{i,N_{\mathrm{MP},i}-1},\mathbb{E}\{1/\Upsilon_i\}\}T_{\mathrm{st},i,N_{\mathrm{MP},i}-1}\big)+4\sqrt{\kappa_1\kappa_4}d_i/N_{\mathrm{MP},i}$. At the $(N_{\mathrm{MP},i}-2)^{\mathrm{th}}$ step, $\gamma_{i,N_{\mathrm{MP},i}-1}$ is a random variable. Thus, we have the following averaging

$$\begin{aligned}\mathbb{E}\{J^{\star}_{\mathrm{MP,st},i,N_{\mathrm{MP},i}-1}(T_{\mathrm{st},i,N_{\mathrm{MP},i}-1})\}=\frac{2^{R^{\star}_i}-1}{K}\Bigg(&2\mathbb{E}\left\{\frac{1}{\Upsilon_i}\right\}\frac{\sqrt{\kappa_1/\kappa_4}d_i}{N_{\mathrm{MP},i}} \\ &+\mathbb{E}\left\{\min\left\{\frac{1}{\Upsilon_i},\mathbb{E}\left\{\frac{1}{\Upsilon_i}\right\}\right\}T_{\mathrm{st},i,N_{\mathrm{MP},i}-1}\right)+4\frac{\sqrt{\kappa_1\kappa_4}d_i}{N_{\mathrm{MP},i}}.\end{aligned} \tag{4.10}$$

The $(N_{\mathrm{MP},i}-2)^{\mathrm{th}}$ step of the optimization problem of (4.8) can be solved similarly. By induction, we can backtrack to the j^{th} step. Equations (4.8) and (4.9) can then be easily confirmed in this way. ■

[4]Note that one-step nested expectation means $\mathbb{E}\{1/\Upsilon_i\}$. Similarly, two-step nested expectation means $\mathbb{E}\{\min\{1/\Upsilon_i,\mathbb{E}\{1/\Upsilon_i\}\}\}$. The same rule applies to higher steps.

The optimum strategy of (4.8) results in the robot only stopping once along $\mathcal{T}_i$ to spend all its time budget. The lemma then allows the robot to optimally choose that stop location. More specifically, the nested expectation in (4.8) decreases as the number of nested steps increases. Hence, the nested expectation is small when the robot operates at the beginning of $\mathcal{T}_i$, i.e. when j is small. This means that the robot will spend all the stop time resource at the beginning of $\mathcal{T}_i$ only if the measured value of $\gamma_{i,j}$ is very large. On the other hand, the nested expectation becomes larger towards the end of $\mathcal{T}_i$, i.e. when j is large. This implies that the robot is more likely to choose a location to stop if it is towards the end of the sub-trajectory and it has not found a good spot yet. Intuitively, at the beginning of $\mathcal{T}_i$, the robot is not in a rush to spend the stop time since there is a good chance that a better $\gamma_{i,j}$ can be observed later. However, as the robot approaches the end of $\mathcal{T}_i$, the probability of observing a better $\gamma_{i,j}$ becomes smaller, forcing the robot to choose the stop location quicker.

Note that, for a lognormally-distributed Υ_i, the nested expectation can be found by using (4.11) iteratively,

$$\mathbb{E}\left\{\min\left\{\frac{1}{\Upsilon_i}, c\right\}\right\} = c\Theta\left(\frac{1}{\sigma_{\mathrm{dB},i}}\frac{10}{\ln 10}\ln\left(c\overline{\Upsilon}_i\right)\right) + \frac{1}{\overline{\Upsilon}_i}\exp\left(\left(\frac{\ln 10}{10}\right)^2\frac{\sigma_{\mathrm{dB},i}^2}{2}\right)\Theta\left(-\frac{1}{\sigma_{\mathrm{dB},i}}\frac{10}{\ln 10}\ln\left(c\overline{\Upsilon}_i\right) + \frac{\ln 10}{10}\sigma_{\mathrm{dB},i}\right), \quad (4.11)$$

where c is a constant calculated from the previous iteration (the previous nested expectation) and Θ is the Q function. To reduce the computation, the nested expectation can be found offline before the operation and saved to the memory of the robot.

In summary, the following are the steps of our proposed co-optimization framework. First, the robot predicts the shadowing and path loss components of the channel along the given trajectory, based on a small number of a priori channel measurements in the

same environment. Then, based on the given time budget, the total number of bits of information to be transmitted, and the required target BER, the robot finds the optimum motion speed, stop time, and transmission rate for each sub-trajectory, $\mathcal{T}_i$, by solving (4.2). If $t^{\star}_{\mathrm{st},i} > 0$, for some i, i.e. there is a stop time, the robot evaluates (4.11) iteratively for that corresponding sub-trajectory, and implements (4.8) based on the online measurement of the channel, in order to optimally choose the stop location.

4.3 Simulation Results

In this section, we test our framework by using real channel measurements from downtown San Francisco (data courtesy of W. M. Smith) [119].[5] Fig. 4.2 (a) shows the channel power along a fixed path with the length of 240 m. As can be seen, the channel is dominated by shadowing and multipath fading. This waveform is taken from the real measurements of [119]. Since we do not know the transmit power in that specific measurement, we assume that 1 W of transmit power was used (without loss of generality) to generate the channel power waveform. This will serve as the true channel power for testing our framework in this section. Furthermore, we assume that the receiver noise power is -80 dBm, and the robot has 10% a priori channel samples gathered in the same environment to estimate the channel. We take $d_i = 10$ m ($N_{\mathrm{SH}} = 24$) for all i. Fig. 4.2 (b) then shows the estimated $\mathbb{E}\{1/\Upsilon_i\}$, which is an indication of predicated channel quality along the fixed path (see Remark 1 in Section 2.1). Moreover, the motion parameters are taken as $v_{\max} = 6$ m/s, $\kappa_1 = 4.39$, $\kappa_2 = 24.67$ and $\kappa_4 = 14.77$ [87].

Fig. 4.2 shows the results of our co-optimization framework of Section 4.1 (only adaptation to shadowing and path loss). We have $Q_{\mathrm{tot}}/B = 250$ bits/Hz and $T_{\mathrm{tot}} = 120$ seconds in this example. The optimization problem of (4.2) is solved numerically by

[5] Similar results are obtained with simulated channels.

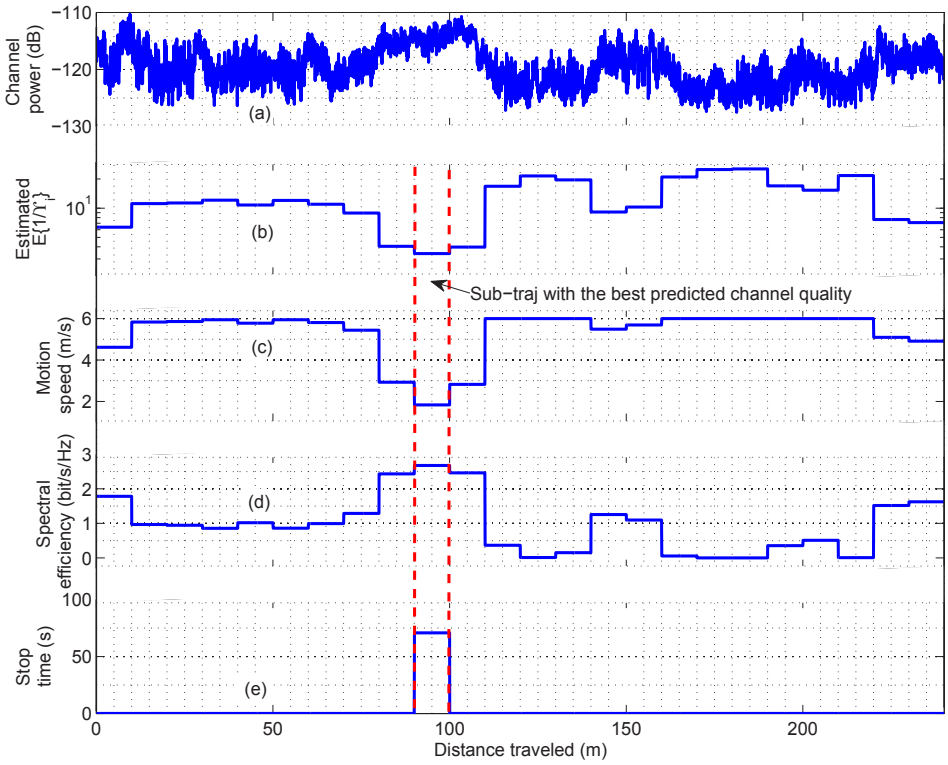

Figure 4.2: Illustration of the performance of our co-optimization strategy. Figures a and b show the signal strength and the predicted channel quality along the trajectory respectively. Figures c, d and e show the optimum motion speed, spectral efficiency, and stop time of our proposed co-optimization framework of Section 4.1 respectively. In this case, the robot predicts the shadowing and path loss components of the channel along its trajectory and plans its strategy accordingly.

using the Optimization Toolbox of MATLAB. As can be seen from Fig. 4.2 (c and d), the robot moves slower and sends faster at the places that have better predicted channel quality. Moreover, the robot stops at the location with the best predicted channel quality, as marked in Fig. 4.2 (e). We next compare the total energy consumption with the two cases of 1) no planning, i.e. the robot travels with the constant speed of D/T_{tot} and chooses the constant spectral efficiency of $Q_{\text{tot}}/(BT_{\text{tot}})$, and 2) separately optimizing the motion speed and the spectral efficiency, i.e. the robot travels with the constant speed of D/T_{tot} and optimizes the spectral efficiency based on the predicted channel quality. As compared to our co-optimization strategy, the robot needs to consume 2.06 times more

energy in the case of no planning, and 1.76 times more in the case of separate optimization of motion speed and spectral efficiency in order to accomplish the same task. With the additional online stop-time adaptation of Section 4.2, the robot further optimizes where to stop in the designated sub-trajectory as it learns the true value of the channel along its path. In this example, this additional optimization can further save 18.4% energy as compared to the case of only implementing our co-optimization framework of Section 4.1.

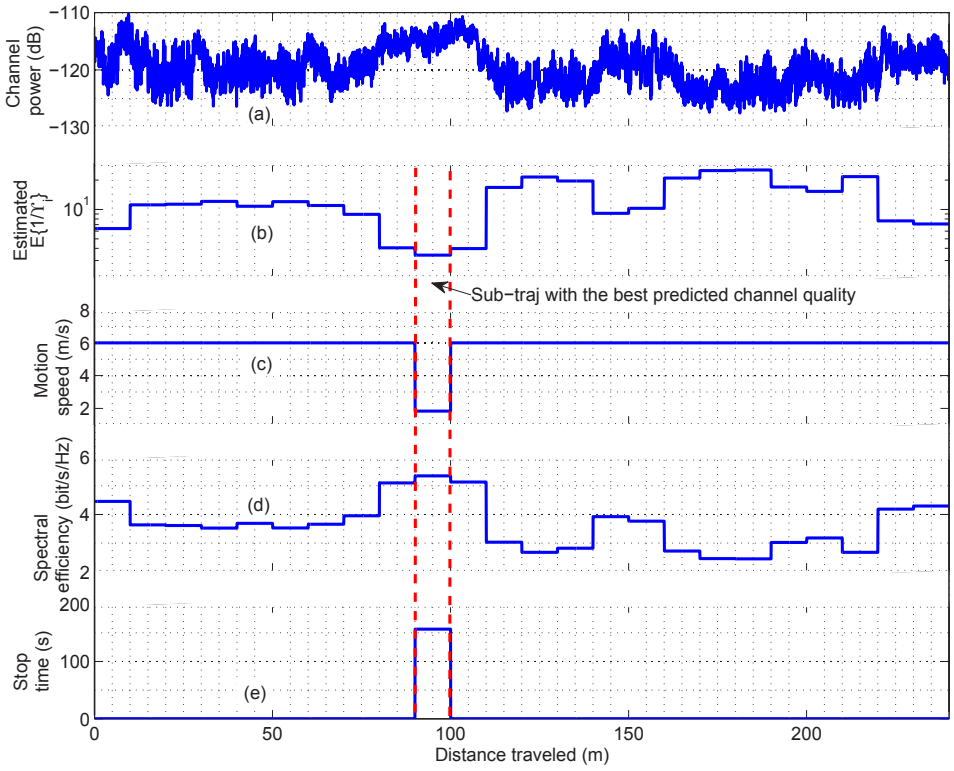

Figure 4.3: Illustration of the performance of our co-optimization strategy for the case of heavy-task load.

Next, Fig. 4.3 and 4.4 show the optimum strategies of the heavy and light-task cases. We have $T_{\text{tot}} = 200$ seconds for both cases, $Q_{\text{tot}}/B = 1000$ bits/Hz for the heavy-task load case and $Q_{\text{tot}}/B = 10$ bits/Hz for the light-task load case.[6] As can be seen in Fig.

[6]We choose a small value for Q_{tot}/B to show the asymptotic behavior of the light-task load case. As such, the optimum solution is not exactly the same as the asymptotic case. But they are very close.

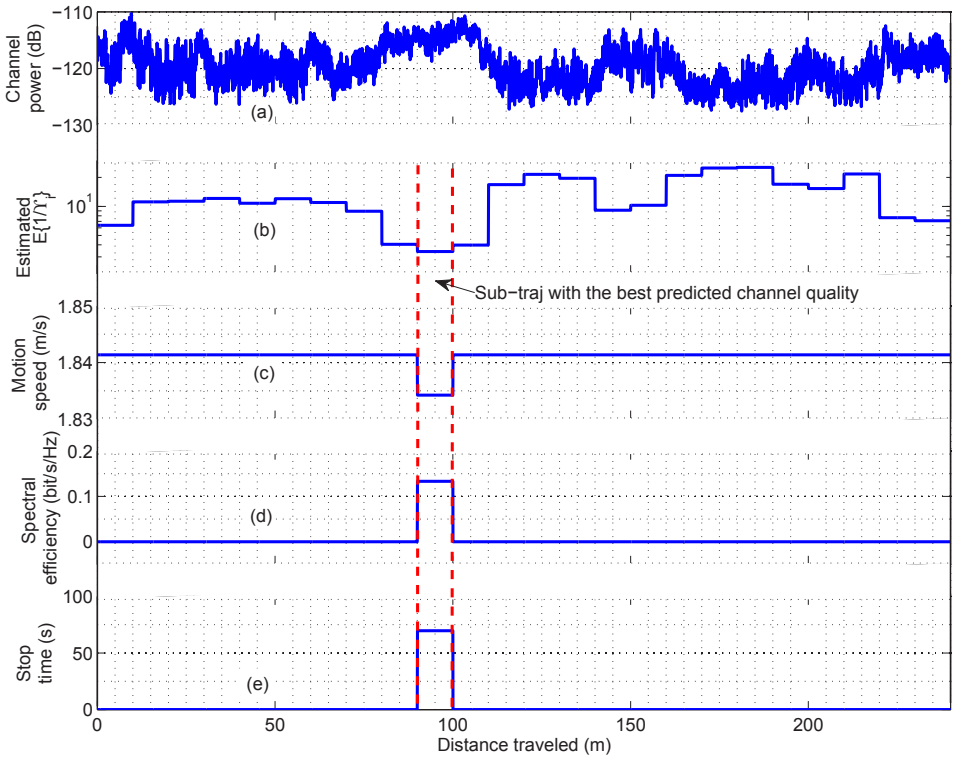

Figure 4.4: Illustration of the performance of our co-optimization strategy for the case of light-task load.

4.3 (c), if the robot has a heavy-task load, it moves with its maximum velocity along the sub-trajectories where the predicted channel quality is not the best. The rest of the time budget (154 seconds) is allocated to the place with the best predicted channel quality. On the other hand, if the task load is light (Fig. 4.4), the robot moves with an almost constant speed along the whole trajectory and transmits at the location with the best predicted channel quality, as shown in Fig. 4.4 (c and d) respectively. Note that $v = \sqrt{\kappa_4/\kappa_1} = 1.83$ m/s minimizes the motion energy cost along $\mathcal{T}$. It can be seen from Fig. 4.4 (c) that the robot moves with a speed very close to this value for the light-load case, as predicted by Lemma 17.

4.4 Extensions to Online Sensing and Data Gathering

So far, we have considered the case where the bits of information that need to be transmitted are fixed and assigned to the robot at the beginning of the operation. In some applications, the robot is required to sense a number of points of interest, gather the sensing data, and then transmit the data to the remote station online and during the operation. In this part, we briefly discuss how our proposed co-optimization framework of Section 4.1 can be generalized to such cases.[7]

Consider the scenario where there are $N_{\rm I}$ points of interest located at $z_i \in \mathcal{T}$, for $i \in \{1, \cdots, N_{\rm I}\}$, that the robot needs to visit. $\mathcal{T}$ is the pre-defined trajectory as defined previously. Let $Q_i > 0$ denote the number of bits of information that the robot can gather at z_i. Also, let $Q_0 \geq 0$ denote the initial number of bits of information that the robot has before starting the operation. Similar to Section 4.1, $\mathcal{T}$ is divided into $N_{\rm SH}$ sub-trajectories ($\mathcal{T}_i$s, for $i \in \{1, 2, \cdots, N_{\rm SH}\}$). Without loss of generality, we also assume that $\mathcal{T}$ is divided in such a way that z_i is located at the beginning of $\mathcal{T}_{{\rm Ind}(z_i)}$, where ${\rm Ind}(z_i)$ represents the index of the sub-trajectory where z_i is located. Then, the optimization framework of (4.2) can be generalized as follows:

$$\begin{aligned}
\text{minimize} \quad & J_{\rm SH} = \sum_{i=1}^{N_{\rm SH}} \frac{2^{R_i}-1}{K} \mathbb{E}\left\{\frac{1}{\Upsilon_i}\right\}(t_{{\rm mo},i} + t_{{\rm st},i}) + \frac{\kappa_1 d_i^2}{t_{{\rm mo},i}} + \kappa_4 t_{{\rm mo},i} \\
\text{subject to} \quad & \sum_{i=1}^{N_{\rm SH}} t_{{\rm mo},i} + t_{{\rm st},i} \leq T_{\rm tot}, \quad \sum_{i=1}^{N_{\rm SH}} R_i(t_{{\rm mo},i} + t_{{\rm st},i}) = \sum_{i=0}^{N_{\rm I}} Q_i/B, \\
& \sum_{i=1}^{{\rm Ind}(z_j)-1} R_i(t_{{\rm mo},i} + t_{{\rm st},i}) \leq \sum_{i=0}^{j-1} Q_i/B, \ \forall\ j \in \{1, \cdots, N_{\rm I}\}, \\
& R_i,\ t_{{\rm st},i} \geq 0,\ t_{{\rm mo},i} \geq d_i/v_{\max},\ \forall\ i \in \{1, \cdots, N_{\rm SH}\}.
\end{aligned} \tag{4.12}$$

[7] The additional online adaptation of Section 4.2 can be readily applied to this case. We therefore only focus on extending the results of Section 4.1 in this part.

Note that, from $\mathcal{T}_1$ to $\mathcal{T}_{\text{Ind}(z_j)-1}$, the total number of bits that can be gathered by the robot is $\sum_{i=0}^{j-1} Q_i$. Thus, the robot cannot send more information than it has gathered so far, which results in the third constraint in (4.12). Similar to Lemma 13, it can also be shown that the constraints of the optimization problem of (4.12) satisfy LICQ at the optimum point. Hence, we have the following properties for the optimum motion and communication co-optimization strategy:

Theorem 3 *The optimum motion speed ($v_i^\star$), transmission rate ($R_i^\star$) and stop time ($t_{\text{st},i}^\star$) of (4.12) satisfy the following properties: if $\mathbb{E}\{1/\Upsilon_i\} < \mathbb{E}\{1/\Upsilon_j\}$ and there is no point of interest between $\mathcal{T}_i$ and $\mathcal{T}_j$, then $v_i^\star \leq v_j^\star$ and $R_i^\star \geq R_j^\star$, where $i, j \in \{1, \cdots, N_{\text{SH}}\}$. Moreover, the robot may stop in more than one sub-trajectory during the operation. Let $\mathcal{K}_{\text{best}}$ denote the collective set of indices where $\mathbb{E}\{1/\Upsilon_i\}$ has its minimum in the following intervals: from $\mathcal{T}_1$ to $\mathcal{T}_{\text{Ind}(z_1)-1}$, from $\mathcal{T}_{\text{Ind}(z_j)}$ to $\mathcal{T}_{\text{Ind}(z_{j+1})-1}$, for $j \in \{1, \cdots, N_{\text{I}} - 1\}$, and from $\mathcal{T}_{\text{Ind}(z_{N_{\text{I}}})}$ to $\mathcal{T}_{N_{\text{SH}}}$. Then, if $t_{\text{st},i}^\star > 0$, we have $i \in \mathcal{K}_{\text{best}}$.*

Proof: It is straightforward to extend the proof of Theorem 2 to this case. The details of the proof are omitted due to page limitation. ■

Similar to Theorem 2, Theorem 3 says that the robot moves slower and transmits faster along $\mathcal{T}_i$, as compared to $\mathcal{T}_j$, if the predicted channel quality along $\mathcal{T}_i$ is better and there is no point of interest between them. If there exists any point of interest between $\mathcal{T}_i$ and $\mathcal{T}_j$, and $j < i$, the same conclusion still holds. However, if $j > i$, then the robot may need to reduce its speed and transmit with a higher rate at $\mathcal{T}_j$ in order to ensure the transmission of the newly-gathered information. Also, the robot may stop at more than one location along the trajectory in order to spend long enough time for transmission. Theorem 3 says that, in such cases, the corresponding sub-trajectories must have the best predicted channel quality in their local areas, where each local area is an area that contains no point of interest.

Chapter 5

Co-Optimization With Trajectory Planning

In the previous chapter, we have characterized the case where the robot moves along a pre-defined trajectory. In this part, we extend this scenario and integrate the trajectory design into the co-optimization framework. More specifically, consider the scenario where a mobile robot is tasked with visiting a set of POIs $\mathcal{P} = \{p_2, \cdots, p_m\}$ in a workspace $\mathcal{W} \subset \mathbb{R}^2$, collecting their corresponding information bits, and transmitting them to a remote station under resource constraints. We assume that each POI p_i has $Q_i > 0$ information bits that need to be gathered, where $i \in \{2, \cdots, m\}$. In addition, the robot may initially have some information bits Q_1 in its memory as well. The robot then needs to start from its initial position p_1, visit all the POIs, gather the information bits, and successfully transmit them to a remote station. The robot has limited time and energy budgets for its operation. Furthermore, it experiences realistic communication channels with path loss, shadowing and multipath fading, when transmitting to the remote station. Our goal is then to successfully plan the trajectory of the robot and the transmission

This chapter is an amended version of [120].

of the gathered bits while minimizing the total energy consumption, which *includes both communication and motion energy costs*, and under other resource constraints.

Fig. 5.1 shows an example of our considered scenario. As can be seen, the robot starts from its initial position, plans its trajectory to visit all the POIs in the workspace, and transmits the gathered bits to the remote station.

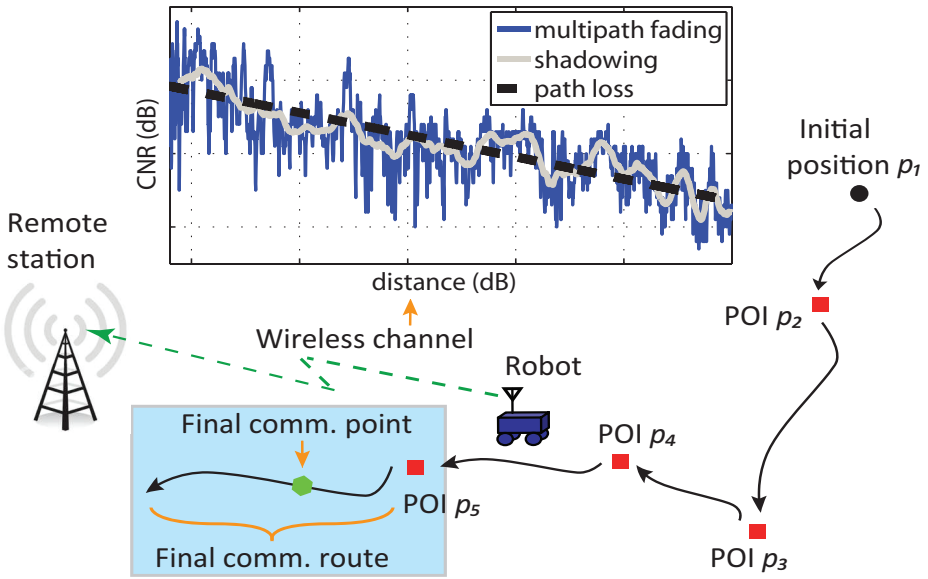

Figure 5.1: A robot starts from its initial position, designs its trajectory to visit four POIs, and finds a final communication point that has a high channel quality. Throughout this operation, it plans its communication and motion strategies to send the collected data to the remote station. The shaded box is the "To Go or Not to Go" problem which is characterized in Section 5.1.

To optimally solve this problem, the robot needs to address the following challenges: *1) find the optimal trajectory that covers all the POIs, and 2) find the corresponding optimal communication and motion strategies along this trajectory to send all the information bits, while satisfying its time and communication reception quality constraints and minimizing its total energy cost.* By optimal communication and motion strategies, we refer to the optimal transmit power/rate, motion speed and stop times throughout the chapter. An important question at the core of this problem is then as follows: when/how should a robot incur motion energy, deviate from a trajectory that would have been opti-

mal by only considering sensing and motion objectives, and move to locations better for communication? Bringing a theoretical understanding to this question in a general setting when the robot can deviate from its trajectory any time is considerably challenging. We thus assume that there is a pre-defined route between any two POIs that the robot can choose to traverse.[1] Without loss of generality, we assume that the pre-defined route between any two POIs is a straight line. Note that this setting still allows us to address the aforementioned question for the following reason. The robot has to decide on the order in which it visits the POIs, which allows it to incur motion energy and choose a longer trajectory for better connectivity, as needed, if that is the optimal thing to do.

Furthermore, once the robot visits the last POI, we allow it to move along a new route, if needed, to find a location better for communication (in case it saves the overall energy consumption). We refer to this final route and location as "final communication route" and "final communication point" respectively, as shown in Fig. 5.1. Note that once the robot reaches the last POI, it needs to decide on if it is better for it to move to find a final communication point or to stay at the last POI and possibly increase its transmission power. Moreover, in this chapter we bring a theoretical understanding to how to choose the final communication point. We refer to this problem as the "To Go or Not to Go" problem, which is not only an important stand alone problem, but also addresses the last piece of our considered scenario. Once we solve this problem, we utilize the gathered insights to solve the overall problem of planning the site visits, finding the final communication point, and designing the communication transmission rate, motion speed and stop times along the whole trajectory. Note that the robot transmits the collected bits to the remote station all over the trajectory and not just at the final communication point.

Intuitively, without considering the communication cost, the optimal order to visit all

[1]The pre-defined route, for instance, could be the only possible route due to environmental constraints.

the POIs should be the one that results in the minimum-length trajectory for the case of linear motion model, in order to minimize the motion energy consumption, as we have seen in Section 2.3. However, the minimum-length trajectory may not be suitable for communication since the channel quality along this trajectory may be very low. Similarly, if the channel quality at the last POI is very high, it may be optimal for the robot to transmit all the bits at the last POI without moving. On the other hand, if the channel quality at the last POI is very low, the robot may want to incur some motion energy to move to a place that is better for communication. Hence, the optimal planning strategy requires a co-optimization of the communication and motion objectives.

The rest of this chapter is organized as follows. In Section 5.1, we characterize the "To Go or Not to Go" problem. In Section 5.2, we first present our overall offline co-optimization framework which is based on the predicted channel quality in the environment. Then, we propose an approach that allows the robot to adapt its strategy online when it observes the true value of the channel along the way. Finally, in Section 5.3, we verify the effectiveness of our proposed framework in a simulation environment.

5.1 To Go or Not to Go?

In this section, we first consider a special case where $\mathcal{P} = \emptyset$ and the total number of bits that needs to be sent is $Q_{\text{tot}} = Q_1$. In other words, the mobile robot does not need to visit any POI in the workspace and already has all the bits that need to be sent. Then, it has to decide if it should move to find a final communication point, and if so, decide on the corresponding optimal motion and communication strategies. This is an important simplified scenario to analyze for the following two reasons. First, this in itself is an important stand alone problem addressing when it is beneficial for a robot to incur motion energy to save the communication energy and the resulting overall energy.

Second, it addresses the last piece of the considered problem of this chapter (see shaded box of Fig. 5.1), where the robot has visited all the POIs and needs to decide if/how it should travel from the last POI to find a good communication point. The theories we derive for this part will then be extended to address the overall problem that also involves visiting sites, as we shall see in Section 5.2.

Thus, in this section we address what we refer to as the "To Go or Not to Go" problem, i.e. should the robot incur motion energy to move to a better spot for communication or should it stay at its current position and increase its transmission power? If it should move, what is the optimal final communication route? Given the optimal final communication route, where is the optimal final communication point (the point where the robot should move to if it decides to move) and what are the corresponding optimal communication and motion strategies along the route? In this section, we start by assuming that the final communication route is given beforehand. We then characterize key properties of the optimal final communication point where the robot should stop and the corresponding optimal communication and motion strategies along the way. We further show under what conditions the robot should move from/stay at its current position. In Section 5.1.3, we then relax the assumption of the pre-defined route and characterize the optimal final communication route under certain conditions.

5.1.1 Properties of the Optimal Final Communication Point and the Corresponding Optimal Communication and Motion Strategies

Let $\mathcal{T}$ denote the pre-defined final communication route that is given beforehand. For the purpose of adapting the communication and motion strategies, we discretize $\mathcal{T}$ into $n_{\mathcal{T}}$ sub-routes $\mathcal{T}_i$s, for $i \in \{1, \cdots, n_{\mathcal{T}}\}$, each with length d_i. Initially, the robot is

located at the beginning of $\mathcal{T}_1$, and can move to any $\mathcal{T}_i$ for any $i \in \{1, \cdots, n_{\mathcal{T}}\}$ (moving through $\mathcal{T}_1$, $\mathcal{T}_2$, $\cdots$, $\mathcal{T}_{i-1}$) if needed. Each d_i should be chosen small enough, such that the channel along $\mathcal{T}_i$ can be considered stationary (see [70] for how to choose the length in practice). To consider the most general case, we further allow d_is to be different in size in order to account for the cases where the route spans over a large area with changing environmental features (such as from indoor to outdoor), resulting in different stationary lengths in different parts of the route. Then, a Gaussian random variable, $\Upsilon_{\mathrm{dB},\mathcal{T}_i}$, with the mean $\overline{\Upsilon}_{\mathrm{dB},\mathcal{T}_i}$ and variance $\sigma^2_{\mathrm{dB},\mathcal{T}_i}$ can best characterize the distribution of CNR (in dB) at $\mathcal{T}_i$ (see Section 2.1). Furthermore, we assume that the robot has reached sub-route $\mathcal{T}_i$ as long as it arrives at the first point in $\mathcal{T}_i$.[2] Then, finding the optimal final communication point becomes determining the optimal final sub-route that the robot should move to. In this chapter, we use communication energy model (2.12) and linear motion model (2.25). We can then formulate the following optimization problem to minimize the total energy

[2]Note that there is no need to move farther since the channel quality is predicted the same over each sub-route.

cost:

$$\text{minimize} \quad J_{\text{fin}} = \sum_{i=1}^{n_{\mathcal{T}}} \underbrace{\sum_{\ell=1}^{n_r} P_{\text{C},i,\ell} t_{\text{tr},i,\ell}}_{\substack{E_{\text{C},i}:\text{communication} \\ \text{cost along } \mathcal{T}_i}} + \sum_{i=1}^{n_{\mathcal{T}}-1} y_{i+1} \underbrace{\kappa_1 d_i + \kappa_2 t_{\text{mo},i}}_{\substack{E_{\text{M},i}:\text{ motion cost} \\ \text{along } \mathcal{T}_i}} \tag{5.1}$$

$$\begin{aligned}
\text{subject to} \quad & 1) \sum_{i=1}^{n_{\mathcal{T}}-1} t_{\text{mo},i} + \sum_{i=1}^{n_{\mathcal{T}}} t_{\text{st},i} \leq T_{\text{tot}}, \quad 2) \sum_{i=1}^{n_{\mathcal{T}}} \sum_{\ell=1}^{n_r} R^{\ell} t_{\text{tr},i,\ell} \geq \frac{Q_{\text{tot}}}{B}, \\
& 3) \sum_{\ell=1}^{n_r} t_{\text{tr},i,\ell} \leq t_{\text{mo},i} + t_{\text{st},i}, \ \forall\ i \in \{1, \cdots, n_{\mathcal{T}}-1\}, \\
& 4) \sum_{\ell=1}^{n_r} t_{\text{tr},n_{\mathcal{T}},\ell} \leq t_{\text{st},n_{\mathcal{T}}}, \quad 5)\ y_i T_{\text{tot}} \geq t_{\text{st},i} \geq 0, \ \forall\ i, \\
& 6)\ t_{\text{tr},i,\ell} \geq 0, \ \forall\ i, \ell, \quad 7)\ y_{i+1} T_{\text{tot}} \geq t_{\text{mo},i} \geq y_{i+1} \frac{d_i}{v_{\max}}, \ \forall\ i, \\
& 8)\ y_1 \geq y_2 \geq \cdots \geq y_{n_{\mathcal{T}}}, \quad 9)\ y_i \in \{0,1\}, \ \forall\ i,
\end{aligned}$$

where the unknown variables to solve for are $t_{\text{tr},i,\ell}$s, $t_{\text{mo},i}$s, $t_{\text{st},i}$s and y_is. More specifically, $t_{\text{tr},i,\ell}$ denotes the transmission time while using the spectral efficiency R^{ℓ} along $\mathcal{T}_i$, $t_{\text{mo},i}$ and $t_{\text{st},i}$ represent the motion and stop times that the robot spends along $\mathcal{T}_i$ respectively, $T_{\text{tot}} > 0$ is the given operation time budget, $Q_{\text{tot}} > 0$ is the total number of bits that needs to be sent, and B is the given fixed bandwidth. Moreover, $E_{\text{C},i}$ and $E_{\text{M},i}$ are the anticipated total communication and motion energy costs along $\mathcal{T}_i$ respectively, and $P_{\text{C},i,\ell} = \big((2^{R^{\ell}} - 1)/K\big)\mathbb{E}\{1/\Upsilon_{\mathcal{T}_i}\}$ with $\Upsilon_{\mathcal{T}_i} = 10^{\Upsilon_{\text{dB},\mathcal{T}_i}/10}$. Finally, binary variable y_i is 1 if the robot reaches $\mathcal{T}_i$ (either moves through or stops at $\mathcal{T}_i$), and is 0 otherwise. Note that if $y_i = 0$, for $\forall\ i \in \{2, \cdots, n_{\mathcal{T}}\}$, then the robot does not move. Furthermore, in this section we use $\mathbb{E}\{1/\Upsilon_i\}$ instead of $\mathbb{E}\{1/\Upsilon_{\mathcal{T}_i}\}$ since there is only one route.

Our optimization framework of (5.1) finds the optimal final communication point along the pre-defined route, and adapts the motion speed, stop time and transmission rate of the robot along each sub-route, while minimizing the total energy cost and satisfying

the total time budget and target BER. Note that, as mentioned in Section 2.3, the motion energy is minimized when $t_{\mathrm{mo},i} = d_i/v_{\max}$. Thus, we have introduced the stop time variables $t_{\mathrm{st},i}$s in (5.1) in order to allow the robot to stop during the operation if needed.

Lemma 19 *Function $f(t) = (2^t - 2^c)/(t-c)$ is strictly increasing with respect to $t \in (c, \infty)$.*

Proof: Lemma 19 can be easily verified by checking the first-order derivative of $f(t)$. ■

In the subsequent sections, we use superscript $\star$ to denote the optimum solution or the optimum value of the corresponding optimization problem. We then have the following results to characterize the optimal communication strategy.

Lemma 20 *Let $J^{\star}_{\mathrm{nComm}}(Q,T)$ be the optimal value of the following optimization problem:*

$$\begin{aligned} &\textit{minimize} \quad J_{\mathrm{nComm}}(Q,T) = \sum_{\ell=1}^{n_r} (2^{R^\ell} - 1) t_{\mathrm{tr},\ell} \\ &\textit{subject to} \quad 1)\ \sum_{\ell=1}^{n_r} R^\ell t_{\mathrm{tr},\ell} = \frac{Q}{B}, \quad 2)\ \sum_{\ell=0}^{n_r} t_{\mathrm{tr},\ell} = T, \quad 3)\ t_{\mathrm{tr},\ell} \geq 0,\ \forall\ \ell, \end{aligned} \tag{5.2}$$

where T is the given total transmission time, Q is the total number of given bits that needs to be sent, and the rest of the parameters are as defined before. Then, we have the following:

1) the optimal transmission times are

$$t^{\star}_{\mathrm{tr},\ell^\star} = \frac{R^{\ell^\star+1}T - Q/B}{R^{\ell^\star+1} - R^{\ell^\star}}, \tag{5.3}$$

$$t^{\star}_{\mathrm{tr},\ell^\star+1} = \frac{Q/B - R^{\ell^\star}T}{R^{\ell^\star+1} - R^{\ell^\star}}, \tag{5.4}$$

and $t^{\star}_{\mathrm{tr},\ell}=0$*, for* $\ell\neq\ell^{\star},\ell^{\star}+1$*, where* $\mathcal{R}=\{R^0,R^1,\cdots,R^{n_r}\}$ *is the set of possible spectral efficiencies,* $\ell^{\star}=\lfloor Q/(BT)\rfloor_{\mathcal{R}}$ *and* $\lfloor\cdot\rfloor_{\mathcal{R}}$ *denotes the largest integer in* $\mathcal{R}$ *that is smaller than or equal to the argument, i.e.* $\lfloor Q/(BT)\rfloor_{\mathcal{R}}=\ell$ *if* $R^{\ell}\leq Q/(BT)<R^{\ell+1}$*. Moreover, we have* $J^{\star}_{\mathrm{nComm}}(Q,T)=a_{\ell^{\star}}Q-b_{\ell^{\star}}T$*, where*

$$a_{\ell}=\frac{2^{R^{\ell+1}}-2^{R^{\ell}}}{B(R^{\ell+1}-R^{\ell})}, \tag{5.5}$$

$$b_{\ell}=\frac{R^{\ell}(2^{R^{\ell+1}}-1)-R^{\ell+1}(2^{R^{\ell}}-1)}{R^{\ell+1}-R^{\ell}}. \tag{5.6}$$

2) $J^{\star}_{\mathrm{nComm}}(Q,T)$ *is monotonically increasing with respect to* Q *and is non-increasing with respect to* T*. In particular, it is monotonically decreasing with respect to* T *for* $T\leq Q/(BR^1)$*. Moreover,* $J^{\star}_{\mathrm{nComm}}(Q,T)\to 0$ *as* $Q\to 0$*.*

Proof: The first part of Lemma 20 implies that 1) the robot at most uses two different spectral efficiencies in $\mathcal{R}$ for transmission, i.e. $t^{\star}_{\mathrm{tr},\ell}>0$ for at most two different $\ell\in\{0,1,\cdots,n_r\}$, and 2) if $t^{\star}_{\mathrm{tr},\ell}>0$ for some ℓ, then it is only possible to have either $t^{\star}_{\mathrm{tr},\ell+1}>0$ or $t^{\star}_{\mathrm{tr},\ell-1}>0$.

We first show that the robot at most uses two different spectral efficiencies in $\mathcal{R}$ for transmission. Consider the dual function of the primal optimization problem as follows:

$$g_{J_{\mathrm{nComm}}}=\sum_{\ell=1}^{n_r}(2^{R^{\ell}}-1)t_{\mathrm{tr},\ell}+\lambda\big(Q/B-\sum_{\ell=1}^{n_r}R^{\ell}t_{\mathrm{tr},\ell}\big)+\mu\big(\sum_{\ell=0}^{n_r}t_{\mathrm{tr},\ell}-T\big)-\sum_{\ell=0}^{n_r}\pi_{\ell}t_{\mathrm{tr},\ell}, \tag{5.7}$$

where λ, μ and π_{ℓ}s are Lagrange multipliers. Then, based on Karush-Kuhn-Tucker (KKT) conditions, we have the following: $\partial g_{J_{\mathrm{nComm}}}/\partial t_{\mathrm{tr},\ell}=(2^{R^{\ell}}-1)-\lambda R^{\ell}+\mu-\pi_{\ell}=0$, $\pi_{\ell}t_{\ell}=0$, and $\pi_{\ell}\geq 0$, $\forall\,\ell$. Suppose that the robot uses three different spectral efficiencies, R^{ℓ_1}, R^{ℓ_2} and R^{ℓ_3}, for transmission, i.e. $t^{\star}_{\mathrm{tr},\ell_1},t^{\star}_{\mathrm{tr},\ell_2},t^{\star}_{\mathrm{tr},\ell_3}>0$. Then, $\pi^{\star}_{\ell_1},\pi^{\star}_{\ell_2},\pi^{\star}_{\ell_3}=0$, resulting in $(2^{R^{\ell}}-1)-\lambda^{\star}R^{\ell}+\mu^{\star}=0$, $\forall\,\ell=\ell_1,\ell_2,\ell_3$. Note that we have an overdetermined system to solve for $\lambda^{\star}$ and $\mu^{\star}$. Without loss of generality, assume that $R^{\ell_1}<R^{\ell_2}<R^{\ell_3}$. Then by

solving $\lambda^\star$ for ℓ_1 and ℓ_2, we have $\lambda^\star_{\ell_1,\ell_2} = (2^{R^{\ell_1}} - 2^{R^{\ell_2}})/(R^{\ell_1} - R^{\ell_2})$. Similarly, by solving $\lambda^\star$ for ℓ_1 and ℓ_3, we have $\lambda^\star_{\ell_1,\ell_3} = (2^{R^{\ell_1}} - 2^{R^{\ell_3}})/(R^{\ell_1} - R^{\ell_3})$. From Lemma 19, we know that $\lambda^\star_{\ell_1,\ell_2} < \lambda^\star_{\ell_1,\ell_3}$, which results in a contradiction. Hence, we have that the robot at most uses two different spectral efficiencies for transmission.

Next, we show that if $t^\star_{\mathrm{tr},\ell} > 0$ for some ℓ, then it is only possible to have either $t^\star_{\mathrm{tr},\ell+1} > 0$ or $t^\star_{\mathrm{tr},\ell-1} > 0$. From the previous part, we know that $t^\star_{\mathrm{tr},\ell} > 0$ for at most two different $\ell \in \{0, \cdots, n_r\}$. Suppose that $t^\star_{\mathrm{tr},\ell_1}, t^\star_{\mathrm{tr},\ell_2} > 0$, $\ell_2 > \ell_1$, and there exists a $\ell_3 \in \{0, 1, \cdots, n_r\}$ such that $\ell_1 < \ell_3 < \ell_2$. Then, by solving $\lambda^\star$ and $\mu^\star$, we have

$$\lambda^\star = \frac{2^{R^{\ell_1}} - 2^{R^{\ell_2}}}{R^{\ell_1} - R^{\ell_2}}, \tag{5.8}$$

$$\mu^\star = \frac{(2^{R^{\ell_1}} - 1)R^{\ell_2} - (2^{R^{\ell_2}} - 1)R^{\ell_1}}{R^{\ell_1} - R^{\ell_2}}. \tag{5.9}$$

Moreover,

$$\begin{aligned}
\pi^\star_{\ell_3} &= 2^{R^{\ell_3}} - 1 - \lambda^\star R^{\ell_3} + \mu^\star \\
&= 2^{R^{\ell_3}} - 1 - \frac{(2^{R^{\ell_2}} - 1)(R^{\ell_3} - R^{\ell_1}) + (2^{R^{\ell_1}} - 1)(R^{\ell_2} - R^{\ell_3})}{R^{\ell_2} - R^{\ell_1}} \\
&< 2^{R^{\ell_3}} - 1 - (2^{R^{\ell_2}\frac{R^{\ell_3} - R^{\ell_1}}{R^{\ell_2} - R^{\ell_1}} + R^{\ell_1}\frac{R^{\ell_2} - R^{\ell_3}}{R^{\ell_2} - R^{\ell_1}}} - 1) \\
&= 2^{R^{\ell_3}} - 1 - (2^{R^{\ell_3}} - 1) = 0,
\end{aligned} \tag{5.10}$$

where the inequality holds since $2^{R^\ell} - 1$ is a convex function of R^ℓ. Clearly, this contradicts the fact that $\pi^\star_{\ell_3} \geq 0$. Hence, if $t^\star_{\mathrm{tr},\ell} > 0$ for some ℓ, then it is only possible to have either $t^\star_{\mathrm{tr},\ell+1} > 0$ or $t^\star_{\mathrm{tr},\ell-1} > 0$.

Based on the two facts proved above, it is easy to see that the optimum solution of (5.2) is to choose spectral efficiencies R^ℓ and $R^{\ell+1}$ such that $R^\ell \leq Q/(BT) < R^{\ell+1}$. This results in the optimal $t^\star_{\mathrm{tr},\ell^\star}$, $t^\star_{\mathrm{tr},\ell^\star+1}$ and $J^\star_{\mathrm{nComm}}(Q,T)$ in the first part of the lemma.

For the second part of the lemma, we have the following for $J^{\star}_{\text{nComm}}(Q,T)$:

$$J^{\star}_{\text{nComm}}(Q,T) = \frac{2^{R^{\ell^\star(Q,T)+1}} - 2^{R^{\ell^\star(Q,T)}}}{R^{\ell^\star(Q,T)+1} - R^{\ell^\star(Q,T)}}\frac{Q}{B} - \frac{R^{\ell^\star(Q,T)}(2^{R^{\ell^\star(Q,T)+1}} - 1) - R^{\ell^\star(Q,T)+1}(2^{R^{\ell^\star(Q,T)}} - 1)}{R^{\ell^\star(Q,T)+1} - R^{\ell^\star(Q,T)}}T, \tag{5.11}$$

where we use notation $\ell^\star(Q,T)$ to explicitly indicate that $\ell^\star$ is a function of Q and T. Clearly, $\ell^\star(Q,T) = 0$ as $Q \to 0$. We then have

$$J^{\star}_{\text{nComm}}(Q,T) = \frac{2^{R^1} - 1}{R^1}\frac{Q}{B} \to 0 \tag{5.12}$$

as $Q \to 0$. Next, we prove the monotonic properties of $J^{\star}_{\text{nComm}}(Q,T)$.

First, consider the case where T is fixed and let $\widetilde{Q} > Q$. If $R^{\ell^\star(Q,T)} \le Q/(BT) < \widetilde{Q}/(BT) < R^{\ell^\star(Q,T)+1}$, then $\ell^\star(\widetilde{Q},T) = \ell^\star(Q,T)$ and

$$J^{\star}_{\text{nComm}}(\widetilde{Q},T) - J^{\star}_{\text{nComm}}(Q,T) = \frac{2^{R^{\ell^\star(Q,T)+1}} - 2^{R^{\ell^\star(Q,T)}}}{R^{\ell^\star(Q,T)+1} - R^{\ell^\star(Q,T)}}(\widetilde{Q}/B - Q/B) > 0. \tag{5.13}$$

Moreover, if $R^{\ell^\star(Q,T)} \le Q/(BT) < R^{\ell^\star(Q,T)+1} \le \widetilde{Q}/(BT) < R^{\ell^\star(Q,T)+2}$, then $\ell^\star(\widetilde{Q},T) = \ell^\star(Q,T) + 1$ and $J^{\star}_{\text{nComm}}(\widetilde{Q},T) \ge J^{\star}_{\text{nComm}}(BR^{\ell^\star(Q,T)+1}T,T) > J^{\star}_{\text{nComm}}(Q,T)$. By induction, it can be seen that $J^{\star}_{\text{nComm}}(\widetilde{Q},T) > J^{\star}_{\text{nComm}}(Q,T)$ for any $\widetilde{Q} > Q$, i.e. $J^{\star}_{\text{nComm}}(Q,T)$ is monotonically increasing with respect to Q.

Next, consider the case where $Q \neq 0$ is fixed and let $T < \widetilde{T} \le Q/(BR^1)$. Note that in this case, $\ell^\star(Q,T) \ge 1$ and $\ell^\star(Q,\widetilde{T}) \ge 1$, i.e. $R^{\ell^\star(Q,T)} > 0$ and $R^{\ell^\star(Q,\widetilde{T})} > 0$. Similar to the previous part, if $R^{\ell^\star(Q,T)} \le Q/(B\widetilde{T}) < Q/(BT) < R^{\ell^\star(Q,T)+1}$, then $\ell^\star(Q,\widetilde{T}) = \ell^\star(Q,T)$,

and

$$J^{\star}_{\mathrm{nComm}}(Q,\widetilde{T}) - J^{\star}_{\mathrm{nComm}}(Q,T) = \frac{R^{\ell^{\star}(Q,T)}(2^{R^{\ell^{\star}(Q,T)+1}}-1) - R^{\ell^{\star}(Q,T)+1}(2^{R^{\ell^{\star}(Q,T)}}-1)}{R^{\ell^{\star}(Q,T)+1} - R^{\ell^{\star}(Q,T)}}(T-\widetilde{T}) < 0. \tag{5.14}$$

Moreover, if $R^{\ell^{\star}(Q,T)-1} \leq Q/(B\widetilde{T}) < R^{\ell^{\star}(Q,T)} \leq Q/(BT) < R^{\ell^{\star}(Q,T)+1}$, then $\ell^{\star}(Q,\widetilde{T}) + 1 = \ell^{\star}(Q,T)$ and $J^{\star}_{\mathrm{nComm}}(Q,\widetilde{T}) < J^{\star}_{\mathrm{nComm}}\big(Q, Q/(BR^{\ell^{\star}(Q,T)})\big) \leq J^{\star}_{\mathrm{nComm}}(Q,T)$. By induction, it can be seen that $J^{\star}_{\mathrm{nComm}}(Q,\widetilde{T}) < J^{\star}_{\mathrm{nComm}}(Q,T)$ for any $T < \widetilde{T} \leq Q/(BR^1)$, i.e. $J^{\star}_{\mathrm{nComm}}(Q,T)$ is monotonically decreasing with respect to T for $T \leq Q/(BR^1)$.

Finally, it can be easily seen that if $T > Q/(BR^1)$, $\ell^{\star}(Q,T) = 0$. As a result,

$$J^{\star}(Q,T) = \frac{2^{R^1}-1}{R^1}\frac{Q}{B}, \tag{5.15}$$

for all $T > Q/(BR^1)$, i.e. $J^{\star}_{\mathrm{nComm}}(Q,T)$ is a constant with respect to T for $T > Q/(BR^1)$. Hence, we have that $J^{\star}_{\mathrm{nComm}}(Q,T)$ is non-increasing with respect to T. This concludes the second part of the lemma. ■

Note that $J^{\star}_{\mathrm{nComm}}(Q,T)$ can be considered as the optimal normalized communication cost to send Q bits in time T. Next, we prove the key properties of the optimal solution of (5.1) for the case that the robot has to move.

Theorem 4 *Let $i^{\star}$ denote the index of the optimal final sub-route that the robot should move to. Then the optimal solution of (5.1) satisfies the following properties:*

1) $\mathbb{E}\{1/\Upsilon_{i^{\star}}\} < \mathbb{E}\{1/\Upsilon_i\}$, for $\forall\ i \in \{1,\cdots,i^{\star}-1\}$

2) $t^{\star}_{\mathrm{mo},i} = d_i/v_{\max}$, for $\forall\ i \in \{1,\cdots,i^{\star}-1\}$;

3) $t^{\star}_{\mathrm{st},i} = 0$, for $\forall\ i \in \{1,\cdots,i^{\star}-1\}$, and $t^{\star}_{\mathrm{st},i^{\star}} = T_{\mathrm{tot}} - \sum_{i=1}^{i^{\star}-1} d_i/v_{\max}$;

4) If $\mathbb{E}\{1/\Upsilon_i\} < \mathbb{E}\{1/\Upsilon_j\}$, for $i,j \in \{1,\cdots,i^{\star}\}$, then $\sum_{\ell=1}^{n_r} R^{\ell} t^{\star}_{\mathrm{tr},i,\ell}/(t^{\star}_{\mathrm{mo},i} + t^{\star}_{\mathrm{st},i}) \geq \sum_{\ell=1}^{n_r} R^{\ell} t^{\star}_{\mathrm{tr},j,\ell}/(t^{\star}_{\mathrm{mo},j} + t^{\star}_{\mathrm{st},j})$.

Proof: We prove Theorem 4 by contradiction.

1) Suppose that $\mathcal{T}_{i^\star}$ is the optimal final sub-route that the robot should move to, and $\mathbb{E}\{1/\Upsilon_{i^\star}\} \geq \mathbb{E}\{1/\Upsilon_i\}$, for some $i \in \{1, \cdots, i^\star - 1\}$. Then, there exists a $j < i^\star$ such that $\mathbb{E}\{1/\Upsilon_j\} = \min_{i\in\{1,\cdots,i^\star\}} \mathbb{E}\{1/\Upsilon_i\}$. Let $t^\star_{\mathrm{mo},i}$, $t^\star_{\mathrm{st},i}$ and $t^\star_{\mathrm{tr},i,\ell}$ denote the optimal solution given the optimal final sub-route $\mathcal{T}_{i^\star}$. We can always choose another feasible solution as follows. Choose $\mathcal{T}_j$ as the final sub-route, $t_{\mathrm{mo},i} = t^\star_{\mathrm{mo},i}$, $t_{\mathrm{st},i} = t^\star_{\mathrm{st},i}$, $t_{\mathrm{tr},i,\ell} = t^\star_{\mathrm{tr},i,\ell}$, for $i \in \{1, \cdots, j-1\}$, $t_{\mathrm{st},j} = \sum_{i=j}^{i^\star-1} t^\star_{\mathrm{mo},i} + \sum_{i=j}^{i^\star} t^\star_{\mathrm{st},i}$ and $t_{\mathrm{tr},j,\ell} = \sum_{i=j}^{i^\star} t^\star_{\mathrm{tr},i,\ell}$. Clearly, by using this feasible solution we have the following: $E_{\mathrm{C},i} = E^\star_{\mathrm{C},i}$, $E_{\mathrm{M},i} = E^\star_{\mathrm{M},i}$, for $i \in \{1, \cdots, j-1\}$, and $E_{\mathrm{C},j} \leq \sum_{i=j}^{i^\star} E^\star_{\mathrm{C},i}$, resulting in $J_{\mathrm{fin}} < J^\star_{\mathrm{fin}}$. This means that we can always find a feasible solution that performs better than the optimal solution, which contradicts the optimality of the final sub-route $\mathcal{T}_{i^\star}$. Hence, $\mathbb{E}\{1/\Upsilon_{i^\star}\} < \mathbb{E}\{1/\Upsilon_i\}$, for $\forall\, i \in \{1, \cdots, i^\star - 1\}$.

2) Let $t^\star_{\mathrm{mo},i} > d_i/v_{\max}$, for some $i \in \{1, \cdots, i^\star - 1\}$, be the optimal motion time along $\mathcal{T}_i$. Then, by choosing the following feasible solution: $t_{\mathrm{mo},i} = d_i/v_{\max}$, $t_{\mathrm{st},i} = t^\star_{\mathrm{st},i} + t^\star_{\mathrm{mo},i} - d_i/v_{\max}$ and $t_{\mathrm{tr},i,\ell} = t^\star_{\mathrm{tr},i,\ell}$, we can show that $E_{\mathrm{C},i} = E^\star_{\mathrm{C},i}$ and $E_{\mathrm{M},i} < E^\star_{\mathrm{M},i}$. This means that the optimal solution incurs more energy which is contradicting. Hence, $t^\star_{\mathrm{mo},i} = d_i/v_{\max}$, for $\forall\, i \in \{1, \cdots, i^\star - 1\}$.

3) Let $t^\star_{\mathrm{st},i} > 0$, for some $i \in \{1, \cdots, i^\star - 1\}$, be the optimal stop time along $\mathcal{T}_i$. We can always choose the following feasible solution: $t_{\mathrm{st},i} = 0$, $t_{\mathrm{st},i^\star} = t^\star_{\mathrm{st},i^\star} + t^\star_{\mathrm{st},i}$, $t_{\mathrm{tr},i,\ell} = t^\star_{\mathrm{tr},i,\ell} t^\star_{\mathrm{mo},i}/(t^\star_{\mathrm{st},i} + t^\star_{\mathrm{mo},i})$ and $t_{\mathrm{tr},i^\star,\ell} = t^\star_{\mathrm{tr},i^\star,\ell} + t^\star_{\mathrm{tr},i,\ell} t^\star_{\mathrm{st},i}/(t^\star_{\mathrm{st},i} + t^\star_{\mathrm{mo},i})$. In this feasible solution, the robot sends less information bits along $\mathcal{T}_i$ and more information bits along $\mathcal{T}_{i^\star}$. Based on the first part of the theorem, it can be seen that this feasible solution consumes less energy, since the predicted channel quality is better along $\mathcal{T}_{i^\star}$. This contradicts the assumption that $t^\star_{\mathrm{st},i} > 0$ is the optimal stop time. Hence, we have $t^\star_{\mathrm{st},i} = 0$, for $\forall\, i \in \{1, \cdots, i^\star - 1\}$, and $t^\star_{\mathrm{st},i^\star} = T_{\mathrm{tot}} - \sum_{i=1}^{i^\star-1} d_i/v_{\max}$.

4) Suppose that $\sum_{\ell=1}^{n_r} R^\ell t^\star_{\mathrm{tr},i,\ell}/(t^\star_{\mathrm{mo},i} + t^\star_{\mathrm{st},i}) < \sum_{\ell=1}^{n_r} R^\ell t^\star_{\mathrm{tr},j,\ell}/(t^\star_{\mathrm{mo},j} + t^\star_{\mathrm{st},j})$ and $\mathbb{E}\{1/\Upsilon_i\} <$

$\mathbb{E}\{1/\Upsilon_j\}$ for some $i, j \in \{1, \cdots, i^\star\}$. Let $0 < t_c \leq \min\{t^\star_{\mathrm{mo},i} + t^\star_{\mathrm{st},i}, t^\star_{\mathrm{mo},j} + t^\star_{\mathrm{st},j}\}$, and define $\widetilde{t}^\star_{\mathrm{tr},i,\ell} = t^\star_{\mathrm{tr},i,\ell} t_c/(t^\star_{\mathrm{mo},i} + t^\star_{\mathrm{st},i})$ and $\widetilde{t}^\star_{\mathrm{tr},j,\ell} = t^\star_{\mathrm{tr},j,\ell} t_c/(t^\star_{\mathrm{mo},j} + t^\star_{\mathrm{st},j})$. Clearly, we have $\sum_{\ell=1}^{n_r} R^\ell \widetilde{t}^\star_{\mathrm{tr},i,\ell} < \sum_{\ell=1}^{n_r} R^\ell \widetilde{t}^\star_{\mathrm{tr},j,\ell}$. Moreover, since $\sum_{\ell=0}^{n_r} \widetilde{t}^\star_{\mathrm{tr},i,\ell} = \sum_{\ell=0}^{n_r} \widetilde{t}^\star_{\mathrm{tr},j,\ell} = t_c$, we have $\sum_{\ell=1}^{n_r} (2^{R^\ell} - 1)\widetilde{t}^\star_{\mathrm{tr},i,\ell} < \sum_{\ell=1}^{n_r} (2^{R^\ell} - 1)\widetilde{t}^\star_{\mathrm{tr},j,\ell}$ based on Lemma 20. We can then choose a feasible solution as follows: $t_{\mathrm{tr},i,\ell} = t^\star_{\mathrm{tr},i,\ell} - \widetilde{t}^\star_{\mathrm{tr},i,\ell} + \widetilde{t}^\star_{\mathrm{tr},j,\ell}$ and $t_{\mathrm{tr},j,\ell} = t^\star_{\mathrm{tr},j,\ell} - \widetilde{t}^\star_{\mathrm{tr},j,\ell} + \widetilde{t}^\star_{\mathrm{tr},i,\ell}$ for all ℓ. It is straightforward to see that using this feasible solution consumes less energy since $E_{\mathrm{C},i} + E_{\mathrm{C},j} < E^\star_{\mathrm{C},i} + E^\star_{\mathrm{C},j}$, resulting in a contradiction. Hence, we must have $\sum_{\ell=1}^{n_r} R^\ell t^\star_{\mathrm{tr},i,\ell}/(t^\star_{\mathrm{mo},i} + t^\star_{\mathrm{st},i}) \geq \sum_{\ell=1}^{n_r} R^\ell t^\star_{\mathrm{tr},j,\ell}/(t^\star_{\mathrm{mo},j} + t^\star_{\mathrm{st},j})$ if $\mathbb{E}\{1/\Upsilon_i\} < \mathbb{E}\{1/\Upsilon_j\}$. ■

Part 1 of Theorem 4 says that if the robot chooses to move, then the optimal final sub-route should have the property that its predicted channel quality is better than that of all the sub-routes before it. This is intuitive since it is not optimal for the robot to spend more motion energy to go to a location that has a worse predicted channel quality. Part 2 of Theorem 4 shows that the robot should always travel with its maximum speed to save motion energy. If it needs to spend more time at some positions where the predicted channel quality is high, it chooses to stop rather than reducing its speed. Part 3 of Theorem 4 says that the robot only stops once and at the optimal final sub-route, where the predicted channel quality is the best. Moreover, note that $\sum_{\ell=1}^{n_r} R^\ell t^\star_{\mathrm{tr},i,\ell}/(t^\star_{\mathrm{mo},i} + t^\star_{\mathrm{st},i})$ is the optimal average spectral efficiency along $\mathcal{T}_i$. Then, part 4 of Theorem 4 says that the robot should increase its transmission rate (send with a higher average spectral efficiency) at the regions where the predicted channel quality is higher to save the communication energy.

Remark 9 *Parts 3 and 4 of Theorem 4 imply that the robot sends most of its information bits at the optimal final sub-route if T_{tot} is large.*

Based on Theorem 4, the optimization problem of (5.1) can be greatly simplified. Let $\mathcal{N}_{\mathrm{acpt}}(\mathcal{T}) = \{N_1, \cdots, N_{|\mathcal{N}_{\mathrm{acpt}}(\mathcal{T})|}\}$ be a set of acceptable sub-route indices for stopping,

where $N_1 = 1$, N_j denotes the j^{th} index such that $\mathbb{E}\{1/\Upsilon_{N_j}\} < \mathbb{E}\{1/\Upsilon_i\}$, for $\forall\ i \in \{1, \cdots, N_j - 1\}$, and $|\mathcal{N}_{\text{acpt}}(\mathcal{T})|$ is the total number of sub-routes in $\mathcal{T}$ that satisfy this condition. In other words, $\mathcal{N}_{\text{acpt}}(\mathcal{T})$ contains index 1 (the current position) and all the indices of the sub-routes where the predicted channel quality is better than that of all the sub-routes before them. By using the properties of Theorem 4, it is easy to verify that the number of variables in (5.1) can be reduced from $(3 + n_r)n_{\mathcal{T}} - 1$ to $n_r N_{|\mathcal{N}_{\text{acpt}}(\mathcal{T})|} + 2|\mathcal{N}_{\text{acpt}}(\mathcal{T})|$. We skip presenting the details of the simplified optimization problem for brevity.

5.1.2 Should the Robot Move or Should the Robot Stay?

So far, we have characterized some properties of the optimal solution if it is the best that the robot moves. In this part we focus on one of the fundamental questions raised at the beginning of this section: Under what conditions should the robot spend its energy on motion to move to a better spot for communication and under what conditions should it stay at its initial position and increase its transmission power? Theorem 5 provides two sufficient conditions along this line. Before presenting the theorem, we first introduce the fixed average-rate strategy, which will be utilized in the subsequent proofs.

Lemma 21 (fixed average-rate strategy) *Suppose that the final sub-route is $\mathcal{T}_{N_j}$, for some $j \in \{1, \cdots, |\mathcal{N}_{\text{acpt}}(\mathcal{T})|\}$. Then, the following (sub-optimal) transmission strategy has a fixed average rate along all the sub-routes:*

$$t_{\text{tr},i,\ell^\star} = \frac{d_i}{v_{\max}} \frac{R^{\ell^\star+1} - Q_{\text{tot}}/(T_{\text{tot}}B)}{R^{\ell^\star+1} - R^{\ell^\star}}, \tag{5.16}$$

$$t_{\text{tr},i,\ell^\star+1} = \frac{d_i}{v_{\max}} \frac{Q_{\text{tot}}/(T_{\text{tot}}B) - R^{\ell^\star}}{R^{\ell^\star+1} - R^{\ell^\star}}, \tag{5.17}$$

for $i \in \{1, \cdots, N_j - 1\}$,

$$t_{\mathrm{tr},N_j,\ell^\star} = \left(T_{\mathrm{tot}} - \sum_{i=1}^{N_j-1} \frac{d_i}{v_{\max}}\right) \frac{R^{\ell^\star+1} - Q_{\mathrm{tot}}/(T_{\mathrm{tot}}B)}{R^{\ell^\star+1} - R^{\ell^\star}}, \tag{5.18}$$

$$t_{\mathrm{tr},N_j,\ell^\star+1} = \left(T_{\mathrm{tot}} - \sum_{i=1}^{N_j-1} \frac{d_i}{v_{\max}}\right) \frac{Q_{\mathrm{tot}}/(T_{\mathrm{tot}}B) - R^{\ell^\star}}{R^{\ell^\star+1} - R^{\ell^\star}}, \tag{5.19}$$

and $t_{\mathrm{tr},i,\ell} = 0$, *for all* i *and* $\ell \neq \ell^\star, \ell^\star+1$, *where* $\ell^\star$ *is the largest integer in* $\mathcal{R}$ *that is smaller than or equal to* $Q_{\mathrm{tot}}/(BT_{\mathrm{tot}})$. *Moreover, the normalized communication cost along* $\mathcal{T}_i$ *is* $\big(d_i/(v_{\max}T_{\mathrm{tot}})\big)J^\star_{\mathrm{nComm}}(Q_{\mathrm{tot}}, T_{\mathrm{tot}})$, *for* $i \in \{1, \cdots, N_j-1\}$, *and is* $\big(1-\sum_{i=1}^{N_j-1} d_i/(v_{\max}T_{\mathrm{tot}})\big)$ $\times J^\star_{\mathrm{nComm}}(Q_{\mathrm{tot}}, T_{\mathrm{tot}})$, *for* $i = N_j$.

Proof: The lemma can be easily confirmed by calculating the average rate

$$\frac{\sum_{\ell=\ell^\star}^{\ell^\star+1} R^\ell t_{\mathrm{tr},i,\ell}}{\sum_{\ell=\ell^\star}^{\ell^\star+1} t_{\mathrm{tr},i,\ell}} \tag{5.20}$$

and the normalized communication cost. ■

Theorem 5 *1) The robot should stay at its initial position if*

$$\frac{1}{K}\mathbb{E}\left\{\frac{1}{\Upsilon_1}\right\} J^\star_{\mathrm{nComm}}(Q_{\mathrm{tot}}, T_{\mathrm{tot}}) \leq \sum_{i=1}^{N_2-1} \kappa_{\mathrm{M}} d_i. \tag{5.21}$$

2) The robot should at least move to sub-route $\mathcal{T}_{N_j}$, *for* $j \in \{2, \cdots, |\mathcal{N}_{\mathrm{acpt}}(\mathcal{T})|\}$, *if*

$$\underbrace{\sum_{i=N_k}^{N_j-1} \kappa_{\mathrm{M}} d_i}_{\substack{\textit{equivalent} \\ \textit{motion cost}}} \leq \underbrace{\frac{1}{K} M_{\mathrm{eq,ch}}(\mathcal{T}_{N_j}, \mathcal{T}_{N_k}) J^\star_{\mathrm{nComm}}(Q_{\mathrm{tot}}, T_{\mathrm{tot}})}_{\textit{equivalent communication cost}}, \tag{5.22}$$

for $\forall\ k \in \{1, \cdots, j-1\}$, *where*

$$M_{\text{eq,ch}}(\mathcal{T}_{N_j}, \mathcal{T}_{N_k}) = \text{DQ}(\mathcal{T}_{N_k}, \mathcal{T}_{N_j}) + \sum_{i=1}^{N_j-1} \text{DQ}(\mathcal{T}_{N_j}, \mathcal{T}_i) \frac{d_i}{T_{\text{tot}} v_{\max}} \tag{5.23}$$

and $\text{DQ}(\mathcal{T}_i, \mathcal{T}_j) = \mathbb{E}\{1/\Upsilon_i\} - \mathbb{E}\{1/\Upsilon_j\}$ *denotes the difference in the metric that characterizes the channel prediction quality at* $\mathcal{T}_i$ *and* $\mathcal{T}_j$.

Proof: The total energy cost of sending all the bits at the initial position is $\mathbb{E}\{1/\Upsilon_1\}\, J^{\star}_{\text{nComm}}(Q_{\text{tot}}, T_{\text{tot}})/K$ while the motion energy cost of moving to sub-route $\mathcal{T}_{N_2}$ is $\sum_{i=1}^{N_2-1} \kappa_{\text{M}} d_i$. The first part of the theorem then easily follows. To prove the second part of the theorem, consider the sub-optimal fixed average-rate strategy of Lemma 21. After some derivations, we can prove that this strategy results in the following upper bound on the total energy cost when choosing $\mathcal{T}_{N_j}$ as the final sub-route: $\big(-M_{\text{eq,ch}}(\mathcal{T}_{N_j}, \mathcal{T}_{N_k}) + \mathbb{E}\{1/\Upsilon_{N_k}\}\big) J^{\star}_{\text{nComm}}(Q_{\text{tot}}, T_{\text{tot}})/K + \sum_{i=1}^{N_j-1} \kappa_{\text{M}} d_i$. It is also straightforward to see that choosing any other sub-route $\mathcal{T}_{N_k}$, for $k \in \{1, \cdots, j-1\}$, as the final sub-route at least consumes the following amount of energy: $\mathbb{E}\{1/\Upsilon_{N_k}\}\, J^{\star}_{\text{nComm}}(Q_{\text{tot}}, T_{\text{tot}})/K + \sum_{i=1}^{N_k-1} \kappa_{\text{M}} d_i$. Hence, the robot should move at least to $\mathcal{T}_{N_j}$ if (5.22) holds for all k. ■

Note that $M_{\text{eq,ch}}(\mathcal{T}_{N_j}, \mathcal{T}_{N_k})$ can be thought of as an equivalent measure of channel prediction quality. Hence, the right hand side of (5.22) can be interpreted as an equivalent communication energy cost, given Q_{tot} and T_{tot}.

From Lemma 20, we know that $J^{\star}_{\text{nComm}}(Q_{\text{tot}}, T_{\text{tot}})$ is monotonically increasing with respect to Q_{tot}. It can be seen from part 1 of Theorem 5 that if the motion cost is high (i.e. κ_{M} is large), the communication demand is low (i.e. Q_{tot} is small), K is large (i.e. required reception quality is low), and/or the predicted channel quality at the initial position is high enough, it is better for the robot to simply stay at its initial position to send the bits. Similarly, part 2 of Theorem 5 says that if the communication demand is high (i.e. Q_{tot} is large) and $M_{\text{eq,ch}}(\mathcal{T}_{N_j}, \mathcal{T}_{N_k})$ is positive (this is always true given a

sufficiently large T_{tot} or $v_{\max}$),[3] it is more efficient to spend energy on motion to move to the regions where the predicted channel quality is high. Then, whether the robot should move to $\mathcal{T}_{N_j}$ or stop at $\mathcal{T}_{N_k}$ can be determined by comparing the equivalent motion and communication costs, as shown in (5.22). Theorem 5 then mathematically characterizes the corresponding sufficient conditions to decide on when to move or stay.

Remark 10 *In general, there is no monotonic relation between the motion decision of the robot in terms of how far it should travel, and the total time budget* T_{tot}.

5.1.3 Impact of Underlying Channel Parameters

We next consider a special case where the shadowing component of the channel is uncorrelated, i.e. $\beta \to 0$, to see how the underlying channel parameters impact the motion decision of the robot. Based on (2.4) and (2.5), we then have $\overline{\Upsilon}(q, q_b) = \alpha_{\text{PL}}/\|q - q_b\|^{n_{\text{PL}}}$ and $\sigma^2_{\text{dB}}(q, q_b) = \xi^2_{\text{dB}} + \rho^2_{\text{dB}} = \chi^2_{\text{dB}}$, where $\alpha_{\text{PL}} = 10^{\alpha_{\text{PL,dB}}/10}$. *It is straightforward to show that for an uncorrelated channel, the optimal final communication point lies on the line segment between the initial position of the robot and the remote station. Hence, the final communication route can be optimally determined in this case.*

Let the pre-defined route $\mathcal{T}$ be the line segment between the initial position of the robot and the remote station. Clearly, in this case we have $\mathcal{N}_{\text{acpt}}(\mathcal{T}) = \{1, \cdots, n_{\mathcal{T}}\}$. The following lemma characterizes if the robot should move farther or not, when it uses the fixed average-rate transmission strategy of Lemma 21.

Lemma 22 *Consider the case where the robot uses the fixed average-rate transmission strategy of Lemma 21. Let* $\mathcal{T}_j$ *denote the current position of the robot. Then, the robot should move closer to the remote station, i.e. move to* $\mathcal{T}_{j+1}$ *instead of stopping at* $\mathcal{T}_j$*, if*

[3]Note that $\text{DQ}(\mathcal{T}_{N_j}, \mathcal{T}_i) < 0$ and $\text{DQ}(\mathcal{T}_{N_k}, \mathcal{T}_{N_j}) > 0$ in $M_{\text{eq,ch}}(\mathcal{T}_{N_j}, \mathcal{T}_{N_k})$.

and only if

$$\kappa_{\mathrm{M}} < \left(\frac{(\sum_{i=j}^{n_{\mathcal{T}}} d_i)^{n_{\mathrm{PL}}} - (\sum_{i=j+1}^{n_{\mathcal{T}}} d_i)^{n_{\mathrm{PL}}}}{\alpha_{\mathrm{PL}} \exp\left(-\varpi \chi_{\mathrm{dB}}^2\right) d_j} \right) \underbrace{\frac{1}{K} \left(1 - \sum_{i=1}^{j} \frac{d_i}{T_{\mathrm{tot}} v_{\max}} \right) J^{\star}_{\mathrm{nComm}}(Q_{\mathrm{tot}}, T_{\mathrm{tot}})}_{\eta_1}. \tag{5.24}$$

Moreover, if d_j is sufficiently small as compared to the remaining distance between the robot and the remote station ($\sum_{i=j+1}^{n_{\mathcal{T}}} d_i$), equation (5.24) can be further simplified as follows:

$$\kappa_{\mathrm{M}} < \underbrace{\frac{n_{\mathrm{PL}} (\sum_{i=j+1}^{n_{\mathcal{T}}} d_i)^{n_{\mathrm{PL}}-1}}{\alpha_{\mathrm{PL}} \exp\left(-\varpi \chi_{\mathrm{dB}}^2\right)}}_{\eta_2} \eta_1. \tag{5.25}$$

Proof: The robot should move to $\mathcal{T}_{j+1}$ instead of stopping at $\mathcal{T}_j$, if and only if the following equation is satisfied: $\sum_{i=j}^{j+1} \sum_{\ell=\ell^\star}^{\ell^\star+1} P_{\mathrm{C},i,\ell} t_{\mathrm{tr},i,\ell}(\mathcal{T}_{j+1}) - P_{\mathrm{C},j,\ell} t_{\mathrm{tr},j,\ell}(\mathcal{T}_j) + d_j < 0$, where $t_{\mathrm{tr},i,\ell}(\mathcal{T}_j)$ denotes the transmission time using the fixed average-rate strategy of Lemma 21 for the case of stopping at $\mathcal{T}_j$. The lemma can then be confirmed after some straightforward calculations. ■

We can interpret (5.25) as follows. Consider κ_{M} as the derivative of the motion energy cost $\kappa_{\mathrm{M}} d_i$ with respect to d_i, and $-\eta_2$ as the derivative of the predicted channel quality ($\mathbb{E}\{1/\Upsilon_i\}$) with respect to d_i. Then, the robot has an incentive to move towards the remote station if and only if the rate of decrease of the average communication energy cost is larger than the rate of increase of the motion energy cost.

It can be seen that η_2 is monotonically increasing with respect to the remaining distance between the robot and the remote station ($\sum_{i=j+1}^{n_{\mathcal{T}}} d_i$), the variance of the channel prediction error (χ_{dB}^2), and the path loss exponent (n_{PL}).[4] Therefore, the robot should

[4]Note that the monotonic behavior with respect to n_{PL} holds if and only if $(\sum_{i=j+1}^{n_{\mathcal{T}}} d_i)^{n_{\mathrm{PL}}} > e^{-1}$,

move closer to the remote station if the path loss exponent, the remaining distance between the robot and the remote station, and/or the channel prediction error variance are larger, in order to save the overall energy cost. Moreover, η_1 is monotonically increasing with respect to Q_{tot} and $v_{\max}$. Hence, the robot should move closer to the remote station if the communication demand is higher (it has more bits to send) and/or if it can move faster. Finally, the robot should move closer to the remote station if the motion cost is lower, i.e. κ_{M} is smaller.

Remark 11 *Note that the analysis in this section also holds for the case where the channel is fully correlated, i.e.* $\beta \to \infty$.

5.1.4 Choosing the Set of Final Communication Routes

In general, finding the optimal final communication route is considerably challenging. However, the following observations allow us to come up with a strategy that can be near-optimal for several cases, yet simple enough for implementation. First, from the third and fourth parts of Theorem 4, we know that the robot spends most of its time budget and sends most of the bits at the final communication point, given that the time budget is large enough. This means that the total communication cost is mostly dominated by the communication cost along the optimal final sub-route. Second, the motion cost of the robot is proportional to the distance that the robot travels, as shown in (2.26). These two imply that a line route that ends at a location with high communication quality can be near-optimal for several cases. In particular, if the channel is uncorrelated or fully correlated, the line segment between p_i and the remote station becomes the optimal final communication route, as we have shown in 5.1.3. Then, we consider the following strategy in the next section where we solve the overall problem of visiting the sites and

which should be satisfied in most practical applications.

communicating the information under resource constraints. Given the last POI p_i, choose a set of n_s points in the workspace, $\mathcal{S}_i = \{s_{i,1}, \cdots, s_{i,n_s}\}$, such that the predicted channel quality at $s_{i,j}$s is high. For instance, $\mathcal{S}_i$ can include the position of the remote station, or a point that is close to p_i with a high predicted channel quality. Then, the final communication route can be chosen from the set of line segments that traverse from p_i to the points in the set $\mathcal{S}_i$, in case p_i becomes the last POI. Note that we allow different sets for different p_is in order to keep it more general. Furthermore, in case the robot decides it has to move, it not only has to choose which of its possible final routes to take but also needs to find the optimal final communication point across that route (i.e. it may not be optimal to go to the end point of a final route).

5.2 Communication-Aware Site Visiting and Information Gathering

In this section, we build on the results of the previous section to solve our original problem of visiting the POIs, deciding on the final communication point, and designing the communication and motion strategies along the whole trajectory. We show how this problem can be formulated as a Mixed Integer Linear Program (MILP). We then characterize some properties of the optimal solution. It should be noted that these three components (planning the site visits, deciding on the final communication point and designing the communication and motion strategies) are coupled and should be concurrently optimized.

Let $\mathcal{E}_{i,j}$ denote the pre-defined route from p_i to p_j. Similar to the previous section, we discretize $\mathcal{E}_{i,j}$ into $n_{\mathcal{E}_{i,j}}$ sub-routes, $\mathcal{E}_{i,j,k}$s, for $k \in \{1, \cdots, n_{\mathcal{E}_{i,j}}\}$, each with length $l_{i,j,k}$, where $\sum_{k=1}^{n_{\mathcal{E}_{i,j}}} l_{i,j,k} = l_{i,j}$, with $l_{i,j}$ denoting the distance between p_i and p_j. Variables $l_{i,j,k}$s

are chosen such that the channel along each sub-route can be considered stationary. The predicted channel quality along $\mathcal{E}_{i,j,k}$ is then characterized by $\mathbb{E}\{1/\Upsilon_{\mathcal{E}_{i,j,k}}\}$. Moreover, for each POI p_i, for $i \in \{1, \cdots, m\}$, we have the set of possible final communication routes $\mathcal{S}_i$ as discussed in Section 5.1.4. Let $\mathcal{L}_{i,j}$ denote the route from POI p_i to $s_{i,j}$. Similarly, we discretize $\mathcal{L}_{i,j}$ into $n_{\mathcal{L}_{i,j}}$ sub-routes, $\mathcal{L}_{i,j,k}$s, for $k \in \{1, \cdots, n_{\mathcal{L}_{i,j}}\}$, each with length of $d_{i,j,k}$. The predicted channel quality along $\mathcal{L}_{i,j,k}$ is then characterized by $\mathbb{E}\{1/\Upsilon_{\mathcal{L}_{i,j,k}}\}$. Similar to Section 5.1.1, let $\mathcal{N}_{\text{acpt}}(\mathcal{L}_{i,j}) = \{N_{i,j,1}, \cdots, N_{i,j,|\mathcal{N}_{\text{acpt}}(\mathcal{L}_{i,j})|}\}$ be a set of acceptable sub-route indices for stopping, where $N_{i,j,1} = 1$, $N_{i,j,k}$ denotes the k^{th} index such that $\mathbb{E}\{1/\Upsilon_{\mathcal{L}_{i,j,N_{i,j,k}}}\} < \mathbb{E}\{1/\Upsilon_{\mathcal{L}_{i,j,\ell}}\}$, for $\forall\ \ell \in \{1, \cdots, N_{i,j,k} - 1\}$, and $|\mathcal{N}_{\text{acpt}}(\mathcal{L}_{i,j})|$ is the total number of sub-routes in $\mathcal{L}_{i,j}$ that satisfy this condition.

To formulate the MILP, we introduce the following binary variables: $x_{i,j}$ for $i, j \in \{1, \cdots, m\}$ and $i \neq j$, $y_{i,j,k}$ for $i \in \{1, \cdots, m\}$, $j \in \{1, \cdots, n_s\}$ and $k \in \mathcal{N}_{\text{acpt}}(\mathcal{L}_{i,j})$, and z_i for $i \in \{1, \cdots, m\}$. Let $x_{i,j} = 1$ if the trajectory of the robot contains the route from p_i to p_j, and $x_{i,j} = 0$ otherwise. Also, let $y_{i,j,k} = 1$ if the robot moves through or stops at $\mathcal{L}_{i,j,k}$, given the last POI is p_i, and $y_{i,j,k} = 0$ otherwise. Finally, let $z_i = 1$ if the last visited POI is p_i, and $z_i = 0$ otherwise. Then, we can formulate the following MILP:

$$\begin{aligned}
\min.\quad J_{\text{overall}} = &\sum_{i=1}^{m}\sum_{\substack{j=1\\ j\neq i}}^{m}\left(x_{i,j}\kappa_1 l_{i,j} + \kappa_2\sum_{k=1}^{n_{\mathcal{E}_{i,j}}}\tau_{\text{mo},i,j,k}\right) + \sum_{i=1}^{m}\sum_{j=1}^{n_s}\sum_{k=2}^{|\mathcal{N}_{\text{acpt}}(\mathcal{L}_{i,j})|} y_{i,j,k}\sum_{\ell=N_{i,j,k-1}}^{N_{i,j,k}-1}\kappa_{\text{M}} d_{i,j,\ell}\\
&+\sum_{i=1}^{m}\sum_{\substack{j=1\\ j\neq i}}^{m}\sum_{k=1}^{n_{\mathcal{E}_{i,j}}}\sum_{\ell=1}^{n_r}\frac{2^{R^\ell}-1}{K}\mathbb{E}\left\{\frac{1}{\Upsilon_{\mathcal{E}_{i,j,k}}}\right\}\tau_{\text{tr},i,j,k,\ell}\\
&+\sum_{i=1}^{m}\sum_{j=1}^{n_s}\sum_{k=1}^{N_{i,j,|\mathcal{N}_{\text{acpt}}(\mathcal{L}_{i,j})|}}\sum_{\ell=1}^{n_r}\frac{2^{R^\ell}-1}{K}\mathbb{E}\left\{\frac{1}{\Upsilon_{\mathcal{L}_{i,j,k}}}\right\}t_{\text{tr},i,j,k,\ell} \qquad (5.26)\\
\text{s.t.}\quad 1)\ &\sum_{i=1}^{m}\sum_{\substack{j=1\\ j\neq i}}^{m}\sum_{k=1}^{n_{\mathcal{E}_{i,j}}}(\tau_{\text{mo},i,j,k}+\tau_{\text{st},i,j,k}) + \sum_{i=1}^{m}\sum_{j=1}^{n_s}\sum_{k=2}^{|\mathcal{N}_{\text{acpt}}(\mathcal{L}_{i,j})|} y_{i,j,k}\sum_{\ell=N_{i,j,k-1}}^{N_{i,j,k}-1}\frac{d_{i,j,\ell}}{v_{\max}}\\
&+\sum_{i=1}^{m}\sum_{j=1}^{n_s}\sum_{k\in\mathcal{N}_{\text{acpt}}(\mathcal{L}_{i,j})} t_{\text{st},i,j,k} \le T_{\text{tot}},\quad 2)\ \sum_{k=1}^{n_{\mathcal{E}_{i,j}}}\sum_{\ell=1}^{n_r} R^\ell\tau_{\text{tr},i,j,k,\ell} \le V_i,\ \forall\ i,j,\\
&3)\ V_j \ge V_i - \sum_{k=1}^{n_{\mathcal{E}_{i,j}}}\sum_{\ell=1}^{n_r} R^\ell\tau_{\text{tr},i,j,k,\ell} + Q_j + Q_{\text{tot}}(x_{i,j}-1),\ \forall\ i,j,\\
&4)\ \sum_{i=1}^{m}\sum_{j=1}^{n_s}\sum_{k=1}^{N_{i,j,|\mathcal{N}_{\text{acpt}}(\mathcal{L}_{i,j})|}}\sum_{\ell=1}^{n_r} R^\ell t_{\text{tr},i,j,k,\ell} \ge V_i + Q_{\text{tot}}(y_{i,j,1}-1),\ \forall\ i,j,\\
&5)\ \tau_{\text{mo},i,j,k} \ge x_{i,j}\frac{l_{i,j,k}}{v_{\max}},\ \forall\ i,j,k,\quad 6)\ \sum_{\ell=1}^{n_r}\tau_{\text{tr},i,j,k,\ell} \le \tau_{\text{mo},i,j,k}+\tau_{\text{st},i,j,k},\ \forall\ i,j,k,\\
&7)\ 0 \le \tau_{\text{st},i,j,k} \le x_{i,j}T_{\text{tot}},\ \forall\ i,j,k,\quad 8)\ \sum_{\ell=1}^{n_r} t_{\text{tr},i,j,h,\ell} \le y_{i,j,k}\frac{d_{i,j,h}}{v_{\max}},\ \forall\ i,j,\\
&\text{and } k\in\{2,\cdots,|\mathcal{N}_{\text{acpt}}(\mathcal{L}_{i,j})|\}, h\in\{N_{i,j,k-1}+1,\cdots,N_{i,j,k}-1\},\\
&9)\ \sum_{\ell=1}^{n_r} t_{\text{tr},i,j,N_{i,j,k},\ell} \le y_{i,j,k+1}\frac{d_{i,j,N_{i,j,k}}}{v_{\max}} + t_{\text{st},i,j,N_{i,j,k}},\ \forall\ i,j,\ \text{and } k\in\{1,\cdots,|\mathcal{N}_{\text{acpt}}(\mathcal{L}_{i,j})|-1\},\\
&10)\ \sum_{\ell=1}^{n_r} t_{\text{tr},i,j,N_{i,j,|\mathcal{N}_{\text{acpt}}(\mathcal{L}_{i,j})|},\ell} \le t_{\text{st},i,j,N_{i,j,|\mathcal{N}_{\text{acpt}}(\mathcal{L}_{i,j})|}},\ \forall\ i,j,\\
&11)\ y_{i,j,1} \ge y_{i,j,2} \ge \cdots \ge y_{i,j,|\mathcal{N}_{\text{acpt}}(\mathcal{L}_{i,j})|},\ \forall\ i,j,\\
&12)\ 0 \le t_{\text{st},i,j,N_{i,j,k}} \le y_{i,j,k}T_{\text{tot}},\ \forall\ i,j,\ \text{and } k\in\{1,\cdots,|\mathcal{N}_{\text{acpt}}(\mathcal{L}_{i,j})|\},\\
&13)\ t_{\text{tr},i,j,k,\ell},\tau_{\text{tr},i,j,k,\ell} \ge 0,\ \forall\ i,j,k,\ell,\quad 14)\ \sum_{\substack{i=1\\ i\neq j}}^{m} x_{i,j} = 1,\ \forall\ j\neq 1,\quad 15)\ \sum_{j=2}^{m} x_{1,j} = 1,\\
&16)\ z_i + \sum_{\substack{j=1\\ j\neq i}}^{m} x_{i,j} = 1,\ \forall\ i\neq 1,\quad 17)\ \sum_{i=1}^{m} z_i = 1,\quad 18)\ \sum_{j=1}^{n_s} y_{i,j,1} = z_i,\ \forall\ i,\\
&19)\ u_i - u_j + (m-1)x_{i,j} \le m-2,\ \forall\ i,j\neq 1, i\neq j,\quad 20)\ 2\le u_i\le m,\ \forall\ i\neq 1,\\
&21)\ x_{i,j},\ y_{i,j,k},\ z_i\in\{0,1\},\quad u_i\in\mathbb{Z}.
\end{aligned}$$

As can be seen, the first and second terms in the objective function of (5.26) denote the total motion cost to visit all the POIs and the motion cost to move from the last POI to the final sub-route respectively, where $\tau_{\mathrm{mo},i,j,k}$ is the motion time that the robot spends along sub-route $\mathcal{E}_{i,j,k}$. The third and fourth terms represent the total communication cost to send all the bits along the entire trajectory, where $\tau_{\mathrm{tr},i,j,k,\ell}$ and $t_{\mathrm{tr},i,j,k,\ell}$ denote the transmission times with the spectral efficiency R^{ℓ} along the sub-routes $\mathcal{E}_{i,j,k}$ and $\mathcal{L}_{i,j,k}$ respectively. Moreover, constraint 1 ensures that the robot accomplishes the task in the given time budget T_{tot}, where $\tau_{\mathrm{st},i,j,k}$ and $t_{\mathrm{st},i,j,k}$ are the stop times assigned to $\mathcal{E}_{i,j,k}$ and $\mathcal{L}_{i,j,k}$ respectively. Constraint 2 guarantees that the robot does not send more than the available bits in its memory, where V_i (a variable to solve for) denotes the number of the bits on board of the robot when it leaves the i^{th} POI. Constraints 3 and 4 force the robot to send all the collected bits to the remote station, where Q_i is the number of generated/collected information bits at p_i and $Q_{\mathrm{tot}} = \sum_{i=1}^{m} Q_i$. Constraint 5 is the maximum velocity constraint of the robot. Constraints 6, 8, 9 and 10 force the total transmission time along each sub-route to be smaller than or equal to the total time that is spent along the corresponding sub-route. Constraints 7 and 12 guarantee that the stop time is zero if the corresponding sub-route is not part of the whole trajectory. Constraint 14 forces each POI to exactly have one degree in. Constraints 15 and 16 force the initial position and each POI, except for the last one, to exactly have one degree out. If a certain POI is the last POI that the robot visits (i.e. $z_i = 1$), then it should have zero degree out to other POIs. Constraint 17 guarantees that the robot only chooses one POI to visit at last. Constraint 18 ensures that the robot chooses to move along $\mathcal{L}_{i,j}$ for some j only if the last visited POI is p_i. Finally, constraints 19 and 20 are sub-tour elimination constraints, where u_is are auxiliary integer variables. Here, we use Miller-Tucker-Zemlin (MTZ) formulation [121], which is a classic approach in Traveling Salesman Problem (TSP). Note that although we aim to find a trajectory rather than

a tour, MTZ formulation can still be used to eliminate sub-tours. Furthermore, note that we have applied the properties of Theorem 4 in (5.26) to simplify the formulation. The MILP of (5.26) can be solved using existing efficient solvers such as IBM ILOG CPLEX [122].

5.2.1 Properties of the Optimal Solution

In this part, we extend the results in Section 5.1.1 and characterize some properties of the optimal solution of (5.26).

Theorem 6 *Let $\mathcal{T}^\star$ be the optimal trajectory which contains the routes between the POIs as well as the route between the last visited POI and the optimal final communication point. Let $\mathcal{T}_h^\star$ be the h^{th} stationary sub-trajectory of $\mathcal{T}^\star$, where $h \in \{1, \cdots, n_{\mathcal{T}^\star}\}$ and $n_{\mathcal{T}^\star}$ is the total number of stationary sub-trajectories of $\mathcal{T}^\star$. Consider the case where sub-route $\mathcal{E}_{i,j,k}$ is part of $\mathcal{T}^\star$, i.e. $\mathcal{E}_{i,j,k} = \mathcal{T}_h^\star$ for some h. We then have the following properties for the optimal communication and motion strategies:*

1) $\tau^\star_{\text{mo},i,j,k} = l_{i,j,k}/v_{\max}$, for $\forall\ i, j, k$;

2) If $\tau^\star_{\text{st},i,j,k} > 0$, then the predicted channel quality along $\mathcal{E}_{i,j,k}$ must be better than that of the remaining part of the optimal trajectory, i.e. $\mathbb{E}\left\{1/\Upsilon_{\mathcal{E}_{i,j,k}}\right\} = \mathbb{E}\left\{1/\Upsilon_{\mathcal{T}_h^\star}\right\} < \mathbb{E}\left\{1/\Upsilon_{\mathcal{T}_\ell^\star}\right\}$, for $\forall\ \ell \in \{h+1, \cdots, n_{\mathcal{T}^\star}\}$, where $\mathbb{E}\left\{1/\Upsilon_{\mathcal{T}_\ell^\star}\right\}$ is the predicted channel quality along sub-trajectory $\mathcal{T}_\ell^\star$;

3) If sub-routes $\mathcal{E}_{i,j,k}$ and $\mathcal{E}_{i,j,h}$ are part of $\mathcal{T}^\star$, and $\mathbb{E}\{1/\Upsilon_{\mathcal{E}_{i,j,k}}\} < \mathbb{E}\{1/\Upsilon_{\mathcal{E}_{i,j,h}}\}$, then $\sum_{\ell=1}^{n_r} R^\ell t^\star_{\text{tr},i,j,k,\ell}/(\tau^\star_{\text{mo},i,j,k} + \tau^\star_{\text{st},i,j,k}) \geq \sum_{\ell=1}^{n_r} R^\ell t^\star_{\text{tr},i,j,h,\ell}/(\tau^\star_{\text{mo},i,j,h} + \tau^\star_{\text{st},i,j,h})$.

Proof: Theorem 4 can be easily extended to prove Theorem 6. We omit the details for brevity. ■

As expected, the robot should travel with its maximum velocity to save motion energy. Moreover, if needed, it should only stop at the places that have better predicted channel

quality than that of the remaining part of the optimal trajectory. Between each two POIs, it should send faster at the places that have better predicted channel quality. Note that Theorem 4 further characterizes the properties of the optimal strategy after the last POI is visited.

The following theorem characterizes the corresponding properties of the optimal trajectory of (5.26) when the communication demand is significantly low or high.

Theorem 7 *1) Let $\mathcal{S}_{\mathcal{T}_{\min}}$ denote the set of all the minimum-length trajectories that cover all the POIs and $L_{\min}$ represent the corresponding minimum length. Moreover, let L be the minimum length of all the other possible trajectories, i.e. $L = \min_{\mathcal{T}\notin\mathcal{S}_{\mathcal{T}_{\min}}} |\mathcal{T}|$. Then, the optimal trajectory is in the set $\mathcal{S}_{\mathcal{T}_{\min}}$ if there exists a $\mathcal{T} \in \mathcal{S}_{\mathcal{T}_{\min}}$ such that*

$$\frac{1}{K}\mathbb{E}\left\{\frac{1}{\Upsilon_{\mathcal{T}_{n_\mathcal{T}}}}\right\} J^{\star}_{\mathrm{nComm}}\left(Q_{\mathrm{tot}}, T_{\mathrm{tot}} - \frac{L_{\min}}{v_{\max}}\right) \leq \kappa_{\mathrm{M}}(L - L_{\min}), \tag{5.27}$$

where $n_\mathcal{T}$ is the total number of sub-trajectories of $\mathcal{T}$.

2) Let $\mathcal{S}_{\mathcal{T}_{\mathrm{comm}}}$ denote the set that contains all the trajectories that end at the sub-trajectory with the best predicted channel quality, and $\overline{\mathcal{S}}_{\mathcal{T}_{\mathrm{comm}}}$ be the complement of $\mathcal{S}_{\mathcal{T}_{\mathrm{comm}}}$, i.e. it contains all the other trajectories that do not end at the sub-trajectory with the best predicted channel quality. Then, if there exists a $\mathcal{T} \in \mathcal{S}_{\mathcal{T}_{\mathrm{comm}}}$ such that

$$\underbrace{\kappa_{\mathrm{M}}(|\mathcal{T}| - \widetilde{L})}_{\textit{equivalent motion cost}} \leq \underbrace{\frac{1}{K}\widetilde{M}_{\mathrm{eq,ch}} J^{\star}_{\mathrm{nComm}}(Q_{\mathrm{tot}}, T_{\mathrm{tot}})}_{\textit{equivalent communication cost}}, \tag{5.28}$$

where $\widetilde{M}_{\mathrm{eq,ch}} = \sum_{i=1}^{n_\mathcal{T}-1}\left(\iota - \mathbb{E}\left\{1/\Upsilon_{\mathcal{T}_i}\right\}\right) d_i/(T_{\mathrm{tot}} v_{\max}) + \varkappa - \iota$, $\iota = \min_{\mathcal{T}\in\mathcal{S}_{\mathcal{T}_{\mathrm{comm}}}} \mathbb{E}\{1/\Upsilon_{\mathcal{T}_{n_\mathcal{T}}}\}$, $\varkappa = \min_{\mathcal{T}\in\overline{\mathcal{S}}_{\mathcal{T}_{\mathrm{comm}}}, i\in\{1,\cdots,n_\mathcal{T}\}} \mathbb{E}\{1/\Upsilon_{\mathcal{T}_i}\} > \iota$ and $\widetilde{L} = \min_{\mathcal{T}\in\overline{\mathcal{S}}_{\mathcal{T}_{\mathrm{comm}}}} |\mathcal{T}|$, the optimal trajectory must be in the set $\mathcal{S}_{\mathcal{T}_{\mathrm{comm}}}$. This means that the robot finally moves to the sub-trajectory that has the best predicted channel quality after it has covered all the POIs. Moreover,

the robot only stops at the last sub-trajectory.

Proof: The proof of Theorem 5 can be extended straightforwardly to this case. The details are omitted for brevity. ■

Theorem 7 shows two special cases of the optimal trajectory. It can be seen that the left and right hand sides of (5.27) are the upper bound on the communication cost along the minimum-length trajectory and the minimum extra motion cost to deviate from it respectively. Then, the first part of Theorem 7 says that, if (5.27) holds, the minimum-length trajectory is optimal. Similar to the second part of Theorem 5, $\widetilde{M}_{\text{eq,ch}}$ and the right hand side of (5.28) can also be interpreted as an equivalent measure of channel prediction quality and an equivalent communication energy cost given Q_{tot} and T_{tot} respectively. Moreover, the equivalent motion energy cost on the left hand side of (5.28) is the extra motion cost to choose a trajectory in $\mathcal{S}_{\mathcal{T}_{\text{comm}}}$. Then, whether the robot should move to the sub-trajectory that has the best predicted channel quality can be determined by comparing the equivalent motion and communication costs of (5.28). Note that if the communication demand is sufficiently high and $\widetilde{M}_{\text{eq,ch}}$ is positive (this always holds given a sufficiently large T_{tot} or $v_{\max}$), equation (5.28) can be satisfied and the robot will finally move to the sub-trajectory that has the best predicted channel quality.

5.2.2 Online Adaptation

Our framework can also be generalized to the case where the initial knowledge of the environment is uncertain, for instance due to channel prediction uncertainty. In this case, the robot can adjust its strategy online once it has learned the environment better by resolving (5.26) after visiting each POI. This, however, could be computationally expensive. One possible sub-optimal strategy is to only adapt the transmission power/rate

and stop times of the robot without changing the order in which it will visit the POIs. This adaptation strategy can be posed as a linear program by simplifying (5.26), which can be solved more efficiently. We omit the details for brevity.

Another source of uncertainty is multipath fading. In order to reduce the energy cost more, the robot can further adjust its transmit power/rate and stop times online based on the online observations of the real channel values in each sub-trajectory. Here, we present an approach that is slightly different from the one we have proposed in Section 4.2. Note that the approach in Section 4.2 can also be applied to this case.

Let $\mathcal{T}_h^\star$ denote the h^{th} stationary sub-trajectory of $\mathcal{T}^\star$ that is found by solving (5.26). We divide $\mathcal{T}_h^\star$ into $n_{\text{MP},h}$ equal-length chunks, $\mathcal{T}_{h,i}^\star$, for $i \in \{1, \cdots, n_{\text{MP},h}\}$. The robot now adapts to the channel changes from one chunk to another. We use $\Delta l_{\mathcal{T}_h^\star}$ to represent the length of each chunk, over which the channel is considered constant. Moreover, we discretize the distribution of the channel along $\mathcal{T}_h^\star$ such that we use $n_{\text{ch},h}$ constants, $\gamma_{\mathcal{T}_h^\star,j}$, for $j \in \{1, \cdots, n_{\text{ch},h}\}$, to approximate all the possible CNR values. Then, $p_{\mathcal{T}_h^\star,j}$, for $j \in \{1, \cdots, n_{\text{ch},h}\}$, are the probabilities that the real channel value along each chunk is approximated by $\gamma_{\mathcal{T}_h^\star,j}$, for $j \in \{1, \cdots, n_{\text{ch},h}\}$, respectively.[5] Hence, our goal is to assign a proper number of bits and corresponding time budget to each $\mathcal{T}_{h,i}^\star$ based on the online observation of the real channel value, while guaranteeing that the total bits assigned to $\mathcal{T}_h^\star$ are transmitted within the allocated time budget. Note that the total allocated bits and time budget along $\mathcal{T}_h^\star$ are already obtained from the solution of (5.26).

Consider the case where the mobile robot moves to $\mathcal{T}_{h,i}^\star$ and observes its real channel value. Note that the motion cost along $\mathcal{T}_{h,i}^\star$ is given, since it is always optimal to travel with the maximum velocity, as we have shown previously. Hence, we aim to minimize the average communication cost $\sum_{j=1}^{n_{\text{ch},h}} J_{\text{nComm}}^\star(Q_{\mathcal{T}_{h,i}^\star,j}, T_{\mathcal{T}_{h,i}^\star,j}) p_{\mathcal{T}_h^\star,j}/(K\gamma_{\mathcal{T}_h^\star,j})$, where $Q_{\mathcal{T}_{h,i}^\star,j}$

[5]We assume that multipath fading component is normally distributed in the dB domain, with its mean and variance estimated by Lemma 2.

and $T_{\mathcal{T}^\star_{h,i},j}$ denote the assigned number of bits and time budget to $\mathcal{T}^\star_{h,i}$ respectively, if the instantaneous channel value along $\mathcal{T}^\star_{h,i}$ is approximated by $\gamma_{\mathcal{T}^\star_h,j}$. It can be seen that $J^\star_{\text{nComm}}(Q_{\mathcal{T}^\star_{h,i},j}, T_{\mathcal{T}^\star_{h,i},j})$ is a piecewise-linear function of $Q_{\mathcal{T}^\star_{h,i},j}$ and $T_{\mathcal{T}^\star_{h,i},j}$, which is equal to $\max_{\ell\in\{1,\cdots,n_r\}}\{a_\ell Q_{\mathcal{T}^\star_{h,i},j} - b_\ell T_{\mathcal{T}^\star_{h,i},j}\}$. Based on this observation, we can solve the following Linear Program (LP) for online adaptation:

$$\begin{aligned}
\text{minimize} \quad & \sum_{j=1}^{n_{\text{ch},h}} \frac{\pi_j}{K\gamma_{\mathcal{T}^\star_h,j}} p_{\mathcal{T}^\star_h,j} && (5.29)\\
\text{subject to} \quad & 1)\ a_\ell Q_{\mathcal{T}^\star_{h,i},j} - b_\ell T_{\mathcal{T}^\star_{h,i},j} \le \pi_j,\ \forall\ j,\ell,\\
& 2)\ \sum_{j=1}^{n_{\text{ch},h}} Q_{\mathcal{T}^\star_{h,i},j} p_{\mathcal{T}^\star_h,j} = Q^{\text{rem}}_{\mathcal{T}^\star_{h,i}}/(B(n_{\text{MP},h}-i+1)),\\
& 3)\ \sum_{j=1}^{n_{\text{ch},h}} T_{\mathcal{T}^\star_{h,i},j} p_{\mathcal{T}^\star_h,j} = T^{\text{rem}}_{\mathcal{T}^\star_{h,i}}/(n_{\text{MP},h}-i+1),\\
& 4)\ 0 \le Q_{\mathcal{T}^\star_{h,i},j} \le R_{n_r} T_{\mathcal{T}^\star_{h,i},j},\ \forall\ j,\\
& 5)\ R_{n_r}(T^{\text{rem}}_{\mathcal{T}^\star_{h,i}} - T_{\mathcal{T}^\star_{h,i},j}) \le Q_{\mathcal{T}^\star_{h,i},j} \le Q^{\text{rem}}_{\mathcal{T}^\star_{h,i}},\ \forall\ j,\\
& 6)\ \Delta l_{\mathcal{T}^\star_h}/v_{\max} \le T_{\mathcal{T}^\star_{h,i},j} \le T^{\text{rem}}_{\mathcal{T}^\star_{h,i}} - (n_{\text{MP},h}-i)\Delta l_{\mathcal{T}^\star_h}/v_{\max},\ \forall\ j, && (5.30)
\end{aligned}$$

where π_j, for $j \in \{1,\cdots,n_{\text{ch},h}\}$, are auxiliary variables, and $Q^{\text{rem}}_{\mathcal{T}^\star_{h,i}}$ and $T^{\text{rem}}_{\mathcal{T}^\star_{h,i}}$ are the remaining number of bits and time budget that are assigned to $\mathcal{T}^\star_h$ respectively, when the robot reaches $\mathcal{T}^\star_{h,i}$. Once the LP is solved, the robot can assign the proper $Q_{\mathcal{T}^\star_{h,i},j}$ and $T_{\mathcal{T}^\star_{h,i},j}$ to $\mathcal{T}^\star_{h,i}$ based on the instantaneous channel value.

5.3 Simulation Results

Consider the case where the workspace is a 50 m $\times$ 50 m square region with the coordinates shown in Fig. 5.2. The remote station is located at the origin and there are 7 POIs in the workspace. The channel in the workspace is generated using the probabilistic

channel simulator (which probabilistically generates path loss, shadowing and multipath fading components of the channel) [68], with the following real channel parameters that are extracted from real channel measurements in downtown San Francisco (data courtesy of W. M. Smith) [119]: $n_{\mathrm{PL}} = 4.4$, $\xi_{\mathrm{dB}} = 2.6$ and $\beta = 22.6$ m. Furthermore, the multipath fading is taken to be uncorrelated Rician fading with parameter $K_{\mathrm{ric}} = 3.9$. We assume that the robot has 5% a priori channel samples gathered in the same environment. Then, it uses the probabilistic channel prediction framework of Section 2.1 to predict the channel quality at unvisited locations in the workspace. We choose $\mathcal{R} = \{0, 2, 4, 6, 8\}$ bits/Hz/s and $B = 10$ MHz, and the receiver noise power is chosen to be the realistic value of -104 dBmW [123]. We also use the real motion parameters of the Pioneer 3DX robot as follows: $\kappa_2 = 7.4$, $\kappa_4 = 0.29$ and $v_{\max} = 1$ m/s [86]. Moreover, $\mathcal{S}_i$ is chosen as a set that only contains the position that has the best predicted channel quality in the workspace, for $\forall\, i$. The MILP of (5.26) is solved using IBM ILOG CPLEX Studio in MATLAB [122].

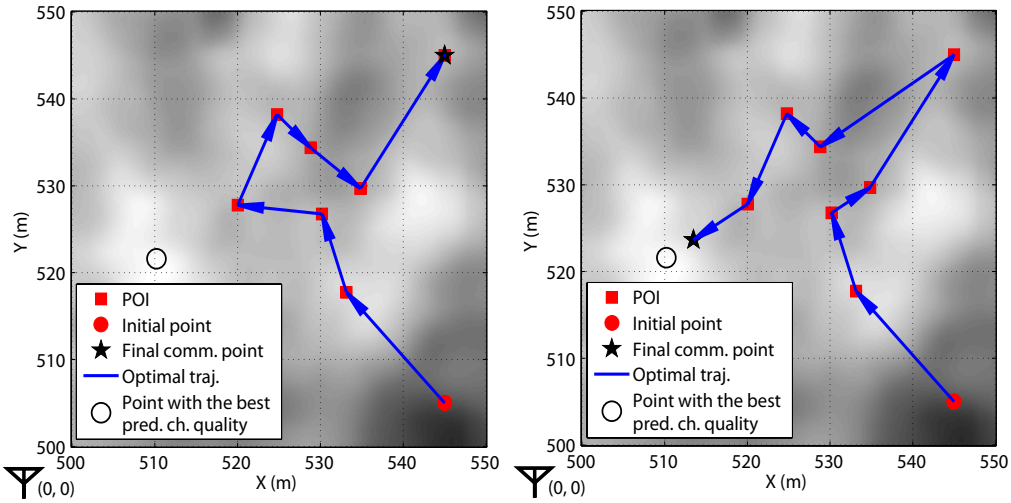

Figure 5.2: Comparison of the optimal trajectories of (5.26) when the communication demands are low (left figure) and high (right figure) respectively. The position of the remote station is marked in both figures. The backgrounds show the predicted channel quality (the predicted channel quality is lower if the background color is darker).

Fig. 5.2 compares the optimal trajectories of (5.26) with different (yet realistic) communication demands. In Fig. 5.2 (left), we have $Q_i/B = 20$ bits/Hz for $\forall\, i$ and $T_{\text{tot}} = 300$ s, resulting in a low communication demand. As can be seen, the optimal trajectory is therefore the minimum-length trajectory that covers all the POIs, which has the total length of 80.1 m. Also, the robot does not move beyond the last POI after it has covered all the POIs. In Fig. 5.2 (right), on the other hand, we have $Q_i/B = 100$ bits/Hz and $T_{\text{tot}} = 300$ s, resulting in a high communication demand. It can be seen that the optimal trajectory is longer (94.9 m), as compared to the previous case, and deviates from the minimum-length one in order to pass through areas with high connectivity. Moreover, the robot moves way beyond the last POI and towards the remote station where the predicted channel quality is high, after visiting the last POI. We have also applied our online adaptation strategy to the high communication demand case, which can further save 13.3% total energy cost in this example. It should be noted that Fig. 5.2 shows two extreme cases. There are several cases where the robot chooses to travel on a final communication route but the final communication point is not necessarily at the end point.

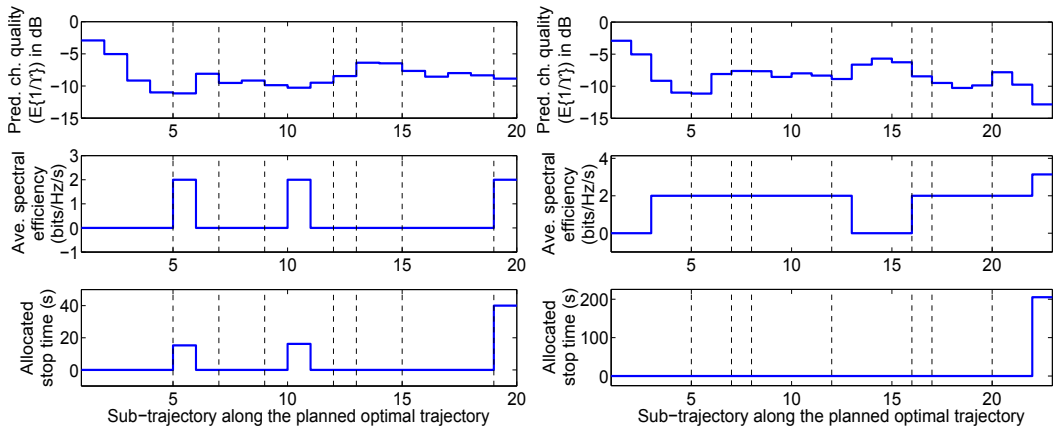

Figure 5.3: Comparison of the optimal communication and motion strategies of Fig. 5.2 when the communication demands are low (left figure) and high (right figure) respectively. The vertical dashed lines represent the locations of the POIs. The observed behavior is as predicted by Theorems 4 and 6.

Fig. 5.3 shows the optimal communication and motion strategies along the optimal trajectories of Fig. 5.2. As shown in Theorem 6, between each two POIs, the robot sends faster (higher average spectral efficiency) at the sub-trajectories that have a better predicted channel quality. Also, the robot only stops at the sub-trajectories where the predicted channel quality is better than that of the remaining part of the trajectory. For the case of high communication demand, the robot only stops at the last sub-trajectory where the predicted channel quality is the best, as shown in the second part of Theorem 7.

Remark 12 (on computational complexity) *It takes 34.7 s and 2396.0 s to solve (5.26) when the communication demands are low and high respectively on a 3.4 GHz CPU.*

So far, the simulation results confirmed that there are cases where the robot has to incur motion energy for better connectivity. Next, we show a simulation result that explicitly focuses on the "To Go or Not to Go" problem, by considering $\mathcal{P} = \emptyset$. The goal is to explicitly show that incurring motion energy for better connectivity can save the overall energy in several realistic cases, which may be against the common belief in the current literature that communication is always much cheaper than motion. Fig. 5.4 shows the total energy saving of utilizing motion to find a final communication point for the case where $\mathcal{P} = \emptyset$. In this simulation, the remote station is located at the origin. The initial position of the robot is chosen at $(400\text{ m}, 0\text{ m})$. Moreover, the final communication route is pre-defined as the line segment from the initial position of the robot to the remote station. The underlying channel parameters are taken the same as Fig. 5.2. Since the planning strategy and the performance depend on each realization of the channel, we average the performance over 100 runs of independent channel samples (but with the same underlying parameters). We compare our strategy with the case

where the robot sends all the data at its initial position, for two different sets of real motion parameters [86]. Fig. 5.4 (left) shows the performance of our strategy (optimal value of (5.1)) as a function of Q_{tot}/B, and for $T_{\text{tot}} = 100$ s. Clearly, the total energy costs of all cases increase as Q_{tot}/B increases. It can be seen that when Q_{tot}/B is small, i.e. the communication demand is low, the robot does not benefit from the motion and sending the data at the initial point can become optimal. However, when Q_{tot}/B is large, i.e. the communication demand is high, incurring motion cost for better connectivity can save the total energy considerably. Fig. 5.4 (right) shows the performance of our strategy as a function of T_{tot}, for $Q_{\text{tot}}/B = 300$ bits/Hz. Similarly, the figure confirms that incurring motion cost for better connectivity can be considerably beneficial depending on the scenario.

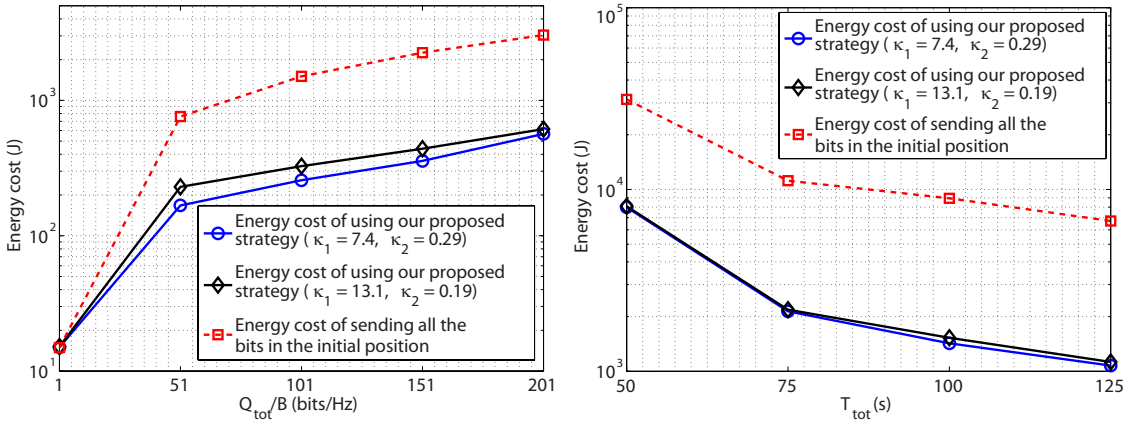

Figure 5.4: Performance of our strategy as compared with the case where the robot sends all its data at its initial position. The saving is considerable.

Chapter 6

Clustering and Path Planning Strategies for Robotic Data Collection

Consider a scenario where a robot is tasked with periodically collecting data from a fixed wireless sensor network. The robot does not know the exact positions of the sensors, but only the probability distribution of their positions. More specifically, we assume that a total of m stationary sensors are independent and identically distributed according to a probability density function (pdf) $p(x)$ in a square workspace $\mathcal{W}$ with the side length of S. Each sensor collects the data from the environment with a rate of ϱ bits/second and caches it in its memory. A robot is then tasked with gathering the up-to-date data from all the sensors in a given period T_{tot}. Our goal is to minimize the total energy cost of the whole operation in each period, *including the communication energy cost of the sensors and the motion cost of the robot*. Clearly, the motion cost is minimized if the robot stays at some point in the workspace while the sensors transmit their gathered

This chapter is an amended version of [124].

bits to it. However, such a strategy is not energy efficient for communication. On the other hand, the communication cost can be minimized if the robot visits each sensor to download the data. However, this strategy causes a high motion cost for the robot.

In this chapter, we propose a strategy that properly combines the ideas of clustering and robotic data collection in a wireless sensor network. In such a strategy, all the sensors are divided into a number of clusters. A stop position is chosen in each cluster for the robot to collect the data (via single-hop wireless transmissions) from the sensors in the corresponding cluster. In this chapter, we assume that the shadowing component of the channel is uncorrelated. Moreover, we assume that the robot can only collect data when it stops at its stop positions. The robot then periodically visits all the stop positions and gathers the data from the network. Fig. 6.1 shows an example of our considered scenario. In general, the motion cost can increase as the number of clusters increases since the robot needs to travel a longer distance in each period. On the other hand, the communication cost can decrease as the number of clusters increases, since the transmission distances of the sensors decrease (see (2.4) and (2.5)). Hence, in this problem, we need to jointly optimize the number of clusters, the clustering of the network, the stop positions, and the path planning and motion strategy of the robot, in order to minimize the total energy cost.

Remark 13 *For simplicity, we only consider the case of single-hop transmissions in this chapter. Moreover, we assume that the sensors can send their information bits to the robot only when it stops at its stop positions. As a result, the communication cost only depends on the clusters and stop positions, as we shall show later. For the case of multi-hop transmissions, routing strategies in each cluster also need to be jointly designed. If the robot is allowed to collect data while moving, the communication cost will depend on the trajectory of the robot rather than the stop positions.*

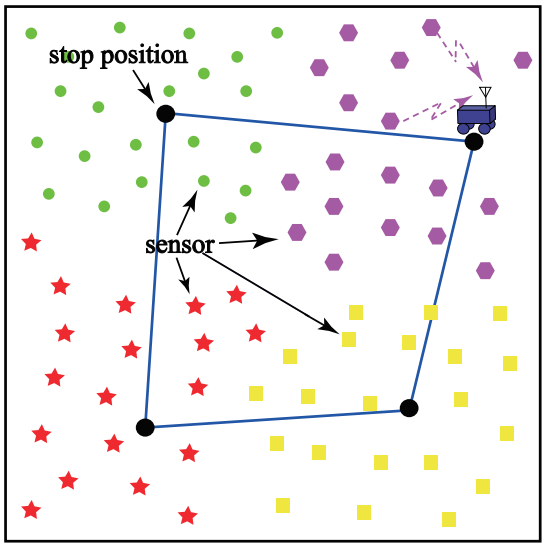

Figure 6.1: An example of using a robot to gather the data from a sensor network. The sensors are divided into 4 clusters. Markers with the same color and shape represent the sensors that are clustered together. The robot has to decide on an optimal stop position in each cluster and then visits all the stop positions periodically to wirelessly collect the data from the sensors in the corresponding clusters.

The rest of this chapter is organized as follows. In Section 6.1, we introduce the concept of space-filling curves which we shall use for algorithm design and performance analysis. We then formulate the general optimization problem that we need to solve in Section 6.2. Section 6.3 presents our proposed computationally-efficient approach based on space-filling curves for the case of uniformly-distributed sensors, and characterizes its performance bound. In Section 6.4, we further extend our approach to the case of non-uniformly-distributed sensors. Finally, in Section 6.6, we show the effectiveness of our proposed approach in a simulation environment.

6.1 Space-Filling Curves

A space-filling curve [104, 125] is a one-dimensional curve that passes through every point of a two-dimensional square. Some of the most celebrated ones are the Hilbert

curve, Peano curve and Sierpiński curve. Readers are referred to [104] for more details on various space-filling curves and how to recursively construct them.

Because of their recursive and self-similar construction, one of the most important properties of space-filling curves is the *locality* property, which means that any two points that are close in the one-dimensional space are mapped to two points that are close in the 2D space. More specifically, let $\mathrm{SF}(\cdot) : \mathcal{C} \to \mathcal{W}$ denote the continuous mapping of a space-filling curve from the unit circle to the $[0, D]^2$ square workspace, where $\mathcal{C} = [0, 1)$ represents the unit circle with a fixed reference point at 0. Note that $\phi \in \mathcal{C}$ represents a point on $\mathcal{C}$, clockwise, from the reference point. Then, we have [104, 126]

$$\|x_1 - x_2\| \leq C_{\mathrm{SF}} \times S \times \mu(\phi_1, \phi_2), \tag{6.1}$$

where $\phi_1, \phi_2 \in \mathcal{C}$, $x_1 = \mathrm{SF}(\phi_1) \in \mathcal{W}$, $x_2 = \mathrm{SF}(\phi_2) \in \mathcal{W}$, C_{SF} is a constant depending on the type of the space-filling curve, $\mu(\phi_1, \phi_2) = \min\{|\phi_1 - \phi_2|, 1 - |\phi_1 - \phi_2|\}^{1/2}$, and $\|\cdot\|$ and $|\cdot|$ denote the Euclidean norm and absolute value of the argument respectively. See Fig. 6.2 for an illustration of the mapping. For Sierpiński curves, for instance, $C_{\mathrm{SF}} = 2$ [104, 126].[1] Note that $\mathrm{SF}(\cdot)$ is not a one-to-one mapping. Different points in $\mathcal{C}$ can be mapped to the same point in $\mathcal{W}$. See [104, 126, 127] for more details on how $\mathrm{SF}(\cdot)$ and $\mathrm{SF}^{-1}(\cdot)$ are evaluated in practice.

Due to this *locality* property, space-filling curves are widely used in computational science [104]. The application that is most related to this chapter is to solve the Traveling Salesman Problem (TSP) as follows [126, 127]. First, map all the points in the square into the unit circle using $\mathrm{SF}^{-1}(\cdot)$. Then, order the mapped points on the unit circle in a clockwise or counter-clockwise direction. Finally, build the tour by connecting the

[1] In this chapter, we use Sierpiński curves in our simulations. This is because constant C_{SF} of Sierpiński curves is among the smallest in the space-filling curves family [104]. This then has the potential to improve the performance of heuristic algorithms which take advantage of their locality property.

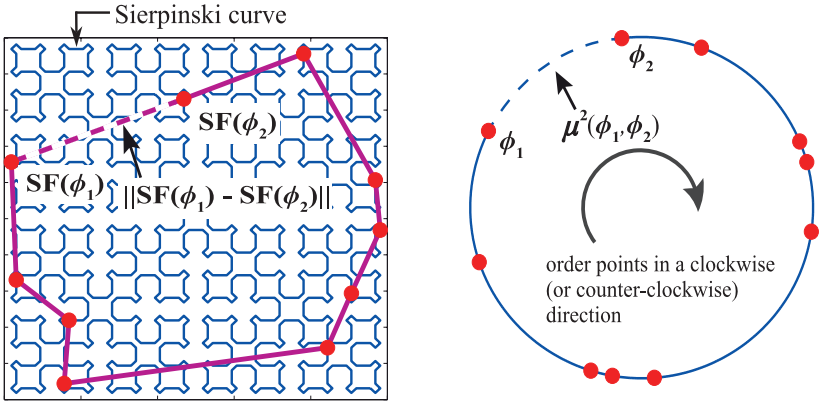

Figure 6.2: The blue curve in the left figure shows the construction of the Sierpiński curve after four recursions in the 2D workspace. The right figure then shows the corresponding 1D curve (circle). The red dots in the left and right figures show the positions of the points in the square and their corresponding mapping in the unit circle respectively. The figure then shows an illustration of the mapping SF$(\cdot)$ and $\mu(\cdot,\cdot)$. The figure also shows how this mapping can be used to solve a TSP problem, where the line segments that connect the points in the square form the tour obtained based on the ordering of the points in the unit circle.

corresponding points in the square based on this order. Fig. 6.2 shows an illustration of solving the TSP problem by using this approach. When the points are independent and identically distributed (i.i.d.) and the number of points are large, the heuristic tour is roughly 35% away from the optimum [127]. However, the computational complexity of this approach is extremely low. In [125], we showed how to utilize the space-filling curves to solve a communication-aware dynamic coverage problem. In this chapter, we utilize them for clustering and data collection in a sensor network.

Remark 14 *There are a number of efficient heuristic algorithms in the TSP literature that can be potentially used towards solving the considered problem [128, 129]. In this chapter, however, we use space-filling curves since they allow us to not only efficiently choose the stop positions and plan the TSP tour but also to characterize the performance bound of our proposed approach.*[2]

[2]The computational complexity of the approaches proposed in [128] and [129] are $O(N^2)$ and $O(N(\log(N))^{O(c)})$, respectively, where N is the number of TSP stop positions and c is a constant.

6.2 Optimization Framework

In this part, we formulate the general optimization problem that we need to solve. Consider the case where the robot divides the sensors into N clusters. Note that N is an unknown variable. Let $\{\mathcal{W}_i\}_{i=1}^{N}$ denote a partition of the workspace such that the sensors in $\mathcal{W}_i$ form a cluster. Also, let q_i, for $i \in \{1, \cdots, N\}$, represent the stop position to collect data from the sensors in the i^{th} cluster. Then, based on the communication model in Section 2.2, the total average communication cost of the sensors can be characterized as follows:

$$E_{\text{C,tot}}(N, \mathcal{Q}, \{\mathcal{W}_i\}_{i=1}^{N}) = m \sum_{i=1}^{N} \int_{\mathcal{W}_i} p(x) P_{\text{C}}(x, q_i) \frac{\varrho T_{\text{tot}}}{BR} dx,$$

where $\mathcal{Q} = \{q_1, \cdots, q_N\}$ denotes the set of stop positions, R is the fixed spectral efficiency, B is the bandwidth, and $P_{\text{C}}(x, q_i) = \big((2^R - 1)/K\big)\mathbb{E}\{1/\Upsilon(x, q_i)\}$ denotes the average communication power cost of the transmission from a sensor at x to the robot at q_i, with $\Upsilon(x, q_i)$ denoting the predicted CNR during the transmission by using the channel prediction framework. Since we assume an uncorrelated shadowing component, we then have $\overline{\Upsilon}(x, q_i) = \alpha_{\text{PL}}/\|x - q_i\|^{n_{\text{PL}}}$ and $\sigma^2_{\text{dB}}(x, q_i) = \xi^2_{\text{dB}} + \rho^2_{\text{dB}} = \chi^2_{\text{dB}}$ (see (2.4) and (2.5)), where $\alpha_{\text{PL}} = 10^{\alpha_{\text{PL,dB}}/10}$. As a result, we have

$$\begin{aligned}
\mathbb{E}\left\{\frac{1}{\Upsilon(x, q_i)}\right\} &= \exp\left(\left(\frac{\ln 10}{10}\right)^2 \frac{\chi^2_{\text{dB}}}{2}\right) \frac{1}{\overline{\Upsilon}(x, q_i)} \\
&= \exp\left(\left(\frac{\ln 10}{10}\right)^2 \frac{\chi^2_{\text{dB}}}{2}\right) \frac{1}{\alpha_{\text{PL}}} \|x - q_i\|^{n_{\text{PL}}} \\
&= \alpha \|x - q_i\|^{n_{\text{PL}}}, \qquad (6.2)
\end{aligned}$$

For comparison, the complexity of the space-filling-based approach [126] is $O(N\log(N))$.

where $\alpha = \exp\left((\ln 10/10)^2 \chi_{\mathrm{dB}}^2/2\right)/\alpha_{\mathrm{PL}}$. Note that for the uncorrelated channel model, the average communication power cost is monotonically increasing with respect to the communication distance. Moreover, in this chapter we use motion model (2.17) to characterize the motion cost. Therefore, we have the following optimization problem to minimize the total energy cost of the network:

$$\begin{aligned}
\text{minimize} \quad & E_{\mathrm{tot}}(N, \mathcal{Q}, \{\mathcal{W}_i\}_{i=1}^N, \{t_{\mathrm{mo},i,j}\}_{i,j=1}^N, \mathcal{T}) = \\
& \underbrace{m \sum_{i=1}^{N} \int_{\mathcal{W}_i} p(x) P_{\mathrm{C}}(x, q_i) \frac{\varrho T_{\mathrm{tot}}}{BR} dx}_{E_{\mathrm{C,tot}}(N, \mathcal{Q}, \{\mathcal{W}_i\}_{i=1}^N)} + \varpi \underbrace{\sum_{i=1}^{N} \sum_{j=1, j\neq i}^{N} z_{i,j} E_{\mathrm{M}}(\|q_i - q_j\|, t_{\mathrm{mo},i,j})}_{E_{\mathrm{M,tot}}(N, \mathcal{Q}, \{t_{\mathrm{mo},i,j}\}_{i,j=1}^N, \mathcal{T})} \\
\text{subject to} \quad & 1) \sum_{i=1, i\neq j}^{N} z_{i,j} = 1, \forall\, j, \quad 2) \sum_{j=1, j\neq i}^{N} z_{i,j} = 1, \forall\, i, \\
& 3)\ u_i - u_j + (N-1) z_{i,j} \leq N - 2, \forall\, i, j \neq 1, i \neq j, \\
& 4) \sum_{i=1}^{N} \sum_{j=1, j\neq i}^{N} z_{i,j} t_{\mathrm{mo},i,j} \leq T\left(1 - \frac{m\varrho}{BR}\right), \\
& 5)\ t_{\mathrm{mo},i,j} \geq 0, \forall\, i, j, \quad 6)\ z_{i,j} \in \{0, 1\}, \forall\, i, j, \\
& 7)\ u_i \in \{2, \cdots, N\}, \forall\, i \neq 1, \quad 8)\ q_i \in \mathcal{W}, \forall\, i,
\end{aligned} \tag{6.3}$$

where $E_{\mathrm{tot}}(N, \mathcal{Q}, \{\mathcal{W}_i\}_{i=1}^N, \{t_{\mathrm{mo},i,j}\}_{i,j=1}^N, \mathcal{T})$ and $E_{\mathrm{M,tot}}(N, \mathcal{Q}, \{t_{\mathrm{mo},i,j}\}_{i,j=1}^N, \mathcal{T})$ represent the total cost of the network and the total motion energy cost, respectively, $\varpi > 0$ is a weight balancing the importance of the average communication energy cost of the sensors and the motion energy cost of the robot, $\mathcal{T}$ is the tour of the robot to visit the stop positions, $t_{\mathrm{mo},i,j}$ is the motion time moving from q_i to q_j, $z_{i,j}$ denotes a binary variable which is 1 if the tour of the robot contains the line segment from q_i and q_j and is 0 otherwise, and u_i is an auxiliary integer variable, which designs the tour.

The first and second constraints in (6.3) guarantee that each stop position has one degree out and one degree in, respectively. The third constraint is the Miller-Tucker-Zemlin (MTZ) sub-tour elimination constraint [121]. Hence, constraints 1-3 ensure that the solution will form a Hamiltonian cycle.[3] The fourth constraint guarantees that the sum of the total motion and communication times is less than or equal to the total time budget.

The variables to solve for are N, q_i, $\mathcal{W}_i$, $t_{\mathrm{mo},i,j}$, $z_{i,j}$ and u_i. Note that we assume $BR \geq m\varrho$ such that the problem is feasible. It is straightforward to see that if the equality holds, the optimal solution is that the robot stays at some position in the workspace to collect the data without moving. Also, without loss of generality, we only consider the case where the robot travels along the line segments between the stop positions, since the motion cost is monotonically increasing with respect to the travel distance between any two stop positions, as can be seen in (2.17). Hence, the tour $\mathcal{T}$ is completely determined by variable $z_{i,j}$, i.e. the order in which to visit the stop positions.

As can be seen, the optimization problem (6.3) is a mixed integer nonlinear program. Moreover, all the variables are coupled. For instance, N and $\mathcal{Q}$ affect not only the communication cost of the sensors (since each sensor transmits to its closest stop position), but also the motion cost of the robot. However, even for fixed N, $\mathcal{Q}$ and $\{\mathcal{W}_i\}_{i=1}^{N}$, jointly determining the tour and the corresponding motion times, i.e. solving $z_{i,j}$ and $t_{\mathrm{mo},i,j}$, is still NP-hard.

In the rest of the chapter, we then show how to sub-optimally but efficiently solve (6.3). More specifically, we first determine the number of clusters and design an initial

[3] As an example, suppose that we have four stop positions labeled as 1, 2, 3 and 4, respectively. Consider a solution where $z_{1,2} = 1$, $z_{2,1} = 1$, $z_{3,4} = 1$, $z_{4,3} = 1$, and $z_{i,j} = 0$ otherwise. As can be seen, this is not a valid tour (since there are two sub-tours) while constraints 1 and 2 are still satisfied. Constraint 3 helps to eliminate such situations. For this example, we have $u_3 - u_4 + 3 \leq 2$ and $u_4 - u_3 + 3 \leq 2$. Then, it becomes impossible to choose u_3 and u_4 to satisfy the previous inequalities. On the other hand, if the solution is a valid tour, it is easy to verify that there exists corresponding u_is to satisfy constraint 3.

solution by taking advantage of the locality property of the space-filling curves (Algorithm 1 for the case of uniformly-distributed sensors and Algorithm 3 for the case of non-uniformly-distributed sensors, as we shall discuss in Sections 6.3 and 6.5 respectively). Then, we propose an iterative approach (Algorithm 2) to optimize the stop positions, the clustering strategy, and the path and motion strategy of the robot after the initial phase. Fig. 6.3 shows a flow chart of our approach. We shall see how each step of our proposed approach boils down to solving a series of convex optimization problems.

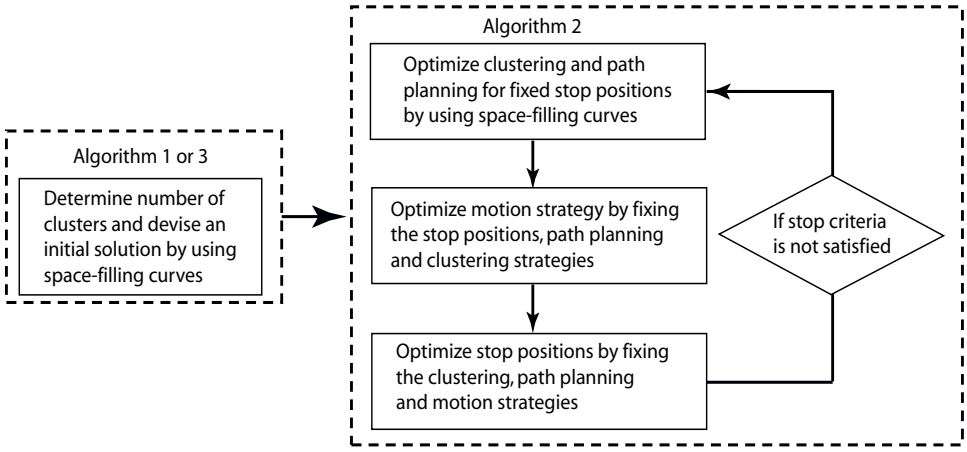

Figure 6.3: Flow chart of our proposed approach. We first determine the number of clusters and design an initial solution by using space-filling curves (Algorithm 1 for the case of uniformly-distributed sensors and Algorithm 3 for the case of non-uniformly-distributed sensors). Then, we iteratively optimize the stop positions, the clustering strategy, and the path and motion strategy of the robot (Algorithm 2).

Lemma 23 *If the stop positions $\mathcal{Q}$ are given, the optimal solution of $\{\mathcal{W}_i\}_{i=1}^N$ for the case of uncorrelated channels will always be the Voronoi partition $\{\mathcal{V}_i(\mathcal{Q})\}_{i=1}^N$.*[4]

Proof: Since the communication cost is monotonically increasing with respect to the distance between a sensor and the robot, the result follows straightforwardly. ■

[4]The Voronoi partition $\{\mathcal{V}_i(\mathcal{Q})\}_{i=1}^N$ of the workspace $\mathcal{W}$ generated by a set of stop positions $\mathcal{Q}$ is defined as follows: $\mathcal{V}_i(\mathcal{Q}) = \{x \in \mathcal{W} | \|x - q_i\| \leq \|x - q_j\|, \forall\, i \neq j\}$, for all i. See [130] for more details on Voronoi diagrams.

Lemma 23 implies that the underlying variables to solve for are N, q_i, $t_{\mathrm{mo},i,j}$, $z_{i,j}$ and u_i in (6.3). We will use Lemma 23 in the subsequent sections when designing our algorithm.

6.3 Joint Clustering and Path Planning

In this section, we present the initial phase of our proposed approach to solve the optimization problem of (6.3) based on space-filling curves. We consider uniformly-distributed sensors in this part, i.e. $p(x) = 1/S^2$. We show how the initial design can be simplified to solving a series of convex optimization problems. Moreover, we characterize how the number of clusters is related to the communication and motion parameters. Finally, we compare the upper bound of the performance of the proposed approach to the case of no clustering (i.e. the whole workspace is one cluster) to show its benefits. We then extend our results to the case of non-uniformly-distributed sensors in Section 6.5.

6.3.1 Our Proposed Approach

Consider the case where there is no clustering, i.e. there is only one cluster (the whole workspace). In the rest of the chapter, this case will serve as a benchmark for comparison. It can be easily seen that the optimal stop position ($q_1^\star$) is the center of the workspace in this case since the sensors are uniformly distributed. The optimal value of (6.3) is as follows for $N = 1$:

$$E_{\mathrm{tot,noCl,unif}} = m \int_{\mathcal{W}} \frac{1}{S^2} P_{\mathrm{C}}(x, q_1^\star) \frac{\varrho T_{\mathrm{tot}}}{BR} dx = \frac{m\alpha S^{n_{\mathrm{PL}}} (2^R - 1) \varrho T_{\mathrm{tot}} C_1}{KBR}, \tag{6.4}$$

where $E_{\text{tot,noCl,unif}}$ denotes the total energy cost for the case of no clustering and $C_1 = \int_{-0.5}^{0.5}\int_{-0.5}^{0.5} \|x\|^{n_{\text{PL}}} dx$.

Note that optimally solving our general optimization problem of (6.3) is not possible. Instead, we propose the following approach to efficiently decouple the optimization of the stop positions, the tour, and the motion times.

Optimization of the stop positions (variables q_is)

Since the sensors are uniformly distributed, we expect that in general the stop positions should be evenly located across $\mathcal{W}$, especially when the communication cost is dominant. This design can be easily achieved in the space-filling curve domain. We then map the 2D workspace $\mathcal{W}$ to $\mathcal{C}$ by using $\text{SF}^{-1}(\cdot)$.

Lemma 24 ([126]) *Consider space-filling mapping* $\text{SF}(\cdot)$. *If the sensors are uniformly distributed in* $\mathcal{W}$, *they will be uniformly distributed in* $\mathcal{C}$.

Let $\{\phi_i\}_{i=1}^N$ and $\{q_{\text{SF},i}\}_{i=1}^N$ denote the stop positions in $\mathcal{C}$ and their corresponding mappings in $\mathcal{W}$, respectively. Without loss of generality, we assume that $0 \leq \phi_1 \leq \phi_2 \cdots \leq \phi_N < 1$. Moreover, let $\Delta_{i-1,i} = \phi_i - \phi_{i-1}$, for $i \in \{2, \cdots, N\}$, be the length of the arc from ϕ_{i-1} to ϕ_i, and $\Delta_{N,1} = \phi_1 + 1 - \phi_N$ be the length of the arc from ϕ_N to ϕ_1. Note that $\sum_{i=2}^N \Delta_{i-1,i} + \Delta_{N,1} = 1$. Then, the total communication cost in $\mathcal{W}$ can be

characterized as follows:

$$
\begin{aligned}
&E_{\mathrm{C,tot,unif}}(N, \mathcal{Q}_{\mathrm{SF}}, \{\mathcal{W}_{\mathrm{SF},i}\}_{i=1}^{N}) = m \sum_{i=1}^{N} \int_{\mathcal{W}_{\mathrm{SF},i}} \frac{1}{S^2} P_{\mathrm{C}}(x, q_{\mathrm{SF},i}) \frac{\varrho T_{\mathrm{tot}}}{BR} dx \\
&\leq m \sum_{i=1}^{N} \int_{\mathrm{SF}(\mathcal{C}_i)} \frac{1}{S^2} P_{\mathrm{C}}(x, q_{\mathrm{SF},i}) \frac{\varrho T_{\mathrm{tot}}}{BR} dx \\
&\leq \frac{m\alpha(2^R - 1)\varrho T_{\mathrm{tot}}}{KBR} \sum_{i=1}^{N} \int_{\mathcal{C}_i} C_{\mathrm{SF}}^{n_{\mathrm{PL}}} S^{n_{\mathrm{PL}}} \left|\phi - \phi_i\right|^{n_{\mathrm{PL}}/2} d\phi \\
&= \frac{m\alpha C_{\mathrm{SF}}^{n_{\mathrm{PL}}} S^{n_{\mathrm{PL}}} (2^R - 1)\varrho T_{\mathrm{tot}}}{KBR(n_{\mathrm{PL}}/2 + 1)2^{n_{\mathrm{PL}}/2}} \left(\sum_{i=2}^{N} \Delta_{i-1,i}^{n_{\mathrm{PL}}/2+1} + \Delta_{N,1}^{n_{\mathrm{PL}}/2+1} \right),
\end{aligned} \tag{6.5}
$$

where $E_{\mathrm{C,tot,unif}}(N, \mathcal{Q}_{\mathrm{SF}}, \{\mathcal{W}_{\mathrm{SF},i}\}_{i=1}^{N})$ is the total communication energy cost for the case of uniformly distributed sensors, $\mathcal{Q}_{\mathrm{SF}} = \{q_{\mathrm{SF},1}, \cdots, q_{\mathrm{SF},N}\}$, $\{\mathcal{W}_{\mathrm{SF},i}\}_{i=1}^{N}$ is the Voronoi partition generated by $\mathcal{Q}_{\mathrm{SF}}$ in the 2D workspace, and $\{\mathcal{C}_i\}_{i=1}^{N}$ is the Voronoi partition generated by $\{\phi_i\}_{i=1}^{N}$ in the space-filling curve domain. Note that the first and second inequalities in (6.5) are obtained based on Lemma 23 and (6.1), respectively. Also, we can prove that the sensors in 1D are uniformly distributed by applying Lemma 24. Moreover, the boundary of the two neighboring Voronoi partitions in 1D can be easily obtained by choosing the middle point between the corresponding stop positions. Then, the last equality of (6.5) follows straightforwardly.

As can be seen, the upper bound of $E_{\mathrm{C,tot,unif}}(N, \mathcal{Q}_{\mathrm{SF}}, \{\mathcal{W}_{\mathrm{SF},i}\}_{i=1}^{N})$ is a convex function of $\Delta_{i-1,i}$ and $\Delta_{N,1}$, and is minimized by choosing $\Delta_{i-1,i}^{\star} = \Delta_{N,1}^{\star} = 1/N$, for $i \in \{2, \cdots, N\}$, i.e. the stop positions are chosen to be equally-spaced in the space-filling curve domain. Without loss of generality, we choose $\phi_i^{\star} = (2i - 1)/(2N)$ and

$q^\star_{\mathrm{SF},i} = \mathrm{SF}(\phi^\star_i)$, for $i \in \{1, \cdots, N\}$. As a result, we have

$$\begin{aligned} E_{\mathrm{C,tot,SF,unif}}(N) &= E_{\mathrm{C,tot,unif}}(N, \mathcal{Q}^\star_{\mathrm{SF}}, \{\mathcal{W}^\star_{\mathrm{SF},i}\}_{i=1}^N) \\ &\leq \frac{m\alpha C_{\mathrm{SF}}^{n_{\mathrm{PL}}} S^{n_{\mathrm{PL}}} (2^R - 1)\varrho T_{\mathrm{tot}}}{(n_{\mathrm{PL}}/2 + 1)(2N)^{\frac{n_{\mathrm{PL}}}{2}} KBR}, \end{aligned} \tag{6.6}$$

where $E_{\mathrm{C,tot,SF,unif}}(N)$ is the communication cost in the 2D workspace by using the above stop position selection strategy, $\mathcal{Q}^\star_{\mathrm{SF}} = \{q^\star_{\mathrm{SF},1}, \cdots, q^\star_{\mathrm{SF},N}\}$, and $\{\mathcal{W}^\star_{\mathrm{SF},i}\}_{i=1}^N$ is the Voronoi partition generated by $\mathcal{Q}^\star_{\mathrm{SF}}$ (we know this is optimal from Lemma 23). Note that in this chapter, we use superscript $\star$ to denote the optimal solutions or the optimal values of the corresponding optimization problems.

Optimization of the tour (variables $z_{i,j}$s and u_is)

Next, consider the motion of the robot. Note that a minimum-distance tour will not be the optimal solution anymore. This is due to the fact that the robot needs to accelerate and decelerate between adjacent stop positions along the tour (there is an acceleration cost). Thus, the total motion cost not only depends on the total length of the tour, but also depends on the lengths of individual line segments. We next show that the minimum-length tour minimizes a tight upper bound on the motion cost if t_{mo} is not very small. More specifically, we consider an upper bound of (2.17) as follows:

$$E_{\mathrm{M,upper}}(d, t_{\mathrm{mo}}) = \frac{\kappa_1 d^2}{t_{\mathrm{mo}} - 2\sqrt{\kappa_3/\kappa_1}} + \kappa_2 d + \kappa_4 t_{\mathrm{mo}}, \tag{6.7}$$

assuming $t_{\mathrm{mo}} > 2\sqrt{\kappa_3/\kappa_1}$. Note that this bound is tight when t_{mo} is not close to zero. Without loss of generality, for a fixed given tour $\mathcal{T}$, we label the stop positions such that the robot visits them by the order of their labels. Then, the upper bound of the total motion cost is given by $E_{\mathrm{M,tot,upper}}(N, \mathcal{Q}, \{t_{\mathrm{mo},i,i+1}\}_{i=1}^{N-1}, t_{\mathrm{mo},N,1}, \mathcal{T}) =$

$\sum_{i=1}^{N-1} E_{\mathrm{M,upper}}(\|q_{i+1}-q_i\|, t_{\mathrm{mo},i,i+1}) + E_{\mathrm{M,upper}}(\|q_N - q_1\|, t_{\mathrm{mo},N,1})$. We then have the following lemma.

Lemma 25 *Given a fixed total motion time budget $T_{\mathrm{mo}} > 2\sqrt{\kappa_3/\kappa_1}N$ and a fixed set of stop positions $\mathcal{Q}$, the optimal value of the following optimization problem is monotonically increasing with respect to the total travel distance $d_{\mathrm{tot}}(\mathcal{Q},\mathcal{T}) = \sum_{i=1}^{N-1}\|q_{i+1}-q_i\| + \|q_N - q_1\|$:*

$$\begin{aligned} \textit{minimize} \quad & E_{\mathrm{M,tot,upper}}(N, \mathcal{Q}, \{t_{\mathrm{mo},i,i+1}\}_{i=1}^{N-1}, t_{\mathrm{mo},N,1}, \mathcal{T}) \\ \textit{subject to} \quad & 1)\ t_{\mathrm{mo},N,1} + \sum_{i=1}^{N-1} t_{\mathrm{mo},i,i+1} \le T_{\mathrm{mo}}, \\ & 2)\ t_{\mathrm{mo},i,i+1} \ge 2\sqrt{\kappa_3/\kappa_1}, \forall\, i, \quad t_{\mathrm{mo},N,1} \ge 2\sqrt{\kappa_3/\kappa_1}, \end{aligned} \tag{6.8}$$

where $E_{\mathrm{M,upper}}(d, t_{\mathrm{mo}})$ is defined to be ∞ if $t_{\mathrm{mo}} = 2\sqrt{\kappa_3/\kappa_1}$.

Proof: It is easy to show that the optimization problem of (6.8) is convex. Then, the dual function of the primal problem is $g = \sum_{i=1}^{N-1} E_{\mathrm{M,upper}}(\|q_{i+1}-q_i\|, t_{\mathrm{mo},i,i+1}) + E_{\mathrm{M,upper}}(\|q_N - q_1\|, t_{\mathrm{mo},N,1}) + \lambda(t_{\mathrm{mo},N,1} + \sum_{i=1}^{N-1} t_{\mathrm{mo},i,i+1} - T_{\mathrm{mo}}) - \sum_{i=1}^{N-1}\nu_{i,i+1}(t_{\mathrm{mo},i,i+1} - 2\sqrt{\kappa_3/\kappa_1}) - \nu_{N,1}(t_{\mathrm{mo},N,1} - 2\sqrt{\kappa_3/\kappa_1})$, where λ, $\nu_{i,i+1}$ and $\nu_{N,1}$ are Lagrange multipliers. Based on the Karush-Kuhn-Tucker (KKT) conditions [111], we have $\partial g/\partial t_{\mathrm{mo},i,i+1} = -\kappa_1\|q_{i+1}-q_i\|^2/(t_{\mathrm{mo},i,i+1} - 2\sqrt{\kappa_3/\kappa_1})^2 + \lambda - \nu_{i,i+1} + \kappa_4 = 0$, for all i, and $\partial g/\partial t_{\mathrm{mo},N,1} = -\kappa_1\|q_N - q_1\|^2/(t_{\mathrm{mo},N,1} - 2\sqrt{\kappa_3/\kappa_1})^2 + \lambda - \nu_{N,1} + \kappa_4 = 0$.

Since constraint 2 can never be active when $T_{\mathrm{mo}} > 2\sqrt{\kappa_3/\kappa_1}N$, we have $\nu^\star_{i,i+1} = 0$, for all i, and $\nu^\star_{N,1} = 0$. Moreover, if $T_{\mathrm{mo}} \ge \sqrt{\kappa_1/\kappa_4}d_{\mathrm{tot}}(\mathcal{Q},\mathcal{T}) + 2\sqrt{\kappa_3/\kappa_1}N$, we have $\lambda^\star = 0$, $t^\star_{\mathrm{mo},i,i+1} = \sqrt{\kappa_1/\kappa_4}\|q_{i+1}-q_i\| + 2\sqrt{\kappa_3/\kappa_1}$, for all i, and $t^\star_{\mathrm{mo},N,1} = \sqrt{\kappa_1/\kappa_4}\|q_N - q_1\| + 2\sqrt{\kappa_3/\kappa_1}$. As a result, the optimal value of (6.8) is

$$(2\sqrt{\kappa_1\kappa_4} + \kappa_2)d_{\mathrm{tot}}(\mathcal{Q},\mathcal{T}) + 2\kappa_4\sqrt{\kappa_3/\kappa_1}N, \tag{6.9}$$

which is monotonically increasing with respect to $d_{\text{tot}}(\mathcal{Q}, \mathcal{T})$. For the case where

$$2\sqrt{\kappa_3/\kappa_1}N < T_{\text{mo}} < \sqrt{\kappa_1/\kappa_4}d_{\text{tot}}(\mathcal{Q}, \mathcal{T}) + 2\sqrt{\kappa_3/\kappa_1}N,$$

it is straightforward to show that $t^{\star}_{\text{mo},i,i+1} = \|q_{i+1} - q_i\|(T_{\text{mo}} - 2\sqrt{\kappa_3/\kappa_1}N)/d_{\text{tot}}(\mathcal{Q}, \mathcal{T}) + 2\sqrt{\kappa_3/\kappa_1}$, for all i, and $t^{\star}_{\text{mo},N,1} = \|q_N - q_1\|(T_{\text{mo}} - 2\sqrt{\kappa_3/\kappa_1}N)/d_{\text{tot}}(\mathcal{Q}, \mathcal{T}) + 2\sqrt{\kappa_3/\kappa_1}$, resulting in the following optimal value:

$$\frac{\kappa_1 d^2_{\text{tot}}(\mathcal{Q}, \mathcal{T})}{T_{\text{mo}} - 2\sqrt{\kappa_3/\kappa_1}N} + \kappa_2 d_{\text{tot}}(\mathcal{Q}, \mathcal{T}) + \kappa_4 T_{\text{mo}}. \tag{6.10}$$

Clearly, the optimal value is monotonically increasing with respect to $d_{\text{tot}}(\mathcal{Q}, \mathcal{T})$, which completes the proof. ■

Lemma 25 shows that the minimum-distance tour minimizes the upper bound of the motion cost. Thus, we choose the minimum-distance tour to cover $\mathcal{Q}$ in 2D. Such a tour can be found by simply ordering the stop positions in the space-filling curve domain, as discussed in Section 6.1.

Optimization of the motion times (variables $t_{\text{mo},i,i+1}$s and $t_{\text{mo},N,1}$)

Based on the previous stop position selection and path planning strategy, the remaining variables to solve for are the number of clusters and the motion times. Then, the

optimization problem of (6.3) can be simplified as follows:

$$\begin{aligned}
\text{minimize} \quad & E_{\text{tot,SF,unif}}(N, \{t_{\text{mo},i,i+1}\}_{i=1}^{N-1}, t_{\text{mo},N,1}) \\
& = E_{\text{tot,unif}}(N, \mathcal{Q}^{\star}_{\text{SF}}, \{\mathcal{W}^{\star}_{\text{SF},i}\}_{i=1}^{N}, \{t_{\text{mo},i,j}\}_{i,j=1}^{N}, \mathcal{T}^{\star}_{\text{SF}}) \\
& = \underbrace{m \sum_{i=1}^{N} \int_{\mathcal{W}^{\star}_{\text{SF},i}} \frac{1}{S^2} P_{\text{C}}(x, q^{\star}_{\text{SF},i}) \frac{\varrho T_{\text{tot}}}{BR} dx}_{E_{\text{C,tot,SF,unif}}(N)} \\
& \quad + \varpi \underbrace{\left(\sum_{i=1}^{N-1} E_{\text{M}}(\|q^{\star}_{\text{SF},i+1} - q^{\star}_{\text{SF},i}\|, t_{\text{mo},i,i+1}) + E_{\text{M}}(\|q^{\star}_{\text{SF},N} - q^{\star}_{\text{SF},1}\|, t_{\text{mo},N,1}) \right)}_{E_{\text{M,tot,SF}}(N, \{t_{\text{mo},i,i+1}\}_{i=1}^{N-1}, t_{\text{mo},N,1}) = E_{\text{M,tot}}(N, \mathcal{Q}^{\star}_{\text{SF}}, \{t_{\text{mo},i,j}\}_{i,j=1}^{N}, \mathcal{T}^{\star}_{\text{SF}})}
\end{aligned} \tag{6.11}$$

$$\begin{aligned}
\text{subject to} \quad & 1) \ \sum_{i=1}^{N-1} t_{\text{mo},i,i+1} + t_{\text{mo},N,1} \leq T_{\text{tot}} \left(1 - \frac{m\varrho}{BR}\right), \\
& 2) \ t_{\text{mo},i,i+1} \geq 0, \forall\, i, \quad t_{\text{mo},N,1} \geq 0,
\end{aligned}$$

where $E_{\text{tot,unif}}(N, \mathcal{Q}^{\star}_{\text{SF}}, \{\mathcal{W}^{\star}_{\text{SF},i}\}_{i=1}^{N}, \{t_{\text{mo},i,j}\}_{i,j=1}^{N}, \mathcal{T}^{\star}_{\text{SF}})$ is the total cost for the case of uniformly distributed sensors, $\mathcal{T}^{\star}_{\text{SF}}$ is the minimum-distance tour obtained by ordering the stop positions in the space-filling curve domain, and $E_{\text{tot,SF,unif}}(N, \{t_{\text{mo},i,i+1}\}_{i=1}^{N-1}, t_{\text{mo},N,1})$ and $E_{\text{M,tot,SF}}(N, \{t_{\text{mo},i,i+1}\}_{i=1}^{N-1}, t_{\text{mo},N,1})$ denote the total cost and total motion cost in the 2D workspace, respectively, based on the stop position selection and path planning strategy in the space-filling curve domain. For a fixed N, equation (6.11) becomes a convex optimization problem since $E_{\text{M,tot,SF}}(N, \{t_{\text{mo},i,i+1}\}_{i=1}^{N-1}, t_{\text{mo},N,1})$ is a convex function of the motion times (as shown in Lemma 3).

Optimization of the number of clusters (variable N)

Finally, we find the best N by characterizing (6.11) for integer Ns up to $N_{\max}$ and finding where the minimum occurs. We show how to choose $N_{\max}$ in Section 6.3.2.

We then propose Algorithm 1 for the initial phase of our framework. More specifically, we first find the cost for the case of no clustering. Then, we solve (6.11) for each $N \in \{2, \cdots, N_{\max}\}$ to obtain $E^{\star}_{\text{tot,SF,unif}}(N)$, where $E^{\star}_{\text{tot,SF,unif}}(N)$ is the optimal value of (6.11) for a fixed N, and $N_{\max}$ is the maximum number of clusters (more discussions on $N_{\max}$ in Section 6.3.2). Next, we find $N^{\star}$ by minimizing $E^{\star}_{\text{tot,SF,unif}}(N)$, for $N \in \{1, \cdots, N_{\max}\}$, with $E^{\star}_{\text{tot,SF,unif}}(N = 1) = E^{\star}_{\text{tot,noCl,unif}}$. If $N^{\star} = 1$, we do not cluster the workspace and choose the center of the workspace as the only stop position. Otherwise, we choose the stop positions as the mapping of the $N^{\star}$ equally-spaced points in the space-filling curve domain. The tour is also readily given by ordering the stop positions in the space-filling curve domain. The clustering is then obtained by the Voronoi partition generated by the stop positions in $\mathcal{W}$. Finally, the motion times are given by the optimal solution of (6.11) for $N = N^{\star}$.

Algorithm 1 Our proposed approach: Initial phase

find $E^{\star}_{\text{tot,noCl,unif}}$ by using (6.4)
solve (6.11), for $N \in \{2, \cdots, N_{\max}\}$
find $N^{\star}$ that minimizes $E^{\star}_{\text{tot,SF,unif}}(N)$
if $N^{\star} = 1$
    return no clustering
else
    choose $N^{\star}$ equally-spaced stop positions in $\mathcal{C}$
    find the tour by ordering the stop positions
    map the stop positions and the tour from $\mathcal{C}$ to $\mathcal{W}$
    choose the clusters to be the Voronoi partition generated by the stop positions in $\mathcal{W}$
    use the corresponding optimal solution of (6.11) for the motion times
end

6.3.2 Upper Bound Derivation

Since the stop positions are equally-spaced in the space-filling curve domain, the distance between the neighboring stop positions in 2D is bounded from above by $C_{\text{SF}} S/\sqrt{N}$

using (6.1). As a result, the total distance of the tour in the 2D workspace is bounded from above by $C_{\mathrm{SF}}S\sqrt{N}$. Hence, based on the proof of Lemma 25, if $BR > m\varrho$ and T_{tot} satisfies $(1-m\varrho/(BR))T_{\mathrm{tot}} \geq \sqrt{\kappa_1/\kappa_4}C_{\mathrm{SF}}S\sqrt{N}+2\sqrt{\kappa_3/\kappa_1}N$, we then have the following upper bound for the total motion cost:

$$\begin{aligned} E_{\mathrm{M,tot,SF}}(N, \{t^{\star}_{\mathrm{mo},i,i+1}\}_{i=1}^{N-1}, t^{\star}_{\mathrm{mo},N,1}) &< \kappa_{\mathrm{M},1}C_{\mathrm{SF}}S\sqrt{N} + \kappa_{\mathrm{M},2}N \\ &< (\kappa_{\mathrm{M},1}C_{\mathrm{SF}}S + \kappa_{\mathrm{M},2})N, \end{aligned} \tag{6.12}$$

where $t^{\star}_{\mathrm{mo},i,i+1}$, for all i, and $t^{\star}_{\mathrm{mo},N,1}$ are the optimal motion times obtained by solving (6.11), $\kappa_{\mathrm{M},1} = 2\sqrt{\kappa_1\kappa_4} + \kappa_2$ and $\kappa_{\mathrm{M},2} = 2\kappa_4\sqrt{\kappa_3/\kappa_1}$. Moreover, the upper bound for the communication cost is given by (6.6). Then, the optimal solution of (6.11) for a fixed N is bounded from above by

$$\begin{aligned} E^{\star}_{\mathrm{tot,SF,unif}}(N) &< E_{\mathrm{tot,SF,unif,upper}}(N) \\ &= \frac{m\alpha C_{\mathrm{SF}}^{n_{\mathrm{PL}}} S^{n_{\mathrm{PL}}}(2^R-1)\varrho T_{\mathrm{tot}}}{(n_{\mathrm{PL}}/2+1)(2N)^{\frac{n_{\mathrm{PL}}}{2}}KBR} + \varpi(\kappa_{\mathrm{M},1}C_{\mathrm{SF}}S + \kappa_{\mathrm{M},2})N. \end{aligned} \tag{6.13}$$

Note that the exact communication and motion costs in the 2D workspace are not strictly decreasing and increasing with respect to N, respectively. As a consequence, it is challenging to select an $N_{\max}$ to ensure that there is no $N \geq N_{\max}+1$ that can result in a smaller $E^{\star}_{\mathrm{tot,SF,unif}}(N)$. However, as can be seen, their upper bounds (6.6) and (6.12), which are obtained by using (6.1), do have the corresponding monotonic properties. Hence, we can use (6.13) to find an appropriate $N_{\max}$.

Note that although N is subject to an integer constraint, $E_{\mathrm{tot,SF,unif,upper}}(N_c)$ is a convex function of N_c for a continuous $N_c \in [2,\infty)$. Then, we can find the optimal N_c

by solving the following convex optimization problem:

$$\begin{aligned} \text{minimize} \quad & \frac{m\alpha C_{\mathrm{SF}}^{n_{\mathrm{PL}}} D^{n_{\mathrm{PL}}} (2^R - 1)\varrho T}{(n_{\mathrm{PL}}/2+1)(2N_c)^{\frac{n_{\mathrm{PL}}}{2}} KBR} + \varpi(\kappa_{\mathrm{M},1} C_{\mathrm{SF}} D + \kappa_{\mathrm{M},2}) N_c \\ \text{subject to} \quad & N_c \geq 2. \end{aligned} \tag{6.14}$$

Define the dual function of (6.14) as follows:

$$\frac{m\alpha C_{\mathrm{SF}}^{n_{\mathrm{PL}}} D^{n_{\mathrm{PL}}} (2^R - 1)\varrho T}{(n_{\mathrm{PL}}/2+1)(2N_c)^{\frac{n_{\mathrm{PL}}}{2}} KBR} + \varpi(\kappa_{\mathrm{M},1} C_{\mathrm{SF}} D + \kappa_{\mathrm{M},2}) N_c - \lambda(N_c - 2),$$

where λ is the Lagrange multiplier. Then, we have the following KKT conditions:

$$\begin{aligned} -\frac{n_{\mathrm{PL}} m\alpha C_{\mathrm{SF}}^{n_{\mathrm{PL}}} D^{n_{\mathrm{PL}}} (2^R - 1)\varrho T}{(n_{\mathrm{PL}}/2+1)(2N_c)^{\frac{n_{\mathrm{PL}}}{2}+1} KBR} + \varpi(\kappa_{\mathrm{M},1} C_{\mathrm{SF}} D + \kappa_{\mathrm{M},2}) - \lambda = 0, \\ \lambda \geq 0, \\ \lambda(N_c - 2) = 0. \end{aligned}$$

As a result, we have the following optimal solution by solving the previous equations:

$$N_c^\star = \begin{cases} \dfrac{1}{2}\left(\dfrac{n_{\mathrm{PL}} m\alpha C_{\mathrm{SF}}^{n_{\mathrm{PL}}} S^{n_{\mathrm{PL}}} (2^R - 1)\varrho T_{\mathrm{tot}}}{(n_{\mathrm{PL}}/2+1) KBR\varpi(\kappa_{\mathrm{M},1} C_{\mathrm{SF}} S + \kappa_{\mathrm{M},2})}\right)^{\frac{2}{n_{\mathrm{PL}}+2}}, \\ \qquad\qquad \text{if } \left(\dfrac{n_{\mathrm{PL}} m\alpha C_{\mathrm{SF}}^{n_{\mathrm{PL}}} S^{n_{\mathrm{PL}}} (2^R - 1)\varrho T_{\mathrm{tot}}}{(n_{\mathrm{PL}}/2+1) KBR\varpi(\kappa_{\mathrm{M},1} C_{\mathrm{SF}} S + \kappa_{\mathrm{M},2})}\right)^{\frac{2}{n_{\mathrm{PL}}+2}} \geq 4, \\ 2, \quad \text{otherwise.} \end{cases} \tag{6.15}$$

Then, the optimal $N^\star$ that minimizes $E_{\mathrm{tot,SF,unif,upper}}(N)$, for $N \in \{2, 3, \cdots\}$, can be found as

$$N^\star = \underset{N \in \{\lfloor N_c^\star \rfloor, \lceil N_c^\star \rceil\}}{\arg\min} \{E_{\mathrm{tot,SF,unif,upper}}(N)\}. \tag{6.16}$$

A good choice of $N_{\max}$ is $\lceil N_c^\star \rceil$ for the following reason. Note that both (6.6) and

(6.12) depend on inequality (6.1). Moreover, since the communication cost is an integral of a polynomial of order $n_{\rm PL}$ of the distance (see the first line of (6.5)), the error of the approximation is expected to be more amplified in (6.6), as compared to (6.12). This results in an over-estimation of N. We thus expect $\lceil N_c^\star \rceil$ to be larger than the optimum $N^\star$ that minimizes $E^\star_{\rm tot,SF,unif}(N)$ with a high probability.

Theorem 8 *If $BR > m\varrho$ and the total time budget $T_{\rm tot}$ is sufficiently large, such that*

$$T \geq \frac{2^{n_{\rm PL}+2}(n_{\rm PL}/2+1)KBR\varpi(\kappa_{\rm M,1}C_{\rm SF}S+\kappa_{\rm M,2})}{n_{\rm PL}m\alpha C_{\rm SF}^{n_{\rm PL}}S^{n_{\rm PL}}(2^R-1)\varrho}, \tag{6.17}$$

and

$$T \geq \frac{\sqrt{\kappa_1/\kappa_4}C_{\rm SF}S\sqrt{\lceil N_c^\star\rceil}+2\sqrt{\kappa_3/\kappa_1}\lceil N_c^\star\rceil}{1-m\varrho/(BR)}. \tag{6.18}$$

We have the following upper bound for the optimal total cost:

$$\begin{aligned} E^\star_{\rm tot,SF,unif} &= \min_{N\in\{2,3,\cdots\}}\{E^\star_{\rm tot,SF,unif}(N)\} < E^\star_{\rm tot,SF,unif,upper} \\ &< \left(\frac{n_{\rm PL}}{n_{\rm PL}/2+1}\right)^{\frac{2}{n_{\rm PL}+2}}\left(\frac{1}{n_{\rm PL}}+\frac{3}{4}\right)\varpi^{\frac{n_{\rm PL}}{n_{\rm PL}+2}}(\kappa_{\rm M,1}C_{\rm SF}S+\kappa_{\rm M,2})^{\frac{n_{\rm PL}}{n_{\rm PL}+2}} \\ &\quad\times\left(\frac{m\alpha C_{\rm SF}^{n_{\rm PL}}S^{n_{\rm PL}}(2^R-1)\varrho T_{\rm tot}}{KBR}\right)^{\frac{2}{n_{\rm PL}+2}}, \end{aligned} \tag{6.19}$$

where $E^\star_{\rm tot,SF,unif,upper} = \min_{N\in\{2,3,\cdots\}}\{E^\star_{\rm tot,SF,unif,upper}(N)\}$. Moreover, compared to the case of no clustering, we have

$$\begin{aligned} \frac{E^\star_{\rm tot,SF,unif}}{E^\star_{\rm tot,noCl,unif}} < \frac{E^\star_{\rm tot,SF,unif,upper}}{E^\star_{\rm tot,noCl,unif}} &< \frac{C_{\rm SF}^{\frac{2n_{\rm PL}}{n_{\rm PL}+2}}}{C_1}\left(\frac{n_{\rm PL}}{n_{\rm PL}/2+1}\right)^{\frac{2}{n_{\rm PL}+2}}\left(\frac{1}{n_{\rm PL}}+\frac{3}{4}\right) \\ &\quad\times\left(\frac{\varpi(\kappa_{\rm M,1}C_{\rm SF}S+\kappa_{\rm M,2})KBR}{m\alpha S^{n_{\rm PL}}(2^R-1)\varrho T_{\rm tot}}\right)^{\frac{n_{\rm PL}}{n_{\rm PL}+2}}. \end{aligned} \tag{6.20}$$

Proof: Note that if $BR > m\varrho$, and (6.17) and (6.18) are satisfied, then $N_c^\star \geq 2$ and $E^\star_{\text{tot,SF,unif}}(N)$ is bounded from above by $E_{\text{tot,SF,unif,upper}}(N)$ when choosing $N = \lceil N_c^\star \rceil$. Then, we have the following upper bound for $E^\star_{\text{tot,SF,unif}}$:

$$\begin{aligned}
E^\star_{\text{tot,SF,unif}} &< E^\star_{\text{tot,SF,unif,upper}} \leq E_{\text{tot,SF,unif,upper}}(\lceil N_c^\star \rceil) \\
&= \frac{m\alpha C_{\text{SF}}^{n_{\text{PL}}} S^{n_{\text{PL}}}(2^R-1)\varrho T_{\text{tot}}}{(n_{\text{PL}}/2+1)(2\lceil N_c^\star \rceil)^{\frac{n_{\text{PL}}}{2}} KBR} + \varpi(\kappa_{\text{M},1} C_{\text{SF}} S + \kappa_{\text{M},2})\lceil N_c^\star \rceil \\
&< \frac{m\alpha C_{\text{SF}}^{n_{\text{PL}}} S^{n_{\text{PL}}}(2^R-1)\varrho T_{\text{tot}}}{(n_{\text{PL}}/2+1)(2N_c^\star)^{\frac{n_{\text{PL}}}{2}} KBR} + \frac{3}{2}\varpi(\kappa_{\text{M},1} C_{\text{SF}} S + \kappa_{\text{M},2}) N_c^\star \\
&= \left(\frac{n_{\text{PL}}}{n_{\text{PL}}/2+1}\right)^{\frac{2}{n_{\text{PL}}+2}} \left(\frac{1}{n_{\text{PL}}} + \frac{3}{4}\right) (\kappa_{\text{M},1} C_{\text{SF}} S + \kappa_{\text{M},2})^{\frac{n_{\text{PL}}}{n_{\text{PL}}+2}} \\
&\quad \times \varpi^{\frac{n_{\text{PL}}}{n_{\text{PL}}+2}} \left(\frac{m\alpha C_{\text{SF}}^{n_{\text{PL}}} S^{n_{\text{PL}}}(2^R-1)\varrho T_{\text{tot}}}{KBR}\right)^{\frac{2}{n_{\text{PL}}+2}},
\end{aligned}$$

where the third inequality follows from the fact that the first and second terms of $E_{\text{tot,SF,unif,upper}}(N)$ are monotonically decreasing and monotonically increasing with respect to N respectively, for $N \geq 2$. This confirms (6.19).

Equation (6.20) can be easily obtained by substituting the upper bound of (6.19) into $E^\star_{\text{tot,SF,unif,upper}}/E^\star_{\text{tot,noCl,unif}}$. ■

Interpretation of the results: It can be seen from Theorem 8 that the upper bound of $E^\star_{\text{tot,SF,unif}}/E^\star_{\text{tot,noCl,unif}}$ depends on $\varpi(\kappa_{\text{M},1} C_{\text{SF}} S + \kappa_{\text{M},2})KBR/(m\alpha S^{n_{\text{PL}}}(2^R-1)\varrho T_{\text{tot}})$. Hence, the upper bound decreases if the motion cost $(\kappa_{\text{M},1} S + \kappa_{\text{M},2})$ decreases and/or the number of information bits generated in each period $(m\varrho T_{\text{tot}})$ increases. Also, the upper bound decreases as χ^2_{dB} increases, since α is monotonically increasing with respect to χ^2_{dB}. These observations are intuitive, since as the communication demand (the total number of generated information bits in each period) becomes higher and/or the predicted channel quality gets worse, more clustering is preferred in order to reduce the communication cost, as shown in (6.15). As a result, the robot will save more energy, as compared to

the case of no clustering.

It is worth to note that although both sides of (6.18) depend on T_{tot}, we can always find a large enough T_{tot} to satisfy this condition. This is because the increasing order of the right-hand side of (6.18) is $T_{\text{tot}}^{2/(n_{\text{PL}}+2)}$, which is smaller than the increasing order of the left hand side.

6.4 Proposed Iterative Approach for Joint Clustering and Path Planning

In this part, we finalize the co-design of our clustering and path planning in realist communication environments. More specifically, by utilizing our initial design phase and Lloyd's algorithm [130], we propose an iterative approach to fine tune the initial design.

Algorithm 2 Proposed iterative approach

initialize $\mathcal{Q}^{(1)}$, $\{\mathcal{W}_i^{(1)}\}_{i=1}^N$, $\{t_{\text{mo},i,j}^{(1)}\}_{i,j=1}^N$ and $\mathcal{T}^{(1)}$ by using Algorithm 1
for $k = 1, 2, \cdots$
  optimize $\mathcal{Q}$ for fixed $\{\mathcal{W}_i^{(k)}\}_{i=1}^N$, $\{t_{\text{mo},i,j}^{(k)}\}_{i,j=1}^N$ and $\mathcal{T}^{(k)}$ to obtain $\mathcal{Q}^{(k+1)}$
  find Voronoi partition $\{\mathcal{W}_i^{(k+1)}\}_{i=1}^N$ for fixed $\mathcal{Q}^{(k+1)}$
  find a new tour $\mathcal{T}^{(k+1)}$ for fixed $\mathcal{Q}^{(k+1)}$
  optimize $\{t_{\text{mo},i,j}\}_{i,j=1}^N$ for fixed $\mathcal{Q}^{(k+1)}$, $\{\mathcal{W}_i^{(k+1)}\}_{i=1}^N$ and $\mathcal{T}^{(k+1)}$ to obtain $\{t_{\text{mo},i,j}^{(k+1)}\}_{i,j=1}^N$
  if the total cost increases as compared to the last iteration
    reject the new TSP solution and assign $\mathcal{T}^{(k+1)} = \mathcal{T}^{(k)}$
    optimize $\{t_{\text{mo},i,j}\}_{i,j=1}^N$ again for fixed $\mathcal{Q}^{(k+1)}$, $\{\mathcal{W}_i^{(k+1)}\}_{i=1}^N$ and $\mathcal{T}^{(k+1)}$
  end
  if the energy no longer decreases
    break
  end
end

We first choose N and initialize variables $\mathcal{Q}$, $\{\mathcal{W}_i\}_{i=1}^N$, $\{t_{\text{mo},i,j}\}_{i,j=1}^N$ and $\mathcal{T}$ in (6.3) by using the solution obtained from Algorithm 1. Then, we fix N and optimize the rest of the

variables in an iterative way as follows. In each iteration, we first optimize $\mathcal{Q}$ in (6.3) for fixed $\{\mathcal{W}_i^{(k)}\}_{i=1}^N$, $\{t_{\mathrm{mo},i,j}^{(k)}\}_{i,j=1}^N$ and $\mathcal{T}^{(k)}$ to obtain a new set of stop positions $\mathcal{Q}^{(k+1)}$, where superscript k denotes that the variables are obtained after the k^{th} iteration. Note that we have a convex optimization problem at this step, which guarantees to have a unique solution. Next, we choose $\{\mathcal{W}_i^{(k+1)}\}_{i=1}^N$ to be the Voronoi partition that is generated by $\mathcal{Q}^{(k+1)}$. Moreover, we find the new TSP tour $\mathcal{T}^{(k+1)}$ for $\mathcal{Q}^{(k+1)}$. Note that we can use space-filling curves or other heuristic approaches [128, 129] to solve the TSP problem sub-optimally but efficiently, as discussed in Section 6.1. Finally, we solve $\{t_{\mathrm{mo},i,j}\}_{i,j=1}^N$ in (6.3) for fixed $\mathcal{Q}^{(k+1)}$, $\{\mathcal{W}_i^{(k+1)}\}_{i=1}^N$ and $\mathcal{T}^{(k+1)}$, which is also a convex optimization problem. It is worth to note that $\mathcal{T}^{(k+1)}$ may have a longer total distance as compared to $\mathcal{T}^{(k)}$. Moreover, even if $\mathcal{T}^{(k+1)}$ has a shorter total distance, it is possible that the total cost after optimizing $\{t_{\mathrm{mo},i,j}\}_{i,j=1}^N$ will become larger than the one obtained in the last iteration. This is because in general the motion cost is not monotonically decreasing with respect to the total distance of the tour, as discussed in Section 6.3.1. To guarantee that our algorithm always reduces the total cost, we accept the new TSP solution only if it reduces the total cost as compared to the last iteration. Otherwise, we reject the new TSP solution, assigning $\mathcal{T}^{(k+1)} = \mathcal{T}^{(k)}$ and solving $\{t_{\mathrm{mo},i,j}\}_{i,j=1}^N$ again. The algorithm repeats these steps until the total cost no longer decreases. We have summarized the proposed approach in Algorithm 2.

6.5 Extension to the Case of Non-Uniformly -Distributed Sensors

So far, we have considered the case where the sensors are uniformly distributed. As a result, we can choose the stop positions such that they are equally-spaced in the space-

filling curve domain. In this part, we extend our previous framework to the case where the sensors are not uniformly distributed.

It is intuitive to expect that the optimal number of clusters in each area of the workspace increases as the density of the sensors in the corresponding area increases, in order to save the communication cost. Hence, we extend the first part of the framework in Section 6.3.1 as follows, in order to add more stop positions to the workspace as needed.[5] We first find the optimal cost for the case where there is no clustering by solving the following optimization problem:

$$\begin{aligned} \text{minimize} \quad & E_{\text{tot,noCl,non}-\text{unif}}(q_1) = \frac{m\alpha(2^R-1)\varrho T_{\text{tot}}}{KBR} \int_{\mathcal{W}} p(x)\|x-q_1\|^{n_{\text{PL}}} dx \qquad (6.21) \\ \text{subject to} \quad & 1)\ q_1 \in \mathcal{W}, \end{aligned}$$

where $E_{\text{tot,noCl,non}-\text{unif}}(q_1)$ denotes the cost for the case of no clustering when the sensors are not uniformly distributed and q_1 is the stop position of the robot. Unlike the uniform case, the optimal $q_1^\star$ in (6.21) depends on $p(x)$ and is not necessary the center of the workspace. It is straightforward to see that the objective function is a convex function of q_1 for typical path loss exponents $n_{\text{PL}} \in [2, 6]$. As a result, we can easily find the global optimum of (6.21).

Similar to Section 6.3.1, for the case of more than one cluster, we determine the number of clusters and the corresponding stop positions by using space-filling curves as follows. First, we map the workspace (including the optimal $q_1^\star$ in (6.21)) to 1D. Without loss of generality, let $\text{SF}^{-1}(q_1^\star) = 0$. Next, we choose an additional stop position at 0.5 in 1D and map it back to the 2D workspace. Similar to the approach proposed in Section

[5]Note that solving this problem optimally is not possible. Furthermore, exactly extending the approach in the previous part is not possible either, since the distribution in 1D is not known for a given non-uniform distribution in 2D. We therefore propose an iterative extension of the proposed approach of the uniform case.

6.3.1, we then solve the following convex optimization problem for $N = 2$:

$$\begin{aligned}
\text{minimize} \quad & E_{\text{tot,SF,non}-\text{unif}}(\{t_{\text{mo},i,i+1}\}_{i=1}^{N-1}, t_{\text{mo},N,1}) = \\
& \frac{m\alpha(2^R-1)\varrho T_{\text{tot}}}{KBR} \sum_{i=1}^{N} \int_{\mathcal{W}_{\text{SF},i}} p(x)\|x - q_{\text{SF},i}\|^{n_{\text{PL}}} dx \\
& + \varpi\left(E_{\text{M}}(d_{N,1}, t_{\text{mo},N,1}) + \sum_{i=1}^{N-1} E_{\text{M}}(d_{i,i+1}, t_{\text{mo},i,i+1}) \right) \qquad (6.22) \\
\text{subject to} \quad & 1) \ \sum_{i=1}^{N-1} t_{\text{mo},i,i+1} + t_{\text{mo},N,1} \leq T_{\text{tot}} \left(1 - \frac{m\varrho}{BR}\right), \\
& 2) \ t_{\text{mo},i,i+1} \geq 0, \forall\, i, \quad t_{\text{mo},N,1} \geq 0,
\end{aligned}$$

where $E_{\text{tot,SF,non}-\text{unif}}(\{t_{\text{mo},i,i+1}\}_{i=1}^{N-1}, t_{\text{mo},N,1})$ is the total cost when the sensors are not uniformly distributed. Here, the variables to solve for are $\{t_{\text{mo},i,i+1}\}_{i=1}^{N-1}$ and $t_{\text{mo},N,1}$. Note that without loss of generality, we label the stop positions such that the robot visits them by the order of their labels in (6.22). Also, we have $q_{\text{SF},1} = q_1^\star$ and $q_{\text{SF},2} = \text{SF}(0.5)$ for $N = 2$. We then compare the optimal value of (6.22) to the case of no clustering. If it has a larger cost, we do not cluster the workspace and terminate the algorithm. Otherwise, we keep this additional stop position. Since it is potentially beneficial to have more clusters in some areas of the workspace, we keep adding stop positions as follows. For the arc $[0, 0.5)$, we further choose 0.25 as an additional stop position and map it back to the 2D workspace. We then find the path of the robot and solve (6.22) again for this new clustering strategy. If it does not increase the total cost, we then keep this new stop position along this arc. Otherwise, we do not choose this new stop position. We use the same strategy for the arc $[0.5, 1)$. Our algorithm stops if no arc between the existing adjacent stop positions needs new stop positions. We summarize our approach in Algorithm 3, where $\mathcal{E}$ and $\mathcal{E}_{\text{new}}$ denote the sets that contain all the arcs at the current and next steps of the algorithm respectively, $\mathcal{F}$ is the set that contains

all the stop positions, and bool_{div} is a boolean variable to determine if we need to keep adding new stop positions.

Algorithm 3 Extension to the case of non-uniformly distributed sensors

find $E^{\star}_{\text{tot,noCl,non-unif}}$ by solving (6.21)
let $\mathcal{E} = \{\mathcal{C}\}$, $\mathcal{F} = \{\text{SF}^{-1}(q_1^{\star})\}$
set bool_{div} to be true
while bool_{div} is true
  set bool_{div} to be false
  for each arc in $\mathcal{E}$
    choose the center of the arc as an additional stop position for this arc
    find the TSP tour and map the stop position to 2D
    solve (6.22)
    if the optimal value of (6.22) does not increase
      divide the arc in half and add the resulting two sub-arcs to $\mathcal{E}_{\text{new}}$
      add the additional stop position to $\mathcal{F}$
      set bool_{div} to be true
    else
      add the original arc to $\mathcal{E}_{\text{new}}$
    end
  end
  set $\mathcal{E}$ to be $\mathcal{E}_{\text{new}}$
end
use the corresponding optimal solution of (6.22) for the motion times

As compared to Algorithm 1, the main difference of Algorithm 3 is that it adds stop positions to the parts of the workspace that can benefit from more clustering. This is intuitive since it is only beneficial to travel a longer distance in the areas that have a larger sensor density. As a result, our proposed algorithm will result in a clustering strategy that depends on $p(x)$. After using Algorithm 3, we then proceed with Algorithm 2 to fine tune the solution.

Remark 15 *In general, finding the upper bound for the case of non-uniformly distributed sensors is very challenging. This is because, given an arbitrary distribution of sensors in the 2D workspace, its corresponding distribution in the space-filling curve domain cannot*

be easily obtained. Characterizing the upper bound for arbitrarily distributed sensors is thus a subject of our future work.

6.6 Simulation Results

Consider the case where the workspace is a 1000 m$\times$1000 m square region with a total of 500 fixed sensors. The channel in the workspace has the following realistic channel parameters [119]: $n_{\mathrm{PL}} = 4.57$ and $\chi^2_{\mathrm{dB}} = 64$. Moreover, we choose $R = 2$ bits/Hz/s, $p_{b,\mathrm{th}} = 10^{-6}$, $B = 500$ MHz and the receiver noise power is chosen to be the realistic value of -204 dBW/Hz. We also use real motion parameters as follows [87]: $\kappa_1 = 0.77$, $\kappa_2 = 10.1$, $\kappa_3 = 5.47$ and $\kappa_4 = 4.24$. Furthermore, we use Sierpiński curves. Finally, we choose $\varpi = 0.1$, a sensing rate of $\varrho = 800$ Kbps for each sensor and $T_{\mathrm{tot}} = 3600$ s.

Fig. 6.4 (left) shows the clusters of the sensors, the stop positions and the tour of the robot by using our proposed framework for the case where the sensors are uniformly distributed. As can be seen, in general, the stop positions are uniformly-spaced in the workspace. Still, the number of clusters, clustering, path planning and motion times need to be jointly optimized as we proposed in this chapter. In this example, the predicted total cost of the whole network is only 1.2% of the energy cost of the case of no clustering, indicating a considerable energy saving achieved through proper co-optimzation. In terms of computational cost, our MATLAB simulation for Fig. 6.4 (left) took 83.9 seconds to run.

Fig. 6.5 and Fig. 6.6 show the benefits of our proposed framework when the sensors are uniformly distributed. We compare our proposed framework to the case of no clustering (Fig. 6.5) as well as to the case where the robot needs to visit each sensor to collect the data (Fig. 6.6). For the second case, we first use space-filling curves to plan the tour of the robot. Then, we optimize the motion strategy of the robot for this fixed tour. It

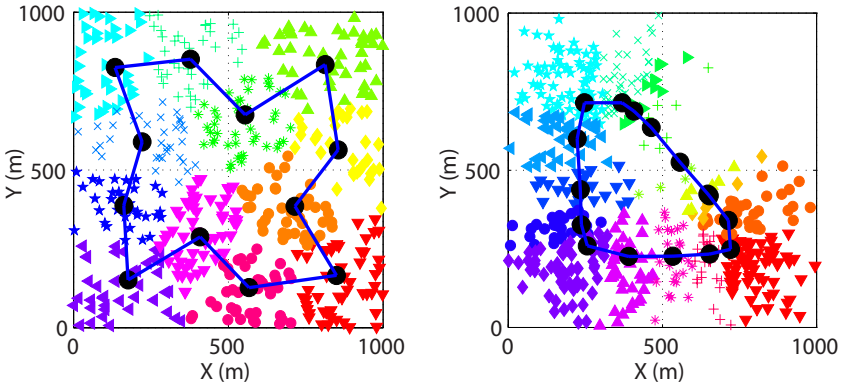

Figure 6.4: The clusters of the sensors, the stop positions and the tours of the robot when the sensors are uniformly distributed (left) and non-uniformly distributed according to $p(x)$ (right), respectively. The figures show the results by using our proposed framework. The black circles and blue line segments indicate the stop positions and the tours of the robot, respectively. The markers with the same shape and color denote the same cluster. In these examples, the predicted total cost of the whole network is only 1.2% and 9.7% of the cost of the case of no clustering, respectively. See the pdf file for a color version.

can be seen that our approach can save the energy considerably as compared to both of these benchmarks. Furthermore, as compared to the case of no clustering, our proposed framework becomes more beneficial as the communication cost becomes more dominant, i.e. the sensing rate or channel variance is higher. On the other hand, as compared to the case of visiting each sensor, our proposed framework becomes more beneficial as the motion cost becomes more dominant, i.e. the sensing rate or channel variance becomes lower.

Fig. 6.4 (right) shows the result when the sensors are not uniformly distributed. In this example, we have $\varrho = 80$ Kbps for each sensor and $p(x) = \widetilde{p}(x)/\int_{\mathcal{W}} \widetilde{p}(x)dx$, where

$$\widetilde{p}(x) = \sum_{i=1}^{3} \mathbb{I}(\pi = i)\mathcal{N}\left(\eta_i, \begin{bmatrix} 125 & 0 \\ 0 & 125 \end{bmatrix}\right).$$

Here, $\eta_1 = [250\ \ 250]^{\mathrm{T}}$, $\eta_2 = [750\ \ 250]^{\mathrm{T}}$, $\eta_3 = [250\ \ 750]^{\mathrm{T}}$, $\mathbb{I}(\cdot)$ denotes an indicator function, $\mathcal{N}(\cdot,\cdot)$ represents a Gaussian distribution with the first and second parameters

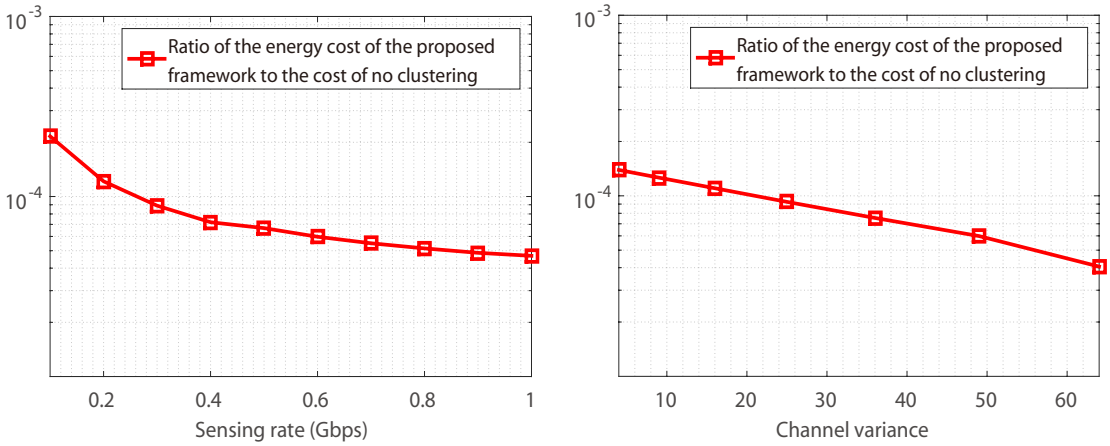

Figure 6.5: The figure shows the ratio of the cost of our proposed framework to the cost of the case of no clustering, for different sensing rates (left) and different channel variances (right) when the sensors are uniformly distributed. The channel variance is 64 for the left figure and the sensing rate is 0.8 Gbps for the right figure. It can be seen that our framework can reduce the total cost considerably, as compared to the case of no clustering.

denoting its mean and covariance respectively, and π denotes a generalized Bernoulli random variable where $\pi = i$ with probability $1/3$ for all i. Fig. 6.4 (right) then shows the results of our proposed approach. It can be seen that we have more clusters in the areas where the density of the sensors is higher, as expected. Moreover, the predicted total cost of the whole network is only 9.7% of the cost of the case of no clustering, indicating a considerable energy saving achieved through proper co-optimization. In terms of computational cost, our MATLAB simulation for Fig. 6.4 (right) took 73.2 seconds to run.

Fig. 6.7 (left and right) shows the benefits of our approach for different sensing rates and different channel variances respectively, when the sensors are distributed according to $p(x)$. Similar to the uniform case, as compared to the case of no clustering, our proposed approach becomes more beneficial as the communication cost becomes higher. On the other hand, as compared to the case of visiting each sensor, our proposed framework becomes more beneficial as the communication cost becomes lower.

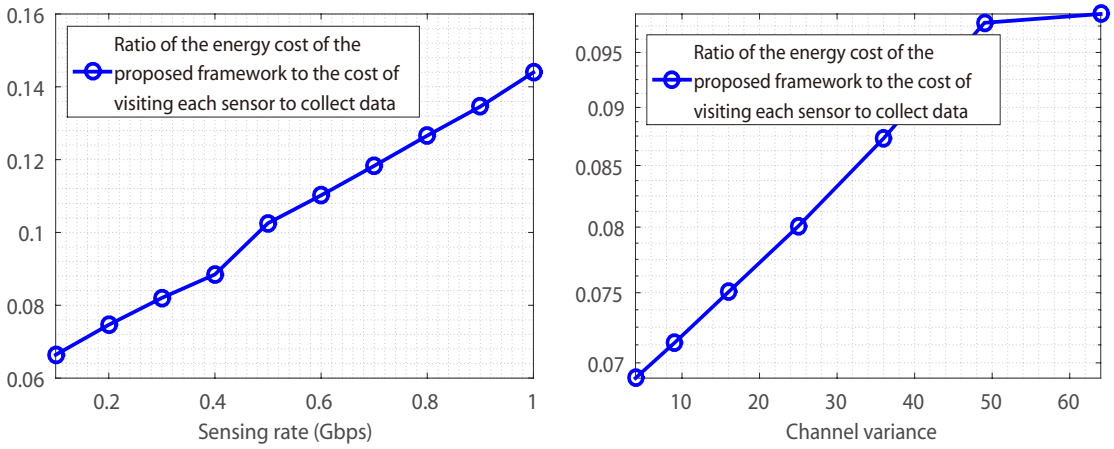

Figure 6.6: The figure shows the ratio of the cost of our proposed framework to the cost of the case of visiting each sensor, for different sensing rates (left) and different channel variances (right) when the sensors are uniformly distributed. The channel variance is 64 for the left figure and the sensing rate is 0.8 Gbps for the right figure. It can be seen that our framework can reduce the total cost considerably, as compared to the case of visiting all the sites.

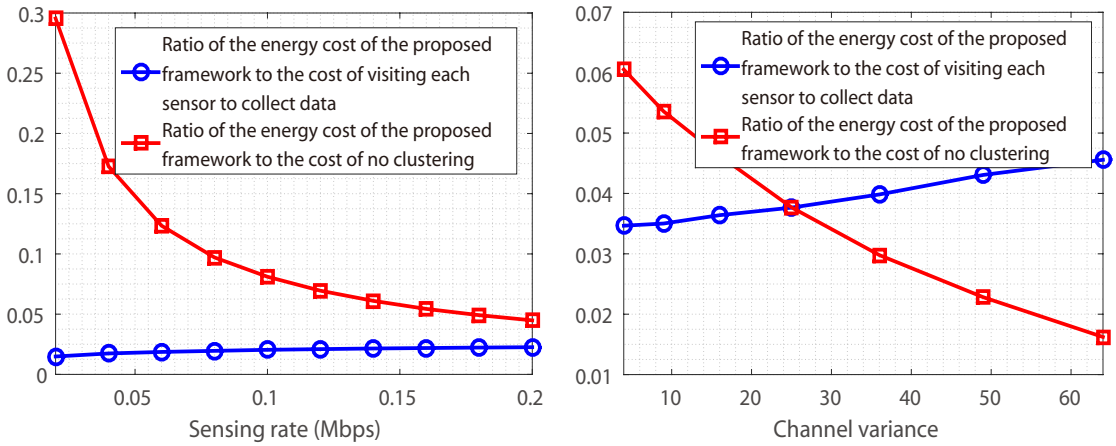

Figure 6.7: The figure shows the ratio of the cost of our framework to the cost of the case of no clustering as well as to the cost of the case of visiting each sensor, for different sensing rates (left) and different channel variances (right) when the sensors are distributed according to $p(x)$. The channel variance is 64 for the left figure and the sensing rate is 1 Mbps for the right figure. It can be seen that our framework can reduce the total cost considerably.

Chapter 7

Conclusions and Future Work

In this chapter, we conclude this dissertation and discuss possible extensions of our considered scenarios.

7.1 Robotic Router Formation

In Chapter 3, we considered the problem of robotic router formation, where two nodes need to maintain their connectivity by using a number of robotic routers. Instead of optimizing the formation of the routers by maximizing the Fiedler eigenvalue, we took a different approach and considered the true reception quality (BER) as a performance metric. We showed how utilizing this metric results in a different robotic configuration with a considerably better performance. We furthermore extended our results to fading environments. We proposed a probabilistic router formation framework by integrating the probabilistic channel prediction approach with robotic router optimization. We showed that our framework can improve the performance considerably as compared to only considering disk models for communication. We also considered power limitations of the network, including both communication and motion costs, and characterized

the underlying tradeoffs. Finally, we showed the performance with a simple preliminary robotic experiment with an emphasis on the impact of localization errors. Along this line, we discussed interesting interplay between the localization quality and channel correlation/learning quality.

One extension of Chapter 3 is to consider multiple transmitter and receiver pairs. Then, the robotic routers need to configure themselves such that the reception quality at all the receivers are guaranteed. Another possible extension is the case of mobile transmitter/receiver, should requires constant online planning and adaptation.

In [131], we have showed preliminary results on the impact of localization errors on the channel prediction. While we had a discussion on the interplay between the localization errors and average end-to-end BER in Chapter 3, it is also interesting to extend the analysis of [131] and mathematically characterize the proposed hypothesis as part of future extensions.

7.2 Co-Optimization Along a Fixed Trajectory

In Chapter 4, we considered the case where a robot is tasked with sending a number of given bits of information to a remote station, as it travels along a pre-defined trajectory and in a given time budget. We showed how the robot can co-plan its motion and communication strategies in order to minimize its total energy consumption (including both the motion and communication costs). We also proved some properties for two special cases of heavy and light-task loads. We then proposed an additional stop-time online adaptation strategy to further fine tune the stop location as the robot moves along its trajectory and measures the true value of the channel. Finally, we briefly discussed how our framework can be generalized to the case of online sensing and data gathering. Our simulation results showed that our proposed framework results in a considerable

performance improvement.

One extension of Chapter 4 is to use the more complete motion model of (2.14) to characterize the motion cost of the robot. In this case, the control input becomes the acceleration rather than the velocity of the robot. As a result, we expect a delayed response of the motion strategy because of the additional constraints/costs on the acceleration. This problem has been investigated in [132].

Another extension is to introduce integer constraints for the spectral efficiency. In this case, we can pose the communication cost as a linear function of the transmission times, as shown in (2.9). It is straightforward to use the corresponding results in Chapter 5 to extend the results.

7.3 Co-Optimization With Trajectory Planning

In Chapter 5, we considered the scenario where a mobile robot needs to visit a number of POIs, gather their generated bits of information, and transmit them to a remote station in a realistic communication environment, while minimizing its total motion and communication energy consumption, and under time and BER constraints. We proposed an energy-aware and communication-aware co-optimization paradigm and characterized several key properties of the co-optimized motion and communication solution. As part of our overall problem, we also brought an understanding to the "To Go or Not To Go" problem, which indicates when to incur motion energy for better connectivity. Finally, our simulation results with real channel and motion parameters confirmed that considerable performance improvement can be achieved.

Similar to the previous case, one extension of Chapter 5 is to use the more complete motion model of (2.14). This may result in different optimal trajectories as compared to the current results. For instance, as discussed in Section 6.3.1, the minimum-distance

trajectory may not minimize the motion cost in this case. Another extension is to design computationally-efficient algorithms to solve the proposed MILP in Section 5.2. Note that the computationally-expensive part of the MILP is to solve the integer variables for the trajectory design. Hence, one possible way to reduce the computational complexity is to use a heuristic algorithm, such as the space-filling-based approach introduced in Section 6.1, to design the trajectory.

7.4 Clustering and Path Planning Strategies for Robotic Data Collection

In Chapter 6, we considered a scenario where a mobile robot is tasked with periodically collecting data from a fixed wireless sensor network. Our goal was to minimize the total cost of the system, including the communication cost of the sensors to the robot, when operating in realistic channel environments, and the motion cost of the robot. We considered a strategy that divides the sensors into a number of clusters and uses a mobile robot to visit each cluster in order to wirelessly collect the corresponding data. We then proposed a sub-optimum but computationally-efficient approach to solve this problem by using space-filling curves. More specifically, we showed how the coupled clustering, stop position selection, path planning and motion design problems can be solved as a series of convex optimization problems. We further mathematically characterized an upper bound for the total energy consumption of our proposed approach for the case of uniformly-distributed sensors, relating it to key motion and communication parameters, such as motor parameters, channel multipath fading and shadowing variances, path loss exponent and target BER. Finally, we verified the effectiveness of our framework in a simulation environment. Our results with realistic channel and motion parameters

showed a considerable energy saving.

One extension of Chapter 6 is to consider multi-hop transmission strategies for the sensors. In this case, we can either integrate the routing design into the optimization framework or use the approach in [103] to approximate the communication energy cost.

Another extension of the considered scenario is to allow the robot to collect data while moving. In this case, the trajectory rather than the stop positions of the robot will affect the communication and motion costs of the network.

Bibliography

[1] J. Cortes, S. Martinez, T. Karatas, and F. Bullo, *Coverage control for mobile sensing networks*, *IEEE Transactions on Robotics and Automation* **20** (April, 2004) 243–255.

[2] I. Hussein and D. Stipanovic, *Effective coverage control for mobile sensor networks*, in *Proceedings of the IEEE Conference on Decision and Control*, pp. 2747–2752, 2006.

[3] M. Schwager, J. Slotine, and D. Rus, *Decentralized, adaptive control for coverage with networked robots*, in *IEEE International Conference on Robotics and Automation*, pp. 3289 – 3294, 2007.

[4] W. Wang, V. Srinivasan, B. Wang, and K. Chua, *Coverage for target localization in wireless sensor networks*, *IEEE Transactions on Wireless Communiations* **7** (February, 2008) 667–676.

[5] J. Cortes, S. Martinez, and F. Bullo, *Robust rendezvous for mobile autonomous agents via proximity graphs in arbitrary dimensions*, *IEEE Transaction on Automatic Control* **51** (August, 2006) 1289–1298.

[6] D. Dimarogonas and K. Kyriakopoulos, *On the rendezvous problem for multiple nonholonomic agents*, *IEEE Transactions on Automatic Control* **52** (May, 2007) 916–922.

[7] X. Wang, M. Fu, and H. Zhang, *Target tracking in wireless sensor networks based on the combination of KF and MLE using distance measurements*, *IEEE Transactions on Mobile Computing* **11** (April, 2012) 567–576.

[8] Y. Mostofi, *Decentralized communication-aware motion planning in mobile networks: An information-gain approach*, *Journal of Intelligent and Robotic Systems* **56** (May, 2009) 233–256.

[9] A. Ghaffarkhah and Y. Mostofi, *Communication-aware motion planning in mobile networks*, *IEEE Transactions on Automatic Control* **56** (October, 2011) 2478–2485.

[10] K. Zhou and S. Roumeliotis, *Multirobot active target tracking with combinations of relative observations*, *IEEE Transactions on Robotics* **27** (August, 2011) 678–695.

[11] A. Ghaffarkhah and Y. Mostofi, *Path planning for networked robotic surveillance*, *IEEE Transactions on Signal Processing* **60** (July, 2012) 3560–3575.

[12] T. He, S. Krishnamurthy, L. Luo, T. Yan, L. Gu, R. Stoleru, G. Zhou, Q. Cao, P. Vicaire, and J. Stankovic, *VigilNet: An integrated sensor network system for energy-efficient surveillance*, *ACM Transactions on Sensor Networks* **2** (February, 2006) 1–38.

[13] A.-J. Garcia-Sanchez, F. Garcia-Sanchez, and J. Garcia-Haro, *Wireless sensor network deployment for integrating video-surveillance and data-monitoring in precision agriculture over distributed crops*, *Computers and Electronics in Agriculture* **75** (February, 2011) 288–303.

[14] R. Olfati-Saber, *Flocking for multi-agent dynamic systems: Algorithms and theory*, *IEEE Transactions on Automatic Control* **51** (March, 2006) 401–420.

[15] H. Tanner, A. Jadbabaie, and G. Pappas, *Flocking in fixed and switching networks*, *IEEE Transactions on Automatic Control* **52** (May, 2007) 863–868.

[16] H. Su, X. Wang, and Z. Lin, *Flocking of multi-agents with a virtual leader*, *IEEE Transactions on Automatic Control* **54** (February, 2009) 293–307.

[17] T. Balch and R. Arkin, *Behavior-based formation control for multirobot teams*, *IEEE Transactions on Robotics and Automation* **14** (December, 1998) 926–939.

[18] A. Das, R. Fierro, V. Kumar, J. Ostrowski, J. Spletzer, and C. Taylor, *A vision-based formation control framework*, *IEEE Transactions on Robotics and Automation* **18** (October, 2002) 813–825.

[19] M. Mesbahi and F. Hadaegh, *Formation flying control of multiple spacecraft via graphs, matrix inequalities, and switching*, *Journal of Guidance, Control, and Dynamics* **24** (March–April, 2001) 369–377.

[20] W. Ren and N. Sorensen, *Distributed coordination architecture for multi-robot formation control*, *Robotics and Autonomous Systems* **56** (April, 2008) 324–333.

[21] T. Liu and Z.-P. Jiang, *Distributed formation control of nonholonomic mobile robots without global position measurements*, *Automatica* **49** (February, 2013) 592–600.

[22] F. Bullo, E. Frazzoli, M. Pavone, K. Savla, and S. L. Smith, *Dynamic vehicle routing for robotic systems*, *Proceeding of the IEEE* **99** (September, 2011) 1482 – 1504.

[23] S. Smith, M. Pavone, F. Bullo, and E. Frazzoli, *Dynamic vehicle routing with priority classes of stochastic demands*, *SIAM Journal on Control and Optimization* **48** (January, 2010) 3224–3245.

[24] M. Pavone, E. Frazzoli, and F. Bullo, *Adaptive and distributed algorithms for vehicle routing in a stochastic and dynamic environment*, *IEEE Transactions on Automatic Control* **56** (June, 2011) 1259–1274.

[25] A. Mainwaring, D. Culler, J. Polastre, R. Szewczyk, and J. Anderson, *Wireless sensor networks for habitat monitoring*, in *Proceedings of the 1st ACM international workshop on Wireless sensor networks and applications*, pp. 88–97, 2002.

[26] F. Ingelrest, G. Barrenetxea, G. Schaefer, M. Vetterli, O. Couach, and M. Parlange, *Sensorscope: Application-specific sensor network for environmental monitoring*, *ACM Transactions on Sensor Networks* **6** (February, 2010) 17–32.

[27] H. Cai and Y. Mostofi, *To ask or not to ask: A foundation for the optimization of human-robot collaborations*, in *IEEE American Control Conference*, (Chicago, IL), July, 2015.

[28] Amazon Prime Air. http://www.amazon.com/b?node=8037720011.

[29] M. M. Zavlanos, M. B. Egerstedt, Y. C. Hu, and G. J. Pappas, *Graph-theoretic connectivity control of mobile robot networks*, *Proceedings of the IEEE* **99** (July, 2011) 1525 – 1540.

[30] M. M. Zavlanos and G. J. Pappas, *Potential fields for maintaining connectivity of mobile networks*, *IEEE Transaction on Robotics* **23** (August, 2007) 812–816.

[31] M. M. Zavlanos, A. Ribeiro, and G. J. Pappas, *Mobility and routing control in networks of robots*, in *Proceedings of IEEE Conference on Decision and Control*, (Atlanta, GA), pp. 7545–7550, December, 2010.

[32] J. Fink, A. Ribeiro, and V. Kumar, *Motion planning for robust wireless networking*, in *Proceedings of the IEEE International Conference on Robotics and Automation*, (Saint Paul, MN), pp. 2419 – 2426, May, 2012.

[33] M. Lindhé and K. H. Johanson, *Using robot mobility to exploit multipath fading*, *IEEE Wireless Communications* **16** (Feb., 2009) 30–37.

[34] C. Ooi and C. Schindelhauer, *Minimal energy path planning for wireless robots*, *Mobile Networks and Applications* **14** (January, 2009) 309 – 321.

[35] A. Ghaffarkhah, Y. Yan, and Y. Mostofi, *Dynamic coverage of time-varying environments using a mobile robot – a communication-aware perspective*, in *Proceedings of IEEE Globecom Workshop on Wireless Networking for Unmanned Autonomous Vehicles*, (Huston, TX), pp. 1297–1302, December, 2011.

[36] J. Fink, A. Ribeiro, and V. Kumar, *Robust control for mobility and wireless communication in cyber–physical systems with application to robot teams*, *Proceedings of the IEEE* **100** (January, 2012) 164–178.

[37] E. Craparo, J. How, and E. Modiano, *Throughput optimization in mobile backbone networks*, *IEEE Transactions on Mobile Computing* **10** (April, 2011) 560–572.

[38] D. Tardioli, A. Mosteo, L. Riazuelo, J. Villarroel, and L. Montano, *Enforcing network connectivity in robot team missions*, *International Jounarl of Robotics Research* **29** (April, 2010) 460–480.

[39] S. Smith, M. Schwager, and D. Rus, *Persistent robotic tasks: Monitoring and sweeping in changing environments*, *IEEE Transaction on Robotics* **28** (April, 2012) 410–426.

[40] D. Bhadauria, O. Tekdas, and V. Isler, *Robotic data mules for collecting data over sparse sensor fields*, *Journal of Field Robotics* **28** (February, 2011) 388–404.

[41] D. Klein, J. Isaacs, S. Venkateswaran, J. Burman, T. Pham, J. Hespanha, and U. Madhow, *Source localization in a sparse acoustic sensor network using UAVs as information seeking data mules*, *IEEE Transactions on Sensor Networks* **9** (November, 2013).

[42] Y. Shi and Y. Hou, *Theoretical results on base station movement problem for sensor network*, in *Proceedings of the 27th IEEE Conference on Computer Communications*, (Phoenix, AZ), pp. 376–384, April, 2008.

[43] Y. Kim and M. Mesbahi, *On maximizing the second smallest eigenvalue of a state-dependent graph laplacian*, *IEEE Transaction on Automatic Control* **51** (April, 2006) 116–120.

[44] M. D. Gennaro and A. Jadbabaie, *Decentralized control of connectivity for multi-agent systems*, in *Proceedings of the 45th IEEE Conference on Decision and Control*, (San Diego, CA), pp. 3628–3633, December, 2006.

[45] M. Zavlanos and G. Pappas, *Controlling connectivity of dynamic graphs*, in *Proceedings of the 44th IEEE Conference on Decision and Control, and the European Control Conference*, (Seville, Spain), pp. 6388–6393, December, 2005.

[46] E. Stump, A. Jadbabaie, and V. Kumar, *Connectivity management in mobile robot teams*, in *Proceeding of the 48th IEEE International Conference on Robotics and Automation*, (Pasadena, CA), pp. 1525–1530, May, 2008.

[47] O. Tekdas, W. Yang, and V. Isler, *Robotic routers: Algorithms and implementation*, *International Journal of Robotics Research* **29** (January, 2010) 110–126.

[48] C. Dixon and E. W. Frew, *Optimizing cascaded chains of unmanned aircraft acting as communication relays*, *IEEE Journal on Selected Areas in Communications* **30** (June, 2012) 883–898.

[49] D. K. Goldenberg, J. Lin, S. A. Morse, B. E. Rosen, and R. Y. Yang, *Towards mobility as a network control primitive*, in *Proceedings of the 5th ACM International Symposium on MobiHoc*, pp. 163–174, 2004.

[50] S. Yu and C. Lee, *Lifetime maximization in mobile sensor networks with energy harvesting*, in *Proceedings of the 51th IEEE International Conference on Robotics and Automation*, (Shanghai), pp. 131–142, May, 2011.

[51] R. Sepulchre, D. Paley, and N. Leonard, *Stabilization of planar collective motion with limited communication*, *IEEE Transactions on Automatic Control* **53** (May, 2008) 706–719.

[52] F. El-Moukaddem, E. Torng, and G. Xing, *Mobile relay configuration in data-intensive wireless sensor networks*, *IEEE Transactions on Mobile Computing* **12** (February, 2013) 261–273.

[53] C. Tang and P. McKinley, *Energy optimization under informed mobility*, *IEEE Transactions on Parallel and Distributed Systems* **17** (September, 2006) 947–962.

[54] H. Jaleel, Y. Wardi, and M. Egerstedt, *Minimizing mobility and communication energy in robotic networks: An optimal control approach*, in *IEEE American Control Conference*, (Portland, OR), pp. 2662–2667, June, 2014.

[55] A. Ghaffarkhah and Y. Mostofi, *Dynamic coverage of time-varying fading environments*, *ACM Transactions on Sensor Networks* **10** (April, 2014) 45 – 83.

[56] J. Luo, J. Panchard, M. Piórkowski, M. Grossglauser, and J.-P. Hubaux, *Mobiroute: Routing towards a mobile sink for improving lifetime in sensor networks*, in *Distributed Computing in Sensor Systems*, pp. 480–497. 2006.

[57] M. Marta and M. Cardei, *Improved sensor network lifetime with multiple mobile sinks*, *Pervasive and Mobile computing* **5** (January, 2009) 542–555.

[58] S. Basagni, A. Carosi, E. Melachrinoudis, C. Petrioli, and Z. Wang, *Controlled sink mobility for prolonging wireless sensor networks lifetime*, *Wireless Networks* **14** (December, 2008) 831–858.

[59] W. Wang, V. Srinivasan, and K.-C. Chua, *Using mobile relays to prolong the lifetime of wireless sensor networks*, in *Proceedings of the 11th annual international conference on Mobile computing and networking*, pp. 270–283, 2005.

[60] Y. Yun and Y. Xia, *Maximizing the lifetime of wireless sensor networks with mobile sink in delay-tolerant applications*, *IEEE Transactions on Mobile Computing* **9** (September, 2010) 1308–1318.

[61] A. Ghaffarkhah and Y. Mostofi, *Optimal motion and communication for persistent information collection using a mobile robot*, (Anaheim, CA), pp. 1532–1537, December, 2012.

[62] A. G. Mehrzad Malmirchegini and Y. Mostofi, *Impact of motion and channel parameters on the estimation of transmitter position in robotic networks*, (Anaheim, CA), pp. 1538–1543, December, 2012.

[63] A. Ghaffarkhah and Y. Mostofi, *A communication-aware framework for robotic field exploration*, (Orlando, FL), pp. 3553–3558, December, 2011.

[64] A. Ghaffarkhah and Y. Mostofi, *Communication-aware surveillance in mobile sensor networks*, (San Francisco, CA), pp. 4032–4038, June, 2011.

[65] A. Ghaffarkhah and Y. Mostofi, *Channel learning and communication-aware motion planning in mobile networks*, pp. 5413 –5420, jun., 2010.

[66] A. Ghaffarkhah and Y. Mostofi, *Communication-Aware Navigation Functions for Robotic Networks*, in *Proceedings of the 28th American Control Conference (ACC)*, (St. Louis, MO), pp. 1316–1322, June, 2009.

[67] A. Ghaffarkhah and Y. Mostofi, *Communication-Aware Motion Planning of Robotic Networks using Navigation Functions - Centralized Case*, in *Proceedings of the 2nd International Conference on Robot Communication and Coordination (ROBOCOMM)*, (Odense, Denmark), March, 2009.

[68] A. Gonzalez-Ruiz, A. Ghaffarkhah, and Y. Mostofi, *A comprehensive overview and characterization of wireless channels for networked robotic and control systems*, *Journal of Robotics* **2011** (October, 2011).

[69] Y. Mostofi, M. Malmirchegini, and A. Ghaffarkhah, *Estimation of communication signal strength in robotic networks*, in *Proceedings of the 50th IEEE International Conference on Robotics and Automation*, (Anchorage, AK), pp. 1946 – 1951, May, 2010.

[70] M. Malmirchegini and Y. Mostofi, *On the spatial predictability of communication channels*, *IEEE Transactions on Wireless Communications* **11** (March, 2012) 964 – 978.

[71] M. Malmirchegini and Y. Mostofi, *An Integrated Sparsity and Model-Based Probabilistic Framework For Estimating the Spatial Variations of Communication Channels, special issue of Elsevier Physical Communication Journal on Compressive Sensing in Communications* **5** (June, 2012) 102–118.

[72] K. Xu, H. Hassanein, G. Takahara, and Q. Wang, *Relay node deployment strategies in heterogeneous wireless sensor networks*, *IEEE Transactions on Mobile Computing* **9** (Feb, 2010) 145–159.

[73] W. Wang, V. Srinivasan, and K.-C. Chua, *Extending the lifetime of wireless sensor networks through mobile relays*, *IEEE Transactions on Networking* **16** (Oct., 2008) 1108–1120.

[74] J. Laneman, D. Tse, and G. Wornell, *Cooperative diversity in wireless networks: Efficient protocols and outage behavior*, *IEEE Transaction on Information Theory* **50** (December, 2004) 3062–3080.

[75] A. Bletsas, A. Khisti, D. P. Reed, and A. Lippman, *A simple cooperative diversity method based on network path selection*, *IEEE Journal on Selected Areas in Communication* **24** (March, 2006) 659–672.

[76] B. Rankov and A. Wittneben, *Achievable rate regions for the two-way relay channel*, in *IEEE International Symposium on Information Theory*, (Seattle, WA), pp. 1668–1672, July, 2006.

[77] Y. Zhao, R. Adve, and T. Lim, *Improving amplify-and-forward relay networks: optimal power allocation versus selection*, *IEEE Transactions on Wireless Communications* **6** (August, 2007) 3114–3123.

[78] J. Luo, R. Blum, L. Cimini, L. Greenstein, and A. Haimovich, *Decode-and-forward cooperative diversity with power allocation in wireless networks*, *IEEE transactions on wireless communications* **6** (March, 2007) 793–799.

[79] A. J. Goldsmith and S.-G. Chua, *Variable-rate variable-power MQAM for fading channels*, *IEEE Transaction on Communications* **45** (October, 1997) 1218–1230.

[80] M. Hasna and M.-S. Alouini, *Optimal power allocation for relayed transmissions over Rayleigh-fading channels*, *IEEE Transactions onWireless Communications* **3** (November, 2004) 1999–2004.

[81] Y. Zhang and K. Letaief, *An efficient resource-allocation scheme for spatial multiuser access in MIMO/OFDM systems*, *IEEE Transactions on Communications* **53** (January, 2005) 107–116.

[82] I. Hammerstrom and A. Wittneben, *Power allocation schemes for amplify-and-forward MIMO-OFDM relay links*, *IEEE Transactions on Wireless Communications* **6** (August, 2007) 2798–2802.

[83] T.-Y. Ng and W. Yu, *Joint optimization of relay strategies and resource allocations in cooperative cellular networks*, *IEEE Journal on Selected Areas in Communications* **25** (February, 2007) 328–339.

[84] A. Barili, M. Ceresa, and C. Parisi, *Energy-saving motion control for an autonomous mobile robot*, in *Proceedings of the IEEE International Symposium on Industrial Electronics*, (Athens), pp. 674–676, July, 1995.

[85] Y. Mei, Y.-H. Lu, Y. Hu, and C. Lee, *Energy-efficient motion planning for mobile robots*, in *Proceedings of IEEE International Conference on Robotics and Automation*, (New Orleans, LA), pp. 4344–4349, April, 2004.

[86] Y. Mei, Y.-H. Lu, Y. Hu, and C. Lee, *Deployment of mobile robots with energy and timing constraints*, *IEEE Transactions on Robotics* **22** (June, 2006) 507–522.

[87] P. Tokekar, N. Karnad, and V. Isler, *Energy-optimal trajectory planning for car-like robots*, *Autonomous Robots* (October, 2013) 279–300.

[88] P. Plonski, P. Tokekar, and V. Isler, *Energy-efficient path planning for solar-powered mobile robots*, *Journal of Field Robotics* **30** (July-August, 2013) 583–601.

[89] Z. Sun and J. Reif, *On finding energy-minimizing paths on terrains*, *IEEE Transactions on Robotics* **21** (February, 2005) 102–114.

[90] C. Kim and B. Kim, *Minimum-energy translational trajectory generation for differential-driven wheeled mobile robots*, *Journal of Intelligent and Robotic Systems* **49** (March, 2007) 367–383.

[91] I. Duleba and J. Sasiadek, *Nonholonomic motion planning based on newton algorithm with energy optimization*, *IEEE Transactions on Control Systems Technology* **11** (May, 2003) 355–363.

[92] S. He, J. Chen, Y. Sun, D. Yau, and N. Yip, *On optimal information capture by energy-constrained mobile sensors*, *IEEE Transactions on Vehicular Technology* **59** (June, 2010) 2472–2484.

[93] S. He, J. Chen, D. Yau, H. Shao, and Y. Sun, *Energy-efficient capture of stochastic events by global-and local-periodic network coverage*, in *Proceedings of the 10th ACM international symposium on Mobile ad hoc networking and computing*, pp. 155–164, 2009.

[94] R. Sugihara and R. Gupta, *Improving the data delivery latency in sensor networks with controlled mobility*, in *Distributed Computing in Sensor Systems*, pp. 386–399. 2008.

[95] R. Sugihara and R. Gupta, *Optimal speed control of mobile node for data collection in sensor networks*, *IEEE Transactions on Mobile Computing* **9** (January, 2010) 127–139.

[96] J. Luo and J.-P. Hubaux, *Joint sink mobility and routing to maximize the lifetime of wireless sensor networks: the case of constrained mobility*, *IEEE/ACM Transactions on Networking* **18** (June, 2010) 871–884.

[97] D. Bhadauria, O. Tekdas, and V. Isler, *Robotic data mules for collecting data over sparse sensor fields*, *Journal of Field Robotics* **28** (February, 2011) 388–404.

[98] W. Heinzelman, A. Chandrakasan, and H. Balakrishnan, *An application-specific protocol architecture for wireless microsensor networks*, *IEEE Transactions on Wireless Communications* **1** (October, 2002) 660–670.

[99] O. Younis and S. Fahmy, *Heed: a hybrid, energy-efficient, distributed clustering approach for ad hoc sensor networks*, *IEEE Transactions on Mobile Computing* **3** (October-December, 2004) 366–379.

[100] G. Xing, T. Wang, W. Jia, and M. Li, *Rendezvous design algorithms for wireless sensor networks with a mobile base station*, in *Proceedings of the 9th ACM international symposium on Mobile ad hoc networking and computing*, pp. 231–240, 2008.

[101] O. Jerew, K. Blackmore, and W. Liang, *Mobile base station and clustering to maximize network lifetime in wireless sensor networks*, *Journal of Electrical and Computer Engineering* **2012** (2012).

[102] M. Ma and Y. Yang, *Sencar: an energy-efficient data gathering mechanism for large-scale multihop sensor networks*, *IEEE Transactions on Parallel and Distributed Systems* **18** (October, 2007) 1476–1488.

[103] A. Somasundara, A. Kansal, D. Jea, D. Estrin, and M. Srivastava, *Controllably mobile infrastructure for low energy embedded networks*, *IEEE Transactions on Mobile Computing* **5** (August, 2006) 958–973.

[104] M. Bader, *Space-Filling Curves: An Introduction with Applications in Scientific Computing*, vol. 9. Springer, 2012.

[105] A. Goldsmith, *Wireless Communications*. Cambridge University Press, 2005.

[106] R. Kirk, *Optimal Control Theory: An Introduction*. Dover Publications, 2004.

[107] Y. Yan and Y. Mostofi, *Robotic Router Formation in Realistic Communication Environments*, *IEEE Transactions on Robotics* **28** (July, 2012) 810–827. © IEEE. Reprint.

[108] D. Johnson and D. Maltz, *Dynamic Source Routing in Ad Hoc Wireless Networks*, vol. 353, ch. 5, pp. 153–181. Kluwer Academic Publishers, 1996.

[109] C. Perkins and E. Royer, *Ad-hoc on-demand distance vector routing*, in *Proceeding of the 2nd IEEE Workshop on Mobile Computing Systems and Applications*, (New Orleans, Louisiana), pp. 90–100, February, 1999.

[110] Y. Yan and Y. Mostofi, *Robotic router formation - a bit error rate approach*, in *Proceeding of IEEE Military Communications Conference*, (San Jose, CA), pp. 1287–1292, November, 2010.

[111] S. Boyd and L. Vandenberghe, *Convex Optimization*. Cambridge University Press, 2004.

[112] A. Abdi and M. Kaveh, *On the utility of gamma pdf in modeling shadow fading (slow fading)*, in *Proceeding of the 49th IEEE Vehicular Technology Conference*, vol. 3, (Houston, TX), pp. 2308–2312, July, 1999.

[113] D. Fox, W. Burgard, and S. Thrun, *Markov localization for mobile robots in dynamic environments*, *Journal of Artifical Intelligence Research* **11** (1999) 391–427.

[114] S. Thrun, W. Burgard, and D. Fox, *Probabilistic Robotics*. MIT Press, 2005.

[115] J. Leonard and H. Durrant-Whyte, *Directed Sonar Sensing for Mobile Robot Navigation*. Springer, 1992.

[116] Y. Yan and Y. Mostofi, *Co-optimization of communication and motion planning of a robotic operation under resource constraints and in fading environments*, *IEEE Transactions on Wireless Communications* **12** (April, 2013) 1562–1572. © IEEE. Reprint.

[117] J. Nocedal and S. Wright, *Numerical Optimization*. Springer, 2nd ed., 2006.

[118] A. Shapiro, D. Dentcheva, and A. Ruszczynski, *Lectures on Stochastic Programming: Modeling and Theory*. SIAM-Society for Industrial and Applied Mathematics, 2009.

[119] W. Smith, *Urban Propagation Modeling for Wireless Systems*. PhD thesis, 2004.

[120] Y. Yan and Y. Mostofi, *To go or not to go: On energy-aware and communication-aware robotic operation*, *IEEE Transactions on Control of Network Systems* **1** (2014), no. 3. © IEEE. Reprint.

[121] C. Miller, A. Tucker, and R. Zemlin, *Integer programming formulation of traveling salesman problems*, *Journal of the ACM* (1960).

[122] "IBM ILOG CPLEX Optimizer." http://www-01.ibm.com/software/integration/optimization/cplex-optimizer/.

[123] K.-L. Du and M. Swamy, *Wireless communication systems: from RF subsystems to 4G enabling technologies*. Cambridge University Press, 2010.

[124] Y. Yan and Y. Mostofi, *Efficient Clustering and Path Planning Strategies for Robotic Data Collection Using Space-Filling Curves*, *Transactions on Control of Network Systems* (2016). conditionally accepted.

[125] Y. Yan and Y. Mostofi, *Efficient communication-aware dynamic coverage using space-filling curves*, in *American Control Conference*, (Portland, OR), 2013.

[126] J. B. III and L. Platzman, *An $O(NlogN)$ planar travelling salesman heuristic based on spacefilling curves*, *Operations Research Letters* **1** (1982), no. 4 121–125.

[127] J. B. III and L. Platzman, *Heuristics based on spacefilling curves for combinatorial problems in euclidean space*, *Management Science* **34** (1988), no. 3 291–305.

[128] S. Lin and B. Kernighan, *An effective heuristic algorithm for the traveling-salesman problem*, *Operations research* **21** (1973), no. 2 498–516.

[129] S. Arora, *Polynomial time approximation schemes for euclidean tra-veling salesman and other geometric problems*, *J. of the ACM* (1998).

[130] Q. Du, V. Faber, and M. Gunzburger, *Centroidal voronoi tessellations: applications and algorithms*, *SIAM review* **41** (1999), no. 4 637–676.

[131] Y. Yan and Y. Mostofi, *Impact of localization errors on wireless channel prediction in mobile robotic networks*, in *Proceedings of the IEEE Globecom Workshops on WiUAV*, (Atlanta, GA), pp. 1374–1379, December, 2013.

[132] U. Ali, Y. Yan, Y. Mostofi, and Y. Wardi, *An optimal control approach for communication and motion co-optimization in realistic fading environments*, in *IEEE American Control Conference*, (Chicago, IL), July, 2015.